Research Experiences for Undergraduates Program

2001 Program Report

National Radio Astronomy Observatory

Research Experiences for Undergraduates Program

2001 Program Report

National Radio Astronomy Observatory

Table of Contents

6

2001 Summer Research Symposium Program (CV)
7

National Radio Astronomy Observatory

REU Program Report

Overview

Fifteen undergraduates participated in the 2001 Research Experiences for Undergraduates Program sponsored by the National Science Foundation, at the NRAO. These students were joined by graduating seniors and graduate students paid for by other funds, to bring the total number of students to 28. 2001 was the forty second year of the NRAO Summer Research Program, which has graduated over 800 students during its tenure. Research initiated in previous years by some students and their mentors continues, giving the program a continuing impact even for students who have departed. In this report we divide the narrative into four main sections, each of which covers activities in the program and research conducted at one of the four main NRAO sites; Charlottesville, Socorro, Green Bank and Tucson. In an Appendix, we include the reports which many of the students wrote as part of their experience. Seven of the research projects will be presented at the 199th meeting of the American Astronomical Society in Washington, D.C. in January, 2002. All of these presentations are expected to be published in astronomical journals during 2001-2.

Several students were supported by non-REU funds--graduate students, graduating seniors, or foreign students. They are included in this report for completeness. REU-supported students are denoted by an NSF logo appearing after their name.

There were 74 applicants to the program, of whom 38 (51%). From these 15 positions were filled in the REU program with 8 women and 7 men. In all, 28 summer students were hired, 15 women and 13 men.

Al Wootten

Charlottesville

17 November, 2001

2001 Research Experiences for Undergraduates Program

National Radio Astronomy Observatory

2001 is the 42nd Anniversary of the NRAO Summer Student Program!

Research Projects by NRAO Site

- Charlottesville
- Socorro
- Green Bank
- Tucson

Charlottesville, Virginia (NRAO Headquarters)

There are five students in the 2001 Summer Student Research Program, four of them under the NSF Research Experience for Undergraduates (REU) program at NRAO-Charlottesville. Highlights of the program included a series of introductory level lectures on aspects of astronomy, particularly radio astronomy, spread over a few weeks. These lectures are intended to aquaint the students with the research which various staff members carry out. The lectures are listed below.

2001 Summer students from Green Bank traveled to Charlottesville to tour the CDL, U. Va. and NRAO HQ. (l-r) Paul Robinson, Matt Lister, Michael Wallace, Richard Simon, Emily Freeland, Julie Rupert, Zach Manganello, Melissa Williams, John Hibbard and Al Wootten.

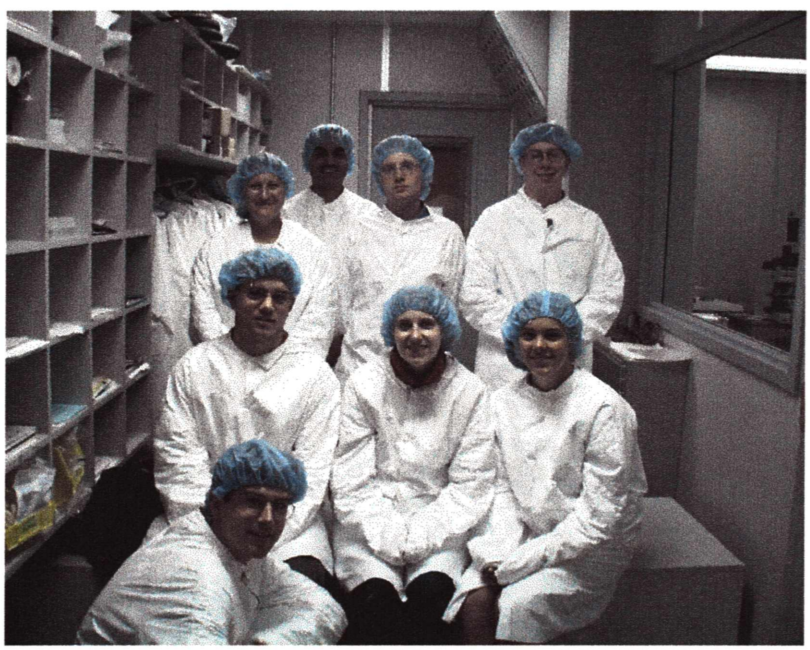

Many of the students in the NRAO-Green Bank program visit Charlottesville for a tour of the Central Development Laboratory, and of the University of Virginia's facility for the fabrication of the Semiconductor-Insulator-Semiconductor detectors used in millimeter wave receivers, the Applied Electrophysics Laboratory.

Students in the Clean Room where SIS mixers are made. (l-r) Michael Wallace, Tim Thacker (second generation NRAO summer student), Skip Thacker (NRAO Summer Student 196?), Paul Robinson, K. Saini and A. Lichtenberger.

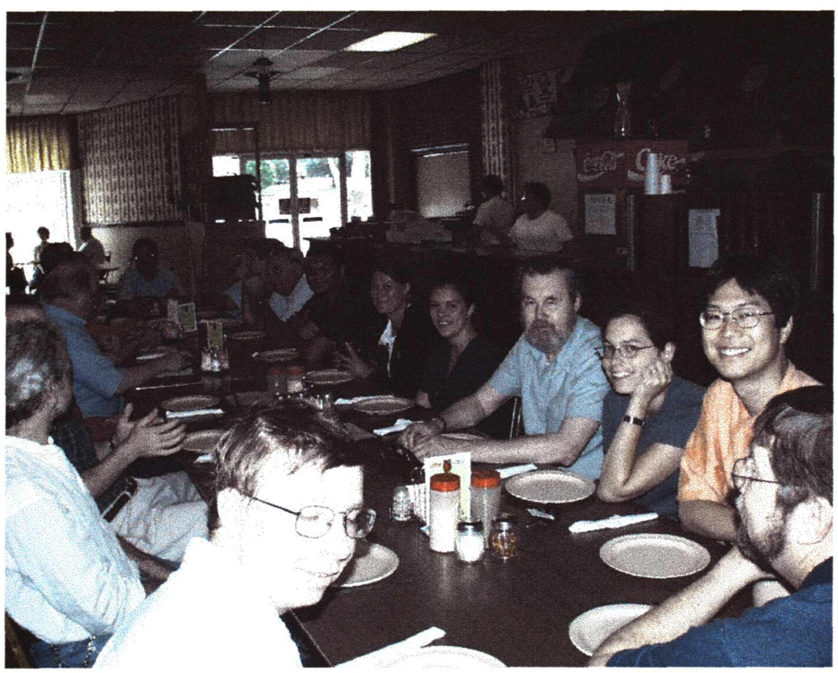

2001 Summer students from Green Bank and Charlottesville met at a pizza lunch get-together with mentors and lecturers and U. Va. personnel in Charlottesville.

The 2001 students enjoy an informal get-together with astronomers from the University of Virginia and NRAO at lunch. followed by a visit with graduate students from the University's Astronomy Department.

Later in the summer, the Charlottesville students visited Green Bank again to tour the NRAO telescopes located there, to meet members of the Green Bank staff, and to attend the annual picnic on 28 July.

One highlight will be initial operations of the Green Bank telescope (GBT), the world's largest steerable telescope. It is an offset parabaloid, 110m across the longest axis, incorporating 16 million lbs of steel in the moving structure.

The 40 ft telescope there is a student telescope, open for any project which students would like to carry out on it (though its instrumentation is limited). If there is interest, we may carry out, probably remotely, a project on the VLA.

We're very excited about the Atacama Large Millimeter Array, which was selected as the top priority for a new astronomical instrument in the 90s back at the beginning of the decade by the Astronomy Survey Committee. Students got to see it take shape as the fourth year of design and development gets underway.

The students give a series of 15 minute talks on their projects during a lunch symposium in Charlottesville before they begin leaving for the summer. They produce short reports describing their summer research.

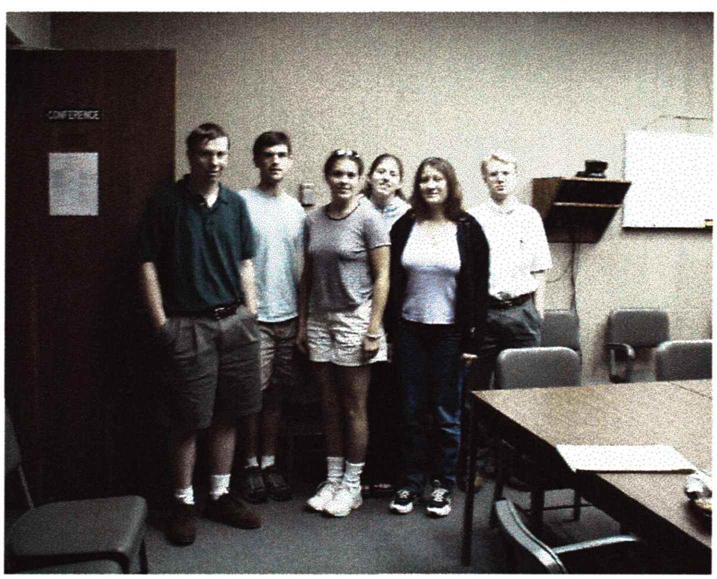

Students (l-r) Michael Wallace, Zach Manganello, Melissa Williams, Emily Freeman, Julie Rupert and Paul Robinson leave full of cosmology after a lecture by Juan Uson.

CV Summer Student Schedule, Summer 2001

Date	Person	Item	Location	Time

18 May	open	Students begin arriving		
4 Jun	open	All students have arrived	at the Observatory	9pm
14 June	Murphy	Introduction to Radio Astronomy	NRAO,Room 317, Stone Hall	9am
15 Jun	open	Public Night at McCormick Observatory	at the Observatory. By the end of public night, Mars should be above the trees, and will be about 19-20" in diameter. Should be an impressive sight, even through a small telescope.	9pm
18 June	Wootten	The REU Program at NRAO; From millivolts to Column Density	NRAO,Room 317, Stone Hall	9am
20 June	Turner	Interstellar Molecules	NRAO,Room 317, Stone Hall	9am
22 June	Condon	Radio Sources	NRAO,Room 317, Stone Hall	9am
25 June	Lister	TBA	NRAO,Room 317, Stone Hall	9am
27 June	Open	TBA	NRAO,Room 317, Stone Hall	9am
29 June	Kempner	Radio Relics and Halos	NRAO,Room 317, Stone Hall	not given
30 June	Goldin	MAP Satellite Launch	Cape Canaveral	??
30 June	Open	Comet LINEAR (C/2001 A2) swings by Earth	Dark skies near you	Look Up!
2 Jul	Open		NRAO,Room 317, Stone Hall	9am
4 July	Fireworks!		McIntire Park	Dark
6 July	Kellerman	The Development of Radio Astronomy	NRAO,Room 317, Stone Hall	Ppnd
6 Jul	open	Public Night at McCormick Observatory	at the Observatory	9pm

9 July	Hogg	Radio Stars	NRAO,Room 317, Stone Hall	9am
11 Jul	Liszt	The Galactic Center	NRAO,Room 317, Stone Hall	9am
13 July	Sarazin	Chandra: X-ray Astronomy	NRAO,Room 317, Stone Hall	9am
16 Jul	Wootten	ALMA and Star Formation	NRAO,Room 317, Stone Hall	9am
18 Jul	Wootten	ALMA and Star Formation (continued)	NRAO,Room 317, Stone Hall	9am
18 Jul	Wootten	Visit of Green Bank Students to Charlottesville	NRAO,Room 317, Stone Hall	pm
19 Jul	Bradley	Central Development Lab Introduction	Rm 228 Ivy Road	9am
19 Jul	Thacker	Tour of Central Development Lab	Rm 228 Ivy Road	10am
19 Jul	All	Pizza Lunch with U. Va.	Anna's Pizza	12pm
19 Jul	Crowe	Tour of U. Va. Device Fabrication Facility	U. Virginia	1:20pm
19 Jul	Wootten	BBQ for CV, GB REUs and mentors	Edgemont Road Garden	6pm
20 July	Uson	Cosmology	NRAO,Room 317, Stone Hall	9am
20 July	open	Public Night at McCormick Observatory	at the Observatory	9pm
23 July	Hibbard	Galaxy Morphology	NRAO,Room 317, Stone Hall	11am
25 July	Hibbard	Interacting Galaxies	NRAO,Room 317, Stone Hall	1pm
27 July	Kempner	Radio Relics and Halos	NRAO,Room 317, Stone Hall	9am
27 July	All	CV REUs -> Green Bank Picnic	Green Bank, W. Va.	evening

28 July	All	CV REUs -> Green Bank Picnic	Green Bank, W. Va.	noon
29 July	All	CV REUs tour GB; return from Green Bank Picnic	Green Bank, W. Va.	noon
30 July	Open	Open	NRAO,Room 317, Stone Hall	9am
31 July	Students	REU research presentations	Rm 317, Stone Hall	high noon
1 August	Open	Open	NRAO,Room 317, Stone Hall	9am
3 Aug	open	Public Night at McCormick Observatory	at the Observatory	9pm
11 August Aug	Leonids	Meteor Shower	Deltaville, Virginia	Midnight

Emily Freeland of Indiana University works with Matt Lister on

Circular Polarization Imaging of Active Galactic Nuclei at 43 GHz

This observational study involves a search for circularly polarized emission in a sample of bright, flat-spectrum AGNs at 43 GHz. The data were taken with the VLBA over the period 1999-2000 and include many well-known blazars such as 3C 273 and 3C 279, both of which have been found to display circular polarization (C.P.) at lower frequencies. Since the data were originally processed with only linear polarization images in mind, this project will involve a careful re-calibration of the data, paying close attention to the relative calibration of the left and right complex antenna gains.

Models of intrinsic circular polarization predict a higher amount of C.P. at 43 GHz than at lower frequencies due to reduced opacity and other effects. These data can therefore provide a useful means of distinguishing between competing intrinsic C.P. and Faraday conversion mechanisms in AGNs. Using the multiple epochs available for 3C 279, it will be possible to check for variations of C.P. in this source at 43 GHz. Homan et al. (1999) found 3C 279's C.P. to be highly stable at 15 GHz, which is unusual given its large variations in linear polarization and intensity. This project is best suited for an advanced undergraduate student or graduating senior who is interested in learning about AGNs and cutting-edge VLBI research. The work is likely to be data-intensive, with a smaller amount of time spent on theory.

Megan Kohring, of The University of Virginia
will work with John Hibbard
in collaboration with J. Barnes (IfA) on

Tidal Dwarf Formation in Tidal Tails

It has long been known (eg Schweizer 1978) that clumps of star formation with properties similar to dwarf galaxies exist within tidal features. Some of these features show enhancements also in the underlying stellar light and in the neutral gas column density and line-profile width, leading to the suggesting that they will evolve into independent dwarf galaxy satellites. This suggestion is supported by detailed numerical simulations which demonstrate that self-gravitating structures can indeed develop in tidal material torn off during galaxy interactions. However, the observational evidence that optical enhancements within the tidal tails are in fact distinct identities is rare or non-existence. Many may be simply unbound collections of young stars recently born within the tail, but destined to fade into obscurity within a few hundred million years.

The goal of the present project is to identify bound clumps within tidal tails generated via numerical simulations of merging galaxies, and to quantify their expected observatial characteristics. Simulated maps of the integrated intensity, velocity field, and velocity dispersion will be generated and examined to see if the location of the bound clumps distinguish themselves from projected (but unbound) enhancements. Next, the student will make simulated measurements of the dynamical mass of the clumps (from the half-light profiles and "observed" velocity dispersion), and compare these values to their "true" mass. Finally, the student will examine high-resolution HI observations of the nearest and most famous

tailed merger, NGC 4038/9
("The Antennae") to see if any of the regions within its tails exhibit the expected behavior of bound clumps.
A report on this research may be read.

2001 Summer students Zach Manganello and Tim Thacker mount the Charlottesville Telescope (CVT) between NRAO and U. Va. Astronomy.

Zachary Manganello , of Middlebury College

works with Lynn Matthews and John Effland
on

The Small Radio Telescope

A version of the Haystack Small Radio Telescope kit will be constructed.

Juliette Rupert , of The University of Oklahoma
works with Richard Simon
on

Identifying Promising Target Stars for the Terrestrial Planet Finder Mission

There is widespread interest in the problem of identifying and characterizing Earth-like planets that might exist around nearby stars. To date, little systematic work has been done on carefully identifying the few hundred nearby stars that are the most promising candidates for a search of this type. By using a combination of careful calculation and detailed work with the literature, it should be possible to create a definitive list of the most promising stars for such searches. This work will have a significant effect on the planning of future space missions and will also prove useful to a number of monitoring programs already underway.

Timothy Thacker, of Virginia Tech works with John Effland on

SIS Mixer Test System

Following our specifications and under the guidance of CDL engineering, the student would design circuits and construct hardware for the SIS mixer test system. This hardware would consist of measurement subsystems such as control of LO frequency and power, amplifier bias supplies, or mixer bias supplies. The student would be required to design analog circuits consisting primarily of op amps and would create mechanical designs using AutoCAD. The student would be expected to write software for automated testing of the hardware. CDL engineering would provide to the student the software design consisting of UML class, sequence, and activity diagrams. The student would be expected to write and document object oriented code that meets the software design requirements.

NRAO/Socorro 2001 Research Experience for

Undergraduates (REU) Program

2001 Summer students from Socorro in a VLA antenna (photo courtesy of J. Anderson).

The summer REU program at NRAO/Socorro in 2000 consists of 4 main categories of activity:

1 - student research projects, in collaboration with an NRAO advisor
2 - lectures to the students by NRAO staff members
3 - a joint student project, involving observations with the Very Large Array (VLA)
4 - guided tours of the VLA, given by the students on weekends

The 2001 REU program at NRAO/Socorro is under the direction of Tracy Clarke and Greg Taylor. Dr. Clarke is Jansky Postdoctoral Researcher at NRAO/Socorro, and Dr. Taylor is a member of the scientific research staff.

Lectures, etc...

Several lectures about radio astronomy and interferometry will be presented, allowing the students to obtain a good understanding of the technique. Talks were also given on general topics in astronomy, presented by members of the scientific staff. The astronomy talks were designed to give the students an understanding of what sort of research goes on at NRAO, and in radio astronomy in general. The detailed list of lectures and events for the summer is in the following table and at the AOC WWW site .

Preliminary 2001 Summer Student Calendar of Events

May 2001

May 18: Colloquium by Steve Myers, "Latest Results from the Cosmic Background Imager"
May 25: Colloquium by David Wilner, "Dusty Disks around Young Stars"
May 30: 10:00 am. VLA Tour #1 by Dave Finley & Vivek Dhawan
May 31: 9:00 am. Safety Lecture #1 by Jon Spargo, 3'rd floor conference room
May 31: 4:00 pm. "What is Radio Astronomy?" by Jim Ulvestad

June 2001

June 1: Colloquium by Lincoln Greenhill, "A Pirate's Treasure Map of Orion BN/KL - X Marks the Spot, but is it a Trick?"
June 5: 11:00 am. "Fundamentals of Radio Astronomy" by Rick Perley
June 7: 4:00 pm. "Imaging and Deconvolution" by Tim Cornwell
June 12: 11:00 am. "Basics of Spectral Line" by Claire Chandler
June 14: 10:00 am. VLA Tour #2 by Dave Finley & Vivek Dhawan
June 15: Colloquium by Mark Gurwell, " Millimeterwave Astronomy of Planetary Atmospheres"
June 19: 11:00 am. "Polarimetry" by Greg Taylor
June 19: 3:00 pm. Safety Lecture #2 by Jon Spargo, auditorium
June 20-22: KPNO/Tucson tour
June 22: Colloquium by David Hughes
June 25: VLA observing run
June 26: 11:00 am. "Radio Evidence for Black Holes in Nearby Galactic Nuclei" by Joan Wrobel
June 28: 4:00 pm. "VLBI" by Craig Walker
June 29: Colloquium by Geoff Marcy

July 2001

July 3: VLA observing run
July 3: 3:00 pm. TBA by Henrique Schmitt
July 4: Holiday

July 5: 4:00 pm. TBA by Dale Frail
July 10: 11:00 am. "Molecular Clouds and Star Formation" by Debra Shepherd
July 12: 4:00 pm. "Atronomical Masers" by Mark Claussen
July 17: 11:00 am. "Magnetic Fields in the Universe" by Crystal Brogan
July 19: 4:00 pm. "Cosmic Microwave Background" by Steve Myers
July 24: 11:00 am. Colloquium by Swarup
July 25: 12 pm Summer student talk by Aaron Boley
July 28: TRIP TO APACHE POINT
July 31: 11:00 am. "Planetary Radio Astronomy" by Bryan Butler

August 2001

Aug 1: 12 pm. Summer student talks by Daniel S., Marj, Jason, and Jenn
Aug 2: 4:00 pm. "Microquasars" by Vivek Dhawan
Aug 7: 12 pm. Summer student talks by Diane, Mike, Matt, and Cristina
Aug 7: 4:00 pm. "Properties of HI in Nearby Galaxies" by Dave Thilker
Aug 8: 12 pm. Summer student talk by Bhasker
Aug 15: 12 pm. Summer student talks by Jim, Katie, Daniel P., and Stacy

Joint Student Research Project

The VLA is in its CnB and C configurations this summer. Some telescope time will be allocated to the summer students to pursue group projects.

Note that last summer one of the NRAO student projects resulted in an exciting discovery of the first radio emission detected from a brown dwarf star! This discovery resulted in a paper in Nature. More details are available on the NRAO press release web page.

Planned Trips

Kitt Peak/Tucson - June 20-22

Apache Point - July 28

Other Stuff

A Basic Information Letter is available from the WWW pages.

Student Research Projects

Each of the REU students will work with one or more advisors on one or more projects throughout the summer. This is the main focus of the program, and the majority of the students' time will be spent on these research endeavors. These projects involved observing, data reduction and analysis, equipment development, and theoretical studies. At the end of the program, each student gave a lunch talk explaining the main project(s) he or she worked on during the summer. The possibility exists for the students to present their original research at scientific meetings deemed appropriate by their advisor(s). Following is a detailed list of the specific projects carried out by the NRAO/Socorro REU students:

Jason Adelstein of Columbia University

works with Steve Myers
on

The CLASS Survey

In the next couple of months, a copy of the full CLASS archive (now only at Jodrell Bank) will be set up here at NRAO. There will be the opportunity to then develop some summer student projects based on the CLASS archive. For example:
- morphological classifications
- polarization properties
- correlations with other surveys (eg. FIRST)
- update of astrometric catalogues (CLASS accuracy is ~15-30 mas)

James Anderson of New Mexico Tech
works with Jim Ulvestad
on

The Flare in NGC 7582--AGN or Supernova?

The Seyfert galaxy NGC 7582 turned from a Seyfert 2 to a Seyfert 1 galaxy in mid-1998; broad permitted emission lines appeared at the same time that an X-ray flare occurred. The optical spectrum during the flare was similar to that of a Type IIn supernova, so it has been suggested that the flare was due to a supernova rather than an AGN associated with a massive black hole. Many Type IIn supernovae are detected as radio sources, peaking at 500-1000 days after their optical flares. Therefore, NGC 7582 was observed twice in the A configuration at 3.6 and 6cm, once in August 1999 and again in December 2000. The project will be to image the 2000 data for comparison to the 1999 data and pre-flare images, and combine the radio results with models for the X-ray emission to see if a type IIn supernova is feasible. In addition, the possibility that the flare is due to an absorbing cloud "uncovering" part of the nucleus will be investigated.

Aaron Boley of Mount Union College works with Mark Claussen on

Methanol Maser Sources--Disks Around Young Stars?

We (Claussen and Beasley) have performed a VLBA snapshot survey of 12 sources in the 12.1 GHz maser line of methanol near compact HII regions. The purpose of the survey is to extend the knowledge of the structure of methanol masers toward more sources and thus test the statistics of Norris et al. (1993, ApJ, 412, 222) in which the claim was made that a large fraction of methanol masers toward HII regions are frequently located along lines or arcs. Norris' et al. interpretation of these structures is that they indicate the existence of edge-on disks around the forming stars.

The summer student project would be to calibrate and image as many sources from the 12.1 GHz VLBA project as possible in the available time and to examine the structure/velocities of the maser sources to determine if they fit a possible disk model.

Kathryn Devine, of Carleton College works with Miller Goss on

OH Masers in the High Excitation 6cm Line Observed with the VLBA

We will have new VLBA data on the excited OH masers at 6 cm.

Jennifer Donley, of Penn State University
works with Henrique Schmitt
on

Radio and Optical Narrow Band Imaging of Seyfert Galaxies

This project involves the use of 3.6cm VLA A-configuration images, as well as HST narrow band [OIII] images of Seyfert galaxies. The student working on this project will learn to reduce and analyze the HST images and how to combine them with the radio images. Since the absolute astrometry of HST has a precision of the order of 0.5 arcsec, dictated by the precision of the the guide star catalog, we will have to devise ways of aligning the optical and radio images to be able to compare them. This dataset will be used to study the origin of the misalignment between the accretion disk axis and the host galaxy plane axis, which can be due to mergers with other galaxies, or by self induced radiation warping. It will also be used to compare the size and shape of the Narrow Line Region of Seyfert 1 and Seyfert 2 galaxies, and to estimate the importance of shocks to the ionization of the gas. Right now we have approximately 30 galaxies for which both optical and radio data are available, but we expect to have at least 50 galaxies by the middle of the year.

Marjorie Frankel, of Wellesley College
works with Tracy Clarke
on

Magnetic Fields Threading Galaxy Cluster Gas

Faraday rotation measure studies of radio sources viewed through the X-ray emitting intracluster gas reveal the presence of magnetic fields threading through the thermal gas. Radio sources located in the central regions of so-called cooling flow clusters show Faraday rotation measures of thousands of radians/square metre with corresponding magnetic field strengths of 10 to 100 microGauss ordered on scales of 1 to 10 kpc (e.g. Dreher et al 1987; Ge and Owen 1993, 1994; Taylor and Perley 1993; Taylor et al 1994). In order to understand how these strong magnetic fields interact with the cooling flow it is necessary to probe the strength and topology of the magnetic fields prior to the onset (or well after the disruption) of the cooling flow. Clarke et al (2001) have studied the central regions of non-cooling flow clusters and find fields of order 5 microGauss coherent on scales of ~10 kpc. Their sample was designed to probe the radial extent of the intracluster magnetic fields and thus they do not have sources viewed through the very cores of the clusters for comparison with the cooling-flow results. I have initiated a series of observations at the VLA with scaled-array polarimetry to probe the magentic field in the cores of the non-cooling flow clusters using a sample of mainly background (plus some embedded) radio sources. Observations have been undertaken at 4 wavelengths in A array and will be followed by two wavelengths in the upcoming B array for a sample of the more compact targets. I would suggest that a summer student could start by making some simple images of the targets (around 17 sources) to find a few 'interesting' objects. To define interesting I would encourage them to use both the image and some background research to target say 3 sources. The student could then carry out Faraday mapping of the chosen targets and possibly assist in the comparison of the structure function with that of the cooling flow sources. If interested, the student could work with a single cluster target and include X-ray analysis in the study. This project could certainly lead to an AAS presentation and likely an ApJ paper.

Matthew Kunz of University of Virginia
works with Claire Chandler
on

The formation and evolution of high-mass protostars is not well understood. Study is hindered by the difficulty of observing the innermost 100 AU around high-mass protostars; these regions are distant, heavily obscured, and dynamically complicated. However, the archetypal high-mass star forming region, Orion BN/KL, exhibits uniquely strong SiO maser emission from several transitions, and the brightness distributions have been mapped with VLBI.

SiO maser emission from the two brightest transitions (7 mm wavelength) traces a biconical outflow from a 100,000 Lsun protostar. The masers lie 20 - 60 AU from the protostar and their proper motions, easily observed with the VLBA, are uniquely well suited to the study of outflow (and possibly accretion) dynamics so close to a high-mass protostar. In projects BG98 and BG118 we have begun a several year-long proper motion study of the SiO masers, with observations scheduled monthly. The project is challenging because data calibration and imaging of the maser source are extremely demanding; dynamic ranges of many thousand must be achieved and the source structure is complex, with dozens of emission components in each < 1 km/s spectral channel.

We propose to work with a student to measure maser proper motions from three epochs of data, to model motions, and to examine in detail deviations from the current simple biconical outflow model in several sub-regions. We will train the student in the necessary VLBI data reduction and post-reduction analysis. In the first four to six weeks, the student will reduce the first epoch of data and construct scripts that will make possible automated reduction of the second two epochs (2 weeks). Experience with scripted reduction at the CfA has demonstrated the feasibility of this schedule. Estimation and analysis of proper motions for a small fraction of the maser components spread throughout the source and for all of the maser components in several sub-regions (4 weeks) will generate results suitable for AAS presentation.

Laura Lindenmayer, of New Mexico Tech,
works with David Thilker
on

Neutral Atomic Hydrogen (HI) in M33

We have completed a high-resolution VLA/WSRT survey of HI in M33. Our data comprise the most detailed HI observations ever obtained for a spiral galaxy other than the Milky Way and reveal many striking properties of the neutral atomic gas. The wealth of information contained by these observations presents a summer student several avenues for research, with the particular choice based on student preference and abilities. One of our principal goals is to compile a list of expanding shells and superbubbles in M33. This task will be addressed using a 3D pattern-recognition technique to initially identify a sample of HI structures. Planned follow-up then consists of comparison with optical imagery (to examine the stellar content and ionized gas associated with each well-defined shell). An alternative focus for the summer student could be the study of 21cm line profile variations as a function of environment within M33. The smooth decrease of mid-plane pressure (with increasing galactocentric radius) and the more localized, disruptive influence of massive star formation will be key factors in this analysis. A general investigation, based on median co-aligned profiles, the spectral correlation function, and velocity coherence imaging, has yet to be undertaken.

Bhasker Moorthyof New Mexico State University
works with Vivek Dhawan
on

Motion of the Galactic Black Hole Binary GRS1915+105

Radio imaging of GRS1915+105 with the VLBA shows, in different states of the black-hole binary, the core is always a compact collimated jet of Tb ~ 10^9 K. This AU-scale jet is observed to vary in ~30min, fed by relativistic plasma ejected from the inner accretion disk. The dynamics of hot corona (emitting inverse-Compton hard x-rays), accretion disk (soft X-rays), and jet (optically thick synchrotron from radio to IR) are complex and very interesting. There are as well occasional big outbursts, with associated superluminal ejecta expelled to 1000's of AU. The relationship between the AU-scale and large scales is unclear. By astrometry relative to the extragalactic frame, the core has been located to about 1.5 milliarcsec, and its motion after allowing for Glactic secular parallax is consistent with the black hole being stationary with respect to its surroundings (+-100km/s, at 12kpc) A better limit on these astrometric results can be obtained by putting the various epochs of observation into a common reference frame, which has changed due to VLBA correlator model updates. Software to do this is now available, and would be tested and applied. The reduction of existing VLBA data would involve learning about phase referencing, imaging, and astrometry. It is a pretty challenging project, but I think it is realistic to have 1 epoch (the earliest) remodelled, which should form the basis of a paper on an improved estimate of proper motion. There also may be the opportunity to take VLA data on this or another X-ray binary as a target of opportunity.

Cristina Murrayof The University of New Mexico
and Michael Fine, of Colgate University
work with Frazer Owen
on

Deep Radio/Optical Surveys of Distant Rich Galaxy Cluster Regions

The students will work on my deep radio/optical surveys of the regions containing rich clusters of galaxies at z=0.25-0.41. There are three clusters fields now with such data. Besides studying the clusters, a major part of the project involves studying the background sources. The main goal is to determine the radio luminosity function of star forming galaxies as a function of redshift. The redshifts are obtained from deep, broadband imaging to which one can fit templates of various galaxy spectral energy distributions. The major goal for the summer would be to obtain these redshifts for the radio identifications. The computer programs exist to do this: both a program to make the catalogs of the optical sources in each of the 10 optical-near IR bands and to fit the templates using various input parameters. The radio data should be reduced before the summer. Some of the basic reductions of the optical data may be necessary. I think it should be possible to have a set of photometic redshifts for at least one of the fields by the end of the summer and thus we should be able to have some initial answers about the star formation history of the universe.

Daniel Stark, of The University of Wisconsin
works with Debra Shepherd
on

The W75N Molecular Outflow

OVRO CO(J=1-0) mosaic data of the W75N outflow will be reduced and imaged. The OVRO data must be reduced with the Caltech MMA reduction package (about 1/3 of the tracks are done so far). A miriad script drafted out can be used for imaging. The student will learn how to reduce and image data. If time permits, 12m CO spectra that are reduced will be used for an optical depth determination of the CO in the outflow. In addition, VLA 7mm continuum data will probe the central region. The VLA and OVRO images will be compared once all is finished. One other possibility is that, if VLBA time is assigned for the source G192.16, water maser observations may trace the dynamics of the disk.

Stacy Teng, of The University of Maryland
works with Jim Ulvestad
on

An Age-ordered Sequence of Merger Galaxies

An age-ordered sequence of merger galaxies is being observed at high resolution with the VLA in order to find the epoch of maximum star formation in the merger process. Each galaxy is being observed in multiple configurations at 6 cm and 3.6 cm. The data are imaged, and areas of compact radio emission identified and measured. Spectral information is used to determine whether particular sources are dominated by supernova remnants or H II regions, which enables estimates to be made of the populations of massive young stars in the galaxies. One galaxy for which much of the work has been completed and published is the nearby merger NGC 4038/9, the "Antennae" (see Neff & Ulvestad, 2000, AJ, 120, 670). The summer project would be to work on analyzing the data on a single galaxy in the sequence, and making the relevant interpretations.

Diane Wong, of Cornell University
works with Greg Taylor and Jim Ulvestad
on

"Sub-parsec radio structure in NGC 4151."

The Seyfert galaxy NGC 4151 has been observed in two epochs with the VLBA, looking for jet speeds near the nucleus, a possible compact thermal disk, and the actual location of the active nucleus. The first epoch was rather low sensitivity, and has already been published (Ulvestad et al., 1998, ApJ, 496, 196). The second epoch was observed with the VLBA and phased VLA in 1998, to very high sensitivity at 3.6 cm and moderate sensitivity at 6 cm. The summer project would be to analyze the data from this second epoch, generate final images of NGC 4151, and address the scientific issues listed above.

Green Bank, West Virginia (NRAO 43m and 100m Telescopes)

Students conducting their research at the NRAO Green Bank Site in West Virginia included the students in the list below, along with others. The program at Green Bank is under the direction of Dr. Ron Maddalena.

2001 Calendar of Events -- West Virginia

The following lists the scheduled activities for the GB students:
-- Student Orientation and tours

June 2001

July 2001

Melissa Williams, of Valdosta State University

works with Jay Lockman
on

Hydrogen in Ursa Major

Melissa Williams is participating in the study of the hydrogen envelope of the Milky Way galaxy far from the galactic disk where it begins to be affected by the interstellar environment. She will be reducing data from the 1995-1999 HI galactic plane survey taken by Jay Lockman and Ed Murphy using the 140 foot telescope at Green Bank, West Virginia. Plans were made to complete several follow-up observations of the 21 cm HI line using the newly commissioned Green Bank Telescope, the world's largest fully steerable telescope. Unfortunately, the GBT will not be fully operational until a few days after the students leave in August. Paul Robinson is also participating in this project (see below).

Paul Robinson, of Appalachian State University
works with Jay Lockman
on

Hydrogen in Ursa Major

Mr. Robinson corrects the data taken in the 43m HI survey for so-called 'stray radiation.' The stray radiation subtraction is especially important, since the data cannot really be reduced until the stray correction is applied. He will also be involved in the reduction and analysis of the survey using AIPS++.

Michael Wallace, of Hampden-Sydney College
works with Dave Parker
on

Accurate Control of the GBT

I worked for Dave Parker in the Laser Metrology Group. I built a computer interface to the HP-5528A Laser Measurement System to perform automated distance measurements accurately to a tenth of a micron. I also participated in recalibrating parts of the laser range finder and monuments. In addition to laser work I helped to produce plots of data concerning the motion and relative strain in the azimuth track on the GBT. I also helped to produce plots of the vertical and horizontal runout data for the Green Bank Telescope's Elevation Gear. These two sets of data were used to check if both the azimuth track and elevation gear met design specs. Most importantly I learned a considerable amount about the engineering required to produce a radio telescope.

Thomas Freismuth , of College of Charleston works with Glen Langston on

The Second Plane Survey and Transient Sources

I am working with Glen Langston on the second epoch of the Galactic Plane Surveys at 8.35 and 14.35 GHz. We are comparing the second to the first in order to search for transient radio sources. The surveys were made using the 45' NASA/NRAO Green Bank Earth Tracking Station. I have also been able to sit third wheel and watch over some commissioning observations for the spectrometer on the Green Bank Telescope. Some details of this work can be found on a WWW page and at the Sgr A or Rosette pages.

Tucson, Arizona (NRAO VLBA Telescope and ALMA Development)

Four summer students conduct research at the NRAO Tucson site in Arizona during the summer of 2001. The program in Tucson is under the direction of Jeff Mangum. As the NRAO offices are across the street from KPNO/NOAO offices, the group shares in the activities of the NOAO REU program there. For more on their activities see the Tucson Student Page.

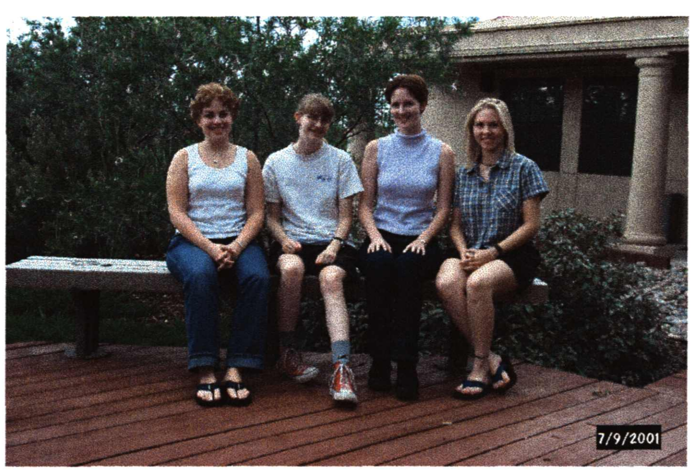

2001 Summer students Rebecca Rosengard, Daisy Raymondson, Sarah Flynn, and Virginia Valentine

In addition to the general activities carried out at the KPNO/NOAO offices, the NRAO and KPNO/NOAO REU students participate in group activities organized by the NRAO staff.

One activity will be a lecture series on millimeter wavelength astronomy given by members of the NRAO scientific staff. Four lectures were given, as listed below. Students also visited the Array Operations Center and Very Large Array in Socorro, NM.

2001 NRAO Tucson Summer Student Calendar of Events

June 2001

June 20-21 - Trip to Kitt Peak with NRAO Socorro REUs

July 2001

July 9-10: Trip to VLA/NRAO Socorro.

July 12: 10:00 am. "Radio Astronomical Observations of the Solar System and Star Formation" by Jeff Mangum

July 19: 10:00 am. "The Cosmic Microwave Background" by Simon Radford

July 24: 10:00 am. "Radio Astronomical Observing Techniques" by Darrel Emerson

August 2001

August 1: 10:00 am. "Interferometric Imaging" by Mark Holdaway

---

2001 Summer students get a tour of the VLA antenna from Jeff Mangum.

The following are sketches describing the work to be done by each REU student at NRAO Tucson.

Sarah Flynn, of State University of New York at Stony Brook works with Jeff Mangum

Molecular Outflow Properties

Ms. Flynn will work on the analysis of CO 2-1 measurements of the molecular outflow properties toward protostellar and young stellar candidates in the Ophiuchus and Taurus molecular cloud regions.

Daisy Raymondson , of The University of California at Davis

works with Jeff Mangum and Simon Radford on

ALMA Amplitude Calibration System

A proposed calibration scheme for ALMA uses two radiators at different temperatures mounted behind the subreflector. Based on a design developed at UC Berkeley, a prototype calibration radiator was constructed and tested in the laboratory. Results were summarized in an internal report.

Rebecca Rosengard, of Wellesley College
works with Simon Radford and Jeff Kingsleyon

The ALMA Nutator Control System

The ALMA subreflector nutator is a high performance, recoilless design. In the laboratory, the dynamic responses of the major components of an engineering demonstration model were characterized. These measurements were used to refine a mathematical model of the mechanism. This model is the basis for tuning the servo system parameters. Results were summarized in an internal report.

Virginia Valentine, of University of Southern California
works with Simon Radford
on

The ALMA Site

Since late 1997, tipping radiometers have measured the submillimeter (350 um) atmospheric transparency at Chajnantor, Mauna Kea, and the South Pole. Data from these instruments were edited and processed to produce a uniform database. Overall observing conditions and diurnal and seasonal variations in conditions at the three sites were compared. Results will appear in a journal paper.

Take me to the 2000 Summer student Home Page
Take me to the 1999 Summer student Home Page
Take me to the 1998 Summer student Home Page
Take me to the 1997 Summer student Home Page
Take me to the 1996 Summer student Home Page
Take me to the 1995 Summer student Home Page
Back to the Home Page

Appendix

Student Presentations at the 199th AAS Meeting

Washington, D. C.

Copies of the abstracts follow.

Meeting Presentations

Part 1. NRAO Summer Student Presentations at the 199th AAS Meeting

Presentation: Interpretations of the Morphologies of 12.2 GHz Methanol Masers Session: 134.16
Authors: A.C. Boley (Mount Union College), M.J. Claussen (NRAO), A.J. Beasley (OVRO/CARMA)

Presentation: OH Masers in the High Excitation 6cm Line Observed with the VLBA Session: 134.19
Authors:K. E. Devine (Carleton College), W. M. Goss (NRAO), P. Palmer (University of Chicago)

Presentation: An [OIII] Study of the Narrow Line Regions of Seyfert Galaxies: Testing the Unified Model
Session: 50.09
Authors:J. Donley (Penn State), H. R. Schmitt (NRAO-Socorro)

Presentation: Faraday Rotation Measure Study of Cluster Magnetic Fields Session: 100.3
Authors:M.M. Frankel (Wellesley College), T.E. Clarke (NRAO)

Presentation: The proper motions of SiO masers around the high-mass protostar, Source I, in Orion
Session: 134.17
Authors:M.W. Kunz (Dept. of Astronomy, University of Virginia), C.J. Chandler (NRAO, Socorro), L.J. Greenhill (Harvard-Smithsonian CfA)

Presentation: Choosing Candidate Stars for the Terrestrial Planet Finder Mission Session: 9.03
Authors:J.T. Rupert (NRAO/University of Oklahoma), R.S. Simon (NRAO)

Presentation: NGC 4151: Radio Morphology on the Sub-Parsec-Scale Session: 50.06
Authors:D.S. Wong, J.S. Ulvestad, G.B. Taylor (NRAO), J.F. Gallimore (Bucknell Univ.)

AAS 199th meeting, Washington, DC, January 2002
Session 134. Formation of Massive Stars
Display, Thursday, January 10, 2002, 9:20am-4:00pm, Exhibit Hall

[Previous] | [Session 134] | [Next]

[134.16] Interpretations of the Morphologies of 12.2 GHz Methanol Masers

A.C. Boley (Mount Union College), M.J. Claussen (NRAO), A.J. Beasley (OVRO/CARMA)

We present VLBA results of 12.2 GHz class II methanol maser observations towards nine massive star forming regions in the Northern Hemisphere. Our results show that 7 out of 9 of the imaged target regions display linear or curved morphologies with smooth velocity gradients. However, sub-solar enclosed masses are derived when using the edge-on circumstellar disk model. Although there are arguments that suggest only a small portion of the edge-on disk is seen, we feel that the edge-on circumstellar disk model for explaining the morphologies of methanol masers is inadequate and cannot explain methanol maser regions with complex and simple morphologies. We will present the results of our observations as well as other possible interpretations of the morphologies of methanol maser regions.

This research has been supported by the National Science Foundation, through its Research Experience for Undergraduates program. NRAO is a facility of the National Science Foundation operated under cooperative agreement by Associated Universities, Inc.

[Previous] | [Session 134] | [Next]**AAS 199th meeting, Washington, DC, January 2002**
Session 134. Formation of Massive Stars
Display, Thursday, January 10, 2002, 9:20am-4:00pm, Exhibit Hall

[Previous] | [Session 134] | [Next]

[134.19] OH Masers in the High Excitation 6cm Line Observed with the VLBA

K. E. Devine (Carleton College), W. M. Goss (NRAO), P. Palmer (University of Chicago)

Results are presented from VLBA observations of OH 4765-MHz masers in the star-forming regions of W3(OH) and K3-50. OH masers at 4765-MHz appear to be correlated with star forming regions and can be among the strongest masers in a region. Existing models explaining the pumping mechanisms of the excited state maser lines of OH propose that 1720-MHz masers and 4765-MHz masers will arise in the same gas. In W3(OH), three regions of maser emission were detected. In K3-50, one region of maser emission was detected. Results are compared to existing data of nearby maser emission at 1720-MHz when available. These observations seek to improve existing models explaining excited state OH maser emission using the high angular resolution possible with the VLBA. With high angular resolution and phase-referenced data, it is possible to obtain accurate absolute positions for the observed masers in W3(OH) and K3-50. Using MERLIN data obtained by Gray et al. (2001) for 1720-MHz masers in W3(OH), spatial coincidence is shown between observations of 4765-MHz masers and the 1720-MHz masers observed by Gray et al. It appears that no 1720-MHz masers in K3-50 exist near the observed 4765-MHz maser, in contrast to existing models of 4765-MHz maser emission. Angular sizes of 4765-MHz masers are also investigated and, when possible, compared to angular sizes of coincident 1720-MHz masers. Larger angular sizes of 4765-MHz masers suggest unsaturated masers at this frequency. Finally, circular polarization in the observations is examined. Theory indicates that no circular polarization should be observed in OH emission at 4765-MHz; however, existing upper limits on observed circular polarization for this maser line are fairly high. Although the circular polarization of our observations is still currently being investigated, out current upper limit on observed circular polarization from this state is ~ 6 %.

The author(s) of this abstract have provided an email address for comments about the abstract: devinek@carleton.edu

[Previous] | [Session 134] | [Next]**AAS 199th meeting, Washington, DC, January 2002**
Session 50. Seyfert Galaxies
Display, Tuesday, January 8, 2002, 9:20am-6:30pm, Exhibit Hall

[Previous] | [Session 50] | [Next]

[50.09] An [OIII] Study of the Narrow Line Regions of Seyfert Galaxies: Testing the Unified Model

J. Donley (Penn State), H. R. Schmitt (NRAO-Socorro)

We present the results of an HST [OIII] study of the narrow line regions (NLRs) of Seyfert galaxies. Our sample consists of Seyfert galaxies selected from nearly isotropic properties, their far-infrared fluxes and warm infrared colors. We discuss the luminosities, projected linear extents, and morphologies of the NLRs of these galaxies as well as the agreement of these properties with the Unified Model. We find that while the Unified Model accurately predicts many of the observed characteristics of the NLRs, certain observed morphologies can not be explained by simple models and require a more careful examination.

This research has been supported by the National Science Foundation, through its Research Experience for Undergraduates program. NRAO is a facility of the National Science Foundation, operated under

cooperative agreement by Associated Universities, Inc.

[Previous] | [Session 50] | [Next]**AAS 199th meeting, Washington, DC, January 2002**
Session 100. Galaxy Clusters and Mergers
Display, Wednesday, January 9, 2002, 9:20am-6:30pm, Exhibit Hall

[Previous] | [Session 100] | [Next]

[100.03] Faraday Rotation Measure Study of Cluster Magnetic Fields

M.M. Frankel (Wellesley College), T.E. Clarke (NRAO)

Magnetic fields are thought to play an important role in galaxy cluster evolution. To this end in this study, we looked at polarized radio sources viewed at small impact parameters to the cores of non-cooling flow clusters. By looking at non-cooling flow clusters we hoped to establish what magnetic fields of clusters look like in the absence of the compressed central magnetic fields of the cooling-flow cores. Clarke, Kronberg and Boehringer (2001) examined Faraday rotation measures of radio probes at relatively large impact parameters to the cores of galaxy clusters. The current study is an extension of the Clarke et al. analysis to probe the magnetic fields in the cores of galaxy clusters. We looked at the Faraday rotation of electromagnetic waves from background or imbedded radio galaxies, which were observed with the VLA in A&B arrays. Our results are consistent with previous findings and exhibit a trend towards higher rotation measures and in turn higher magnetic fields at small impact parameters to cluster cores. This research was made possible through funding from the National Science Foundation.

[Previous] | [Session 100] | [Next]**AAS 199th meeting, Washington, DC, January 2002**
Session 134. Formation of Massive Stars
Display, Thursday, January 10, 2002, 9:20am-4:00pm, Exhibit Hall

[Previous] | [Session 134] | [Next]

[134.17] The proper motions of SiO masers around the high-mass protostar, Source I, in Orion

M.W. Kunz (Dept. of Astronomy, University of Virginia), C.J. Chandler (NRAO, Socorro), L.J. Greenhill (Harvard-Smithsonian CfA)

The BN/KL region of Orion is the nearest region of on-going massive star formation, providing the highest possible spatial resolution. In particular, Source I (the radio counterpart to IRc2) is believed to be the origin of most of the far-infrared luminosity from the region, and drives both an equatorial

low-velocity outflow and a conical high-velocity flow. SiO masers trace the outflows within 150 AU of the embedded protostar. We have recently begun a monthly monitoring program of these masers using the Very Long Baseline Array (VLBA) of the National Radio Astronomy Observatory, in order to follow the dynamics of the outflows, and to search for evidence of angular momentum transfer to the circumstellar material during mass-loss. We will present a movie of the first 3 months worth of data, and a preliminary analysis of the outflow dynamics.

This research was supported by NSF grants towards the NRAO REU program.

[Previous] | [Session 134] | [Next]**AAS 199th meeting, Washington, DC, January 2002**
Session 9. Space Interferometry and Planet Finders
Display, Monday, January 7, 2002, 9:20am-6:30pm, Exhibit Hall

[Previous] | [Session 9] | [Next]

[9.03] Choosing Candidate Stars for the Terrestrial Planet Finder Mission

J.T. Rupert (NRAO/University of Oklahoma), R.S. Simon (NRAO)

Recently, within the scientific community, there has been an increase of enthusiasm in looking for earth-like planets outside our solar system. One mission that will look for stellar systems containing these objects is the Terrestrial Planet Finder (TPF), a space based interferometer. With TPF, it is necessary to have a focused and well thought out list of candidate stars in order to decrease the amount of time spent looking at undesirable systems. Our project was to create a catalogue of stars that satisfy the constraints TPF will be working under. We began with a complete sample of stars out to 7th magnitude in addition to all stars within 20 parsecs and up to 10th magnitude. We then applied selection criteria to narrow the list to the few hundred most promising candidates. In addition to needed calibrations for some desired quantities, a careful analysis of previous work was required to obtain the parameters necessary to complete the project. To assure the candidate stars were indeed of interest, the project incorporated an intense literature search to obtain accurate information about each candidate star (including binarity, variability, and main sequence lifetime). Once completed, the data will then be placed in catalogue form as a list of the few hundred best candidates that can be used when TPF begins.

We would like to thank the National Science Foundation, National Radio Astronomy Observatory, and the University of Oklahoma for their support.

[Previous] | [Session 9] | [Next]**AAS 199th meeting, Washington, DC, January 2002**
Session 50. Seyfert Galaxies
Display, Tuesday, January 8, 2002, 9:20am-6:30pm, Exhibit Hall

[Previous] | [Session 50] | [Next]

[50.06] NGC 4151: Radio Morphology on the Sub-Parsec-Scale

D.S. Wong, J.S. Ulvestad, G.B. Taylor (NRAO), J.F. Gallimore (Bucknell Univ.)

The VLBA and phased-VLA were used to image Seyfert galaxy NGC~4151 at wavelengths of 3.6 and 6 cm, achieving resolutions of ~2 and 3 mas (0.16 and 0.24 pc) respectively. This marks the first time that this Seyfert has been imaged at 3.6 cm with VLBI.

At both wavelengths, two components (previously denoted as D and E) were identified. The brightness temperatures (~10^7-10^8 K) we calculated were consistent with non-thermal emission from D and E. There is no evidence for extended emission of a lower brightness temperature that might be associated with a nuclear torus. The spectral indices of the components and their subcomponents reveal no obvious flat-spectrum source, so the question of whether the nucleus is in component D or E remains unanswered. This is the second time that NGC 4151 has been imaged by the VLBA at 6 cm, enabling derivation of a tentative speed limit of \leq 0.07c on the parsec scale motion of component E with respect to component D.

NRAO is a facility of the National Science Foundation operated under cooperative agreement by Associated Universities, Inc. Further support for D. S. Wong was provided by NSERC of Canada.

The author(s) of this abstract have provided an email address for comments about the abstract: dianew@astro.columbia.edu

[Previous] | [Session 50] | [Next]

Summer Research Project Reports

Part 1. Charlottesville, Virginia Students

Research Report Title: Circular Polarization Measurements in a Sample of AGN at 22 GHz
Authors:E. E. Freeland and Matt Lister

Research Report Title: Mass Estimates of Tidal Dwarf Galaxies in N-body Simulations of Interacting Disk Galaxies
Authors:M. Kohring, J. Hibbard and J. Barnes

Research Report Title: A Small Radio Telescope for Charlottesville
Authors:Zachary Manganello, Lynn Matthews and John Effland

Research Report Title: Choosing Candidate Stars for the Terrestrial Planet Finder Mission
Authors:Juliette Rupert and R. Simon

Research Report Title: Radio Engineering
Authors:Tim Thacker and John Effland
Part 2. Green Bank, West Virginia Students

Research Report Title: Hydrogen in Ursa Major
Authors:P. Robinson

Research Report Title: The Second Plane Survey and Transient Sources
Authors:T. Freismuth

Research Report Title: Accurate Control of the GBT
Authors:Michael Wallace

Research Report Title: Reduction of 21cm HI Galactic Plane Survey
Authors:M. K. Williams
Part 3. Socorro, New Mexico Students

Research Report Title: The CLASS Project

Authors:J. Adelstein and S. T. Myers

Research Report Title: Radio Limits on the Proposed Supernova in NGC7592
Authors:James M. Anderson and James S. Ulvestad

Research Report Title: Discussion on the Interpretations of 12.2 GHz Methanol Masers
Authors:A. C. Boley, M. J. Claussen and A. J. Beasley

Research Report Title: Phase-Referenced VLBA Observations of OH Masers at 4765 MHz
Authors:K. E. Devine, W. M. Goss and P. Palmer

Research Report Title: An [OIII] Study of the NLRs of Seyfert Galaxies: Testing the Unified Model
Authors:J. Donley and H. R. Schmitt

Research Report Title: Using Deep, Multi-band Imaging to Probe High z Radio Galaxies
Authors:M. S. Fine and F. N. Owen

Research Report Title: Faraday Rotation Measures of Intracluster Magnetic Fields
Authors:M. Frankel

Research Report Title: Outflow 25-150 AU from a 10^5 L_{sun} YSO: A Second Generation SiO Maser Proper Motion Study
Authors:Matthew W. Kunz

Research Report Title: VLBA Imaging of the Microquasar GRS1915+105
Authors:B. Moorthy

Research Report Title: Properties of Faint Radio Galaxies
Authors:Cristina Murray-Krezan

Research Report Title: The Molecular Outflow and 3mm Continuum Emission in W75N
Authors:Daniel Stark

Research Report Title: An Age-ordered Sequence of Merger Galaxies
Authors:S. Teng

Research Report Title: NGC4151: Radio Morphology on the Sub-parsec Scale

Authors:Diane Wong
Part 4. Tucson, Arizona Students

Research Report Title: Molecular Outflow Properties
Authors:S. Flynn

Research Report Title: ALMA Amplitude Calibration System
Authors:D. Raymondson

Research Report Title: The ALMA Nutator Control System
Authors:R. Rosengard

Research Report Title: The ALMA Site
Authors:V. Valentine

2001 Summer Research Symposium

Program

(Charlottesville)

31 July 2001

12:15 pm

"Student Engineering at the CDL"

Tim Thacker

NRAO and Virginia Tech

"Circular Polarization Imaging of Active Galactic Nuclei at 22 GHz"

Emily Freeland

NRAO and Indiana University

"Assembling and Testing the SRT (and other things I did this summer)"

Zach Manganello

NRAO and Middlebury College

"Identifying Promising Target Stars for the Terrestrial Planet Finder Mission"

Julie Rupert

NRAO and University of Oklahoma

Summer Research Project Reports

Part 4. Tucson, Arizona Students

Summer Research Project Reports

Part 4. Tucson, Arizona Students

REU Program
NRAO, Vol. Charlottesville, Va, 2001
Summer 2001

Circular Polarization Measurements in a Sample of AGN at 22GHz

Emily E. Freeland

Indiana University

1. Introduction

Circular polarization measurements, while observationally challenging, can help us to gain important knowledge about the source. Along with the linear polarization information, circular polarization can help to constrain the magnetic field geometry, and probe the partcle energy distribution. We can gain information about the composition of the relativistic jets in AGN from their circular polarization spectra.

Active Galactic Nuclei (AGN) represent three percent of all known galaxies. They are among the most energetic objects in the universe, and are seen to produce much more energy that that of all the stars contained in the galaxy. Powered by accretion onto a central, massive black hole, they have relativistic jets which exhibit superluminal motion.

2. Observations and Analysis

The data consist of a sample of thirteen AGN taken in January 1999 at 22GHz with the VLBA (Very Large Baseline Array). The VLBA has circularly polarized feeds, right (R) and left (L) at each antenna. Without instrumental effects, the parallel hands are $RR = I + V$ and $LL = I - V$ where I and V are the total and circularly polarized flux densities, respectively. To measure circular polarization we must take the difference between two large quantities, RR and LL. This process is sensitive to gain errors.

Initially the data were used to look for linear polarization in strong and weakly optically polarized quasars. The sample consists of bright, flat-spectrum sources including well known blazars, 3C279 and 3C273. We have recalibrated the data, paying close attention to the relative calibration of the left and right complex antenna gains, to look for a circular polarization signal. There are 12 hours total at 22 GHz. The sources were cycled through in order to give good uv coverage.

We used the AIPS processing software for our data calibration. Our first step was the a-priori amplitude calibration using the system temperatures recorded at the telescopes during the time the data were taken. We used AIPS task, FRING, to do our fringe fitting to correct for atmospheric and instrumental phase variations. We corrected for polarization feed leakage. This leakage induces errors in the RR and LL data that mimic a circular polarization signal; these errors are not removed by self-calibration. We corrected the absolute position of the electric vectors on the sky, using the previously determined position angle from the jet of 3C279. Difmap was used for imaging and self-calibration to obtain total I models for each source. Later it was used to image in V also. Self-calibration was done in AIPS to solve for antenna amplitudes and phases with no assumption of circular polarization, i.e. $(RR + LL)/2 = I_{mod}$.

3. Results and Discussion

The detection and measurement of circular polarization has been an observational challenge for many years. The amount of circular polarization in a source is often on the order of one percent of the total intensity. This leaves the measurements sensitive to calibration errors.

There are two primary mechanisms involved in the production of circular polarization. The first, often called intrinsic circular polarization, is a component of synchotron emission. This is produced directly by radiating particles. We define $m_c = V/I$ to be the fractional circular polarization.

For intrinsic circular polarization,

$$m_c \propto \nu^{-1/2}$$

This dependency results in a rather flat circular polarization spectrum, if the main mechanism is intrinsic circular polarization in the source.

The second mechanism is Faraday conversion of linear to circular polarization.

In this case,

$$m_c \propto \nu^{-1} \quad \text{to} \quad \nu^{-5}$$

Faraday conversion is a propagation effect, dominated by lower energy relativistic particles in the jet. It converts Stokes U to V and vice versa. If Faraday conversion is the dominant production mechanism for circular polarization then this requires that the electron energy spectrum extend to low energies. This favors an e^- - e^+ jet because of the amount of energy that a $p - e^-$ would carry away. The energy carried away by the jet cannot exceed the total observed energy dissipation; this dissipated energy is energy stored in radio lobes in magnetic fields and relativistic particles and work done against the surrounding environment.

We detected an appreciable level of circular polarization from sources 3C279 and 3C273. In 3C279, the observed circular polarization on the core is 94 mJy, corresponding to 0.41% local fractional circular polarization. In 3C273, the observed circular polarization on the core is -230 mJy, corresponding to 0.8% local fractional circular polarization. It is important to note that 3C273 and 3C279 are located in the same region of sky and are detected here with differing signs on the circular polarization. This indicates that the signal is unlikely to be caused by anything instrumental.

Both of these sources have been examined at lower frequencies. The circular polarization detections here have the same sign (relative to individual sources) as those presented in previous papers. Homan, Attridge and Wardle (2001), present evidence that this sign consistency may persist for decades. This suggests a stable, persistent property in the jets, such as the polarity of a net magnetic flux, that sets the preferred sign of the circular polarization.

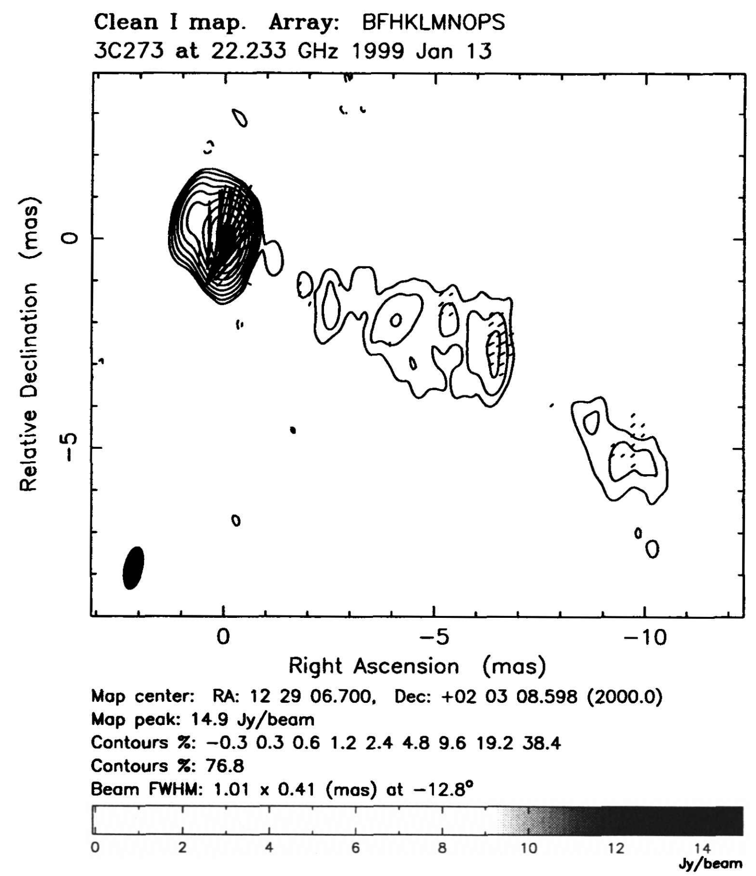

Figure 1. Uniformly weighted total intensity image of 3C273. Linear polarization electric vectors are superimposed

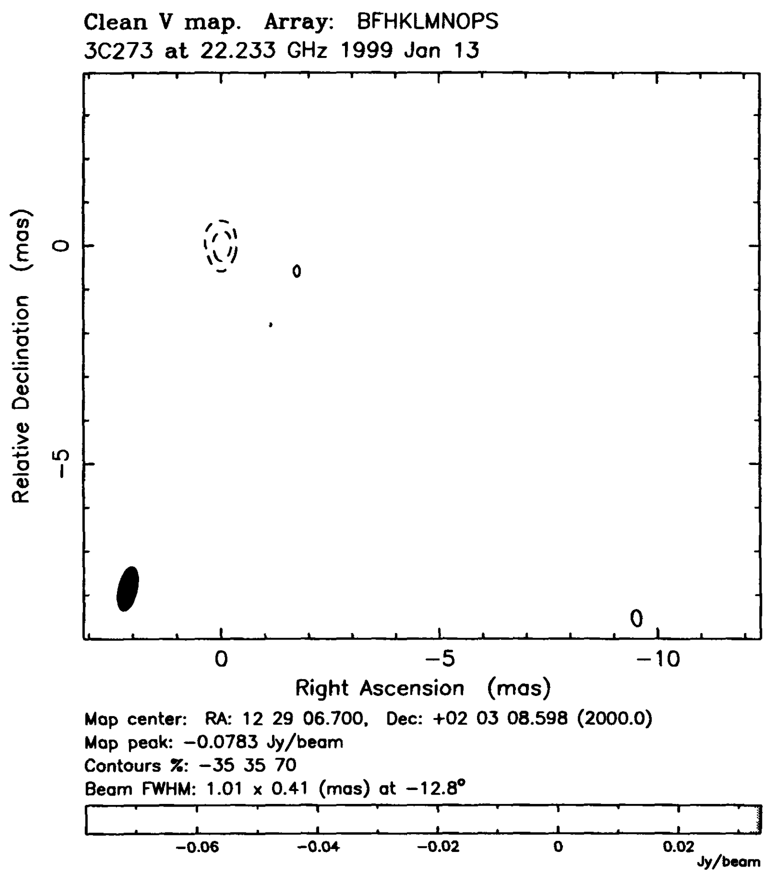

Figure 2. Uniformly weighted circular polarization intensity image of 3C273.

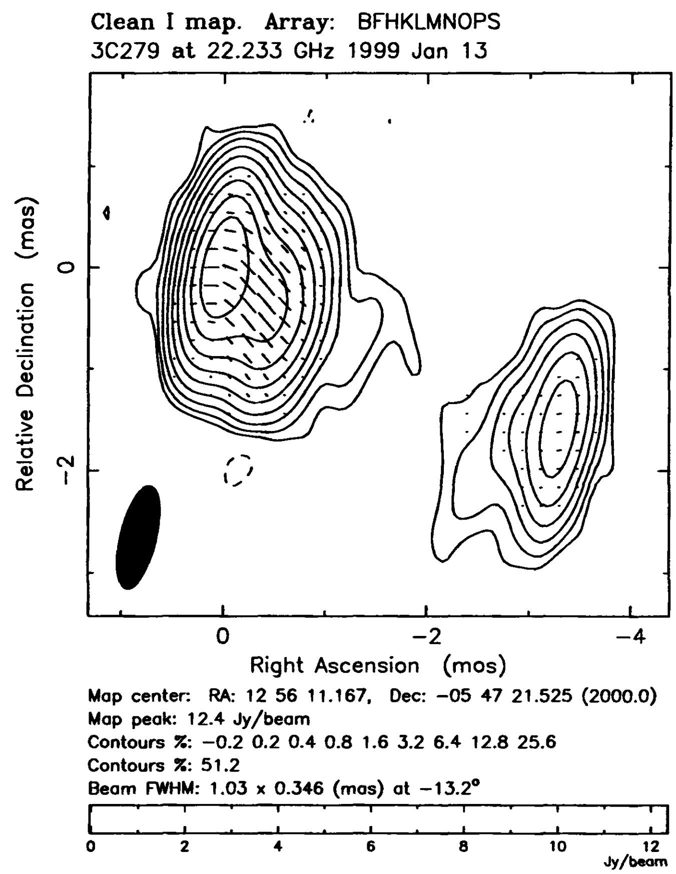

Figure 3. Uniformly weighted total intensity image of 3C279. Linear polarization electric vectors are superimposed.

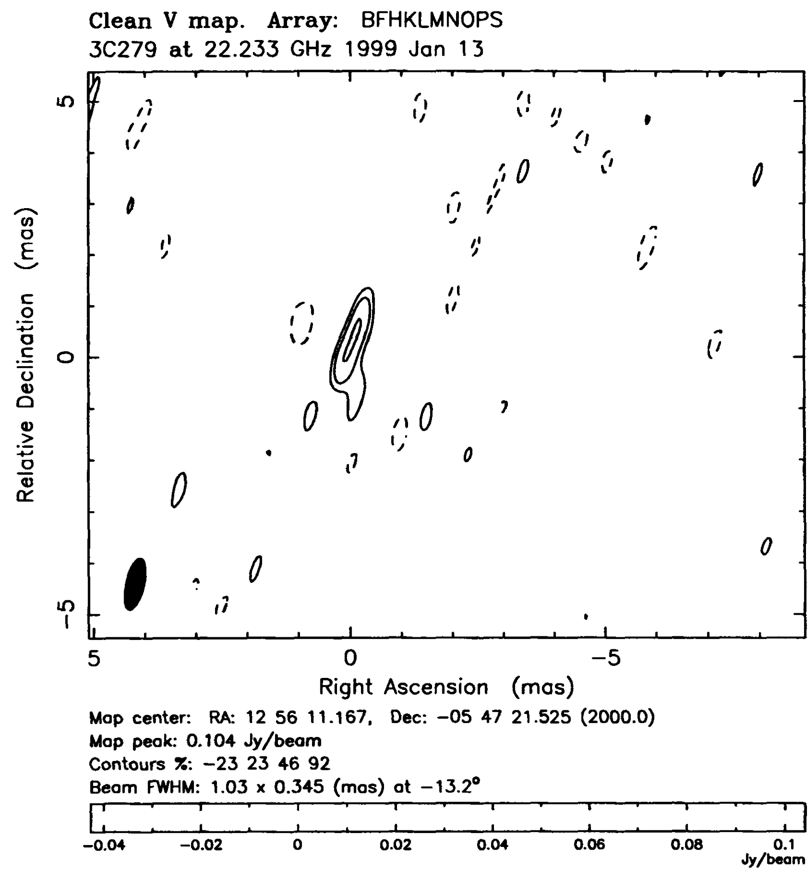

Figure 4. Uniformly weighted circular polarization intensity image of 3C279.

4. Conclusions and Future Work

The signs on our circular polarization measurements are consistent with previous measurements at lower frequencies. Once a detailed error and image noise analysis is done we will be able to compare our levels of detection with previously published levels at other frequencies and look at the circular polarization spectrum. Using this spectrum we will be able to draw conclusions regarding the composition of the AGN jets. Data of these 13 AGN at 43 GHz remains to be examined and will add to the knowledge of the circular polarization spectrum.

References

Homan Attridge, Wardle, ApJ 2001.
Homan & Wardle, 1999 AJ, 118, 1942.

MASS ESTIMATES OF TIDAL DWARF GALAXIES IN N-BODY SIMULATIONS OF INTERACTING DISK GALAXIES

Megan Kohring, University of Virginia

John Hibbard, National Radio Astronomy Observatory

Josh Barnes, Institute for Astronomy

ABSTRACT

Theoretical work (Barnes & Hernquist, 1992) suggests that dwarf galaxies may form within the tidal tails of interacting disk galaxies. Recent observational work purports to identify several so-called "Tidal Dwarf Galaxies" (TDGs) within tidal debris. However, the observational evidence that these TDGs are distinct, dynamical entities is circumstantial or non-existent. N-body simulations of colliding disk galaxies were run and gravitationally bound clumps were identified in the tidal tails. The N-body results were converted to simulated observations (moment maps) and "observable" quantities such as half-light radius, surface brightness and velocity dispersion were extracted from the clumps. From these, the "observed" mass (M_{obs}) and mass-to-light ratio $(M/L)_{obs}$ can be determined, and compared to the true mass (M_{true}) and true mass-to-light ratio $(M/L)_{true}$ of the clumps. We find that the locations of bound clumps in tidal tails often do not correspond to projected density peaks in the moment maps, so simulated observations do not recover the true properties of these regions.

N-BODY SIMULATIONS

Josh Barnes' Zeno software is a self-consistent N-body simulation package available for download at www.ifa.hawaii.edu/~barnes/treecode/treeguide.html Zeno simulates encounters of equal-mass disk galaxies using standard bulge-disk-halo models (for details, see Barnes, J.E. 1992). We ran two simulations with the parameters shown in Table 1.

N	N_{bulge}	N_{disk}	N_{halo}	N_{tot}	M_{bulge}	M_{disk}	M_{halo}	M_{tot}
139264	4096	49152	16384	69632	0.0625	0.1875	1.00	1.25
69632	2048	24576	8192	34816	0.0625	0.1875	1.00	1.25

Table 1. Parameters of galaxy models used in N-body simulations. N is the total number of particles in the simulation; N_{bulge}, N_{disk}, and N_{halo} are the number of particles in each bulge, disk and halo, respectively; N_{tot} is the total number of particles in each galaxy; M_{bulge}, M_{disk}, and M_{halo} are the masses of the bulge, disk and halo, respectively; and M_{tot} is the total mass of each galaxy.

GRIDDING THE DATA AND CALCULATING MOMENT MAPS

In order to turn our N-body data into simulated observations, we grid the data in the x-, y-, and vz-dimensions and compute moment maps using IDL. If i,j, and k represent the indices of the x-, y-, and vz-dimensions, respectively, N_{ijk} is the number of particles in pixel i,j,k of the grid, and V_k is the velocity of the k^{th} channel, then we can calculate moment maps using the following formulae:

$$mom0 = N_{ij} = \sum_k N_{ijk}$$

$$mom1 = V_{ij} = \frac{1}{N_{ij}} \sum_k N_{ijk} V_k$$

$$mom2 = \sigma_{ij} = \sqrt{\frac{1}{N_{ij}} \sum_k (V_k - V_{ij})^2}$$

Mom0 is an integrated "intensity", or the number of particles in each pixel of the grid. Mom1 is an intensity-weighted velocity, and mom2 is an intensity-weighted velocity dispersion. In Figure 1 we show a comparison between the N-body data of our N=139264 simulation and the corresponding mom0 map, and in Figure 2 we show the mom0,1,2 maps for our N=69632 simulation.

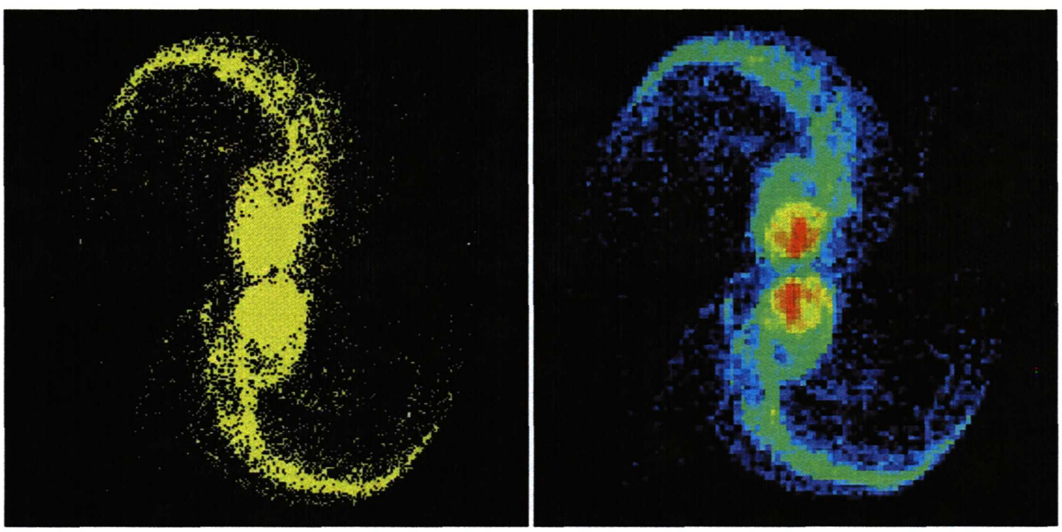

N-body Data **Moment 0 Map**

Figure 1. N-body data and corresponding mom0 map for N=139264 model

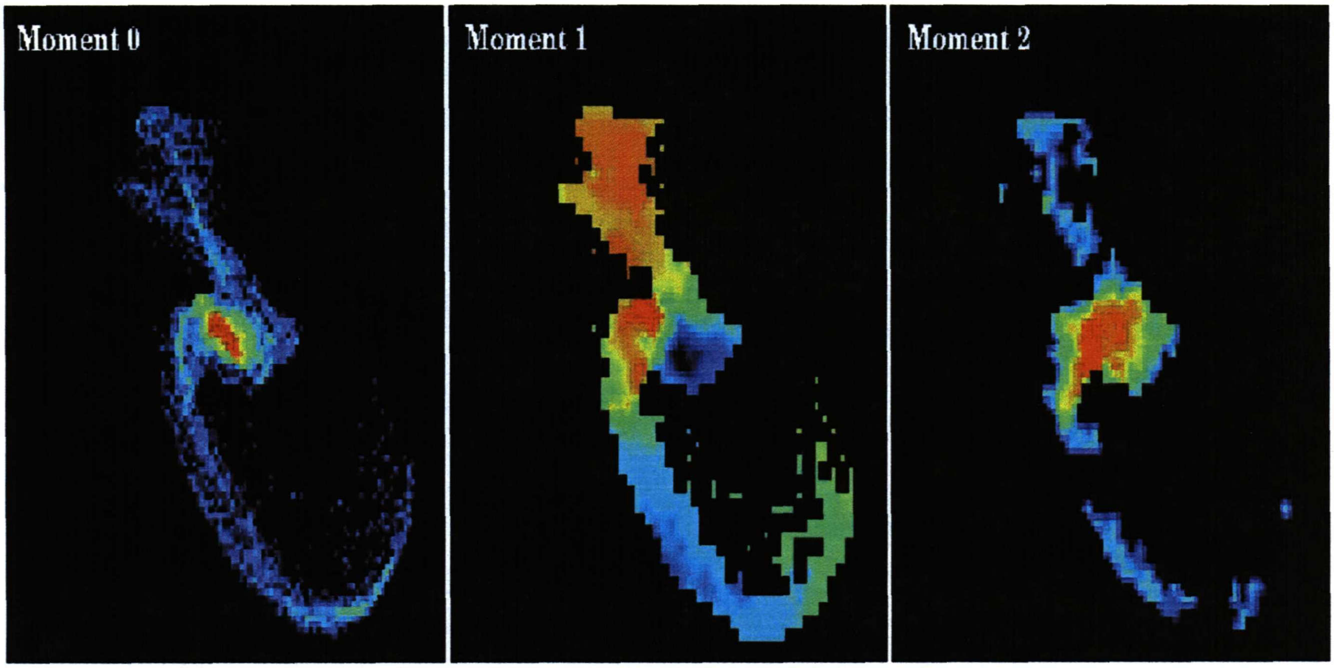

Figure 1. Mom012 maps for N=69632 model

IDENTIFYING GRAVITATIONALLY BOUND REGIONS

Barnes' dwarf-finding procedure in Zeno utilizes a friends-of-friends algorithm which identifies bound regions in the tidal tails. We only consider 'virialized' regions with $T/U < -0.4$, where T is kinetic energy and U is potential energy. The result of the dwarf-finding procedure is shown in Table 2.

Clump #	N	Mass	-T/U	x	y	z	R_m/R_t
1	17	2.8×10^7	0.422	2.698	-3.922	-0.284	0.360
2	23	3.9×10^7	0.400	2.278	-3.935	-0.731	0.868
3	13	2.2×10^7	0.563	2.380	-3.932	-0.611	1.166
4	24	4.0×10^7	0.527	2.939	-3.843	-0.018	0.839
5	12	2.0×10^7	0.412	2.812	-3.880	-0.173	0.399
6	12	2.0×10^7	0.429	-1.023	2.445	2.098	1.521
7	25	4.2×10^7	0.490	0.568	-3.080	-1.801	1.495
8	53	8.9×10^7	0.517	1.716	-4.011	-1.182	1.081
9	37	6.2×10^7	0.570	1.981	-4.018	-0.962	1.039
10	17	2.9×10^7	0.595	3.052	-3.713	0.120	0.875
11	38	6.4×10^7	0.440	3.406	-3.331	0.547	0.936

Table 2. Characteristics of 11 clumps found by Zeno. *N* is the number of particles in each clump; *Mass* is the mass of the clump for a Milky Way progenitor in solar units; *x*, *y*, and *z* are the coordinates of each clump; R_m/R_t is the mean radius divided by the tidal radius; if $R_m/R_t < 1$, the dwarf is expected to lose mass to the parent body as it orbits.

The locations of these 11 clumps are plotted on the mom0 map for our N=69632 simulation in Figure 3 for 4 different viewing angles, corresponding to rotations about the x- and y-axes, respectively (top, l-r). Also shown is a close-up contour map of the southern tidal tail at each viewing angle (bottom, l-r).

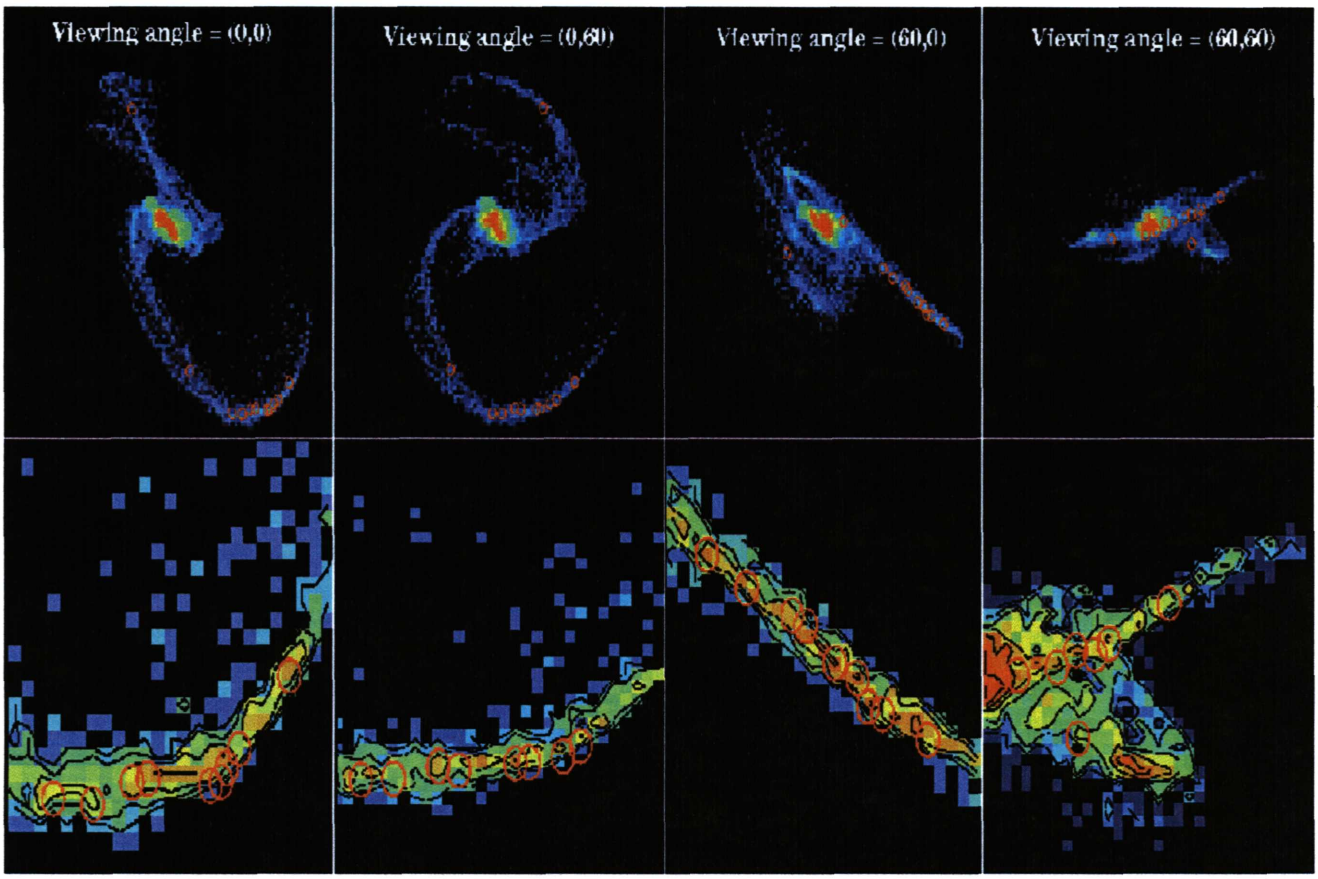

Figure 3. 11 clumps identified by Zeno dwarf-finding algorithm.

OBSERVATIONALLY DERIVED MASS ESTIMATES

From the virial theorem we can derive the virial mass of a bound object in a tidal· tail:

$$M_{vir} = 3\sigma^2 a r_{1/2} G^{-1}$$

where G is the Gravitational constant, â is the 1-dimensional velocity dispersion given by mom2 at the location of a bound region, *a* is a geometric factor (for a uniform density sphere, *a*=2.74), and $r_{1/2}$ is the half-light radius, obtained from fitting a Gaussian profile to the location of the clump in the mom0 map.

(Binney & Tremaine, 1987)

The observed mass-to-light ratio $(M/L)_{obs}$ of the clump is given by:

$$\left(\frac{M}{L}\right)_{obs} = \frac{9}{2\pi G}\frac{\sigma^2}{r_{1/2} I_0}$$

where G, â, and $r_{1/2}$ are the same as above and I_0 is the central surface brightness of the clump. (Richstone & Tremaine, 1986)

NOTE: we fit Gaussians to the known locations of bound regions regardless of whether there is a density peak in the mom0 map or not; this is different from how observers identify TDG candidates.

RESULTS & CONCLUSIONS

We find that the locations of some bound clumps in tidal tails do not correspond to density peaks in the mom0 maps so a Gaussian fit is not possible. In the regions that do correspond to density peaks, the estimations of $r_{1/2}$ and I_0 are too large, which leads to an estimate of M_{vir} that is orders of magnitude too large. This is most likely due to tidal material that is projected near the clumps but not bound to them. Thus, the true properties of bound regions are not recovered by simulated observations. Running higher-N simulations may help to resolve the TDGs in the tidal tails.

REFERENCES

Barnes, J.E. 1992, ApJ, 393, 484

Barnes, J.E., & Hernquist, L. 1992, Nature, 360, 715

Binney, J., & Tremaine, S. 1987, "Galactic Dynamics", (Princeton: Princeton University Press).

Richstone, D. and Tremaine, S. 1986, AJ, 92, 72

Zachary Manganello <k1zk@middlebury.edu>
Student of Physics, Middlebury College
NRAO REU Summer 2001 Student
NRAO Advisors: Lynn Matthews & John Effland
August 14, 2001

END OF SUMMER REPORT

1.1) INTRODUCTION

My work with the National Radio Astronomy Observatory (NRAO) this summer was twofold: I assembled and tested a Small Radio Telescope (SRT), and I worked with the engineers at the Central Development Laboratory on constructing an SIS mixer test rack. This report outlines my experiences and results.

1.2) THE CENTRAL DEVELOPMENT LAB (CDL)

While I was not busy with the Small Radio Telescope, I was working at the CDL. Some of my projects included soldering components to circuit boards, locating parts and taking inventories, building semi-rigid coaxial cables with SMA connectors to be used in the JT-1 dewar, building power cables for the JT-1 bias supply, building mixer bias supply boxes, and writing reports. For me this was an excellent introduction to the world of engineering.

1.3) THE SMALL RADIO TELESCOPE (SRT)

The Haystack Observatory has developed the Small Radio Telescope (SRT), which is capable of making continuum and spectral line observations at L-band (λ=21cm or ν=1.42GHz). Last summer NRAO REU student Charles Fulton of Ohio University assembled an Alpha version of the SRT. NRAO-CV acquired a Beta version of the SRT kit and assigned me to assemble and test the telescope. Assembly and testing of the SRT is valuable not only as an educational experience for me, but will provide Haystack with information they require for further development and improvement of their product.

2.1) ABOUT THE SRT

The Small Radio Telescope is designed primarily as an educational tool, with the purpose of introducing students to the field of radio astronomy. The SRT is a modified 7-foot satellite television dish mounted on a motorized Azimuth-Elevation mount. The Beta kit included hardware for the dish and the motorized mount, a receiver assembly, control and signal cables, and a Control box. Control software and manuals are available online at http://fourier.haystack.edu/SRT.

The following are the characteristics of the SRT claimed on their web site:

2.2) ANTENNA

Manufacturer:	Kaul-Tronics Inc.
Model Number:	(XI-7)
Diameter:	84" (2.1 m)
F/D Ratio:	0.38
Focal Length:	32" (80.9 cm)
Gain at 4.2 GHZ:	40.3 dBi
Weight with Mount:	160 lbs.
Beam Width:	7.0 degrees (L-band)

2.3) MOUNT

Manufacturer:	Kaul-Tronics Inc
Model Number:	Pro-Form H-180 Polar Mounts
Operating Voltage:	20-36 V DC
Operating Current:	2.5 A
Speed:	150 degrees in 70 to 80 seconds

2.4) RADIOMETER

L.O. Frequency range:	1370-1800 MHz
L.O. Tuning steps:	40 kHz
L.O. Settle time:	<5 ms
Rejection of LSB image:	>20 dB
3 dB bandwidth:	40 kHz
I.F. Center:	40 kHz
6 dB I.F. range	10-70 kHz
Preamp frequency range:	1400-1440 MHz
Typical system temperature:	150 K
Typical L.O. leakage out of preamp:	-105 dBm
Preamp input for dB compression From out of band signals:	-24 dBm
Preamp input for intermodlation Interference:	-30 dBm
Square law detector max.:	4000 K at 0 dB attenuation 40,000 K at 10 dB attenuation
Control:	RS-232 2400 baud

A quick calculation confirms the claimed beam width of the SRT:

Beam Width (radians) = (1.22)*λ / D

Where:

λ = Wavelength

and **D** = diameter of dish

For ν=1.42GHz (λ=0.21127m) and with D=2.1m, Beam Width is about 0.1227 radians or about 7 degrees.

3.1) ASSEMBLY

Physical assembly of the SRT went fairly quickly and smoothly. Mechanical systems functioned well. Some holes were not aligned perfectly, and some bolts didn't fit; these problems were solved by enlarging holes with a drill or substituting slightly smaller bolts. The SRT kit included wire nuts for some splices, which I replaced with solder joints and electrical tape. The motorized mounts, which slide over a mounting pipe, have large bolts to secure them to the mounting pipe. These bolts will probably not be enough to keep the antenna from spinning on the mounting pipe. We drilled a hole through the motor assembly mount and through the mounting pipes and secured both with metal pins.

The dish arrived damaged; a dent was found on one of the four quadrants. The feed included with the kit is a crudely modified C-band feed and is poorly designed for operation at L-band.

It was convenient to assemble the SRT on the ground rather than on its final mount ten feet in the air. We had an adapter piece made at a welding shop so the telescope could be installed on a short mount on the ground. We later used a crane and scaffolding to move the SRT up to its final position. The mounting pole is not included in the SRT kit; it was manufactured by the machine shop at the University of Virginia. The assembled SRT is pictured below in Figure 1, just before it is moved up to its position above the roof (note the scaffolding visible in the background):

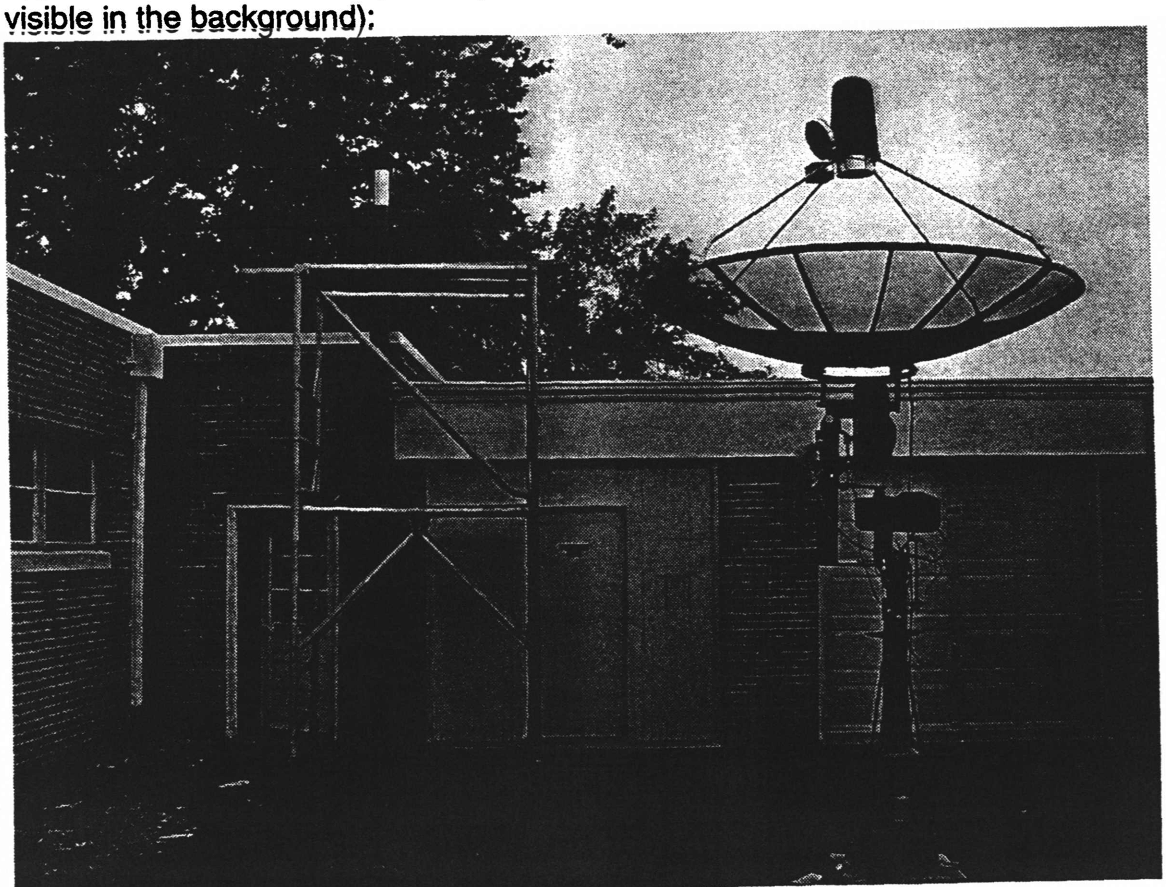

Figure 1: Completed SRT Assembly Ready for Final Installation

The outline for assembly is as follows:

- Assemble Reflector
- Attach Feed Horn to Quad Feed Supports
- Attach Quad Feed Supports to Reflector
- Install Azimuth Drive Assembly
- Attach Adapter Pipe
- Install Elevation Drive Assembly on Adapter Pipe
- Attach Dish to Elevation Drive Assembly
- Fabricate & Install Wiring Harness
- Connect Receiver & LNA
- Focus the Dish
- Install JAVA SRT Control Software
- Make Mount Adjustments and Pointing Corrections

Early on in the assembly process the user is instructed to attach the quad feed supports, but later the user is told to add 3" to the length of the feed supports in order to focus the dish, which requires removing the feed supports. Always read through all of the instructions before beginning any project!

4.1) RECEIVER PERFORMANCE / INSTALLATION

Receiver installation was fairly simple, however there were a few disappointing problems. The SRT receiver has some F-type connectors which carry the 21cm RF. This is unfortunate because this kind of connector is very lossy at such high frequencies. The Low-Noise Amplifier is extremely sensitive to impedance matching.

4.2) THE VANE CALIBRATOR:

The SRT uses an ambient-temperature vane calibrator to obtain a measure of the system noise, background sky, atmosphere, and spillover from the feed. The vane is a circular piece of absorber material attached to a motorized arm that allows the absorber to swing in front of the feed when the "Vane" calibration command is issued. The calibration is the ratio of the power measurement by the receiver with the vane blocking the feed divided by the power measurement by the receiver when the vane is retracted and the signal is received by the sky (this includes contributions from spillover). This ratio is illustrated in the equation below:

$$P_{vane} / P_{sky} = (T_s + T_{vane}) / (T_s + T_{spillover} + T_{sky})$$

Where:

P_{vane} = the power measurement with the vane deployed
P_{sky} = the power measurement with the vane retracted
T_{vane} = the ambient temperature of the vane (FIXED by the software at 300 K)
$T_{spillover}$ = the feed spill-over
T_{sky} = the combined temperature contributions from the sky
And T_s = the system temperature

The minimum signal power that can be distinguished from the random fluctuations in the output of a measuring system caused by noise inherent in the system is the sensitivity of the system. If the system noise has a power, P watts, then the equivalent system temperature or noise temperature can be described by

$$T = P / kB$$

Where:

k = Boltzmann's constant (1.38×10^{-23} w Hz^{-1} K^{-1})
B = the bandwidth
And P = power in watts

The fixed value of 300 K for the noise temperature of the Vane calibrator is assumed by the SRT software. This leads to unacceptable errors in the value for system temperature (T_{sys}) as the actual ambient temperature changes. The electronic noise source calibrator designed by Rodolfo Montez Jr. of the University of Texas at Austin would go a long way in eliminating these errors. An alternative to the electronic noise source is the installation of a thermometer of some sort in the vane itself, and possibly integrating the thermometer's output into the software.

4.2) MINIMUM TEMPERATURE / FLUX

In order to determine which sources the SRT is likely to detect, the minimum detectable temperature must be computed. This is done utilizing the following equations[1]:

$$\Delta T_{min} = (K_s * T_{sys}) / (\Delta v * t * n)^{1/2}$$

and

$$\Delta S_{min} = (2\ k)*(\Delta T_{min}) / A_e$$

Where:

[1] Kraus, John D., Radio Astronomy. Equations (3-121) and (3-123), respectively.

ΔT_{min} is the sensitivity, or minimum detectable temperature (K)
ΔS_{min} is the minimum detectable flux density (J/m^2)
k is Botlzmann's constant (1.38x10^{-23} J/K)
K_s is the sensitivity constant, which is dimensionless and of order unity
T_{sys} is the system temperature (K)
Δv is the predetection bandwidth (Hz)
t is the postdetection integreation time (s)
n is the number of records averaged, which is dimensionless
and A_e is the effective aperture of the antenna (m^2)

A_e is equal to the physical aperture of the antenna in square meters, **A**, multiplied by the aperture efficiency, ε_{ap}, which is dimensionless and ranges from 0 to 1. The SRT is quoted to have an aperture efficiency of 0.5 and a diameter of 2.1 meters.

The aperture of the SRT is then:

$$A = \pi\,(2.1\ /\ 2)^2$$

and hence the effective aperture of the SRT is:

$A_e = \varepsilon_{ap}\,\pi\,(2.1 / 2)^2 = (\pi / 2)\,(2.1 / 2)^2 = (4.41\,\pi) / 8$ or about 1.73 square meters.

Now, given that the SRT has a nosie floor of 282 K, a bandwidth of 40 kHz for each bin, about a 0.5 second integration time, and one record averaged, sensitivity can be computed:

$$\Delta T_{min} = (1)(282\text{ K}) / (40000\text{ s}^{-1} * 0.5\text{ s} * 1)^{1/2} \approx 1.99\text{ K}$$

From the sensitivity the minimum detectable flux density can be computed:

$$\Delta S_{min} = 2 * (1.38\text{x}10^{-23}\text{ J/K})*(1.99\text{ K}) / ((4.41\,\pi) / 8) \approx 7.95\text{x}10^{-24}\text{ J/m}^2$$

5.1) CHARACTERIZATION OF LNA & FILTER

With the help of the Central Development Lab (CDL) of the National Radio Astronomy Observatory (NRAO), I measured the noise temperature of the Low-Noise Amplifier (LNA) on the Small Radio Telescope (SRT) using "Y-factor" measurements.

We employed various techniques for measuring the Y-factor.

- First we ran a crude test which involved simply dipping the load into liquid nitrogen. We used no filtering prior to the power reading, so we were measuring noise temperature averaged over the entire passband. We did not use an isolator, so impedance matching may have been poor, and we did not measure the noise of the stages after the LNA, so we were measuring not the amplifier noise temperature, but the entire receiver noise temperature.

- We used NRAO's calibrated test rack to measure the amplifier noise temperature. One drawback of this system is that its minimum bandwidth is 20 MHz, and since the LNA's passband is only about 100 MHz wide, the measurement does not show as much detail as a narrow-bandwidth system.
- We used a noise diode to generate a known noise level with a spectrum analyzer acting as a filter and a power meter to measure the noise power at the spectrum analyzer's IF output. This technique gives accurate power measurements, but only one frequency at a time.
- Finally, we used the same noise diode to provide the noise level and a spectrum analyzer to filter and measure the noise power. This technique allows us to view trends over a wide frequency range, but power measurements are less accurate.

RESULTS:

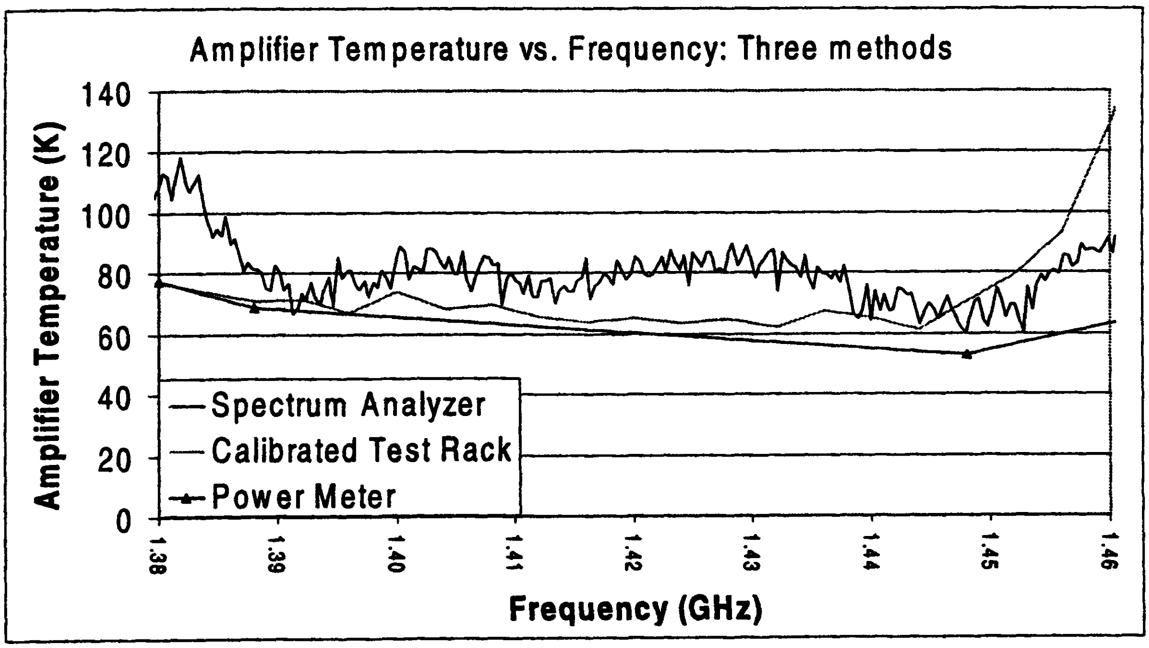

Figure 2: Three Methods for Measuring the Amplifier Temperature

Figure 2 shows our measurements of the receiver noise temperature as a function of frequency. Inside the LNA's passband our different methods are in agreement about the noise temperature of the amplifier, but outside of the passband we found poor agreement. Because it is in the passband of the LNA that operation will take place, we did not attempt to reconcile the out-of-band discrepancies.

The following are averages from each of the data sets collected using various techniques. The average is taken from 1.38 to 1.46 GHz in each applicable case.

Measurement Type	Avg. Receiver Noise Temp.	Avg. Amplifier Noise Temp.
Liquid Nitrogen	128 K	--
NRAO Test Rack	--	73 K
Power Meter	82 K	67 K
Spectrum Analyzer	88 K	80 K

NRAO's test rack and the power meter are the two most accurate methods for measuring noise temperature, and they agree well. The noise temperature of the LNA is about **70 K**.

Reproduced in the appendices at the end of this document are more detailed reports on the characterization of these devices.

Appendix	Subject
A	Gain Measurements
B	Y-Factor Measurements
C	Alignment & System Temperature Measurements

6.1) SRT CONTROL SOFTWARE

The Control software for the SRT is available for download on the SRT web site. This software is written in JAVA. I installed JAVA and a Java Development Kit on a Windows 98 computer and then compiled and installed the SRT software. While the SRT Control software does manage to control the antenna and record data, it is often cumbersome and difficult to use. There is no way to abort commands, there is no integration counter, very little useful documentation, and the 25-point scan produces contour maps that are as mysterious as they are colorful. There is a drawing problem in that if any other window is made active or moved or if the SRT window is moved all previous plots and data points displayed on the screen are not redrawn. What's more, the program is prone to crashing. The SRT control interface is illustrated in Figure 3.

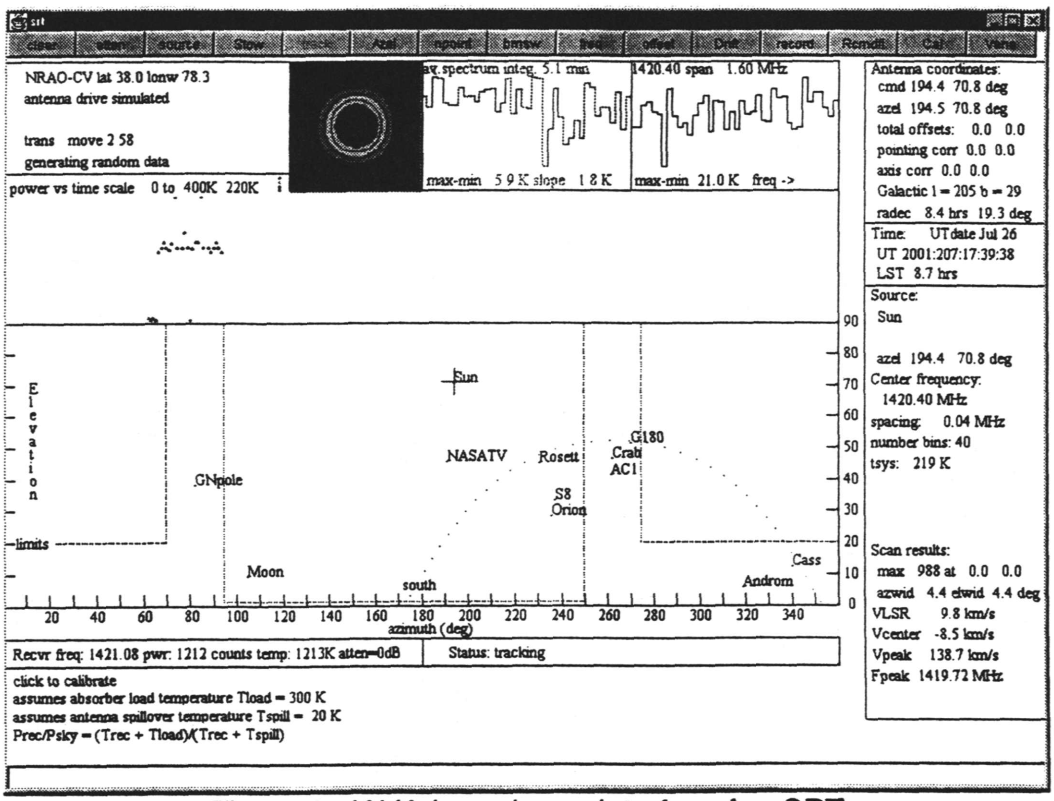

Figure 3: JAVA-based user interface for SRT

It is possible to write observed data to disk in an ascii format. The software saves a set of system temperature measurements to a user-specified or default filename. The file is saved as a .rad file (space delimited), and can be converted for use in a spreadsheet like Excel with some effort. Figure 4 illustrates the format in which the data is written.

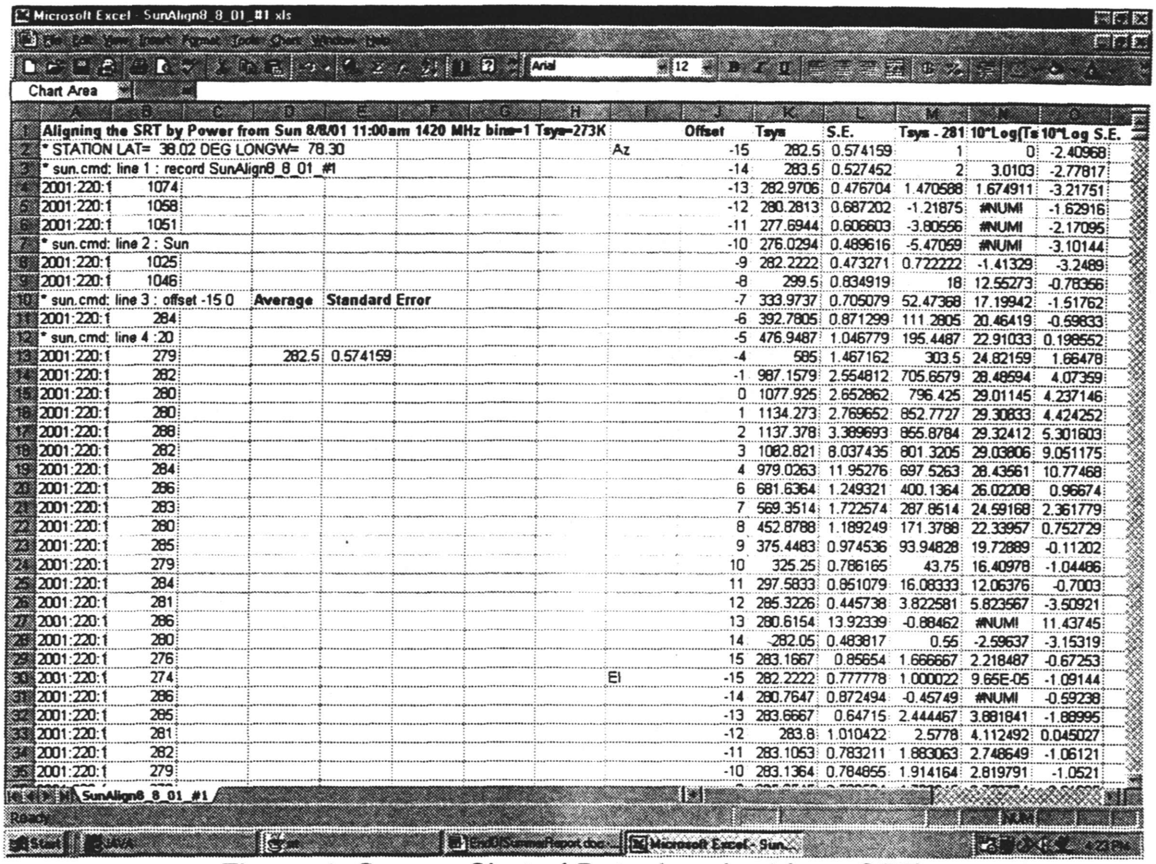

	A	B	D	E	I	J	K	L	M	N	O
1	Aligning the SRT by Power from Sun 8/8/01 11:00am 1420 MHz bins=1 Tsys=273K					Offset	Tsys	S.E.	Tsys - 281	10*Log(Ts	10*Log S.E.
2	* STATION LAT= 38.02 DEG LONGW= 78.30				Az	-15	282.5	0.574159	1	0	-2.40968
3	* sun.cmd: line 1 : record SunAlign8_8_01_#1					-14	283.5	0.527452	2	3.0103	-2.77817
4	2001:220:1	1074				-13	282.9706	0.476704	1.470588	1.674911	-3.21751
5	2001:220:1	1058				-12	280.2813	0.687202	-1.21875	#NUM!	-1.62916
6	2001:220:1	1051				-11	277.6944	0.606603	-3.80556	#NUM!	-2.17095
7	* sun.cmd: line 2 : Sun					-10	276.0294	0.489616	-5.47059	#NUM!	-3.10144
8	2001:220:1	1025				-9	282.2222	0.473271	0.722222	-1.41329	-3.2489
9	2001:220:1	1046				-8	299.5	0.834919	18	12.55273	-0.78356
10	* sun.cmd: line 3 : offset -15 0		Average	Standard Error		-7	333.9737	0.705079	52.47368	17.19942	-1.51762
11	2001:220:1	284				-6	392.7805	0.871299	111.2805	20.46419	-0.59833
12	* sun.cmd: line 4 :20					-5	476.9487	1.046779	195.4487	22.91033	0.198552
13	2001:220:1	279	282.5	0.574159		-4	585	1.467162	303.5	24.82159	1.66478
14	2001:220:1	282				-1	987.1579	2.554812	705.6579	28.48594	4.07359
15	2001:220:1	280				0	1077.925	2.652862	796.425	29.01145	4.237146
16	2001:220:1	280				1	1134.273	2.769652	852.7727	29.30833	4.424252
17	2001:220:1	288				2	1137.378	3.389693	855.8784	29.32412	5.301603
18	2001:220:1	282				3	1082.821	8.037435	801.3205	29.03806	9.051175
19	2001:220:1	284				4	979.0263	11.95276	697.5263	28.43561	10.77468
20	2001:220:1	286				6	681.6364	1.249321	400.1364	26.02208	0.96674
21	2001:220:1	283				7	569.3514	1.722574	287.8514	24.59168	2.361779
22	2001:220:1	280				8	452.8788	1.189249	171.3788	22.33957	0.752729
23	2001:220:1	285				9	375.4483	0.974536	93.94828	19.72889	-0.11202
24	2001:220:1	279				10	325.25	0.786165	43.75	16.40978	-1.04486
25	2001:220:1	284				11	297.5833	0.851079	16.08333	12.06376	-0.7003
26	2001:220:1	281				12	285.3226	0.445738	3.822581	5.823567	-3.50921
27	2001:220:1	286				13	280.6154	13.92339	-0.88462	#NUM!	11.43745
28	2001:220:1	280				14	282.05	0.483817	0.55	-2.59637	-3.15319
29	2001:220:1	276				15	283.1667	0.85654	1.666667	2.218487	-0.67253
30	2001:220:1	274			El	-15	282.2222	0.777778	1.000022	9.65E-05	-1.09144
31	2001:220:1	286				-14	280.7647	0.872494	-0.45749	#NUM!	-0.59238
32	2001:220:1	285				-13	283.6667	0.64715	2.444467	3.881841	-1.88995
33	2001:220:1	281				-12	283.8	1.010422	2.5778	4.112492	0.045027
34	2001:220:1	282				-11	283.1053	0.783211	1.883063	2.748649	-1.06121
35	2001:220:1	279				-10	283.1364	0.784855	1.914164	2.819791	-1.0521

Figure 4: Screen-Shot of Data Acquired from SRT.

The two columns on the left in Figure 4 are what the SRT actually writes, whereas all the other data is processing that must be done by the user. The data the SRT records are: time stamp, antenna position, offsets, and system temperature. The SRT also prints the station latitude and longitude as well as the commands that it executed.

Data from the SRT always appears as values for System Temperature (in Kelvin). These data can be written to file, as described above, but also appears on a power-vs.-time plot as well as on spectral plots in the User Interface. The software is also capable of combining data from a 25-point grid of measurements in order to generate a false-color contour plot of the observed object. This contour plot cannot be exported in any fashion, and our solution was to use the "Print Screen" command and then paste the picture in to some graphics program like Microsoft Paint. No quantitave analysis is possible from the contour plots and no intensity scale is provided by the software.

7.1) CONCLUSION

Assembly and testing of the SRT took most of my ten weeks as an REU student with NRAO. During the time I was not busy with the SRT, I worked at the

CDL on various small projects related to the construction of the JT-1 test rack. The lessons learned and the data collected from the assembly of the SRT have been sent to Haystack, and the completed SRT is installed at the Astronomy Night Lab on the grounds of the University of Virginia for future use by students. Near the end of my tenure with NRAO I gave a 15-minute talk to NRAO employees and UVA students and staff outlining my work this summer.

Respectfully Submitted,
August 14, 2001

Zachary M. Manganello

Appendix A

Small Radio Telescope Gain Measurements

The Small Radio Telescope (SRT) is designed to take continuum and spectral line observations at L-band (1.42 GHz). Because the Bandpass Filter comes before the low noise amplifier (LNA), its gain characteristics are extremely important. **Figure A1** roughly outlines the signal flow from the antenna to the receiver. With the help of the CDL of NRAO-CV, I measured the gain characteristics of both the Bandpass Filter and the LNA on June 20, 2001. Measurements were taken with an HP8722D 50MHz-40GHz Network Analyzer.

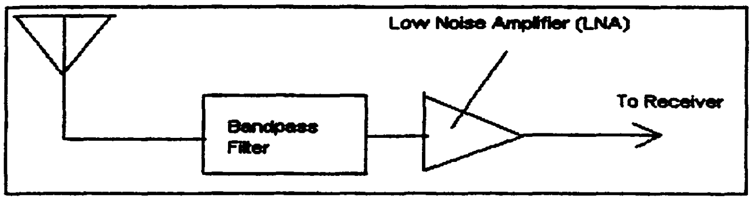

Figure A1

We analyzed the bandpass filter alone, the LNA alone, and the LNA and the filter together as they would be connected once mounted on the radio telescope. For each of these configurations, we took two sets of measurements: wide spectrum (0.5-3.0 GHz) and narrow spectrum (1.35-1.50 GHz). The wide spectrum allows us to see the response of the devices outside of their operating band so we can anticipate possible intermodulation or receiver saturation problems, while the narrow spectrum allows us to see the detailed response of the devices in their operating range.

Figure A2 is the wide spectrum gain measurement of the bandpass filter alone plotted as gain vs. frequency. Two hundred (200) data points were taken.

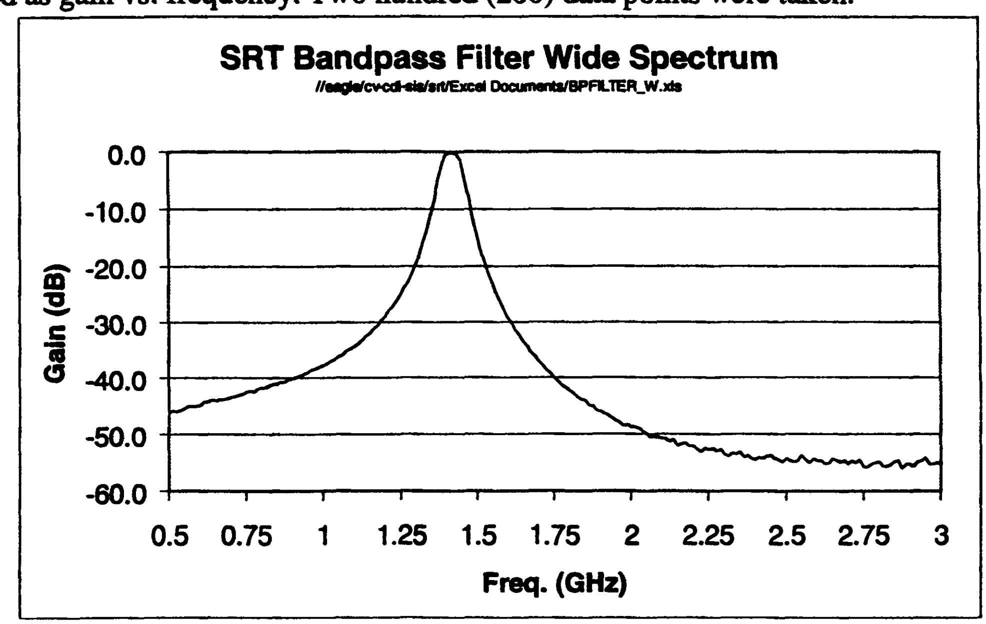

Figure A2

//eagle/cv-cdl-sis/srt/Documents/Small Radio Telescope Gain Measurements.doc

Figure A3 is the narrow spectrum gain measurement of the bandpass filter alone plotted as gain vs. frequency. Two hundred (200) data points were taken.

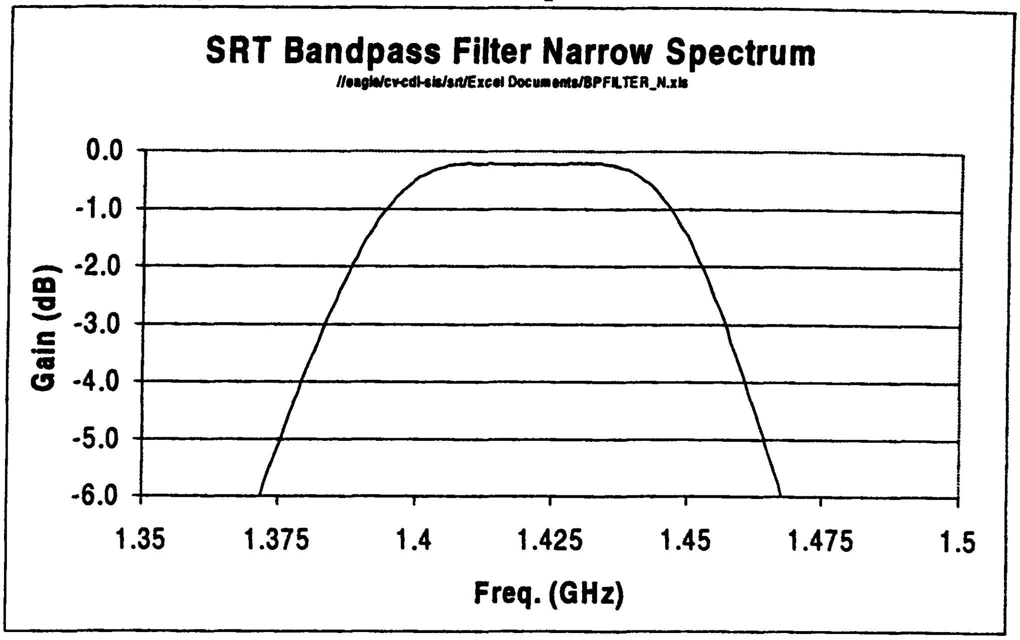

Figure A3

The 3 dB passband is about 73 MHz wide.

Figure A4 is the wide spectrum gain measurement of the LNA alone plotted as gain vs. frequency. Eight hundred (800) data points were taken.

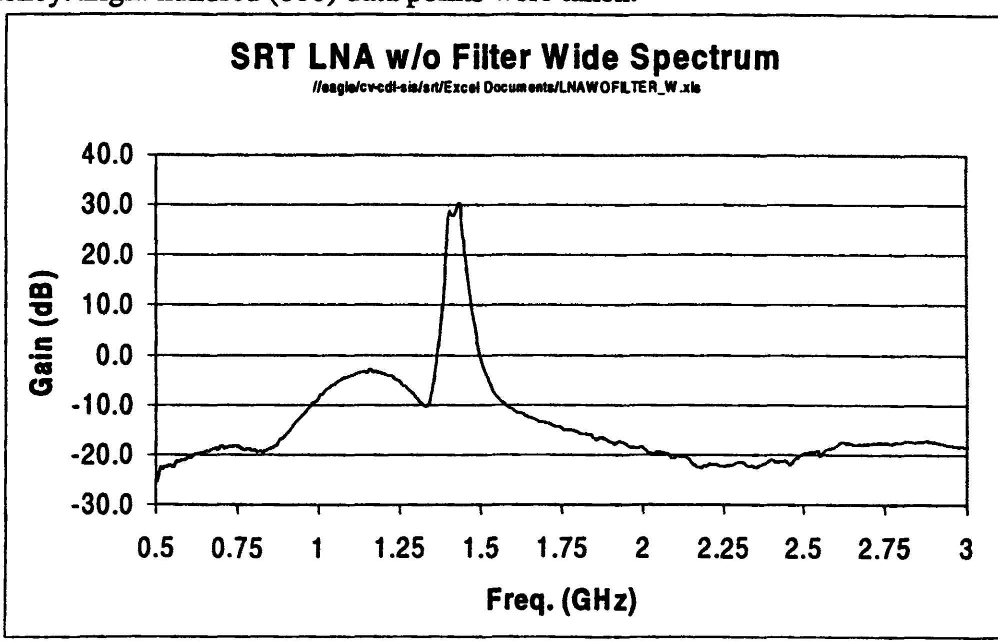

Figure A4

Note that the LNA has a secondary region of gain between about 1.0 and 1.3 GHz.

Figure A5 is the narrow spectrum gain measurement of the LNA alone plotted as gain vs. frequency. Eight hundred (800) data points were taken.

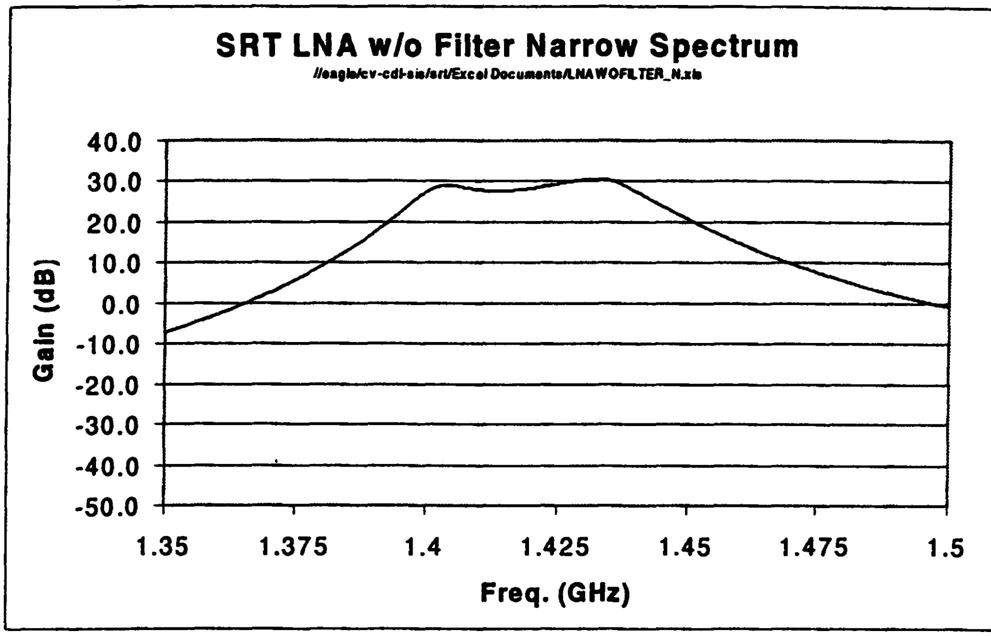

Figure A5

Figure A6 is the wide spectrum gain measurement of the LNA and the bandpass filter together plotted as gain vs. frequency. Eight hundred (800) data points were taken.

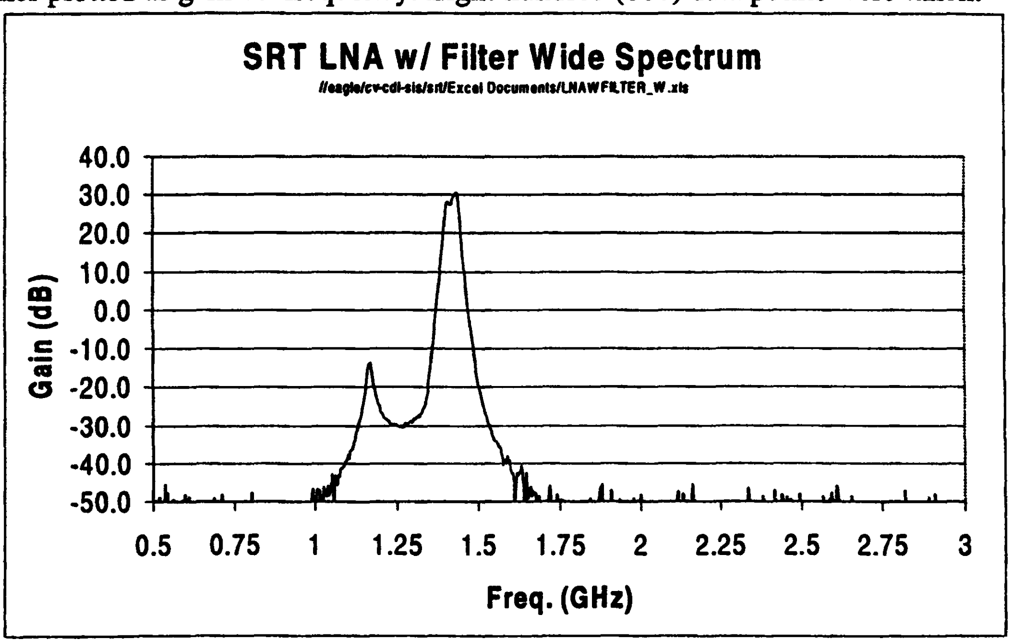

Figure A6

Note that with the bandpass filter in-line, the secondary region of gain seen in **Figure A4** is much narrower.

Figure A7 is the narrow spectrum gain measurement of the LNA and the bandpass filter together plotted as gain vs. frequency. Eight hundred (800) data points were taken.

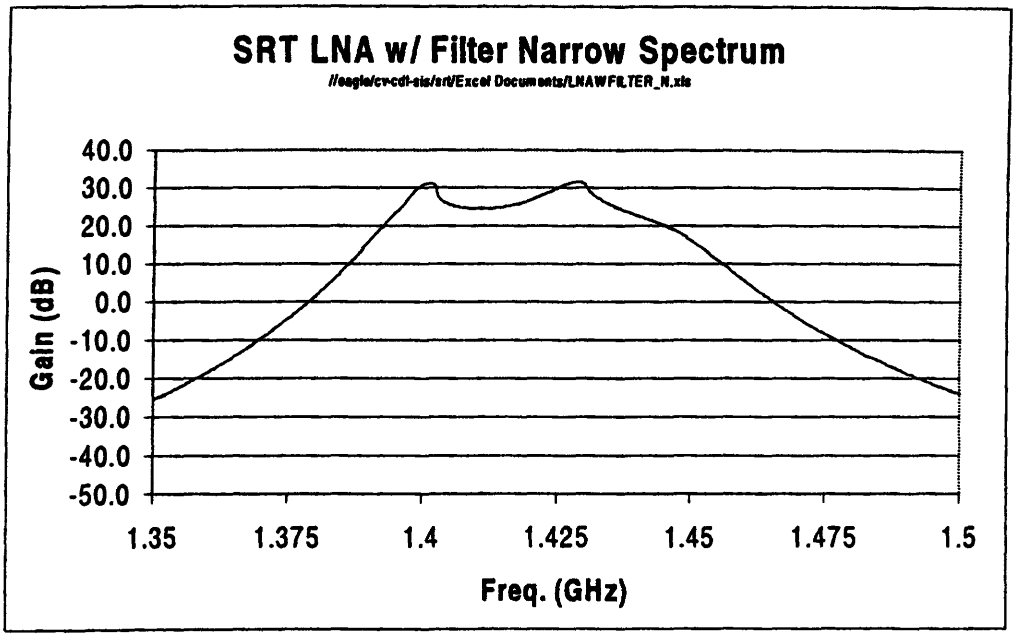

Figure A7

The total gain of both the amplifier and the bandpass filter at the operating frequency (1.42 GHz) is about 27 dB. **Figure A7** shows clearly that the gain is not uniform with frequency; there is a change of about 5 dB between around 1.4 and 1.425 GHz.

Appendix B

Y-FACTOR MEASUREMENTS OF SRT LNA

Radio astronomy requires detection of extremely weak RF radiation, and therefore necessitates sensitive equipment and thorough characterization of such equipment. It is important to know the noise temperature of the Low-Noise Amplifier (LNA) on the Small Radio Telescope (SRT) to account for its noise contribution when using it to detect distant radio sources. With the help of the CDL of NRAO-CV, I measured the noise temperature of this LNA using "Y-factor" measurements.

The measurement is in principle very simple. A hot and a cold load are presented to the LNA, and the ratio of the power outputs from the amplifier is measured. This ratio is called the "Y-factor." Using this number, it is then possible to solve for the noise temperature of the LNA and/or receiver. **Figure B1** illustrates the setup for our first measurements.

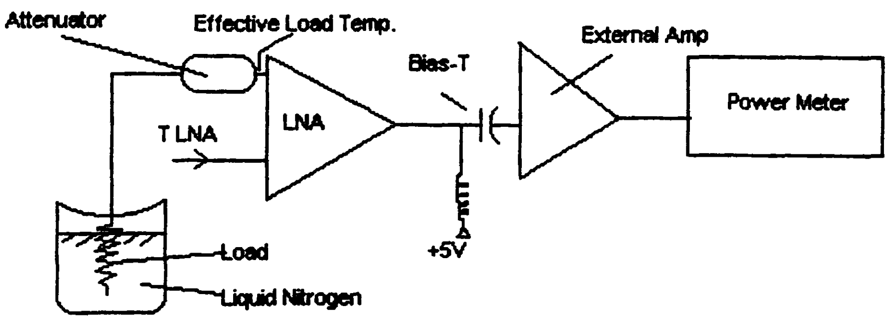

Figure B1

Liquid nitrogen supplies a stable cold temperature, since it boils at 78 K. The load can be dipped into a container of liquid nitrogen in order to take the power reading at the cold temperature. The Bias-T is in-line to supply power to the LNA, which runs on 5V fed through the center conductor. The Bias-T prevents the DC from entering the later stages of the setup. We used another amplifier in the 1.4 GHz frequency range to provide sufficient gain for a usable power meter measurement.

We ran four trials with this configuration. We measured the hot temperature with the LakeShore temperature gauge on a room-temperature Dewer, and used that result, 296.6 K, as our "T_{hot}" value. We used 78 K, the boiling point of liquid nitrogen, as "T_{cold}." When calculating effective source temperature in order to take into account the loss of the semi-rigid cable and any attenuation, we used the following equation[2]:

$\frac{T_{cold}}{Loss} + T_{ambient}(1 - \frac{1}{Loss})$ = effective source temp. (which replaces T_{cold} in the next eq'n)

[2] Pettai, Raoul, Noise in Receiving Systems. New York: John Wiley & Sons, 1984. Equation (8-36).

We used the following equation to solve for noise temperature of the receiver (T_{RX}) after we measured the Y-factor and corrected for loss before the LNA:

$$Y = \frac{T_{hot}+T_{RX}}{T_{cold}+T_{RX}}$$

A useful equation for converting from dBm to power is the following:

$$\text{P (dBm)} = 10 * \log_{10}(\frac{P(Watts)}{0.001})$$

The results from each trial are detailed below:

Trial 1:

In this trial our semi-rigid cable was aluminum and not stainless steel, which caused considerable variation in its temperature and consequentially its loss before the LNA. For this reason we threw away the results from this trial.

Trial 2:

In this trial we used a 1 dB attenuator, and also replaced the aluminum cable with stainless steel cable, which we measured with an HP8722D Network Analyzer to have an insertion loss of 0.3 dB. We used stainless steel because it is more thermally isolated than aluminum, so its loss from cold temperatures as a function of length is more confined when subjected to the cold of the liquid nitrogen.

Total attenuation between load & LNA	1.3 dB
Effective source temperature	133.81 K
Power using hot (296.6 K) load	-27.03 dBm or 1.98×10^{-6} W
Power using cold (78 K) load	-29.28 dBm or 1.18×10^{-6} W
Y-factor ratio	1.68
T_{RX}	**105.6 K**

Trial 3:

In this trial we used no attenuator but kept the same stainless steel cable with 0.3 dB loss. We suspect that without any attenuation beyond the loss of the stainless steel cable, the proper impedance was not being presented to the LNA, therefore making the results from this trial suspect.

Total attenuation between load & LNA	0.3 dB
Effective source temperature	91.75 K
Power using hot (296.6 K) load	-28.93 dBm or 1.28×10^{-6} W
Power using cold (78 K) load	-31.37 dBm or 0.73×10^{-6} W
Y-factor ratio	1.75
T_{RX}	**181.4 K**

Trial 4:

In this trial we used a 3 dB attenuator and the same stainless steel cable with 0.3 dB loss for a total of 3.3 dB of loss.

Total attenuation between load & LNA	3.3 dB
Effective source temperature	193.89 K
Power using hot (296.6 K) load	-42.41 dBm or 57.4×10^{-6} W
Power using cold (78 K) load	-43.72 dBm or 42.5×10^{-6} W
Y-factor ratio	1.352
T_{RX}	**97.9 K**

Trials 2 and 4 have the best agreement and the most similar variables, so might be good approximations of the correct value for T_{RX}. This technique measures the noise temperature average over the entire passband of the LNA because no filtering was used prior to the power reading. Had we used an isolator before the LNA, the impedance matching would have been better and we probably would not have had problems with variations in T_{RX} when we used different attenuations. Also, this measurement gave us a value for receiver temperature, T_{RX}, only. If we had taken similar measurements with the LNA out-of-line, we could have corrected for the second stage amplification and solved for the amplifier temperature, T_{LNA}.

The liquid nitrogen dip test served primarily to introduce me to the concept of Y-factor measurements. The results were not particularly useful, especially because the measurement was only of the receiver temperature, not the LNA temperature. We proceeded with several more tests that were more accurate and actually allowed us to compute values for the noise temperature of the LNA itself. The next section details four more methods for measuring receiver and LNA noise temperatures.

<u>**FOUR MORE METHODS FOR MEASURING RECEIVER AND LNA NOISE TEMPERATURES:**</u>

Because the results from the technique described above are unsatisfactory, we tried several other methods of measuring the noise temperature of the SRT LNA. Each method has advantages and drawbacks. Using a spectrum analyzer we could see noise temperature as a function of frequency, but with less precise measurements for power. A power meter provides very accurate measurements of power, but only at one frequency at a time. We hoped to see agreement between the various methods.

NRAO's CALIBRATED TEST RACK:

The LNA was tested in a calibrated test rack which employs square-law detectors to measure T_{LNA}. This setup calculates just the amplifier's noise temperature (T_{LNA}) by measuring and correcting for the noise figure of the system following the amplifier under test. The bandwidth of the system was 20 MHz. **Figures B2** and B3 detail the results from this trial.

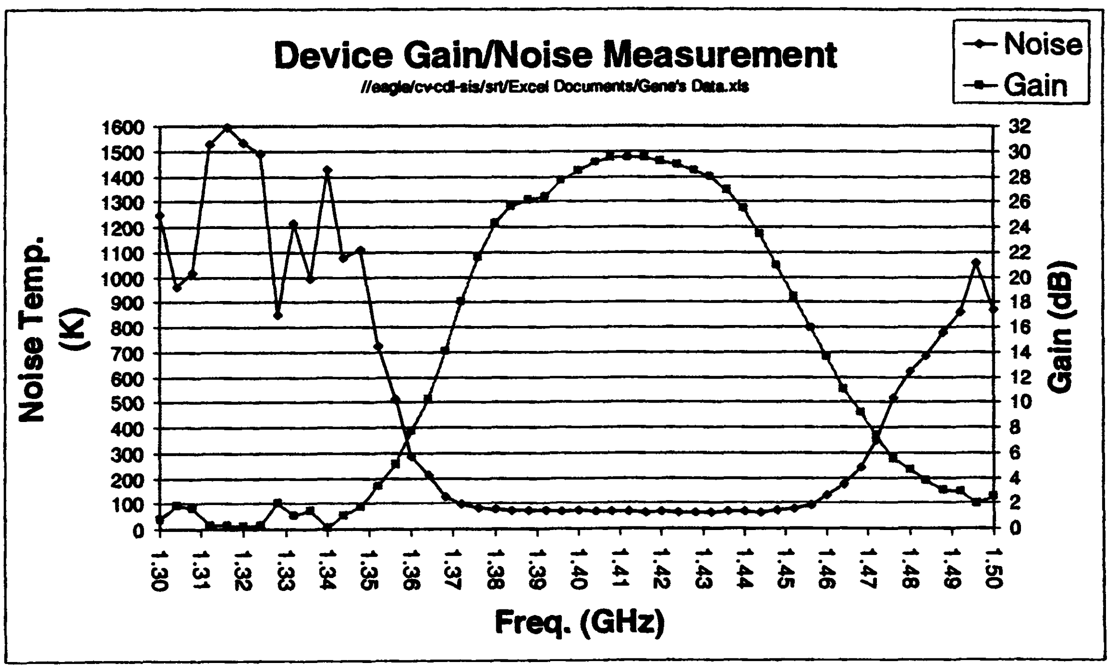

Figure B2: Measurement using NRAO's amplifier test system.

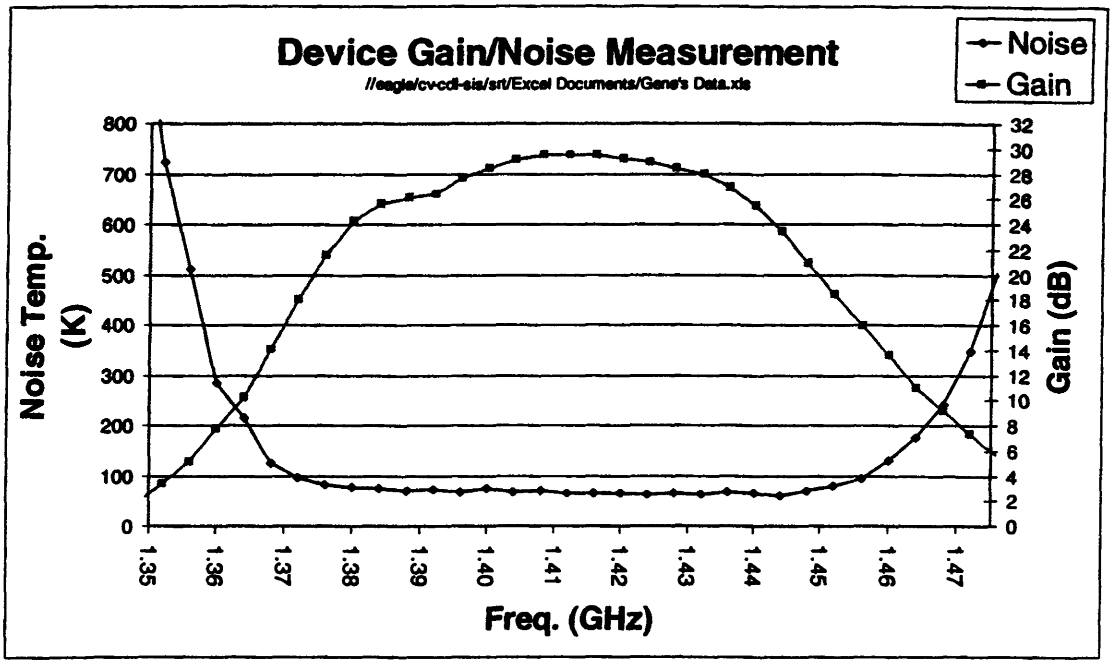

Figure B3: Enlarged version of Figure 2.

MEASURING RECEIVER TEMPERATURE WITH POWER METER:

We employed a power meter (HP E4418B) to measure the receiver temperature by using the spectrum analyzer as a tuned receiver with 1 MHz bandwidth and connecting the power meter to the IF output. In this trial we were measuring the receiver temperature because we were not accounting for the temperatures of all the other devices in the entire receiver. Nevertheless, the shape of the curve we obtained with the power meter was of interest. We expect to see low noise in the passband and noise rising steeply out of the passband. This was indeed what we found for the lower frequencies, but the curve remained surprisingly flat at the high end of the passband. **Figure B4** shows the results from this trial.

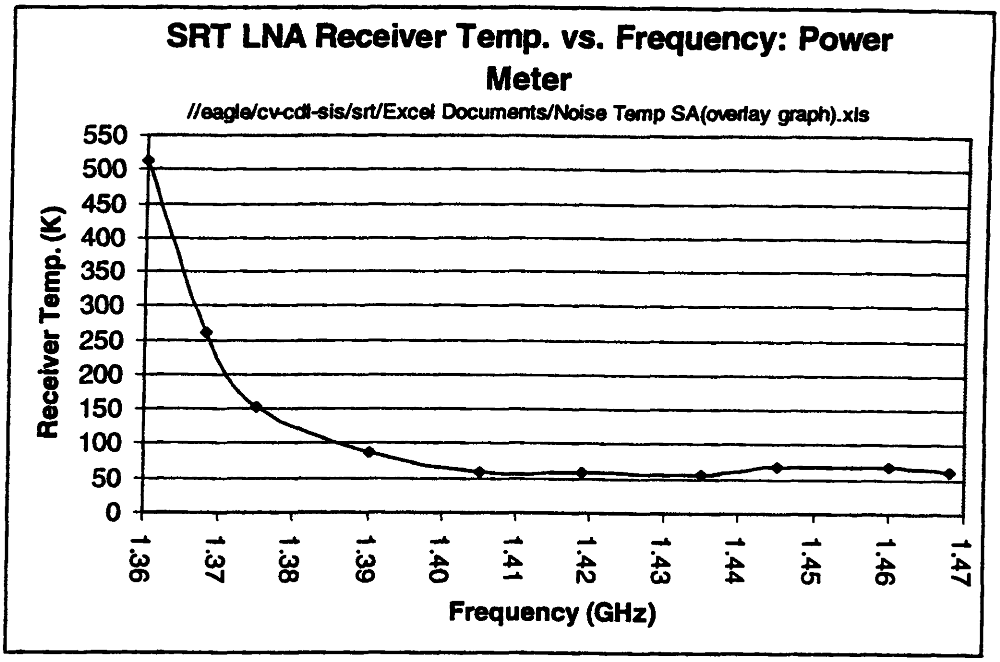

Figure B4: Receiver system noise temperature measured with power meter

MEASURING AMPLIFIER TEMPERATURE WITH POWER METER:

In order to find T_{LNA} we measured noise power for the noise source on and off with the LNA in-line and with it out-of-line. We again used the spectrum analyzer as a tuned receiver, and the power measurement was taken using the power meter connected to the IF output of the spectrum analyzer. This allowed us to calculate the temperature of just the LNA (T_{LNA}) after measuring the receiver noise temperature (T_R) and the noise temperature of the system following the LNA (T_2) and the LNA's gain (G_{LNA}). We then used the following equation to solve for T_{LNA}:

$$T_{LNA} = T_R - \frac{T_2}{G_{LNA}}$$

T_2 varied only slightly with frequency, which was expected since our later amplification stages were broadband. G_{LNA} varied dramatically with frequency; it was very small out of the passband and fairly large in the passband. Again, we expected this for G_{LNA} because the LNA is very narrow-band. T_R also varied with frequency. Our values for T_R came from a calculation using the power difference between the hot and cold sources measured with the LNA in-line. Our values for T_2 came from a similar calculation using the power difference between the hot and cold sources measured with the LNA out-of-line. It is possible to measure the gain of the LNA (G_{LNA}) using the power meter, the derivation for which appears below. **Figure B5** outlines our setup. We used an isolator before the LNA to present the correct impedance to the LNA. Using a spectrum analyzer we measured the loss of the isolator at 0.184 dB, which we accounted for when calculating the effective noise temperature of the noise diode.

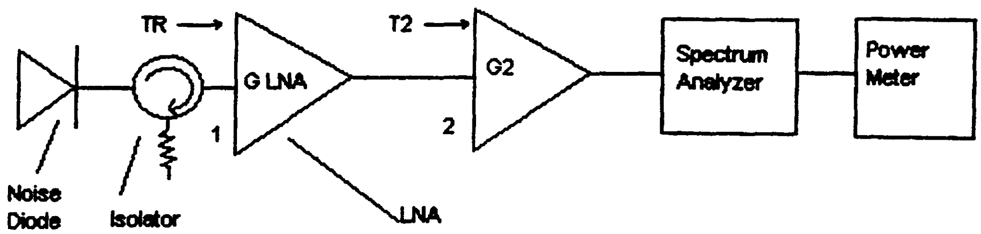

Figure B5

At the input to the LNA (point 1), we know that $\frac{\Delta P}{\Delta T}$ is the following:

$$\frac{P_{H1}-P_{C1}}{T_{H1}-T_{C1}} = \frac{kBG_{LNA}G_2(T_{H1}-T_{C1})}{T_{H1}-T_{C1}} = kBG_{LNA}G_2$$

Where P_{H1} is the power measured with the noise diode turned on, P_{C1} is the power measured with the noise diode turned off, T_{H1} is the noise diode effective temperature when it is turned on, and T_{C1} is the noise diode effective temperature when it is turned off. B is the constant measurement bandwidth and k is Boltzmann's constant. G_{LNA} is the gain of the LNA (the variable for which we would like to solve), and G_2 is the gain of everything after the LNA.

Similarly, at the input to G_2 (point 2), we know that $\frac{\Delta P}{\Delta T}$ is the following:

$$\frac{P_{H2}-P_{C2}}{T_{H2}-T_{C2}} = \frac{kBG_2(T_{H2}-T_{C2})}{T_{H2}-T_{C2}} = kBG_2$$

Where P_{H2} is the power measured with the noise diode turned on, P_{C2} is the power measured with the noise diode turned off, T_{H2} is the hot load temperature, and T_{C2} is the cold load temperature.

Now it is possible to solve for G_{LNA}:

$$G_{LNA} = \frac{kBG_{LNA}G_2}{kBG_2} = \frac{\frac{P_{H1}-P_{C1}}{T_{H1}-T_{C1}}}{\frac{P_{H2}-P_{C2}}{T_{H2}-T_{C2}}}$$

And hence:

$$G_{LNA} = \frac{P_{H1}-P_{C1}}{P_{H2}-P_{C2}} \quad \textit{if } (T_{H1}-T_{C1}) = (T_{H2}-T_{C2})$$

Our results using this method are pictured in **Figure B6**:

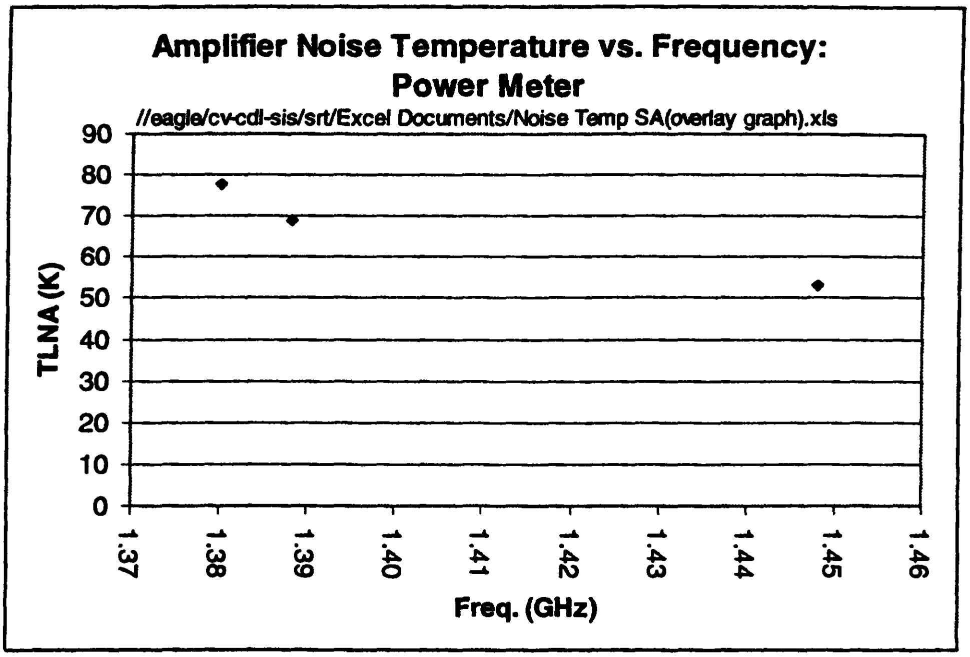

Figure B6: Amplifier Temperature measured with Power Meter.

MEASURING AMPLIFIER TEMPERATURE WITH SPECTRUM ANALYZER:

While a power meter is more accurate for taking power readings, a spectrum analyzer allows us to see power over a broad range of frequencies. We used a spectrum analyzer (HP E4408B) alone to measure power from the amplifier. We measured power from 1.35 to 1.5 GHz with the noise source turned on and with it off. We performed the same measurement with the amplifier out-of-line. We then found the difference in power to calculate the Y-factor, corrected for the spectrum analyzer's noise floor, and using the effective source temperature we calculated the receiver temperature. The equations used to calculate this data are the same as those outlined above for "Measuring Amplifier Temperature with Power Meter." **Figure B7** shows the results from this trial.

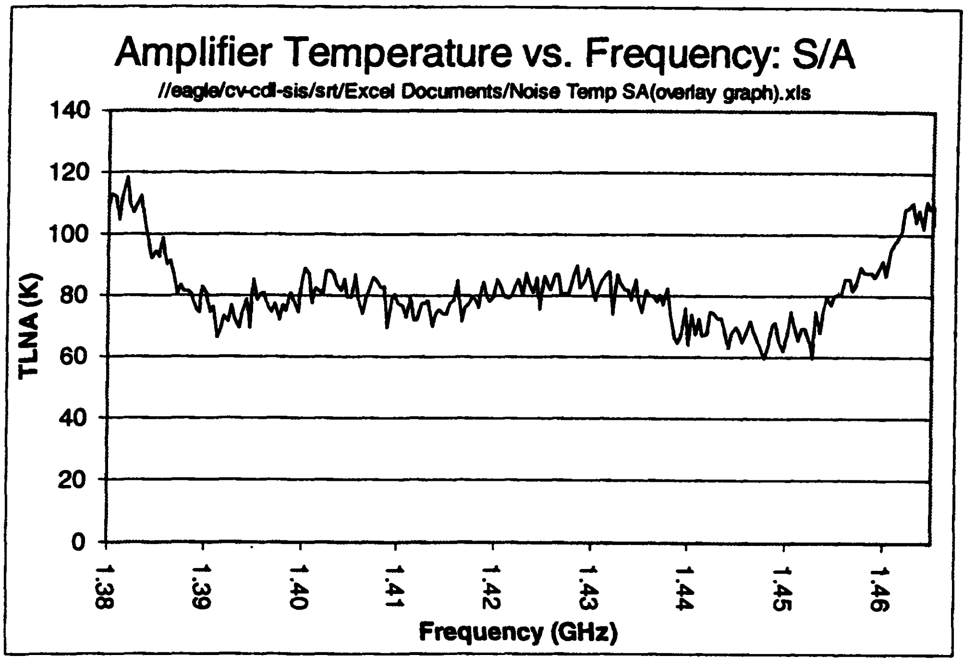

Figure B7: Amplifier noise temperature measured with spectrum analyzer

Figure B8 includes the data shown in **Figure B7**, but over a wider frequency range. **Figure B8** also includes several other results from the same data set: Receiver system noise temperature, the noise temperature of the system following the amplifier (T2), and the gain of the LNA in dB.

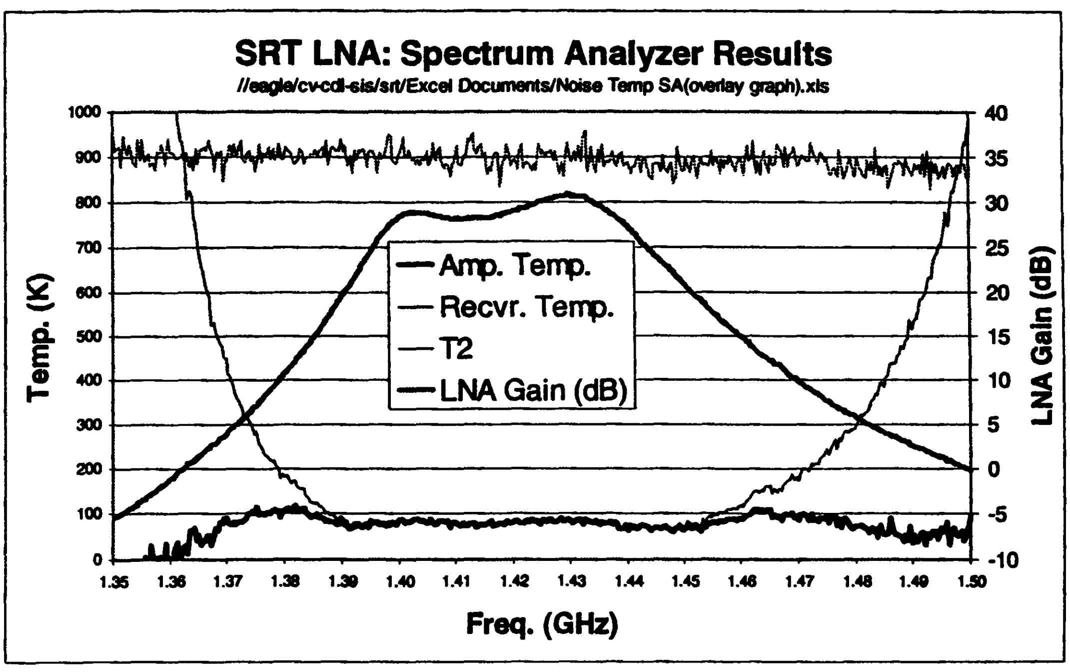

Figure B8: Amplifier, Receiver, and System Noise Temperatures; LNA Gain

The curve for receiver temperature is what we expected: constant noise temperature in the passband with steep slopes to much higher noise temperatures outside of the passband. The gain curve is also reasonable and matches closely the measurements made with the Network Analyzer. Gain drops off sharply out of the passband. The system noise temperature (T2) remains fairly constant, as expected. The plot for receiver temperature (T_{LNA}) agrees well with the other measurements in the passband, but becomes inaccurate outside of the passband due to extreme sensitivity to error.

CONCLUSION:

There is good agreement between the four different methods (shown in **Figure B9**) used to measure temperatures in the passband, but outside of the passband there is poor agreement (**Figure B10**). It should be noted that because the amplifier's noise temperature rises and its gain falls so steeply on the edges that small errors can have very dramatic effects.

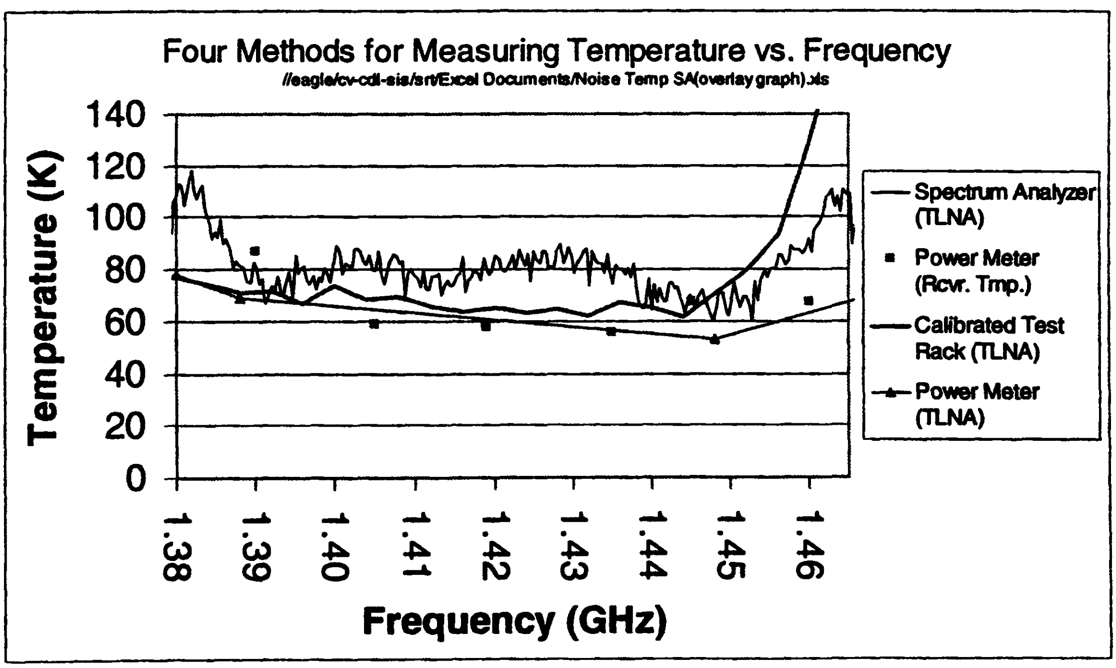

Figure B9: Four methods to find noise temperature – in the passband

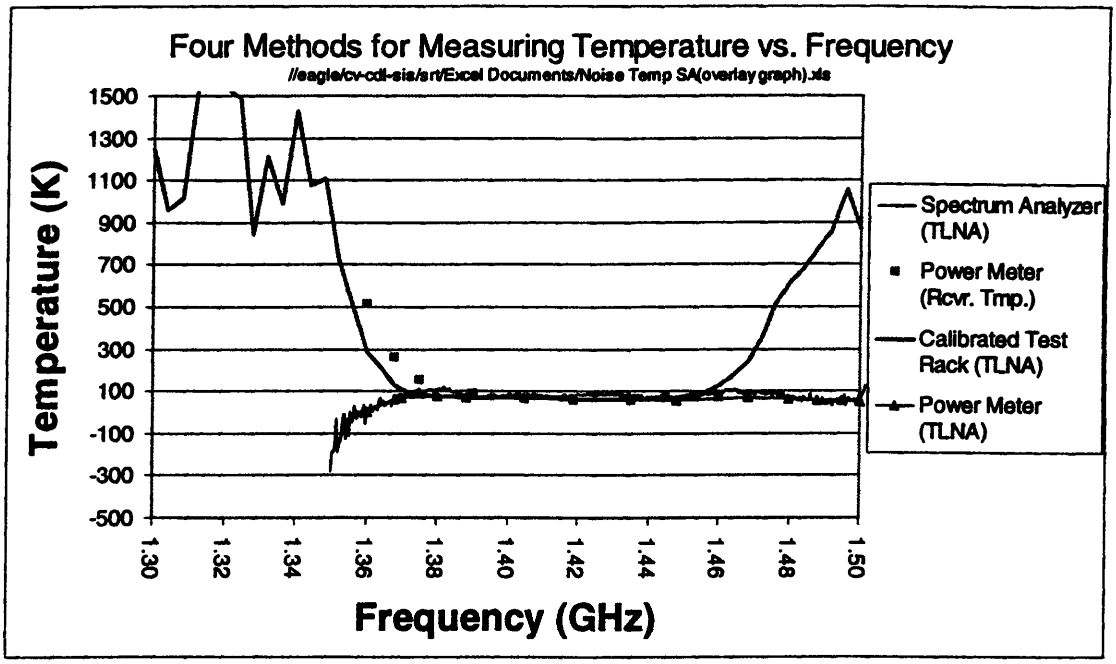

Figure B10: Four methods to find noise temperature – wide spectrum (note poor agreement out of band)

We compared our measurements for gain using the power meter to our earlier gain measurements with the network analyzer. **Figure B11** shows that the curves are very similar. Note, however, that there is a fairly significant difference between the readings – as much as 3 dB – and that this seemingly small difference is enough to drastically change the results for T_{LNA}.

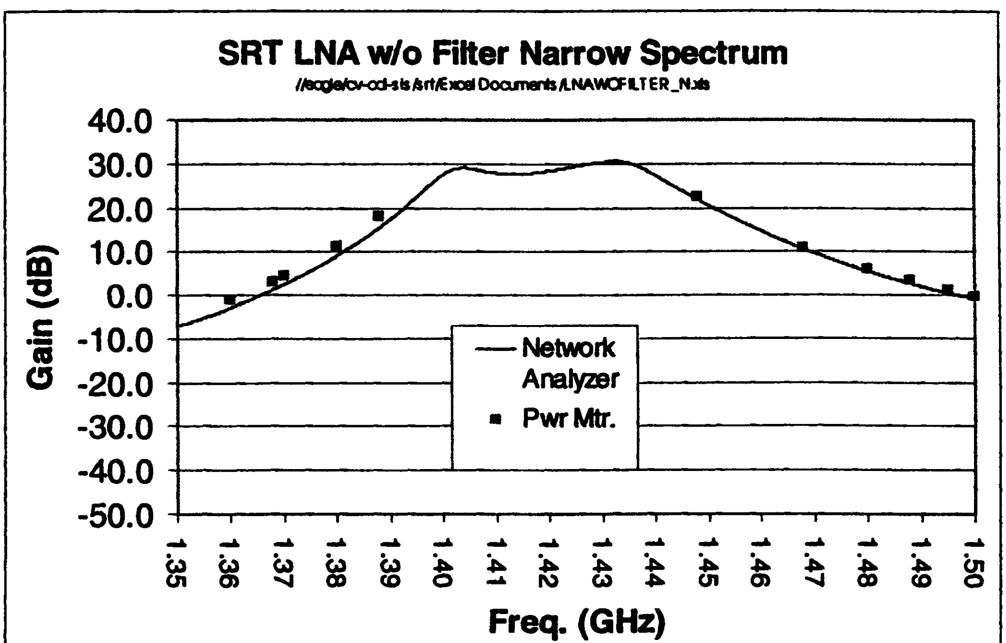

Figure B11: Gain measurements with the network analyzer and with the power meter.

We found the LNA to have fairly good gain (almost 30 dB) and low noise (about 70 K) in the passband. It is important to note that the LNA is sensitive to input impedance, and must be presented with a proper match in order to perform well. With no load the LNA oscillates. While within the passband our various methods for measurement of T_{LNA} were in good agreement, out-of-band the results varied widely.

Appendix C
ALIGNMENT AND SYSTEM TEMPERATURE MEASUREMENTS

Alignment

The SRT manual suggests making antenna pointing corrections in one of two ways: (1) Command the antenna to track the Sun and then make changes in Azimuth and Elevation until the feed horn shadow lines up with the shadow on the center of the dish, or (2) Command the antenna to track the Sun and then make changes in Azimuth and Elevation until the maximum power is observed on the software. The method that involves lining up the shadows is crude and inaccurate, and is especially difficult to perform because the shadow of the Elevation motor assembly gets in the way. I commanded the software to tack the Sun, and then used of "Offset" command to take power readings at points around where the software thought the Sun was. I set the receiver for 1419 MHz and took the following data:

Elevation Offset	Power (K)	Azimuth Offset	Power (K)
5 deg	570	5 deg	580
4 deg	730	4 deg	660
3 deg	845	3 deg	714
2 deg	850	2 deg	730
1 deg	780	1 deg	720
0 deg	690	0 deg	690
-1 deg	555	-1 deg	700
-2 deg	430	-2 deg	622
-3 deg	330	-3 deg	550
-4 deg	280	-4 deg	460
-5 deg	260	-5 deg	370

In graphical form, it is clear that the highest power was at about +2 deg Az and +2 deg El offset. I should adjust my dish up two degrees and right two degrees:

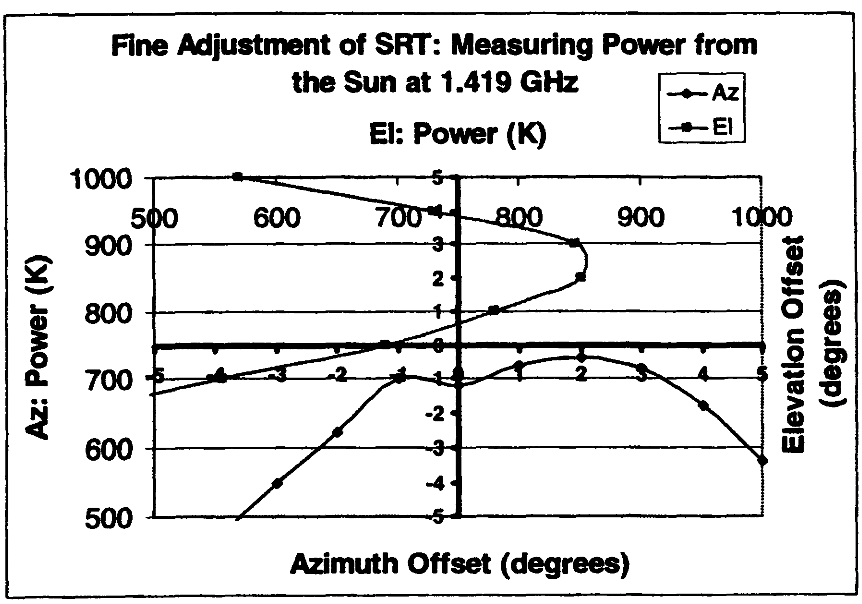

I ran several more alignment tests over a period of a few days with no physical changes to the antenna. Because many of the tests were done with the Sun near its peak elevation in the sky, the curve for azimuth is wider than the curve for elevation. The results from these tests are pictured below:

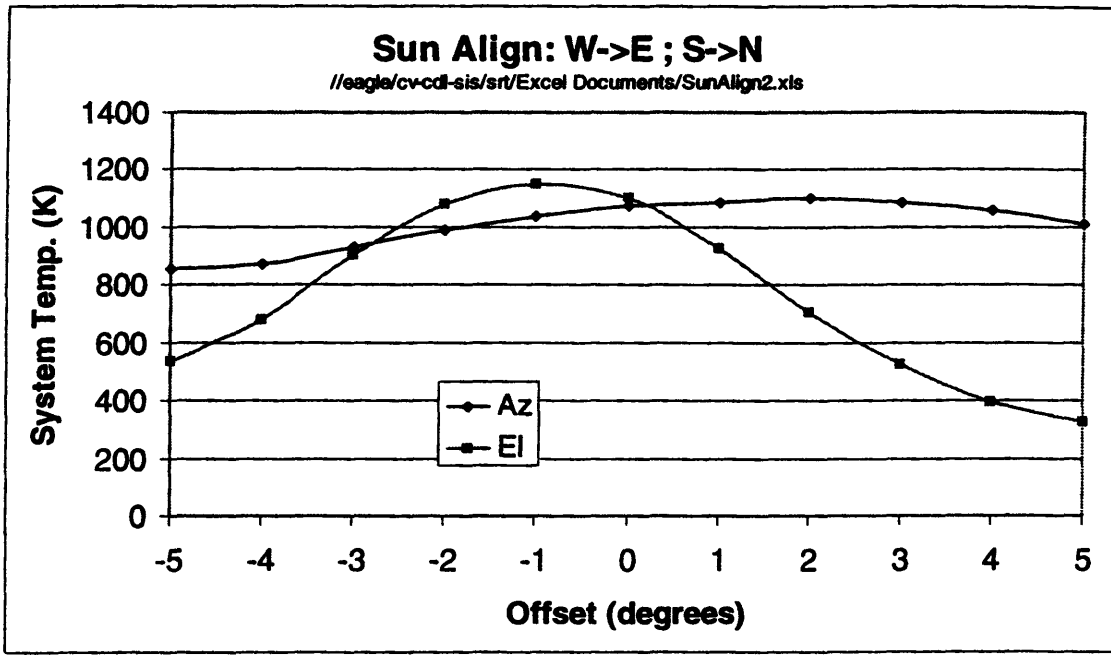

These data were taken 7/13/01, scanning the Sun west-to-east and then south-to-north.

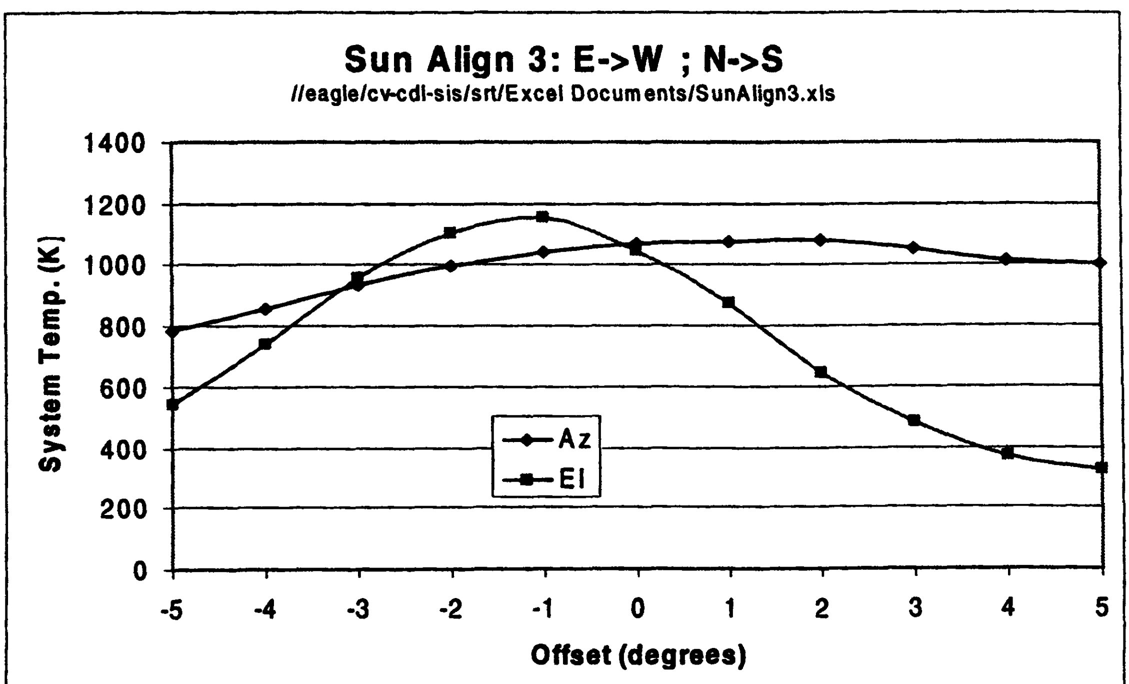

These data were taken 7/13/01, scanning the Sun east-to-west and then north-to-south.

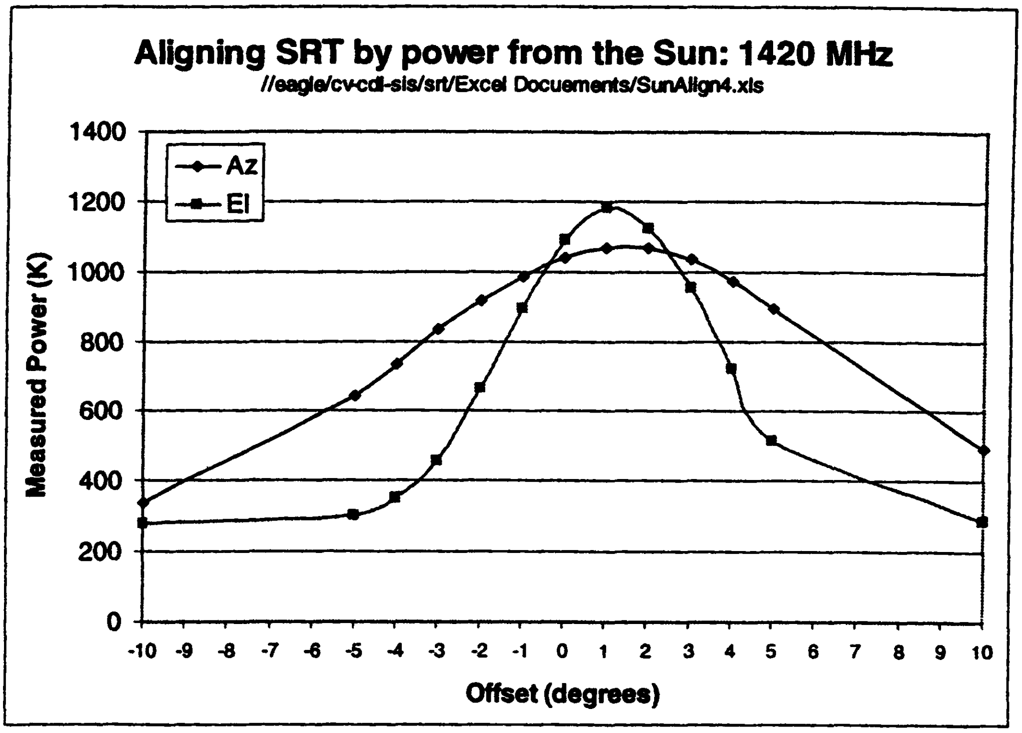

These data, taken 7/16/01, scan the Sun east-to-west, then north-to-south.

It is clear that peak power did not occur for the same offsets in each of the trials. Error may come from resetting the SRT, or possibly from the SRT spinning on its mount.

Using this same technique, it was also possible to look for side-lobes on the SRT. I scanned the sun in azimuth and elevation for thirty different offsets, and then converted system temperature to a logarithmic scale. My results are shown below:

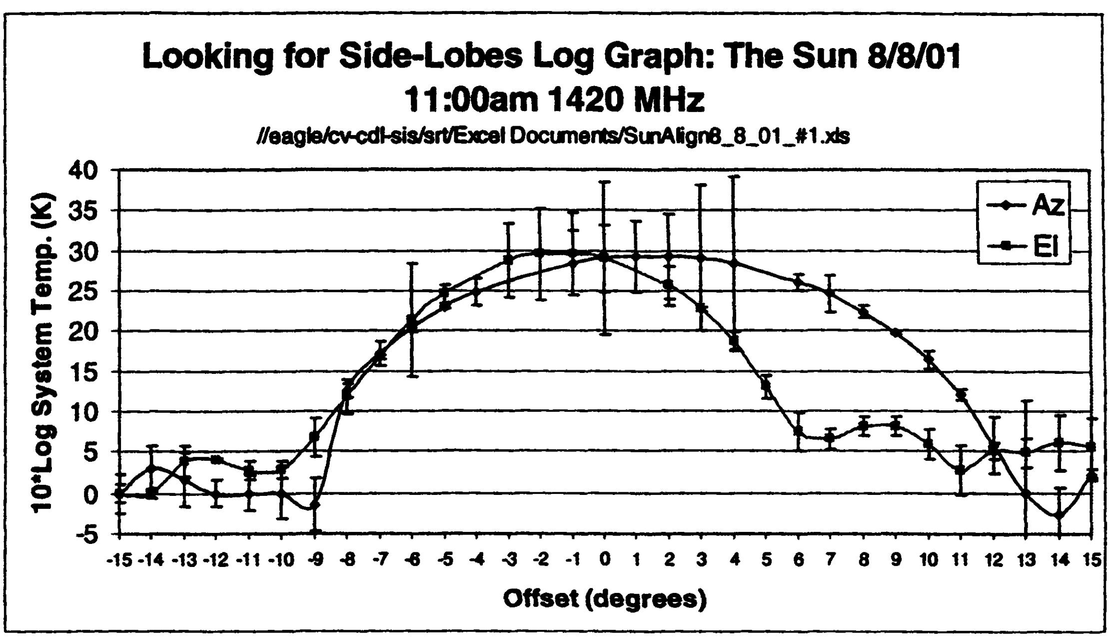

I also ran several 25-point scans on the Sun in an effort to learn more about how this scan works. No physical changes were made to the telescope between trials, but the telescope was commanded to move off-source between each trial. Results are pictured below:

Mosaic of 25-point scans of the Sun taken with the Small Radio Telescope

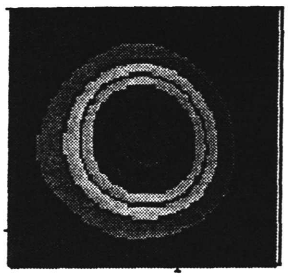

The Sun: Data taken 7/12/01. Center Freq.: 1420.4 MHz ; bins=5, Tsys=231K ; Offset=+2,+2

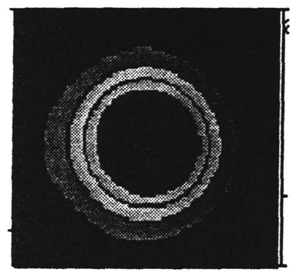

The Sun: Date Taken 7/12/01. Center Freq.: 1420.4 MHz ; bins=5, Tsys=231 K ; Offset=+2,+2

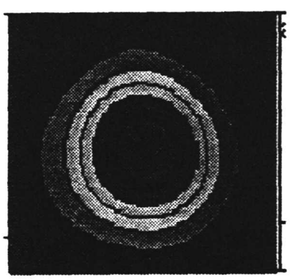

The Sun; Data taken: 7/12/01. Center Freq.: 1420.4 MHz ; bins=1 ; Tsys=231 K. Offset: +2, +2

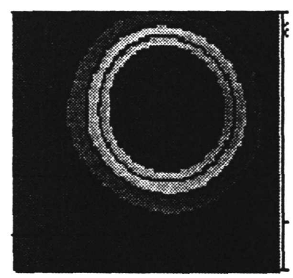

The Sun: Data taken: 7/12/01. Center Freq.: 1420.4 MHz ; bins=1 ; Tsys=231 K ; Offset=0,0

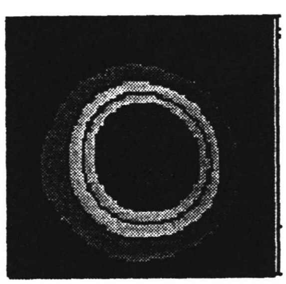

The Sun: Data Taken 7/12/01. Center Freq.: 1420.4 MHz ; bins=1 ; Tsys=231 K ; Offset= +2, +2

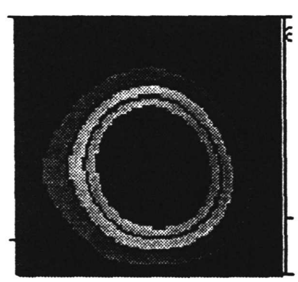

The Sun: Data taken 7/12/01. Center Freq.: 1420.4 MHz ; bins=15 ; Tsys=231 K ; Offset=+2,+2

Note that when the offset was changed from +2deg,+2deg to 0deg,0deg, the image shifted up and right. The number of bins does not appear to affect the image.

System Temperature vs. Antenna Elevation

Next I measured the system temperature (reported as "Tsys" in the JAVA software) as a function of antenna elevation at 1419 MHz. I expected to see higher temperatures at lower elevations due to the greater apparent thickness of the atmosphere and influence of side-lobes at lower elevations. For each elevation I ran the Vane calibrator and recorded the the number for system temperature. I did this test for two azimuth values. I also made note of the temperature read when the load was in place. The results of these tests are as follows:

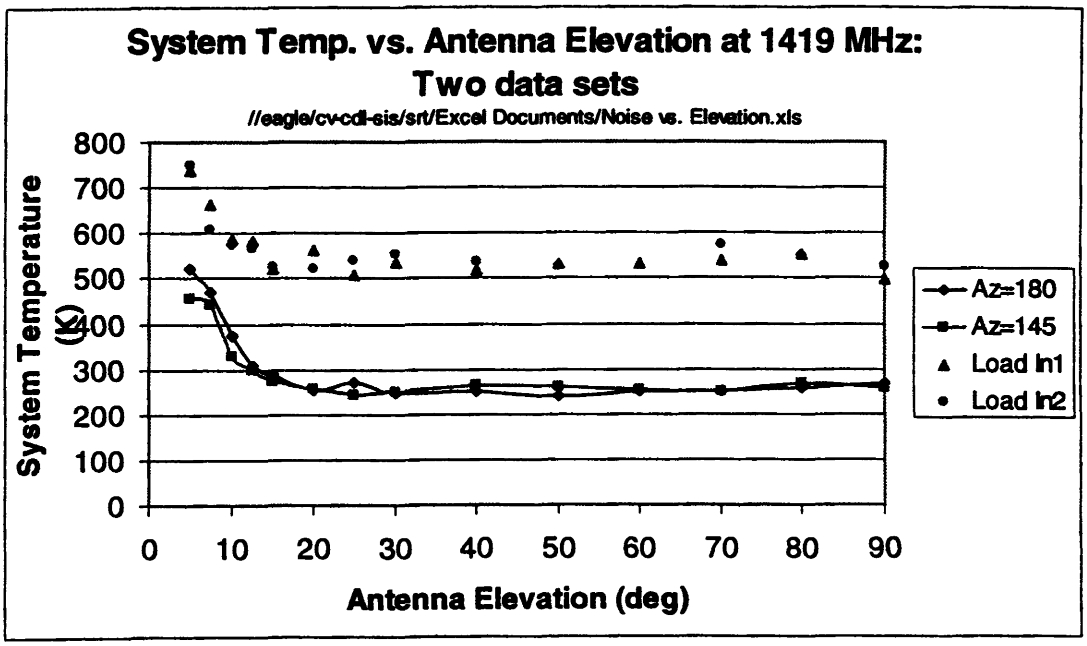

Note that the system temperature with the load in did not remain constant for all elevations (ideally it should); it curves up below 30 degrees elevation. This might be due to the load not completely covering the feed aperture.

At 1419 MHz, I found that for elevations above 30 degrees, the average system temperature with the Vane calibrator in front of the feed is about 550 Kelvin. This number depends on the physical temperature of the load, which is in turn a function of ambient temperature and other factors such as, possibly, the moisture content of the load. The JAVA software assumes the load is at a constant 300 K, which is certainly not always true. An electronic noise source like the one detailed on the SRT web page might produce better results.

Testing the System Noise Floor

The following data were taken in spectral line mode (bins>1) in an effort to see system temperature as a function of frequency. Being a continuum source, the Sun has a fairly constant temperature across the range of frequencies selected, but Rosette appeared to have a sharp spike around 1420.2 MHz corresponding to the spectral line emission from this source. The Sun is a variable source, and could have antenna temperatures at L-band ranging between 264 and 2640 K. The values of around 1000 K are therefore reasonable. In both of the graphs below, the series on top represent data taken with the telescope pointed towards the source, while the series on bottom represent data taken with the telescope pointed towards blank sky (about 15 degrees off-source) in order to see the noise floor. I calibrated the SRT using the Vane calibrator before making any observations. Note the slight upward trend in temperature with increasing frequency in both source and noise floor measurements.

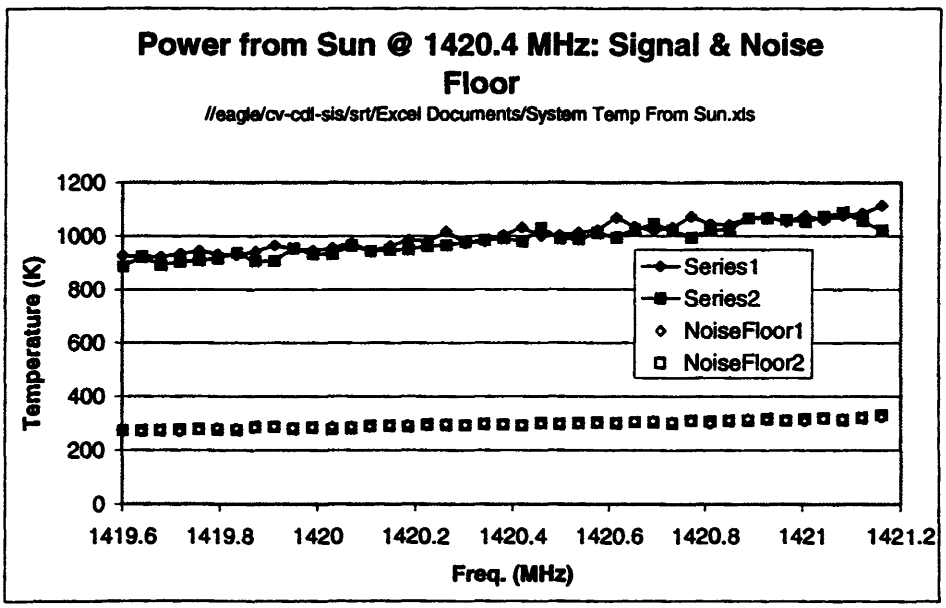

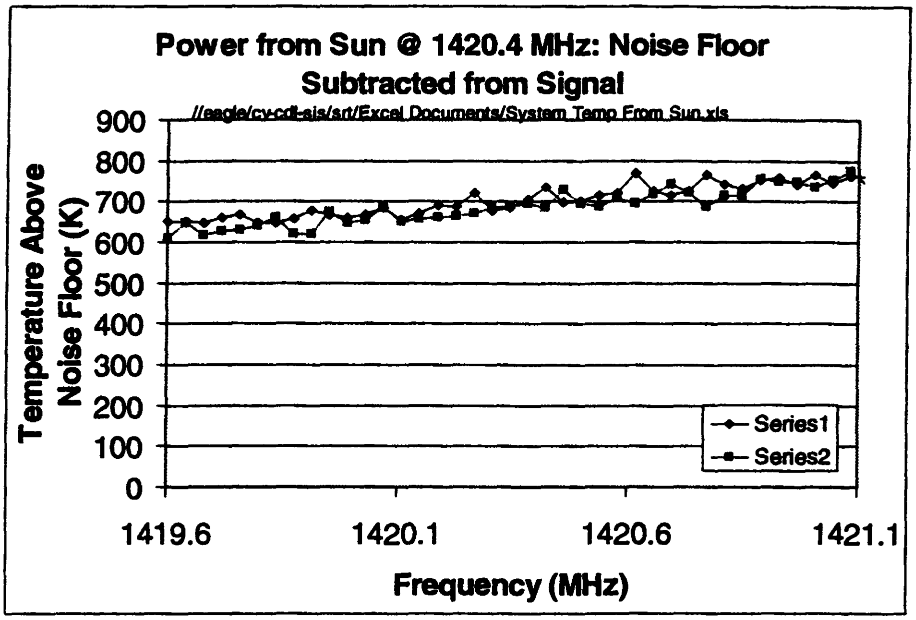
Power from Sun @ 1420.4 MHz: Noise Floor Subtracted from Signal
//eagle/cv-cdl-sis/srt/Excel Documents/System Temp From Sun.xls
Temperature Above Noise Floor (K)
900
800
700
600
500
400
300
200
100
0
Series1
Series2
1419.6
1420.1
1420.6
1421.1
Frequency (MHz)

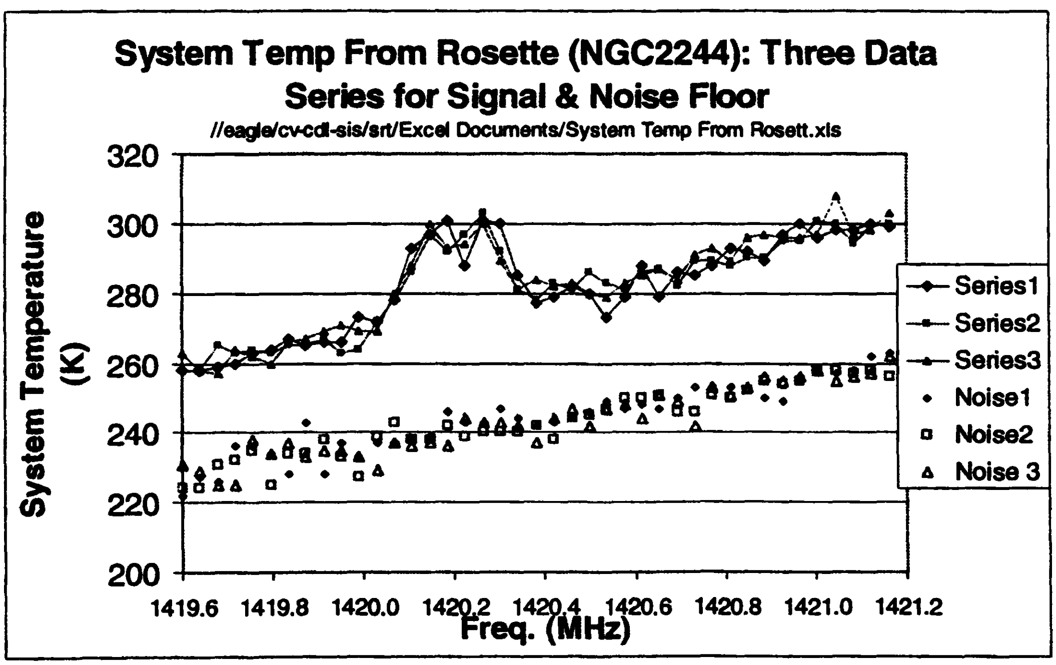
System Temp From Rosette (NGC2244): Three Data Series for Signal & Noise Floor
//eagle/cv-cdl-sis/srt/Excel Documents/System Temp From Rosett.xls
System Temperature (K)
320
300
280
260
240
220
200
Series1
Series2
Series3
Noise1
Noise2
Noise 3
1419.6
1419.8
1420.0
1420.2
1420.4
1420.6
1420.8
1421.0
1421.2
Freq. (MHz)

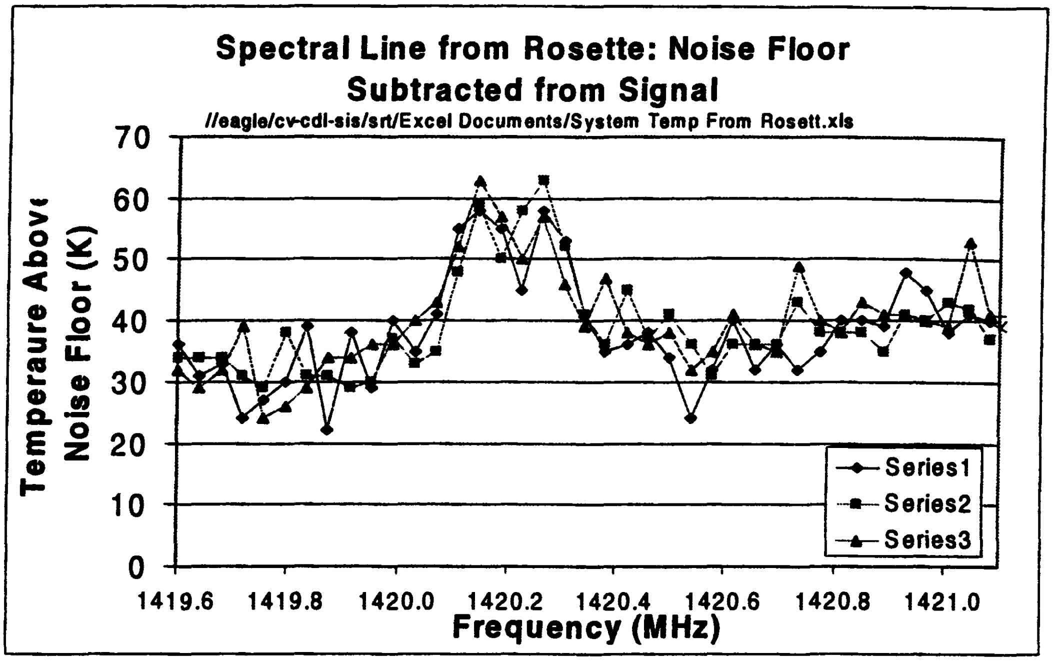
Spectral Line from Rosette: Noise Floor Subtracted from Signal
//eagle/cv-cdl-sis/srt/Excel Documents/System Temp From Rosett.xls
Temperaure Above Noise Floor (K)
70
60
50
40
30
20
10
0
1419.6
1419.8
1420.0
1420.2
1420.4
1420.6
1420.8
1421.0
Frequency (MHz)
Series1
Series2
Series3

Catalogue of the Best Candidate Stars for the Terrestrial Planet Finder Mission

Juliette Rupert, University of Oklahoma

Abstract:

Recently, within the scientific community, there has been an increase of enthusiasm in looking for Earth-Like Planets around stars other than our own. One such mission, which will start in 2007, is the Terrestrial Planet Finder (TPF). With TPF, it is necessary to have a focused and well thought out list of candidate stars. Our project set about creating a catalogue of stars that would satisfy the restraints TPF will be working under. To achieve this, there was a need to understand which aspects and quantities are of most interest when conducting such a project as TPF. To acquire the parameters needed, a careful analysis of previous work was required. Additionally, some calibrations were needed to find certain parameters. In the end, an intense search to obtain accurate information about each candidate star (including binarity, variability, and lifetime) needed to be performed. This data would then be used to form a list of the few hundred best candidates that can be used when TPF begins.

1. Introduction:

The idea that there are planets in other stellar systems has long been of interest. Recently, many Jupiter-size planets have been found and the search is continuing. However, of more interest to the world, is the possibility of life-sustaining, or Earth-like, planets. TPF's mission is to discover planets that have an equilibrium temperature that is equivalent to Earth's. An important aspect of this is in the selection of stars that would be of interest, as significant amounts of time could be wasted looking at stars with undesirable qualities. Nearby and bright stars are at the top of the list for TPF, so this project started by looking at ~15,900 stars that satisfy these particular selection criteria. Some important qualities looked at were angular separation (or the habitable zone), contrast ratios of star and planet, main sequence lifetime, variability, and binarity.

The project began by learning how to efficiently manipulate the software programs that would be needed. Use of Quattro Pro 9 as a calculation base required a knowledge of the program's syntax and method of operation. Bugs in the software also had to be recognized and solutions to them found. The need for graphing software that could handle large numbers of stars was also a necessity. After looking at a variety of plotting software, it was determined that SigmaPlot would most satisfy our needs. Therefore, learning to use SigmaPlot efficiently was another goal.

The next step was verifying and understanding the calculations that would be necessary for the task. Therefore, a thorough understanding of exactly what was occurring within each calculation was required. After re-analyzing the calculations, the real work began. Selection criteria were applied to the Hipparcos Catalogue, finding those stars that would be of most interest to the project.

As the effective temperature (T_{eff}) and the bolometric magnitude (m_{bol}) were not provided in the Hipparcos data, we examined previous studies to help determine these quantities. A calibration had to be created that would satisfy a wide range of V-I color. After the calibration was complete, these parameters were applied to the initial selection, and the remaining calculations of interest were performed.

Further criteria were then applied to reduce the number of interesting stars to a more manageable size. The final selections then had to be looked at carefully to confirm important aspects such as main sequence lifetime, variability, and binarity, as well as to check calculations. After this was done, the final criteria placed on the selections were relaxed to include more stars, applying the same method of verification, until 200-300 stars remained that would be good candidates for TPF.

2. Project Goals:

To obtain our final goal of creating a carefully analyzed catalogue, a variety of steps were taken. The project was split into two main phases. Phase I included the initial selection of stars from the Hipparcos catalogue, the calibration of effective temperature and bolometric correction, and the calculation of the desired parameters such as angular separation and contrast ratio. Phase II incorporated further selection criteria and verification of all essential data that would be put into the catalogue

2.1 Phase I:

In order to begin with a complete sample of candidates that could be useful for TPF, certain criteria were placed on the stars in the Hipparcos catalogue found on the ViZier web site (http://vizier.u-strasbg.fr/cgi-bin/VizieR). As Hipparcos is a relatively complete catalogue out to 10^{th} magnitude stars and includes many 12^{th} magnitude stars, it was the best starting point for the analysis. Using Hipparcos stars with magnitudes greater than 7, in addition to those within 20 parsecs having magnitudes between 7 and 10, were singled out. This initial selection brought the Hipparcos catalogue down from over 118,000 stars to 15,855. These first criteria ensured that the brightest stars, and closest stars, were included, all of which were potentially interesting to the project. In the selection from the Hipparcos catalogue, a number of important parameters such as Parallax, V magnitude, V-I and B-V color, and position were given. The next stage in the project required obtaining some essential quantities that would be needed for the calculations.

Two extremely important and necessary parameters were the effective temperature and the bolometric magnitude. To obtain the latter, the bolometric correction was needed. It would then be added to the V magnitude, given in Hipparcos, resulting in the bolometric magnitude. To calculate these numbers, a calibration that would work for a wide range of T_{eff} and bolometric corrections had to be created. To achieve this, a look at data from previous authors, who had also used stars found in the Hipparcos catalogue and had calibrated values of these quantities, was required. We referred to three important publications: Prieto et. al. (1999), Di Benedetto et al. (1998), and Houdashelt et al.(1999). In using data from three different authors, a good calibration over all V-I was obtained. Individually, each group covered a certain range of V-I, Prieto toward the blue, Di Benedetto within the middle, and Houdashelt with theoretical data for larger V-I. Using a sixth order polynomial, excluding the few outliers that were found, we were able to obtain a good calibration over most of the V-I range for both T_{eff} and bolometric correction (Figures 1 and 2 respectively). The un-smooth curve for V-I < 0.2, found in both figures, is caused by the polynomial fit for the Prieto data, which was done using B-V color (provided in Prieto) instead of V-I. The calibration for the blue end, using Prieto, was added to the calibration of Di Benedetto/Houdashelt. Hence, resulting in a slightly cluttered area at the blue end where the bolometric correction and T_{eff} were plotted versus V-I.

One problem that arose in the effective temperature calibration, due to lack of data, was the failure to extend the fit beyond a V-I of 3.3. To solve this, a T_{eff} of 2850K was adopted for any V-I beyond that value. In the bolometric correction calibration, we lacked data beyond a V-I of 2.7 and therefore did not have a bolometric correction for those stars with V-I greater than that limit. Another difficulty in the bolometric correction calibration was due to the sign difference used in

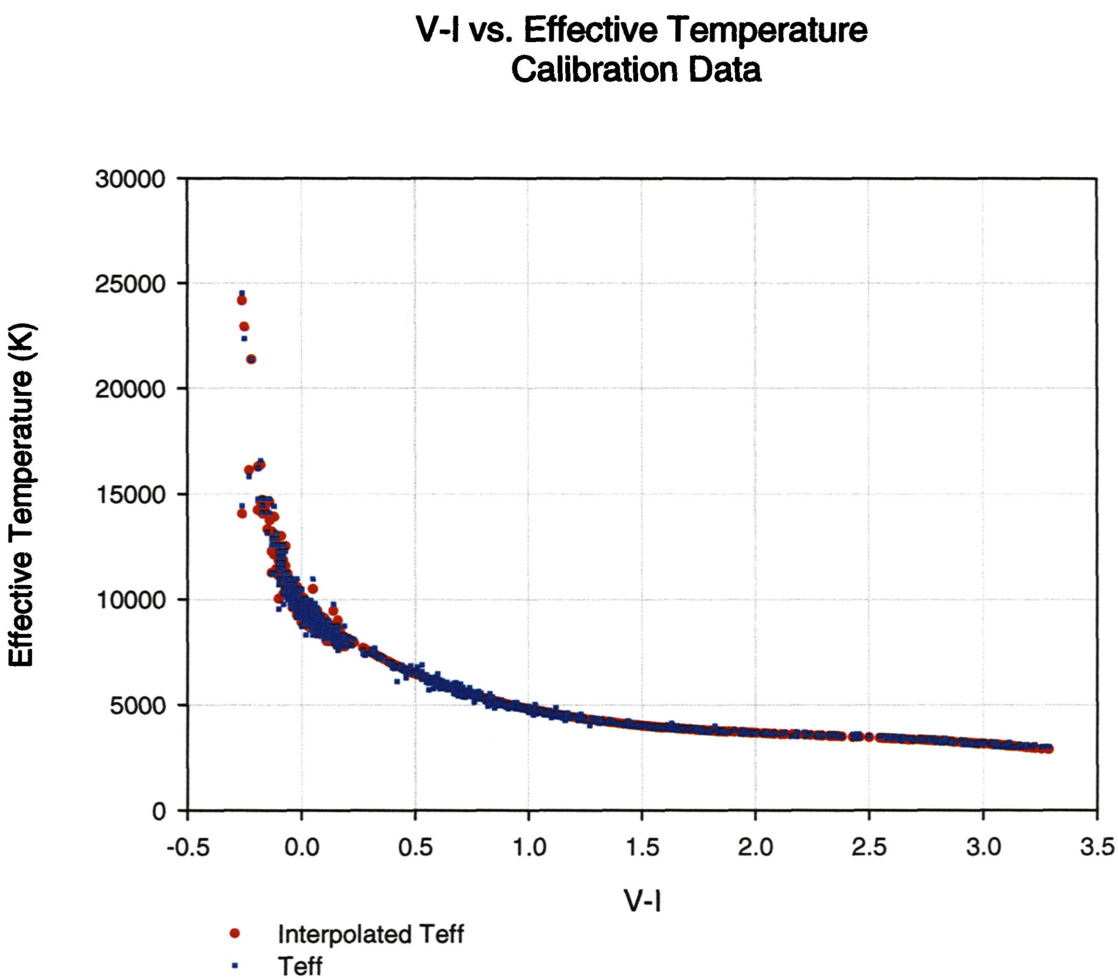

Figure 1: The T_{eff} calibration data that was performed using a 6^{th} order polynomial fit for both Prieto's data and Di Benedetto/Houdashelt. The fit using Prieto's data was applied to those stars with V-I < 0.2, while the Di Benedetto/Houdashelt fit was used for all others. The exceptions were the stars with a V-I greater than 3.3 as there was a lack of reliable data for that limit. Therefore, a T_{eff} of 2850K was adopted for any stars with a color greater than 3.3.

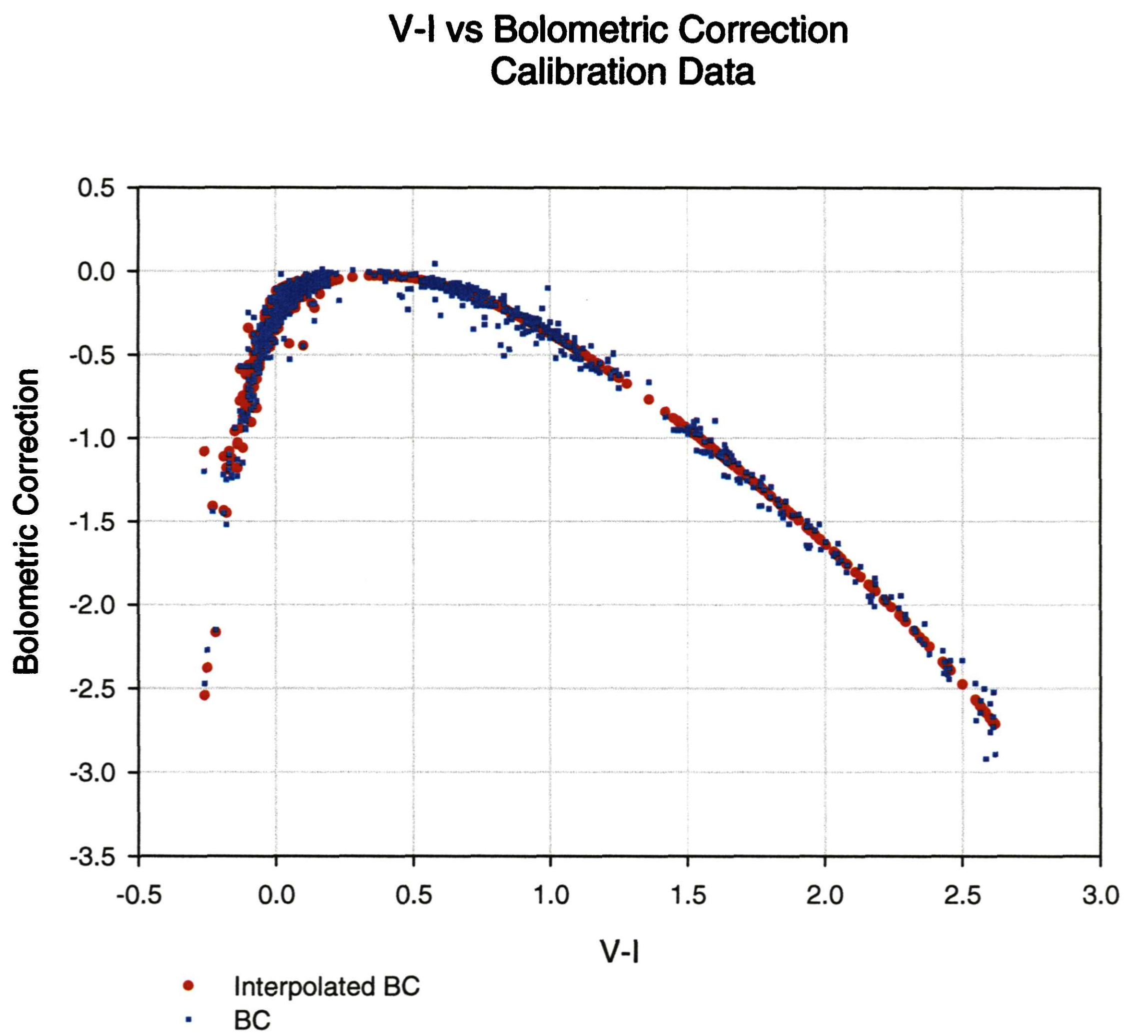

Figure 2: The bolometric correction calibration, done using data from Prieto, Di Benedetto, and Houdashelt. The polynomial fits were then applied to all stars in the initial selection. The fit using Prieto's data was applied to those stars with V-I < 0.2, while the Di Benedetto/Houdashelt fit was used for all others. The exceptions were those stars with V-I greater than 2.7, where the bolometric correction fit would degrade, due to lack of data.

Prieto's bolometric correction data. Since he used a sign opposite that of convention for bolometric corrections, this was taken into account before the fit was performed. When the calibration with Prieto's data was completed, a 0.08 offset in the actual and interpolated data was found. After the offset was corrected, the fit was then re-calculated and added to the Di Benedetto/Houdashelt fit. As Di Benedetto did not have bolometric corrections calculated, as Prieto did, it was necessary to use the bolometric fluxes that were given in his study to find the bolometric corrections. Those stars that did not have a bolometric flux were excluded from the Di Benedetto/Houdashelt polynomial fit.

These interpolated values for T_{eff} and bolometric correction were applied to all 15,855 stars from the initial selection. The bolometric correction was then added to the V magnitude to obtain the bolometric magnitude, which was required for other calculations. As we wanted the most accurate quantities for these parameters, the interpolated values were used only if Di Benedetto or Prieto did not provide them. If all else failed, a previous calibration (by Dr. Richard Simon) based on data from the Hipparcos Input Catalogue was used. This only became necessary for 145 stars.

As our goal was to find stars that would have Earth-like planets, there were two quantities that helped us to further our selection: the angular separation of an Earth-like planet and the contrast ratio, given by the following equations:

$$\text{Angular Separation of the Habitable Zone} \propto (1\text{-}A)^{0.5} / 10^{(mbol/5)} / (T_{planet})^2$$

$$\text{Contrast Ratio} = (\text{Flux density of Star})/(\text{Flux density of Planet})$$

Or

$$(\text{Photons/Sec})_{star}/(\text{Photons/Sec})_{planet}$$

Specifically, we were looking for stars with a habitable zone in which a planet would have the same equilibrium temperature as Earth. Since the angular separation and contrast ratio were of interest in furthering our selection criteria, a plot of the two (Figure 3) was essential to the project. As can be seen, at least one sharp cutoff is visible on the plot. Figure 4, a log-log plot of the same data, has a close up view of the sharp cutoffs. The cutoff extending to the left is due to our selection of stars with magnitudes from 7 to 10 and within 20 parsecs. These are the close stars, which are expected to have a smaller angular separation. The second cutoff that can be seen is a bit more peculiar. After careful analysis, this cutoff was found to be due to the dependency of angular separation on the bolometric magnitude and consequently, from our lack of data for V-I greater than 2.7, it appears.

2.2 Phase II

The next phase, which time did not allow to be completed, was paramount to the project. Phase II began with applying further criteria to the initial selection based on the angular separation and contrast ratio. The criteria were an angular separation of 100 (milli-arc-seconds) or greater and a contrast ratio of 10^{11} or less at 1 micron. After these criteria were applied, there remained 148 stars (Figure 5 shows the angular separation and contrast ratio for these). Each star

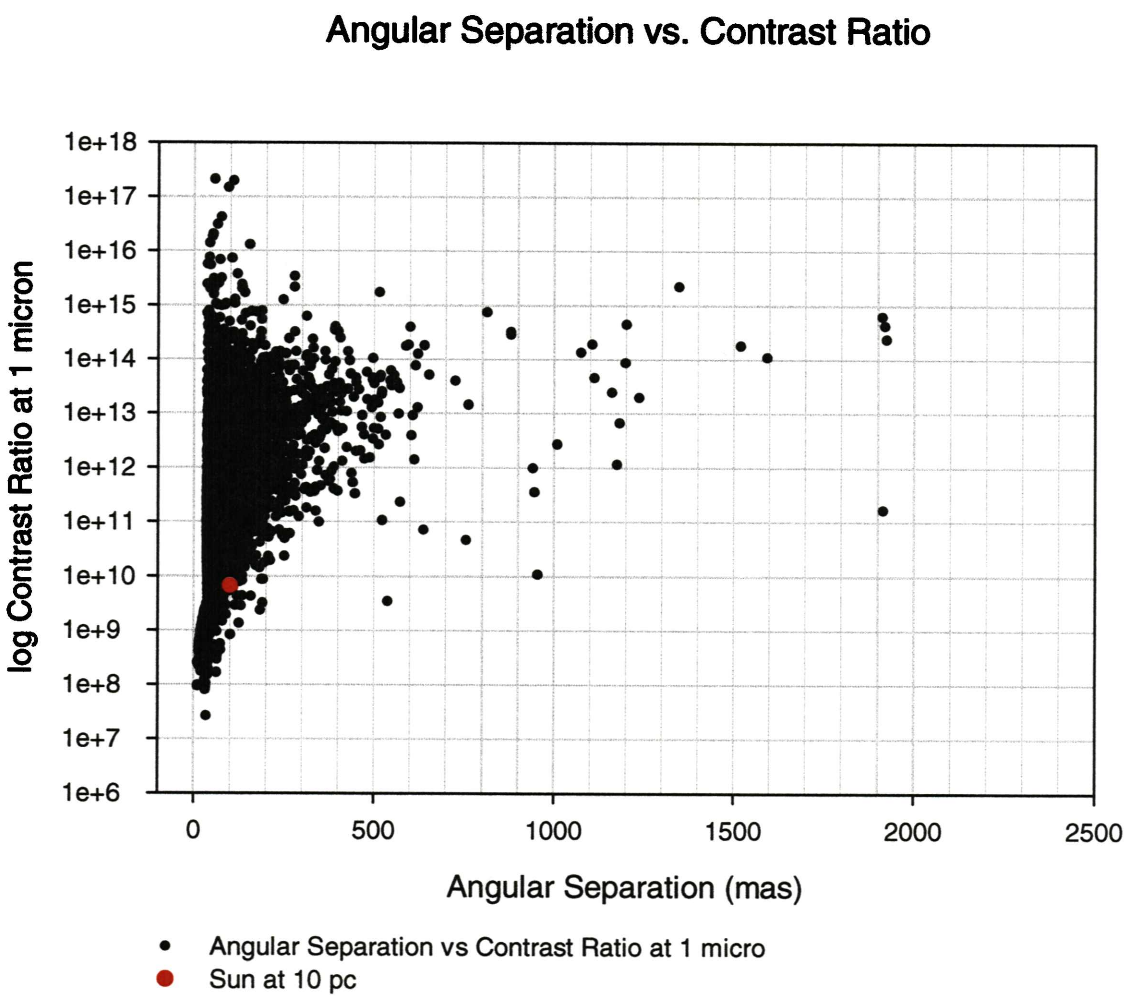

Figure 3: Plot of Angular Separation vs. Contrast Ratio for all 15,855 stars in the initial selection

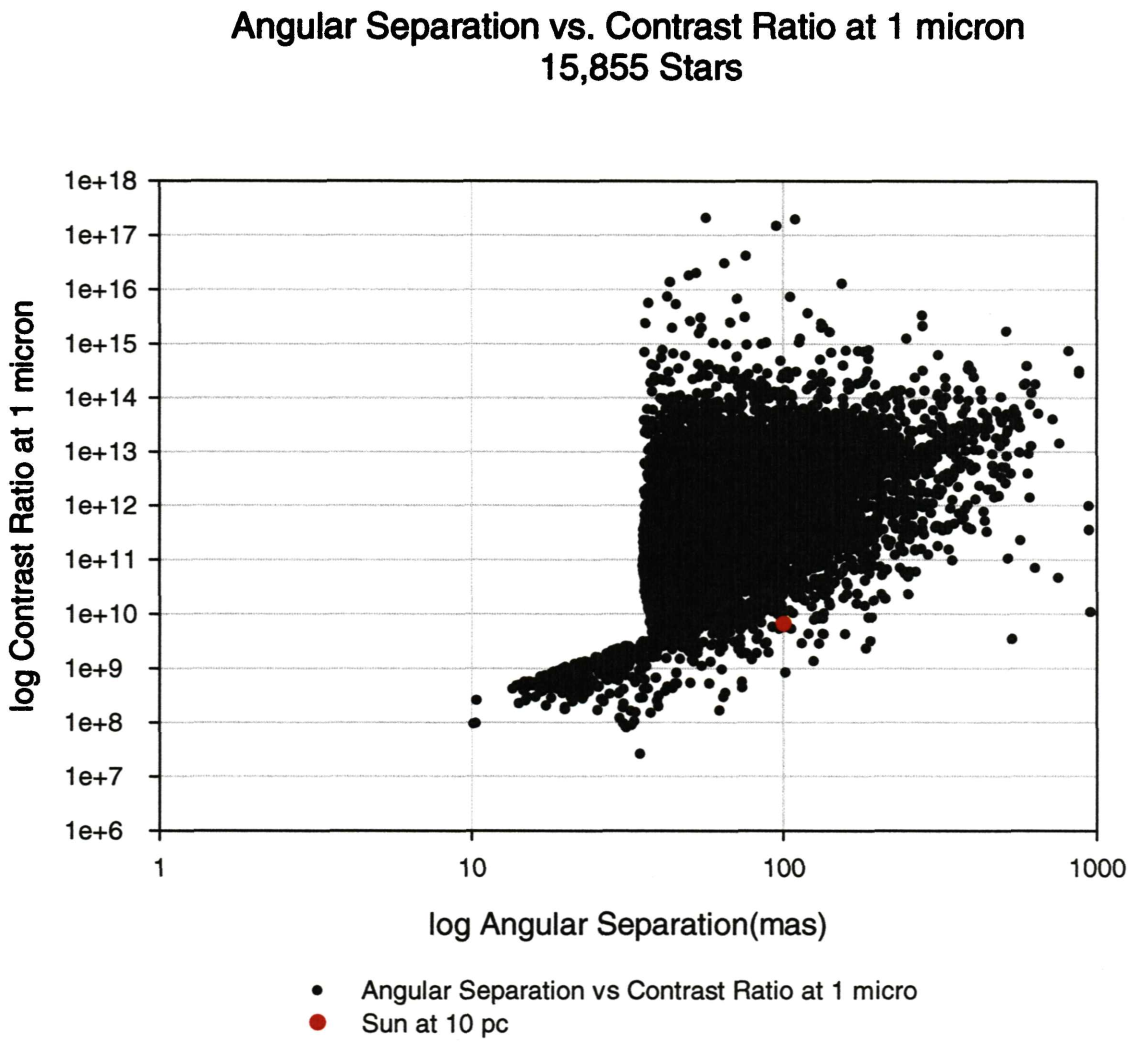

Figure 4: This is the same plot as figure 3 done on a log-log scale in order to more easily see the cutoffs that appeared. The line heading down and to the left is due to our choice of close stars with magnitudes between 7 and 10. The upward cut is caused by the dependency of angular separation on bolometric magnitude.

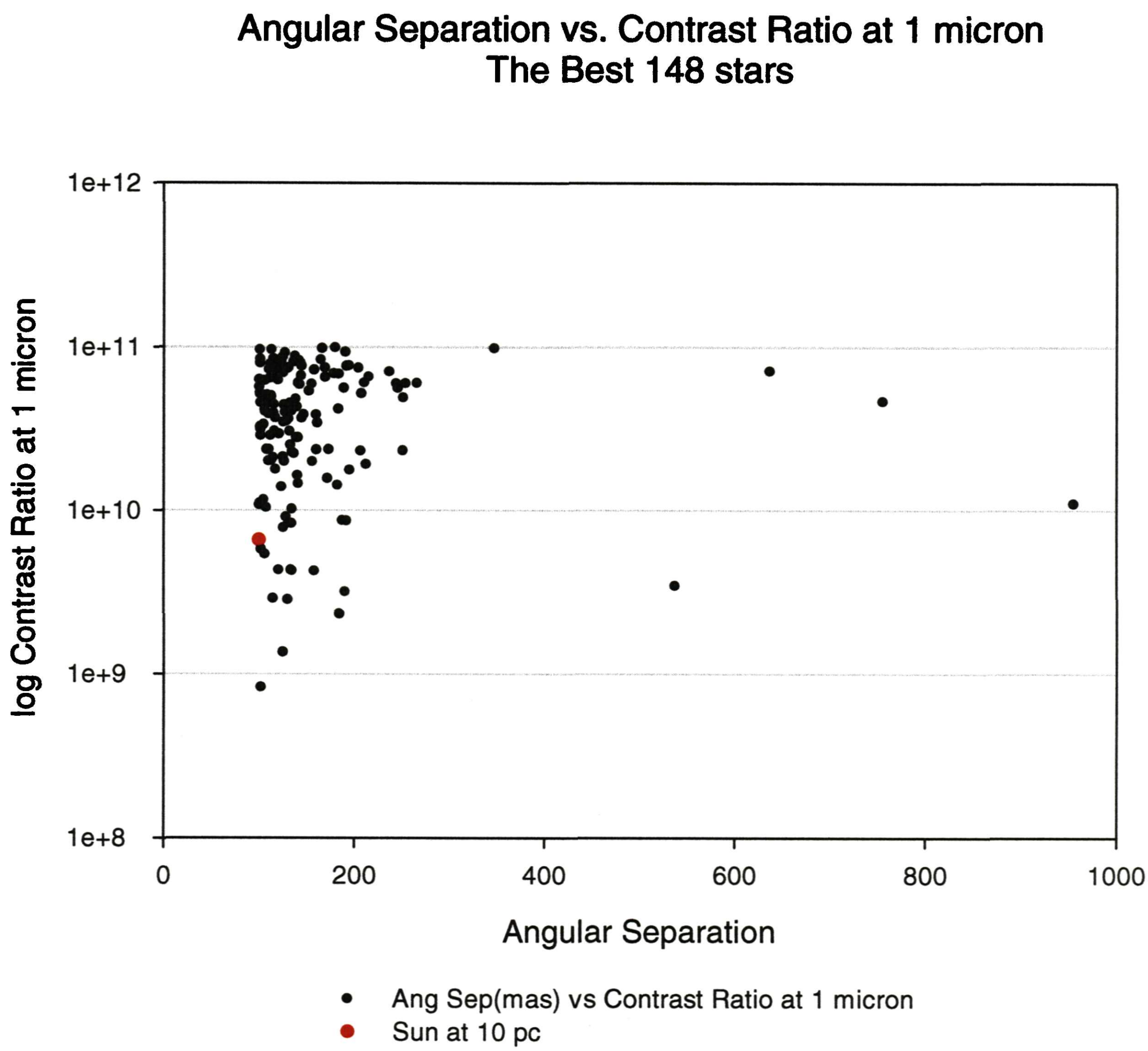

Figure 5: The same angular separation vs. contrast ratio plot done for only the best 148 stars that satisfied the conditions of an angular separation of 100 (mas), or greater, and a contrast ratio of 10^{11}, or less.

had to be carefully looked at through an intensive literature search in order to be positive that the candidates were indeed of interest. Since a complete literature search has not yet been done on the majority of the stars, it is necessary to look at each one with excruciating care, taking extensive measures to verify discontinuities between papers and publications. This is a long process, since each star must be thoroughly examined within the literature to check for main sequence lifetime, variability, and binarity, as well as any odd observations that could arise. Since TPF is interested in detecting Earth-like planets it is necessary that the star be a main sequence, long-lived star, $\geq 10^9$ yrs, and has low variability (~<10%). Binary systems also present problems. A binary system would make detection of a planet more difficult due to the glare from the companion star. The stability of the binary system needs to be looked at as well. Close binaries are not of interest, while those with a separation of 10 arc-seconds or greater are. Using the ViZier web site the literature search was started for these first 148 stars. The project is still in this phase of operation and should be completed in the near future.

3. Future Goals:

After the literature search for these 148 most promising candidates, selection criteria for angular separation and contrast ratio will be relaxed to add a larger number of stars. Depending on the instrumentation used in a certain project, stars with a greater angular separation or a greater contrast ratio might prove interesting. Again, a thorough literature search must be performed on these new additions. This same method of relaxation on the angular separation and contrast ratio, as well as the literature search, will continue until a list of ~200-300 stars can be found that satisfy all requirements. The resulting catalogue will be a good resource for TPF, in addition to being a general catalogue for other missions that require the data found for these stars.

4. Conclusions:

From the beginning, it was known that the project would take longer than time allowed. The necessity for extreme care in selections, calibrations, and verifications made this a reality. The time spent in manipulating the programs and checking calculations only added to the problem. Fortunately, we now have a good calibration that can be used in the future and that can be relied upon. In addition, there will be a more thorough literature search on each of these stars than has previously been performed. As this is an ongoing project, we hope to see completion in the future, resulting in a catalogue that will have many uses and in particular give TPF a starting list for their mission.

References:

Dr. Richard Simon, National Radio Astronomy Observatory, http://www.cv.nrao.edu/~rsimon/aas2001jan.pdf

ViZier, Centre de Données astronomiques de Strasbourg, http://vizier.u-strasbg.fr/viz-bin/Cat?J/A%2bA/352/555

Simbad, http://simbad.u-strasbg.fr/Simbad

Aladin,http://aladin.u-strasbg.fr/java//nph-aladin.pl?frame=launching&-rm=14.1&-server=Aladin

Perryman, M.A.C. et al., 1997, Astronomy and Astrophysics, 323,L49-L52

Prieto C.Allende, Lambert D.L., 1999, Astronomy and Astrophysics, v.352, p.555-562

Di Benedetto G.P., 1998, Astronomy and Astrophysics, v.339, p.858-871

Houdashelt M.L., Bell R.A., Sweigart A.V., 2000, Astronomical Journal. ArXiv:astro-ph/9911367 v1 18 November 1999

Petit M., 1990, Astronomy and Astrophysics Supplement Series 85, 971-987

Petit M., 1989, Astronomy and Astrophysics Supplement Series 77, 497-511

Papers for catalogues used from ViZier:

Hammond, 1927-1982, U.S. Naval Observatory, ViZier catalogue code: I/100A/w10

Boss B., 1937, Carnegie Institute of Washington, 468

Worley, 1983, Published U.S. Naval Observatory, 24, part VII

Morgan, 1933, Published U.S. Naval Observatory, 2nd series, v. XIII

van Altena, W.F., Lee J.T., Hoffleit E.D., 1995, Yale Trigonometric Parallaxes, Fourth Edition

Dommanget, 2000, Astronomy and Astrophysics, 363, 991

Johnson, 1996, Commun. Lunar & Planet Laboratory 4, 99, Table

Kazarovets, 1998, IBVS, 4655, The NSV Supplement Catalog

Gliese,1991, Nearby Stars, Preliminary 3rd Version,V/70A/catalog

Sande (1998) SKY2000 Version 2 Catalog, V/102/sky2000v2

Allen, Poveda, and Herrera, 2000, Astronomy and Astrophysics, v. 356, p. 529-540

Adelman, S.J., 2000, IBVS.4959...1A

Dhillon and Marsh, 1995, MNRAS.275...89D

Kholopov P.N. et. al., 1998, Combined General Catalogue of Variable Stars, ViZier catalogue code: II/214A/gcv

Zakhozhaj V.A., 1979-1996, Vestnik Khar'kovskogo Universiteta 190, 52, ViZier catalogue code: V/101/catalog

Nikoloff I., Hog E., 1982, Perth 75 Catalogue, ViZier catalogue code: I/97/perth75

Smithsonian Astrophysical Observatory Star Catalog, J2000.0 catalogue, ViZier catalogue code: I/131A/sao

Woolley R.v.d.R, Epps E.A., Penston M. J., Pocock S.B., 1970, 1970ROAn....5....1W, ViZier catalogue code: V/32A/catalog

Hoffleit D., Warren Jr W. H., 1991, Astronomical Data Center, ViZier catalogue code: V/50/catalog

Barbera M., et al., 1993, Astrophysical Journal 414, p.846
Keenan(1989), III/150/perkins

Garcia B., 1989, Bulletin Information CDS 36, 27, ViZier catalogue code: III/149/catalog

Guarinos J., 1992, Ph.D. Thesis in Astronomy from Large Databases II, ViZier catalogue code: V/86/ceddu1

Egan M.P., Price S.D., 1996, Astronomical Journal 112, 2862

Worley C.E., Douglass G.G., 1996, Astronomy and Astrophysics Supplement Series 125, 523

Urban S.E., Corbin T.E., and Wycoff G.L., 1997, U.S. Naval Observatory, ViZier catalogue code: I/246/act

Hindsley R., Harrington R., Urban S., 1994, Astronomical Journal 107, 280

Pasinetti-Fracassini L.E., Pastori L., Covino S., Pozzi A., 2001, Astronomy and Astrophysics 367, 521

White N.E., Giommi P., Angelini L., 2000, Laboratory for High Energy Astrophysics, ViZier catalogue code: IX/31/wgacat

Hunsch, Schmitt, Sterzik, and Voges, 1999, Astronomy and Astrophysics Supplement Series 135, 319-338

G.W. Lockwood and B.A. Skiff, 1997, Astrophysical Journal 485,789-811

Fricke W., Kopff A., 1963, Veroff. Astron. Rechen-Inst., Heidelb., No. 10,11, ViZier catalogue code: I/143/fk4_1950

Heiles C., 2000, Astronomical Journal 119, 923

Alekseeva G.A., et al., 1997, Baltic Astron. 6, 481

Gray and Baliunas, 1994, Astrophyscial Journal 427, 1042G

Batten A.H., Fletcher J.M., MacCarthy D.G., 1989, Publ. Dominion Astrophys. Obs. 17

Cayrel de Strobel G., Soubiran C., Ralite N., 2001, Astronomy and Astrophysics 373, 159

Jasinta D.M.D, Raharto M., Soegiartini E., 1995, Astronomy and Astrophysics Supplement Series 114, 487

Henry T.J., McCarthy D.W. Jr, 1993, Astronomical Journal 106, 773

Van Albada-Van Dien E., Panjaitan E., 1987, Astronomy and Astrophysics Supplement Series 68, 117

Luyten W.J.,1940-1987, Publ. Astr. Obs. Univ. Minnesota III, part 3, 35

Marsakov V.A., Shevelev Yu.G., 1988, CDS Inf. Bull., 35, 129

Alzner A., 1998, Astronomy and Astrophysics Supplement Series 132, 237

Ochsenbein F., Halbwachs J.L., 1988, Bull. Inform. CDS 32, 83

Maggio A., et al., 1990, Astrophysical Journal 348, 253

Chen Y.Q., Niessen P.E., Benoni T., Zhao G., 2001, Astronomy and Astrophysics 371, 943

Hog E., et al., 2000, Astronomy and Astrophysics, ViZier catalogue code: I/259/tyc2

To: Al Wootten

From: Tim Thacker

Date: Wednesday, August 01, 2001

Subject: Summer Student Report

The summer was spent in NRAO's Central Development Lab on Ivy Rd in Charlottesville. There I performed a variety of tasks for the engineers. Programming in Visual Basic was done to automate numerous, tedious tasks. Finding the least expensive parts and obtaining quotes from the companies for an intermediate frequency amplifier system for the new ALMA cryogenic Dewar was also performed. The design of amplifier circuits for amplifier gain stability measurements from rack equipment, and modification to the designs of a mixer bias supply were also completed. Those designs were followed by the construction of an amplifier and the repair and modification to the mixer bias supply. Semi-rigid cables, coax cables, heat straps and other parts were fabricated for the new receiver being built for ALMA.

I had to learn Visual Basic to begin coding the various programs that would replace the need for workers to take the time to perform tedious tasks that can be automated. As I already had knowledge of the programming language C++, this task was not as hard as it sounds. The advantage of learning VB is that it has the capability of integrating with MS Excel. This is very useful because it gives the programmer the power to write programs to store data straight to Excel. The first program I completed was a Zero Calibration command for a HP Power Meter. The program initializes the meter and checks for the proper conditions for zeroing to begin. The program then sends the command to start the calibration, and monitors the meter for the completion of the process. The program serially polls one of the meter's status bytes to find out when zeroing has been completed. When the zeroing has finished, the program recognizes this and can be set to immediately start taking data. The LakeShore Temperature Monitor was another piece of equipment for which I wrote a data acquisition program. The program sets up and initializes communication with a LakeShore 218 Temperature Monitor, and reads the data off of various channels.

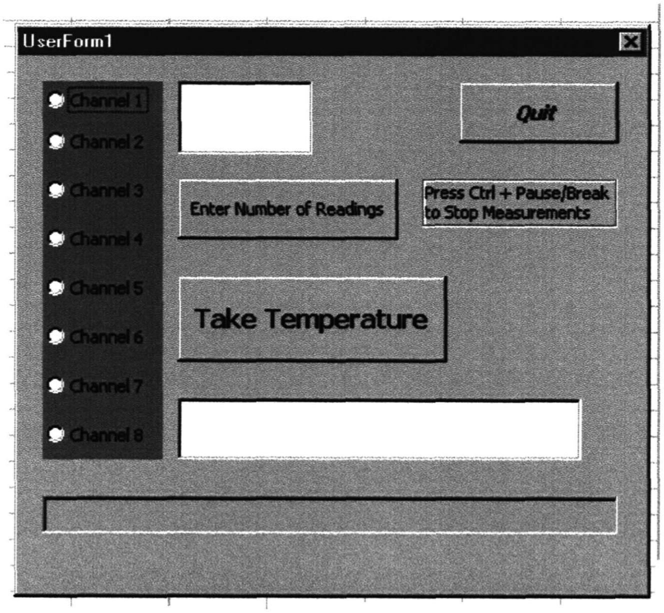

Figure 1: Lakeshore Temperature Meter Software Input Dialog

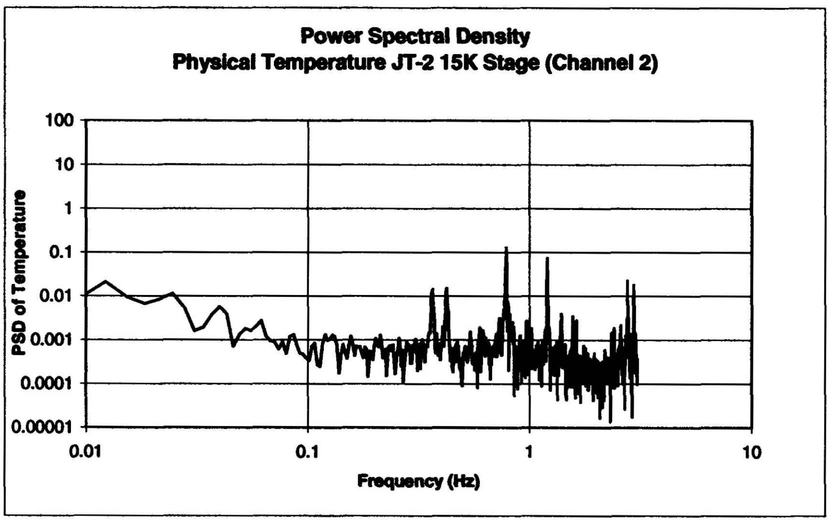

Figure 2: FFT'd results for Lakeshore Temperature Meter Software

The LakeShore Temperature Monitor program takes 30 measurements from a user-selected channel, and averages these readings together. The program will repeat this function until it has done it a specific number of times to which the user has selected. The average of the 30 readings is stored into an array the same size as the total number of readings, and then copied from the array to an Excel spreadsheet. This program provides temperature data in a format suitable for computation of the Fourier Transform, which I did not write, (See Figure 2) that shows temperature spikes at certain repetition rates.

I also wrote a program to monitor and control the temperatures of another cryogenic Dewar system. The program uses the computer's COM port to communicate with an Omega CYD208 Temperature Monitor, and through a GPIB board to control a HP power supply, which is used to control a heater that is connected to the device under test.

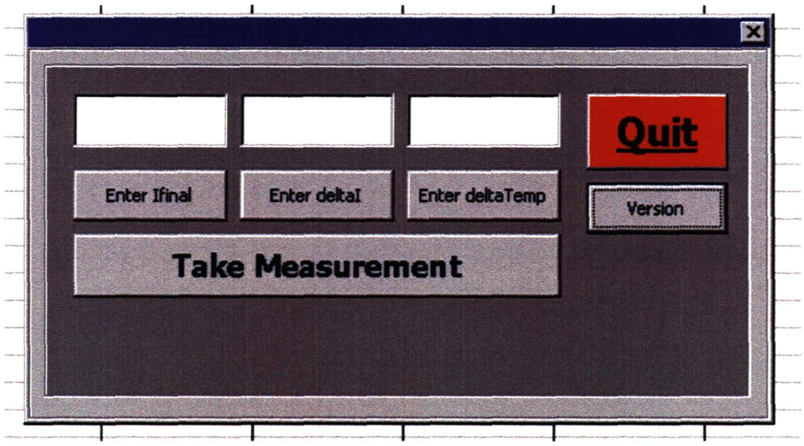

Figure 3: Omega Temperature Meter Input Dialog Box

The program cycles through three channels, taking readings off of them; it takes a temperature reading and a voltage reading off the same channel and then moves on to the next channel. After all three channels have been read, the program reads the current and voltage levels of the power supply. The power supply current is then increased by some amount the user has defined (Figure 3), which increases the temperature of the device under test. The program then runs a test on the temperature monitor to see if the temperature has settled after the power supply has been commanded to the new voltage and current. The test takes 25 readings from each channel on the monitor and creates a standard error. It then compares this error to an error limit the user has input (Figure 3) and if the standard error is within the limit then the program proceeds to repeat this entire cycle. If the standard is outside the limit then the program takes another 25 readings from the channel and tests the standard error. A special test is performed if the standard error is outside the limit and the channel is on channel 3. The program tests to see if the Cryogenic Dewar is out of helium.

In another programming job, I edited the code for the chopper wheel used to take hot/cold load measurements for the Cryogenic Dewar tests. The code had been originally written for a chopper wheel that was approximately twice as big as the current wheel. The wheel's hold current, velocity, and start/stop acceleration had to be adjusted to optimize its performance.

One of the toughest programming tasks was to code for a sweeping circuit using a digital potentiometer. The Digital Pot was constructed using a cascading wiper design. This design required the program to have a continuous loop, as to keep the sweep running, and to be able to change the wipers on the pots to obtain different output values. The outside wipers in the configuration are used to control the sweep's voltage limits, while the inside wipers are cascaded together to allow for the sweeping motion (Figure 4).

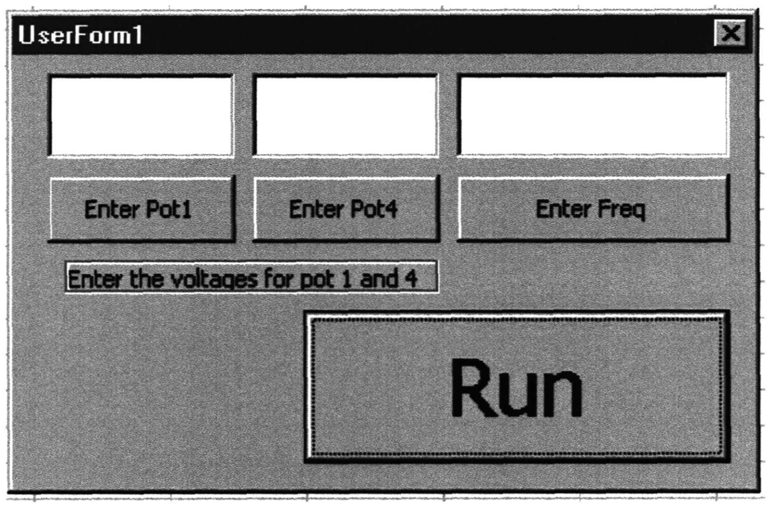

Figure 4: Xicor Digital Potentiometer Input Dialog Box

The trick was to get the cascading wipers to transition smoothly. One of the inside wipers would start its sweep while the other wiper was disabled. Once the first sweeping wiper had reached its limit, the program enables the second wiper, starts its sweep and disables the first wiper all in the same cycle in the loop. The problem encountered on this project was that during the sweep, on the ramping up, the signal produces a spike. The spike occurs at the point where the wipers are switching (enabling/disabling themselves). I believe that these spikes are occurring due to some hardware configuration problems. I think this because when the pots and their wipers are set up in a different configuration, the spikes were still there, but were on the ramp down section of the sweep, instead of the ramp up section. No software was changed when this happened, so this leads me to believe that the problem lies within the hardware.

The hardware design aspect of the summer job was particularly interesting. I was given the task of designing an amplifier circuit that would give a gain of 100 to a signal going into a spectrum analyzer. This would provide the analyzer with a stronger signal for which it could read. This was an interesting task because I had to find an OP-Amp with a gain-bandwidth product of 10 MHz. I found one that had an internal gain of 100, with a frequency range of up to 100 MHz, and it was a low-noise, low-distortion amplifier. The Burr Brown INA103 was just the right OP-Amp for this application. I had to add some voltage regulators to supply power to the amplifier, and some capacitors to filter out any DC noise and smooth out the signal. The other job in design was that I helped modify an old mixer Bias II supply. We basically updated it to be the equivalent of the newer Bias IIC boxes that are on the racks now.

I was able to follow up on my design projects. I constructed the amplifier I designed, and modified the Mixer Bias II box. The amplifier was soldered onto a perforated board and ±15 V regulators were also mounted to the board as well to provide power to the IC. Electrolytic capacitors were also added across the output and ground of the regulators to enhance the noise stability of the regulators' output to the IC. The Bias II box modifications were fairly simple to complete. The hardest part of those modifications was the part when I had to troubleshoot why the potentiometers were not being as sensitive as they should and why when in the hold position the zeroing push button switch wasn't holding the zero, a leak was occurring. The grounding wire on one of the pots had been severed, and once I reconnected it to the ground lead on the board, the problem of the potentiometer's sensitivity was solved. Replacing the dual OP-Amp on the circuit board with two single OP-Amps solved the voltage leak that was occurring. The other tasks for this modification were the addition of wafer switches to control the output impedance and RUN/ZERO/GRND states, OSC/INT switch, UP/HOLD/DOWN switch to control the sweep, and a push button zeroing switch. Another addition to the design was a "÷ by 10" switch, this allowed the user to have better sensitivity over the pots by using a simple voltage divider circuit. I also did some fabrication work. I made 4 semi-rigid, coax cables and 4 heat straps (Figure 5) for the new cryogenic Dewar. The cables were cut to be 4½ inches long and stripped down to the center pin on each end. This was a chore because stainless steel cable both inside and outside is very tough. Once the ends were stripped, they were copper flashed (this helps in the soldering process), and then SMA male connectors were soldered to the ends. The heat straps were made by taking copper braids, and shoving them into wave-guide. They were then soldered into place using a MAPP gas torch. Holes were then drilled into the wave-guides and then the ends were gold plated.

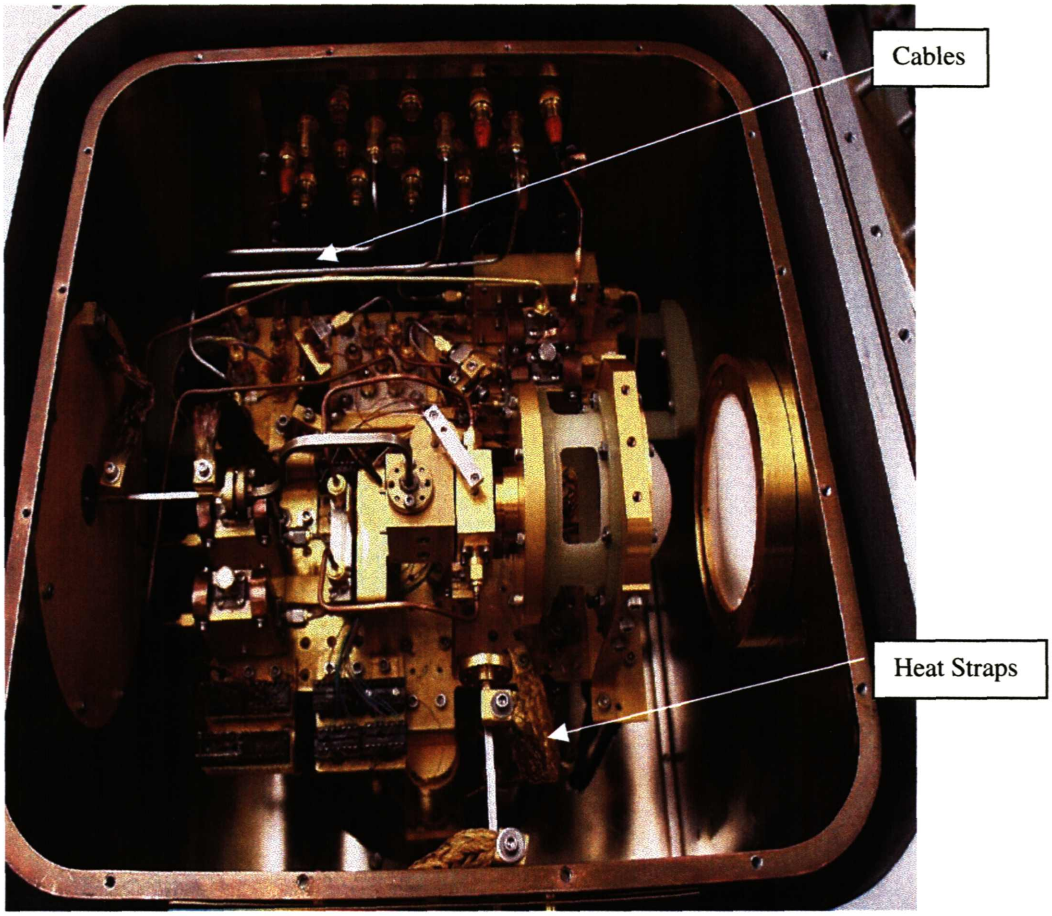

Figure 5: Cryogenic Dewar System with labels for the pieces I fabricated

The misc. work I did this summer was the task of getting quotes for pricing and delivery from various companies to build a new IF plate. This was an important task for this process because it is one of the easiest ways for the CDL to save money. By finding the company that had the best part, for the best price, engineering can help minimize NRAO's expenses. I also helped the another summer student, Zach Manganello, assemble and test a Haystack Small Radio Telescope. I mostly helped him with the physical labor of the project and some of the wiring.

I would like to extend special thanks to the man I worked under, John Effland, along with John Webber and the rest of the CDL staff. Thanks go to NSF and AUI for their funding and support of NRAO and its summer student program as well.

The following attached pages are excepts from the programs I have written, reports about them, flowcharts of them, and other various documentation of my work this summer.

To: John Effland
From: Tim Thacker
Date: Tuesday, June 25, 2001
Subject: HP E4418B – EPM SERIES POWER METER ZEROING CODE

This program automates the power meter 'zeroing calibration command', for the HP E4418B – EPM Series Power Meter. The program communicates with the power meter through a GPIB board.

For accurate measurements the power meter must be 'zeroed' at least once before data is taken. The power meter zeroing process checks the power reading while no power sources are present, hence zero power should be read; but the meter reads a weak power signal. The meter notes this reading and subtracts it from later measurements thus giving the user a set of data with a specific reference. Now this process has been automated and can be executed by this program.

The code instantiates several objects obtained from custom OLE libraries on the server. These modules are called from the function `oPwrMtr.bInit` (`Figure 1`). The three main forms and modules are the `Form1` form, and the `CGPIB` and `CHP4418B` class modules. The form, `Form1`, is the highest level piece of code. It calls the functions that talk to the board and meter, and is basically the link from the user to the meter. The form starts by initializing the meter and setting up a window of command options for the user to choose from (as in `Figure 2`). It lets the user choose either to start the zeroing calibration or to exit the program by hitting the ESC key. The form also initializes a sub-routine, `KeyPreview = True`, that continuously checks to see if the user has pressed the ESC key (at the top in `Figure 2`). Once the ESC key has been pressed, the program resets the power meter and unloads the program (`Figure 3`). This function is basically a kill command. It allows the user to exit the program quickly if they have forgotten to set something up without having to wait for the zeroing process to be completed. When the user presses the ESC key, the function called writes the command `*RST` to the power meter before unloading the program; this resets the meter to its power on state (the write statement in `Figure 4`).

The user clicks the 'Start Zeroing' button to start the zero calibration routine (as illustrated in `Figure 5`). This routine writes to the GPIB board the command to start the zero calibration (`Figure 6`). The board passes this command to the meter, and the program also monitors the board and meter to see if the command has been sent and accepted, if not, error messages pop up and the program is ended. This routine (`Figure 5`) calls the function `oPwrMtr.bZero` (`Figure 6`). This function writes the command `*CLS;CAL:ZERO:AUTO ONCE; *ESE 1` to the meter. The function writes `*CLS` to the meter to clear the status register. This allows the program to check to see if the meter is finished zeroing (`bIsZeroingDone in Figure 7`). The `CAL:ZERO:AUTO ONCE` write to the meter is the command for the meter to start zeroing. The write `*ESE 1` is the command to enable the event status register bit 1. The program next calls 'the function `bReturnWhenZeroingDone`, which serial polls the meter to find out when it has finished zeroing (call made from `Figure 5`). The meter sets a specific register bit to indicate when it has finished zeroing and the program (`bIsZeroingDone in Figure 7`) tests the meter to find when that bit changes. It checks this bit by writing to the meter `*OPC` (the write in `Figure 8`), which tells the meter to set a bit when it has completed its task, and polling the meter's bit (`Figure 8 & 9`) and returning whether or not the meter is busy. `bReturnWhenZeroingDone` loops this function (loop is contained in `Figure 7`) until the meter has finished zeroing and returns a bit of ready to send data. `bIsZeroingDone` checks for a bit value of decimal 32, which is set when the meter is finished zeroing, and returns True (to `Figure 7`) if it has. So now the program knows when the meter is finished zeroing and ready to take data. The routine waits until the meter is ready and then sends the command to return the power meter's measurements (`Figure 5` also shows that it displays the reading in a text window). When the program has finished executing, it resets the meter to the power on state.

Class Diagram of Power Meter Program

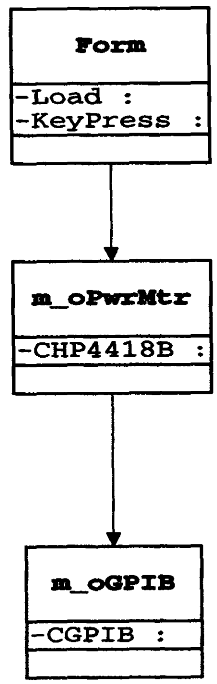

02	tnt	2001-06-04	addition of esc command
01	tnt	2001-05-20	additions of functions
Rev	Who	Date	Notes
National Radio Astronomy Observatory			
Power Meter Zeroing Routines			
Creator: tthacker		Edit Date: 2001/8/3 08:57	
File: Drawing3		Rev: 01	Page 1 of 1

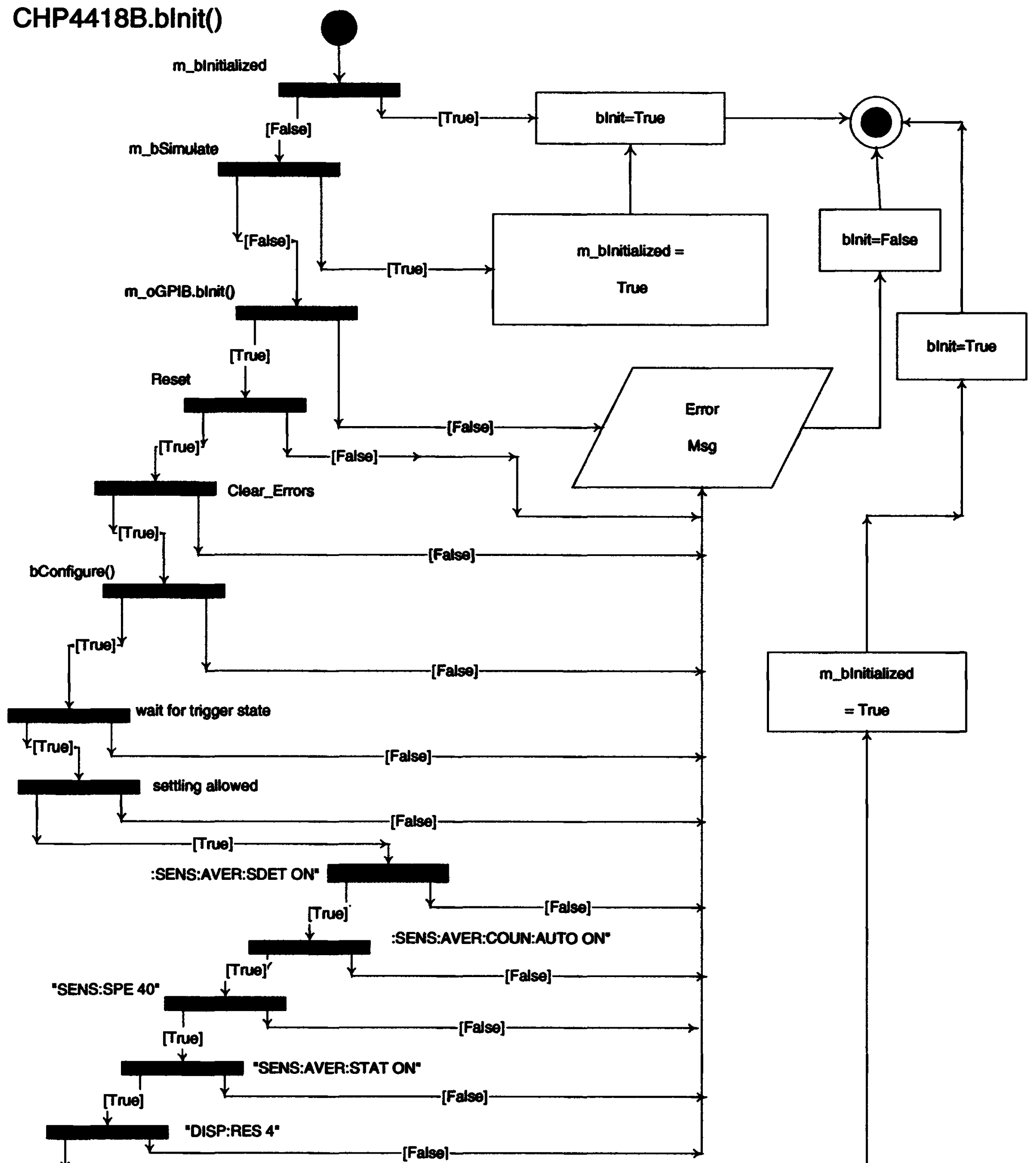

02	tnt	2001-06-04	addition of esc command
01	tnt	2001-05-20	additions of functions
Rev	Who	Date	Notes
National Radio Astronomy Observatory			
Power Meter Zeroing Routines			
Creator: tthacker		Edit Date: 2001/7/24 09:21	
File: PwrMtrdiagrams2.doc		Rev: 01	Page 7 of 10

Figure 1: oPwrMtr.bInit
This function is one of the most important functions. It initializes the power meter. If this function was not called, the user could not communicate to the meter at all.

Sub Form_Load()

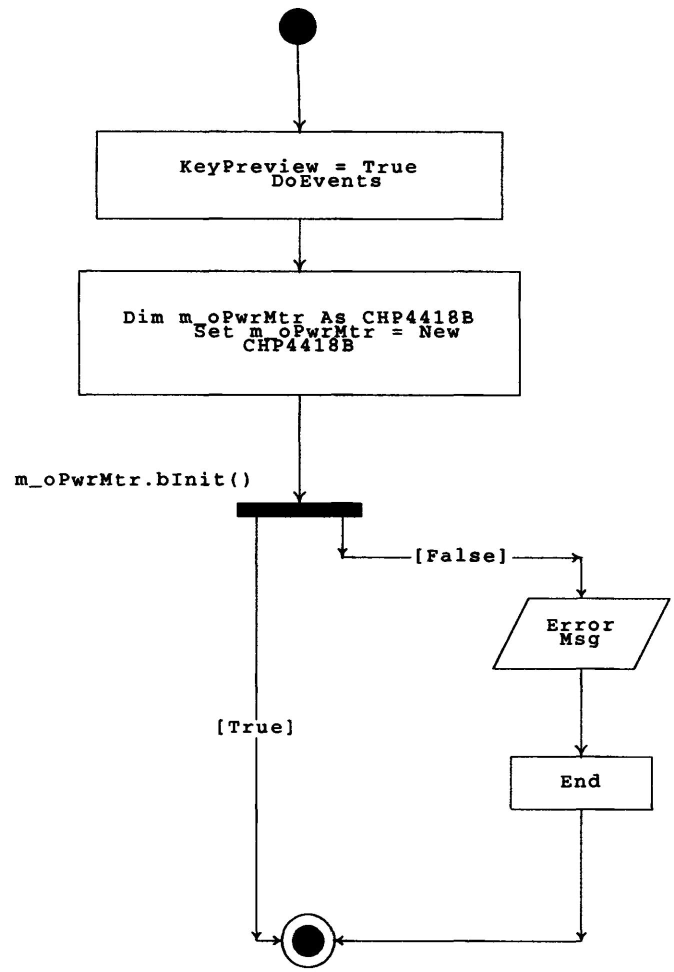

Rev	Who	Date	Notes
02	tnt	2001-06-04	addition of esc command
01	tnt	2001-05-20	additions of functions
National Radio Astronomy Observatory			
Power Meter Zeroing Routines			
Creator: tthacker		Edit Date: 2001/7/24 14:27	
File: PwrMtrdiagrams1.doc		Rev: 02	Page 1 of 10

Figure 2: Sub Form_Load()

This figure outlines how the program initializes the meter while it is loading the form.

Sub Form_KeyPress(iKeyASCII As Integer)

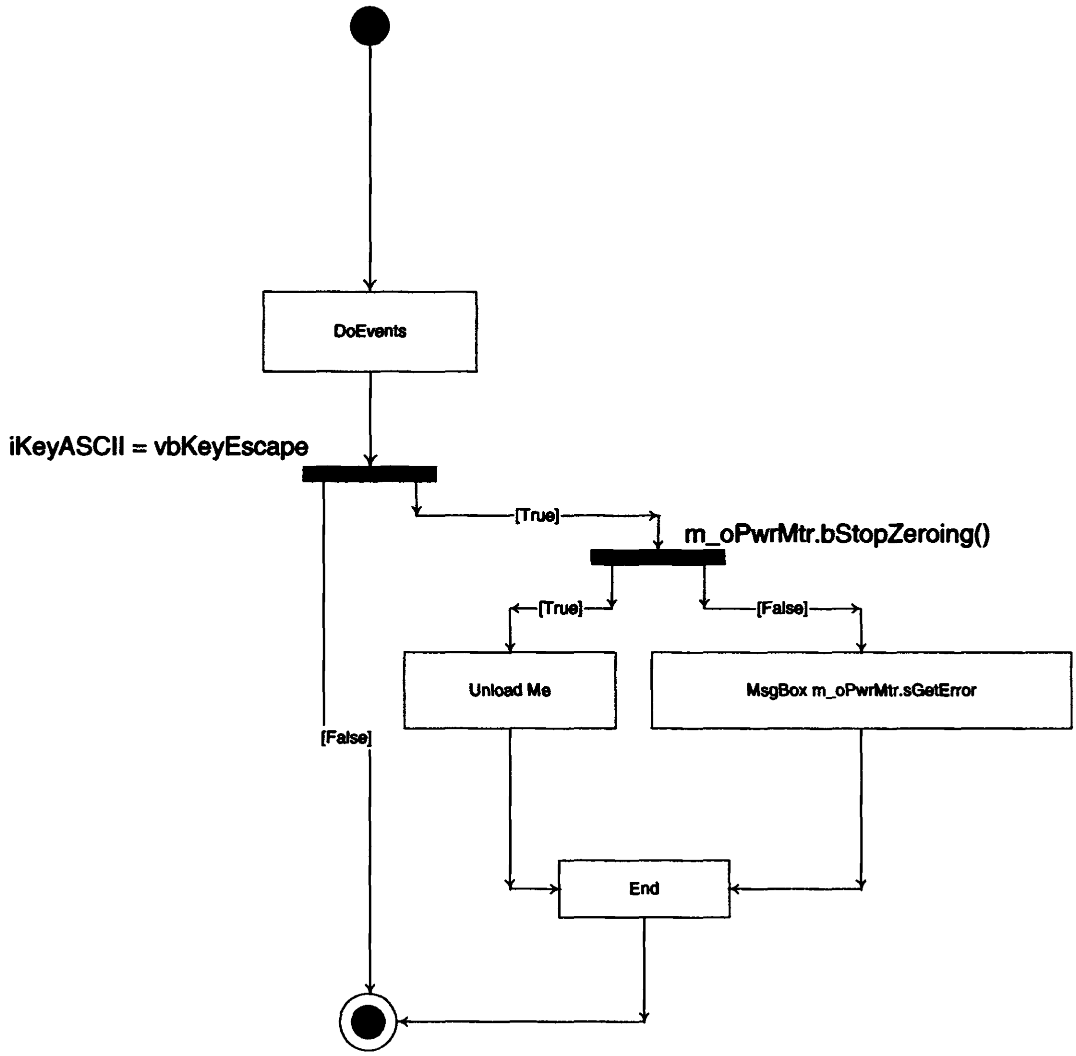

02	tnt	2001-06-04	addition of esc command
01	tnt	2001-05-20	additions of functions
Rev	Who	Date	Notes
National Radio Astronomy Observatory			
Power Meter Zeroing Routines			
Creator: tthacker		Edit Date: 2001/8/1 16:39	
File: PwrMtrdiagrams1.doc		Rev: 01	Page 3 of 10

Figure 3: Sub Form_KeyPress()
The program monitors the keyboard to check to see if the ESC key has been pressed, if the user presses the ESC key to end the program, this sub-routine will call the function bStopZeroing.

CHP4418B.bStopZeroing()

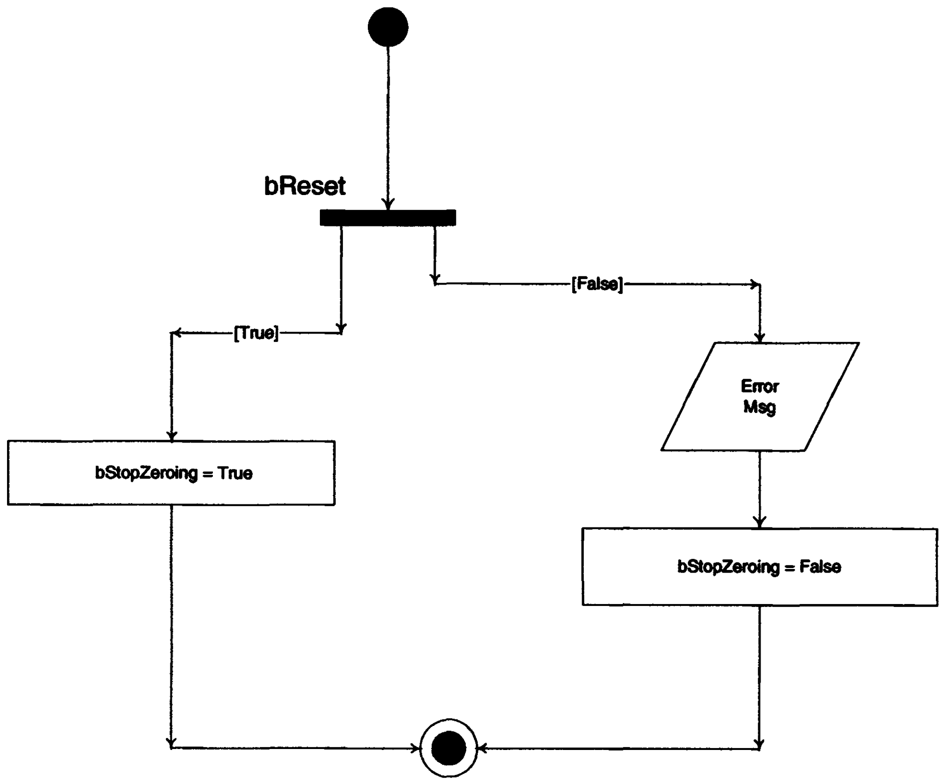

02	tnt	2001-06-04	addition of esc command
01	tnt	2001-05-20	additions of functions
Rev	Who	Date	Notes
National Radio Astronomy Observatory			
Power Meter Zeroing Routines			
Creator: tthacker		Edit Date: 2001/7/24 09:21	
File: PwrMtrdiagrams2.doc		Rev: 01	Page 10 of 10

Figure 4: bStopZeroing
When the user presses the ESC key, the sub-routine Form_KeyPress calls this function to send a command to the meter to stop doing everything and reset itself.

Sub Zeroing_Click()

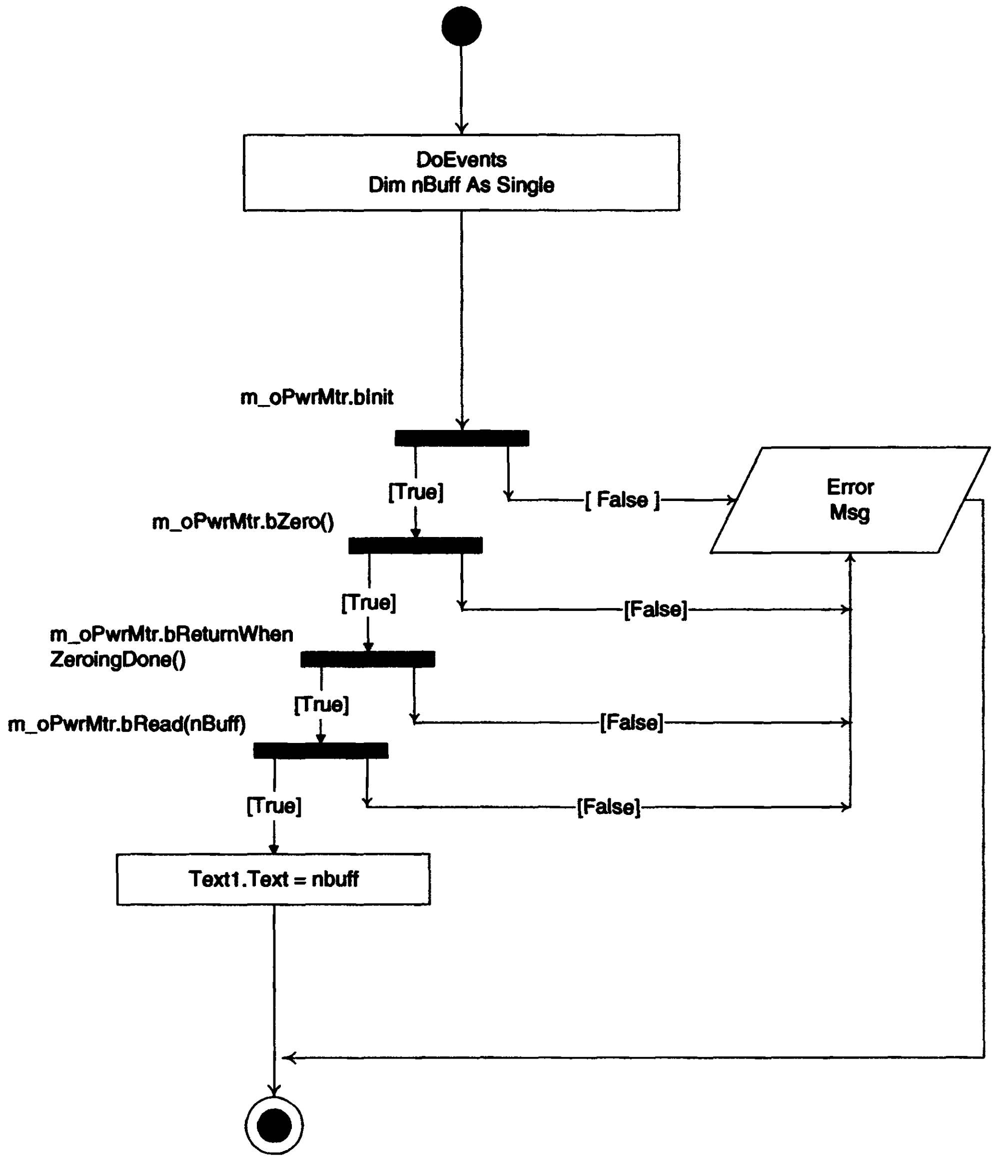

Rev	Who	Date	Notes
02	tnt	2001-06-04	addition of esc command
01	tnt	2001-05-20	additions of functions
National Radio Astronomy Observatory			
Power Meter Zeroing Routines			
Creator: tthacker		Edit Date: 2001/7/24 14:30	
File: PwrMtrdiagrams1.doc		Rev: 01	Page 2 of 10

Figure 5: Sub Zeroing_Click

When the user clicks this button, the program starts the zeroing calibration command (bZero), and also checks to see if zeroing ahs complete (bReturnWhenZeroingDone)

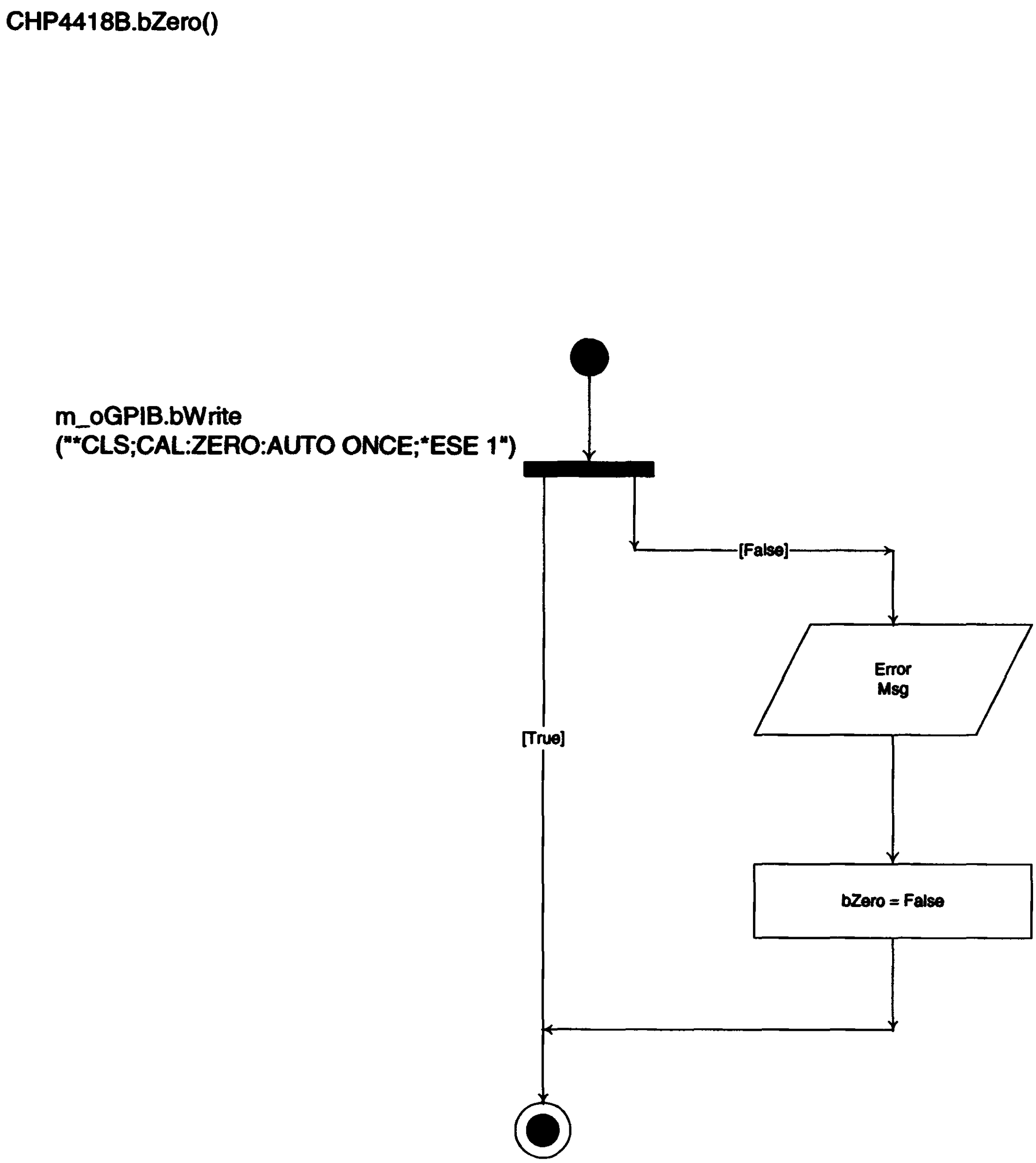

Rev	Who	Date	Notes
02	tnt	2001-06-04	addition of esc command
01	tnt	2001-05-20	additions of functions

National Radio Astronomy Observatory		
Power Meter Zeroing Routines		
Creator: tthacker	Edit Date: 2001/7/24 09:19	
File: PwrMtrdiagrams1.doc	Rev: 01	Page 4 of 10

Figure 6: oPwrMtr.bZero
This figure demonstrates the bZero function. The function writes the command to clear the status register, zero the meter and enable status bit 1 in the status register to the meter.

CHP4418B.bReturnWhenZeroingDone(ByRef bReturn As Boolean)

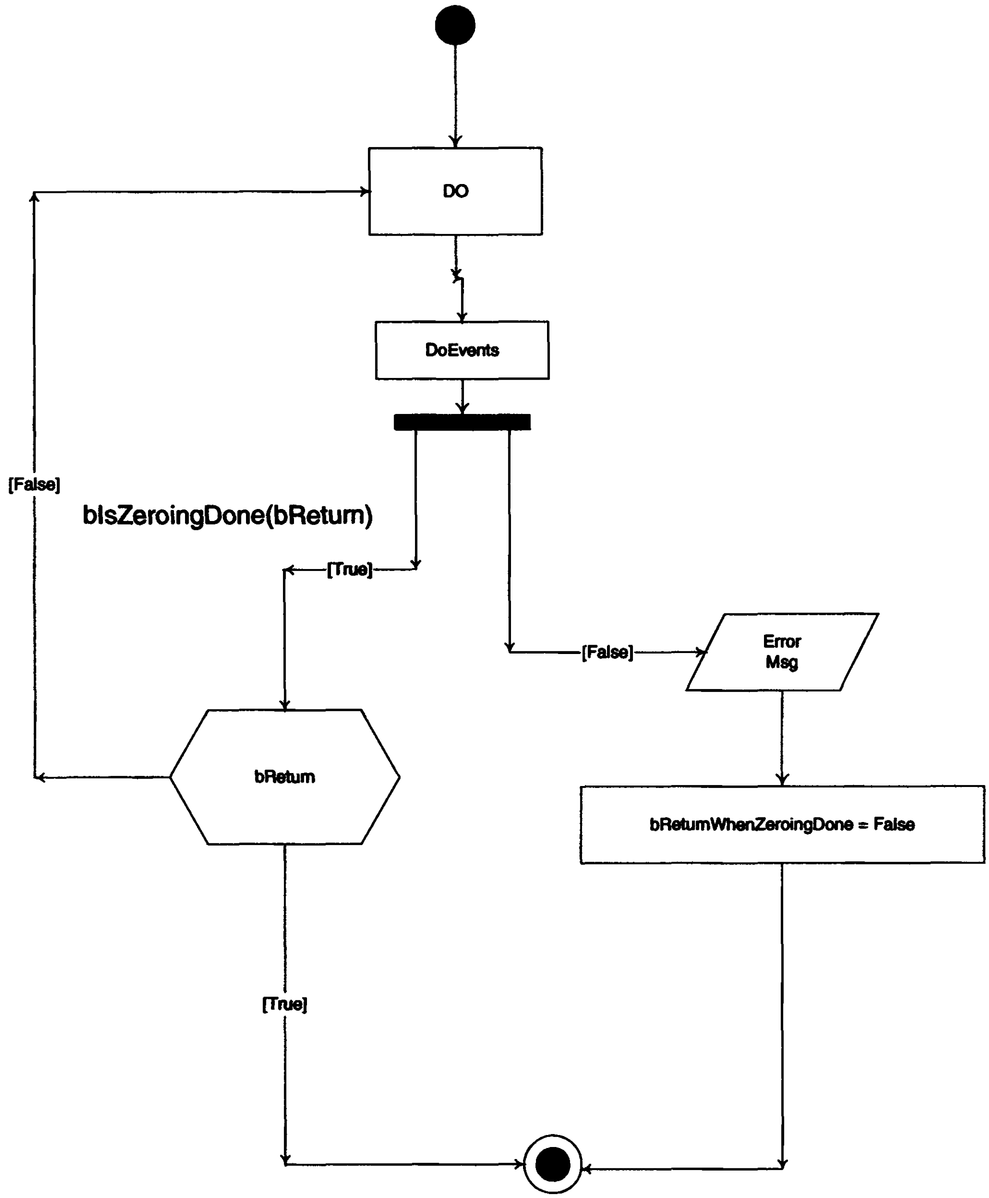

02	tnt	2001-06-04	addition of esc command
01	tnt	2001-05-20	additions of functions
Rev	Who	Date	Notes
National Radio Astronomy Observatory			
Power Meter Zeroing Routines			
Creator: tthacker		Edit Date: 2001/7/24 09:21	
File: PwrMtrdiagrams2.doc		Rev: 01	Page 9 of 10

Figure 7: bReturnWhenZeroingDone
This is the function called by sub-routine Zeroing_Click. It calls the bChckOper & and bIsZeroingDone functions and contains the loop that checks to see if the meter has completed its task.

CHP4418B.bIsZeroingDone

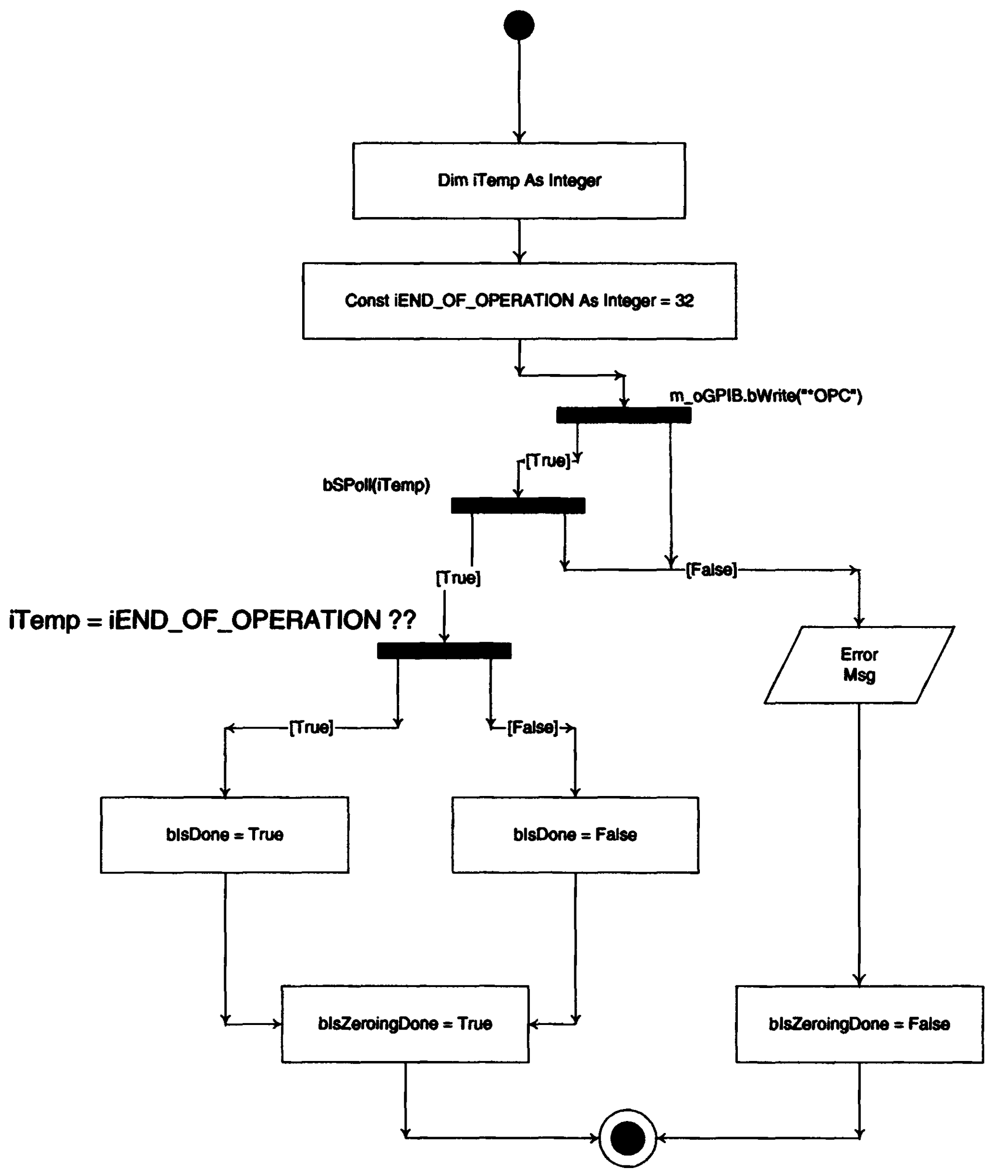

Rev	Who	Date	Notes
02	tnt	2001-06-04	addition of esc command
01	tnt	2001-05-20	additions of functions

National Radio Astronomy Observatory	
Power Meter Zeroing Routines	
Creator: tthacker	Edit Date: 2001/8/1 16:39
File: PwrMtrdiagrams1.doc	Rev: 01 — Page 5 of 10

Figure 8: bIsZeroingDone
This function is called from the function bReturnWhenZeroingDone, and it is the function that serial polls the meter to find out when the status bit changes.

CHP4418B.bSPoll()

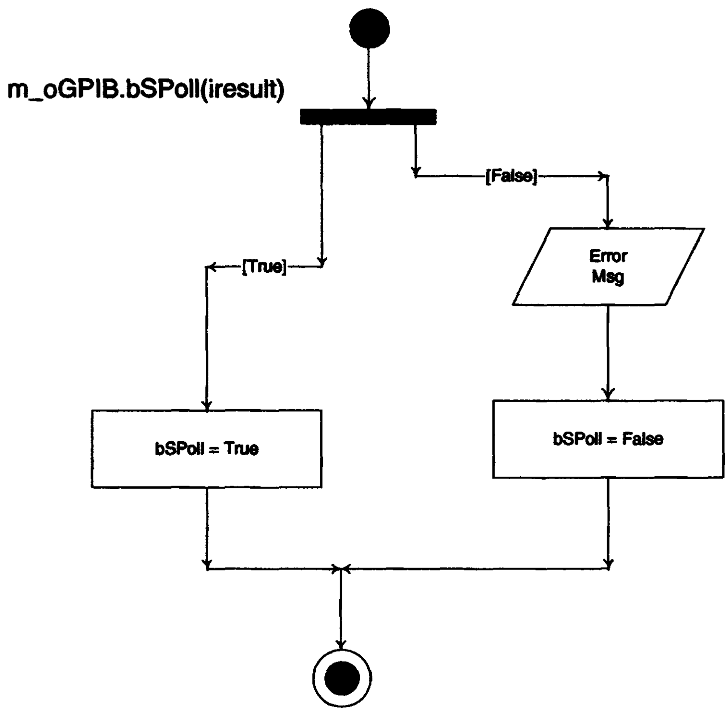

Rev	Who	Date	Notes
02	tnt	2001-06-04	addition of esc command
01	tnt	2001-05-20	additions of functions

National Radio Astronomy Observatory		
Power Meter Zeroing Routines		
Creator: tthacker	Edit Date: 2001/7/24 09:21	
File: PwrMtrdiagrams2.doc	Rev: 01	Page 6 of 10

Figure 9: bSPoll
This function writes to the board the command to serial poll the meter, and return an error message if the write is unsuccessful in any way.

```
)ption Explicit
)im m_oPwrMtr As CHP4418B
'***************************************************************
'ublic Sub Form_Load()
    'This sub-routine loads the form of the program which sets the
    'module-object = to the class module and initializes the power meter.
    '   2001-05-17 tnt

    'keypreview is set to allow computer to watch for keystrokes
    KeyPreview = True
    DoEvents

    'sets meter up as m_oPwrMtr
    Set m_oPwrMtr = New CHP4418B

    'Provides intializations, I/O statements, error messages, etc...
    If Not m_oPwrMtr.bInit(False) Then
        MsgBox m_oPwrMtr.sGetError
        Unload Me
    End If

End Sub
'***************************************************************
?rivate Sub Form_Terminate()
    Set m_oPwrMtr = Nothing
End Sub
'***************************************************************
?rivate Sub Zeroing_Click()
    'The zeroing_click routine performs the zeroing calibration; it
    'writes to the meter to zero, then serially polls the meter to
    'find out if it has finished zeroing.
    '   2001-05-17 tnt

    DoEvents
    'Initializes teh variables
    Dim nBuff As Single

    'Provides intializations, I/O statements, error messages, etc...
    If Not m_oPwrMtr.bInit(False) Then
        MsgBox m_oPwrMtr.sGetError
        Unload Me
    End If

    'writes to bus and tells meter to zero itself
    If Not m_oPwrMtr.bZero() = False Then
        MsgBox m_oPwrMtr.sGetError
        Unload Me
    End If

    'polls meter to determine if zeroing has complete
    If Not m_oPwrMtr.bReturnWhenZeroingDone(False) Then
        MsgBox m_oPwrMtr.sGetError
        Unload Me
    End If

    'reads meter and stores in nBuff
    If Not m_oPwrMtr.bRead(nBuff) Then
        MsgBox m_oPwrMtr.sGetError
        Unload Me
    End If

    Text1.Text = nBuff
End Sub
'***************************************************************
?rivate Sub Form_KeyPress(iKeyASCII As Integer)
    'The form_keypress routine monitors the keyboard to check to see
    'if any keys have been pressed, and if the ESC key was pressed,
    'the program unloads itself.
    '   2001-05-17 tnt
```

```
    DoEvents
    If iKeyASCII = vbKeyEscape Then 'checks to see if the esc key was pressed
        If Not m_oPwrMtr.bStopZeroing() Then
            MsgBox "Power was not stopped!"
        End If
        Unload Me
        End
    End If
End Sub
```

```
' Agilent 4418B Power Meter class
'
' 2001-01-19 jee Genesis from CHP436
' 2001-01-22 jee Added bGetErrors
' 2001-03-08 jee added m_sGOTO_WAIT_FOR_TRIG_STATE
' 2001-06-01 tnt added bZero, bSpoll, bReturnWhenZeroinDone,
'                bIsZeroingDone, bStopZeroing
' State Diagram for Power meter
'
'
'                         +------------+
' :Abort or *RST -------> | Idle State | <----------------------+
'                         +------------+                        ^
'                               |                               |
'                               |                               |
'                               v                               |
'                     +--------------------------+              |
'                    <  INIT[:IMM or :CONT ON] ? >--NO--------->+
'                     +--------------------------+              ^
'                               |                               |
'                              YES                              NO
'                               |                               |
'                               |                         +----------------+
'                               +<------------YES------ <  INIT:CONT ON?   >
'                               |                         +----------------+
'                               |                               ^
'                               v                               |
'TRIG: SOUR IMM          +----------------------+               |
'     : or BUS   ------->|  Wait for Trig State | TRIG:IMM -+   |
'     : or HOLD          +----------------------+           |   |
'                               |                           |   |
'                               |                           |   |
'                               v                           |   |
'                        +---------------------+            |   |
'                        | Wait state TRIG:DEL |            |   |
'                        +---------------------+            |   |
'                               |                           |   |
'                               |                           |   |
'                               +<--------------------------+   |
'                               |                               |
'                               |                               |
'                        +-----------------+                    |
'                        | Triggered State | -------------------+
'                        +-----------------+
'                          |           ^
'                          |           |
'                          v           |
'                        +-----------------+
'                        | Measurements    |
'                        +-----------------+
'
'

'
Option Explicit

' To test all logic except GPIB calls, set this to TRUE
' That is, this allows the software to be used at a machine that isn't
'   connected to any GPIB equipment
Private m_bSimulate As Boolean

' declare reference to GPIB object.
Private m_oGPIB As CGPIB

Private Const m_iGPIB_ADDRESS As Integer = 13        ' GPIB address for 4418B power meter

Private m_sError As String                           ' string containing last error message
Private m_iError As Integer                          ' integer containing last error number
```

```
'     ,m_iError = m_oGPIB.iGetError()
        bReset = False
        Exit Function
    End If

    If Not m_oGPIB.bWrite(m_sRESET) Then
        ' errors resetting unit
        m_sError = "Routine: CHP4418B.bReset: Error resetting Agilent 4418B power meter." & vbCr &
_
                   vbCr & "Routine generating error:" & vbCr & _
                   m_oGPIB.sGetError
        m_iError = m_oGPIB.iGetError()
        bReset = False
        Exit Function
    End If

    m_bInitialized = False

    ' no errors
    bReset = True
End Function
'*****************************************************************
Public Function sGetError() As String
    ' Returns 438 error string
    '1998-09-08 jee    '

    sGetError = m_sError
End Function
'*****************************************************************
Public Function SetSimulate(ByVal bSimulate As Boolean)
    ' sets the class for simulation
    '
    ' Calling Parms: bSimulate - if TRUE, then simulate
    '
    ' 2000-03-13 jee

    m_bSimulate = bSimulate
End Function
'*****************************************************************
Public Function iGetError() As Integer
    ' Returns power meter error number
    ' 2001-01-19 jee

    iGetError = m_iError
End Function
'*****************************************************************
Public Function bZero() As Boolean
    'sends command to power meter to
    '   -clear status byte
    '   -start zeroing calibration
    '   -enable the opertion complete status bit
    '2001-05-17    tnt

    If Not m_oGPIB.bWrite("*CLS;CAL:ZERO:AUTO ONCE;*ESE 1") Then
        ' errors writing clear, zeroing, and enable operations
        m_sError = "Routine: CHP4418B.bZero" & m_oGPIB.sGetError
        m_iError = m_oGPIB.iGetError()
        bZero = False
        Exit Function
    End If
End Function
'*****************************************************************
Public Function bSPoll(ByRef iResult As Integer) As Boolean
    'performs a serial poll on power meter
    '
    ' Returns:  iResult - contents of serial poll
    '           TRUE if polling successful
    '
    '2001-05-17    tnt
```

```
 '    '
   If Not m_oGPIB.bSPoll(iResult) Then
       ' errors on serial polling meter
       m_sError = "Routine: CHP4418B.bSPoll - " & vbCr & vbCr & m_oGPIB.sGetError
       bSPoll = False
   End If

   bSPoll = True
End Function
'*****************************************************************
Public Function bReturnWhenZeroingDone(ByRef bReturn As Boolean) As Boolean
    ' checks whether or notreturns when the zeroing operation is complete
    ' Calling Parms: None
    ' Returns:       bReturn = TRUE after zeroing is complete
    '                Function returns TRUE if no errors
    '
    '2001-05-17    tnt


    Do
        DoEvents
        If Not m_oGPIB.bWrite("*OPC") Then
            ' errors asking for the operation complete bit
            m_sError = "Routine: CHP4418B.bChckOper" & vbCr & vbCr & m_oGPIB.sGetError
            bChckOper = False
            Exit Function
        End If
        If Not bIsZeroingDone(bReturn) Then
            ' error during call
            m_sError = "Routine CHP4418B. bReturnWhenZeroingDone: Error calling:" & _
                    vbCr & vbCr & m_sError
            bReturnWhenZeroingDone = False
            Exit Function
        End If
    Loop While Not bReturn

    bReturnWhenZeroingDone = True
End Function
'*****************************************************************
Public Function bIsZeroingDone(ByRef bIsDone As Boolean) As Boolean
    ' checks if zeroing is complete
    '
    ' Calling Parms: None
    ' Returns:       bIsDone = TRUE when zeroing is complete
    '                TRUE if no errors
    '                FALSE if error during call
    '
    '   2001-05-17    tnt
    '

    Dim iTemp As Integer
    Const iEND_OF_OPERATION As Integer = 32 ' test for end of operation
                                            ' bit set
    If bSPoll(iTemp) Then
        If iTemp = iEND_OF_OPERATION Then
            bIsDone = True
        Else
            bIsDone = False
        End If
        bIsZeroingDone = True
    Else
        ' error during call
        m_sError = "Routine CHP4418B.bIsZeroingDone: Error calling:" & _
                 vbCr & vbCr & m_sError
        bIsZeroingDone = False
    End If
End Function
'*****************************************************************
Public Function bStopZeroing() As Boolean
```

```
. 'function writes to the meter and tells it to reset itself, which
  'effectively ends the reading

  If Not bReset Then
      m_sError = "Routine: CHP4418B.bStopZeroing" & m_oGPIB.sGetError
      m_iError = m_oGPIB.iGetError()
      bStopZeroing = False
  End If

  bStopZeroing = True
:nd Function
```

```
:GPIB - 1

)ption Explicit

 Generic GPIB Class
 1998-09-04 jee

 1998-10-13 jee modified to use with 436 power meter, but now generalized for GPIB
                board
 1998-10-14 jee changed timeout to global value of 300 ms for easier decoding
 1998-10-23 jee changed timeout to 1s to get HP 34401 multimeter to work (with no input)
 1999-02-25 jee change timeout from 1s to 3s so power meter works on lowest range.
 2001-06-01 tnt added bSpoll function

 this is unit descriptor for the GPIB card
'rivate m_UnitDesc As Integer

'rivate m_sError As String                              ' string containing last error message
'rivate m_iError As Integer                             ' integer containing last error number

'rivate Const m_iBOARD_INDEX As Integer = 0             ' GPIB board index
'rivate Const m_iGPIB_SECOND_ADDR As Integer = 0        ' Secondary GPIB address
'rivate Const m_iTIME_OUT As Integer = T3s              ' timeout value for device
'rivate Const m_iEOT As Integer = 1                     ' End or Identify (EOI) line set true with
 last byte
'rivate Const m_iEOS As Integer = &H1C0A                ' End of String:    1 - compare all 8 bits
 of EOS
                                                        '                   C - Set EOI with EOS o
ı write
                                                        '                       and terminate read
 on EOS
                                                        '                   0A - end of string is
ıewline char
'rivate m_bInitialized As Boolean                       ' set true when the HPIB is successfully i
ıitialized
*****************************************************************
'ublic Function bRead(ByRef sBuffer As String) As Boolean
    ' reads the GPIB board and returns the string
    '
    ' Calling Vars: sBuffer - string used to return value read from instrument
    ' Returns:      True - if read successful
    '
    ' 1998-10-22 jee
    ' 2001-01-22 jee added test for sBuffer length = 0
    '                This can be the case if the buffer is null terminated string.
    '
    Dim lBufLength As Long

    If Len(sBuffer) < 1 Then
        lBufLength = 64000
    Else
        lBufLength = Len(sBuffer)
    End If

    Call ilrd(iGetUnitDesc(), sBuffer, lBufLength - 2)
    If ibsta And EERR Then
        'error occured
        m_iError = iberr
        m_sError = "Routine: CGPIB.bRead: Read failed" & vbCr & vbCr & sGetDriverError()
        bRead = False
        Exit Function
    End If

    ' read OK
    m_iError = 0
    m_sError = ""
    bRead = True
:nd Function
*****************************************************************
'ublic Function bWrite(ByRef sBuffer As String) As Boolean
    ' writes to the GPIB board
```

```
,     ,     sBuffer = sBuffer & "Service request line (SRQ) is stuck in on state."

        Case ETAB:
            sBuffer = sBuffer & "Insufficient memory available to hold all GPIB addresses found or
" & vbCr & _
                        "No device in table specified by FINDRQS are requesting service."
        Case Else:
            sBuffer = sBuffer & "Unknown 'iberr' function"
    End Select


    sReturnGPIBError = sBuffer

nd Function
******************************************************************************
ublic Function bSPoll(ByRef iResult As Integer) As Boolean
    'serial polls the meter, asking for its status byte
    'returns:   iResult true if no errors have occurred
    '5/17/01    tnt

    Call ibrsp(iGetUnitDesc(), iResult)
    If ibsta And EERR Then
        'error occured
        m_iError = iberr
        On Error GoTo 0
        m_sError = "Routine: CGPIB.bSPoll - 'Serial Poll' call failed" & vbCr & vbCr & sGetDriverE
rror
        bSPoll = False
        Exit Function
    End If
    On Error GoTo 0
    bSPoll = True

nd Function
```

To: John Effland
From: Tim Thacker
Date: Wednesday, June 27, 2001
Subject: Lake Shore Temperature Monitor Data Collection Program

This program allows the user to select and read into an array one of the eight channels on the LakeShore temperature monitor. Once data collection is finished and stored into the array, the user-defined number of measurements is transferred to an Excel spreadsheet.

The program starts by loading the user interface form (`Figure 1`). When starting the `Form_Load` sub-routine the program calls the temperature monitor's initialization function (which sets up the monitor to talk to the computer through the GPIB board in `Figure 2`). The temperature monitor's initialization function (`Figure 3`) sets up the monitor so it can receive data commands and send temperature measurements via the GPIB board. When the form has finished loading, the program waits for the user to choose from which channel to take measurements (the sub-routine `Option#_Click` in `Figure 4`). Once the user chooses a channel, the program waits for the user to input the number of readings into a text window (the user types the number of readings desired and clicks on the sub-routine button `ArraySize_Click`, `Figure 5`).

The program also has a quit button (the sub-routine `Quit_Click`, `Figure 6`), which when clicked is nothing more than a quick link to the UserForm_Terminate sub-routine (Figure 7). The UserForm_Terminate routine sets the meter and util objects to nothing, and unloads the form and ends the program. This function can be performed anytime, except during measurements. To stop the program from taking measurements the user has to press Ctrl + Pause/Break as the form prompts the user to do under the quit button.

Once the user has chosen a channel (the default channel is 1) and entered the number of readings (the default number of readings is 1) and pressed the `ArraySize_Click` button (as in `Figures 4 & 5`), the user then presses the `TempMeas_Click` button (`Figure 8`). In `Figure 8`, the program sets an array with the number of elements equal to the number of readings, and initializes a loop of same length. The program starts to collect data by means of the `oTempMtr.bReadTemp` function (this function sends commands to the monitor to transmit measurement data back to the computer, as in `Figure 9`). The function starts out testing to see if the system is in a simulation mode, or actually reading real data. If the function determines real data is required, it determines how many readings to take (`Figure 9`). This function sets another loop of identical length to the previous loop in `Figure 8`, and uses it to sweep through and take data from the monitor and return it to the array in `Figure 8`. The function sends the command `KRDG? (Figure 10)`, along with the specific channel. This command tells the meter to make the data available to be read remotely. Once read the loop repeats until all readings are taken then exits the function. The `TempMeas_Click` routine also displays the readings in a second text window as they are being gathered (after `the oTempMtr.bReadTemp` function in `Figure 8`). When all the readings have been collected and stored into the array, the `TempMeas_Click` routine starts another loop of same length, and writes all the data from the array into an Excel spreadsheet.

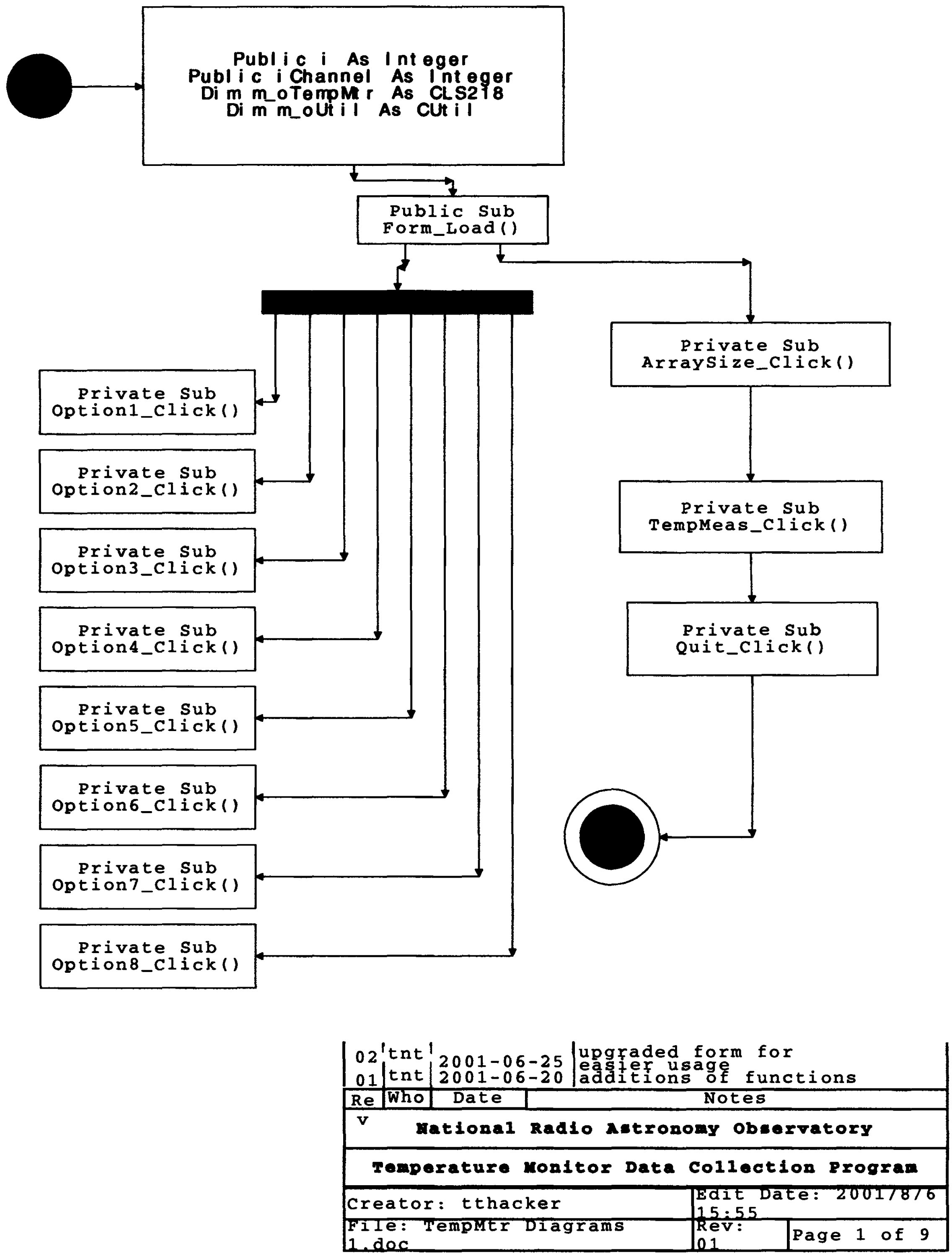

Figure 1:
This figure shows how the program sets up and goes through the different routines.

Public Sub Form_Load()

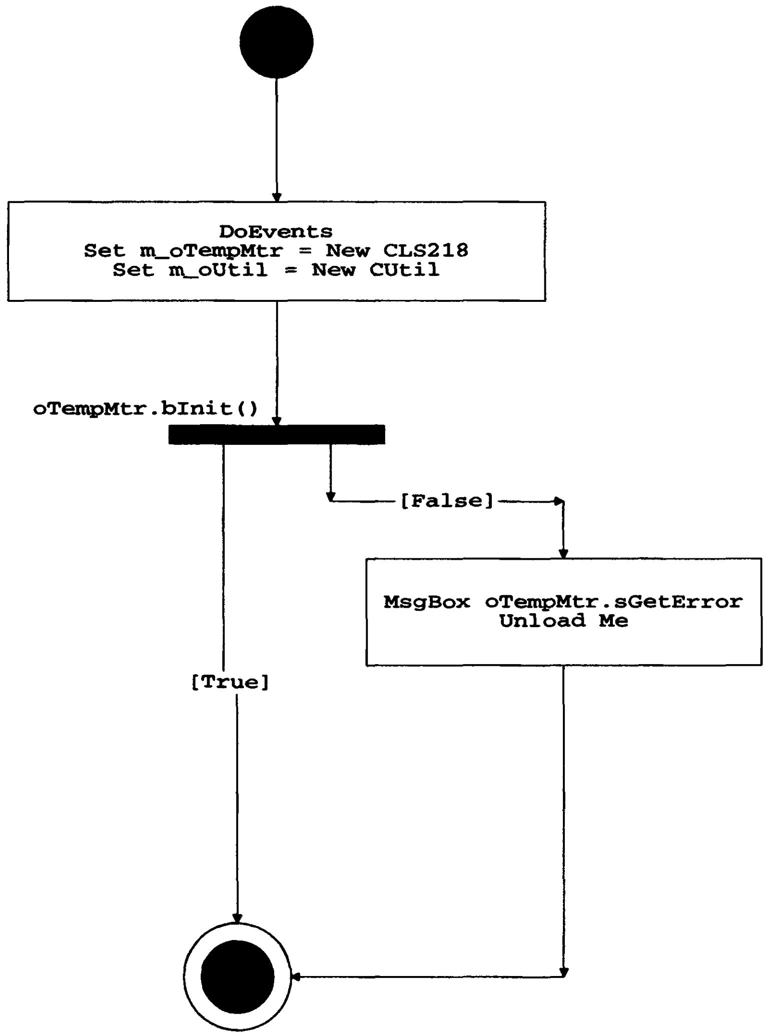

02	tnt	2001-06-25	upgraded form for easier usage
01	tnt	2001-06-20	additions of functions
Rev	Who	Date	Notes
National Radio Astronomy Observatory			
Temperature Monitor Data Collection Program			
Creator: tthacker		Edit Date: 2001/8/6 15:49	
File: TempMtr Diagrams 1.doc		Rev:01	Page 2 of 9

Figure 2: Form_Load

This routine calls the temperature monitor's initialization function, which sets up the monitor to be able to talk to the computer via the GPIB board.

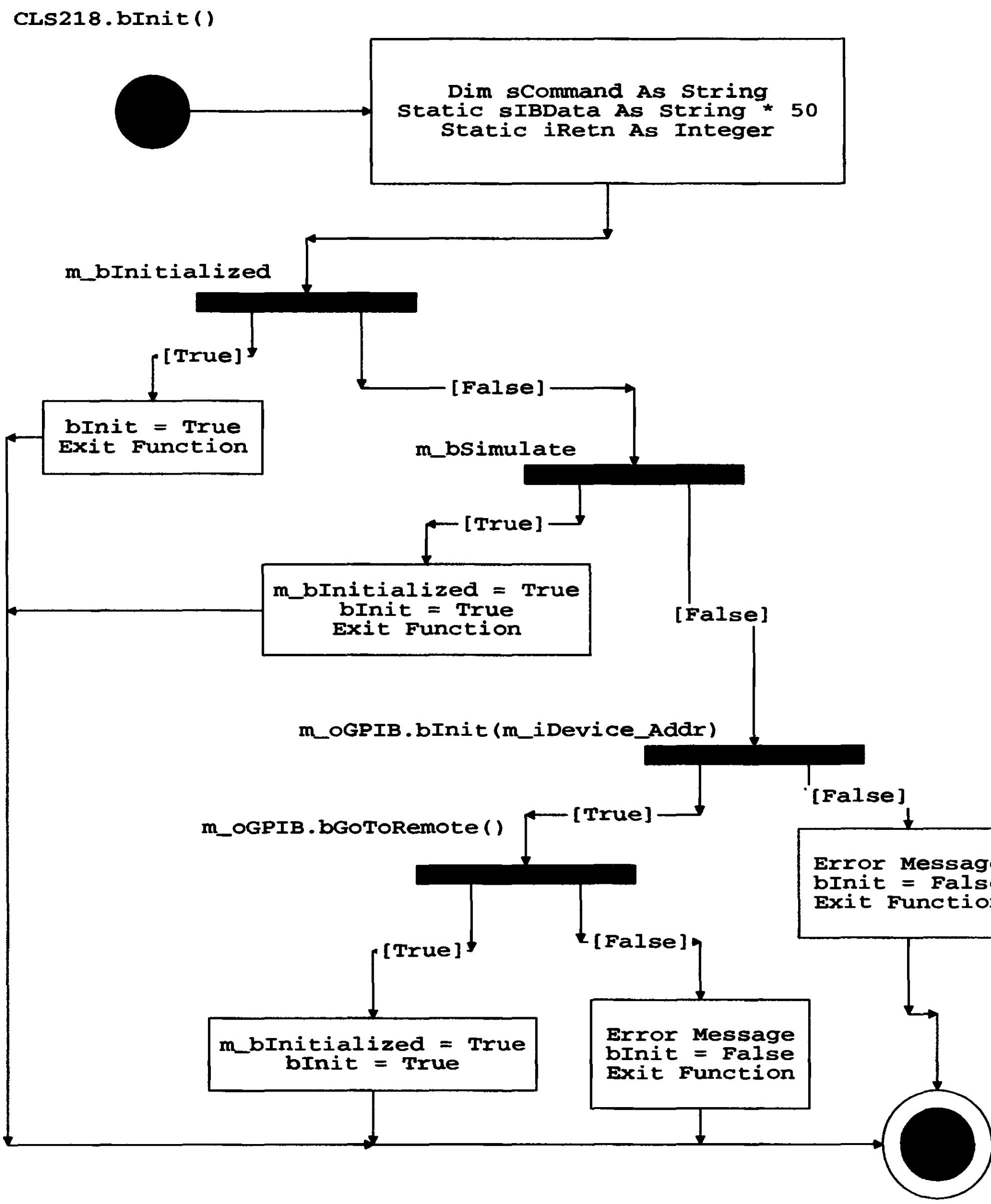

Rev	Who	Date	Notes
02	tnt	2001-06-25	upgraded form for easier usage
01	tnt	2001-06-20	additions of functions

National Radio Astronomy Observatory		
Temperature Monitor Data Collection Program		
Creator: tthacker	Edit Date: 2001/7/24 10:54	
File: TempMtr Diagrams 1.doc	Rev:01	Page 3 of 9

Figure 3: CLS218.bInit

This initialization function allows the computer to communicate with the temperature monitor, without it the computer could not receive data measurements.

```
Private Sub Option#_Click()
```

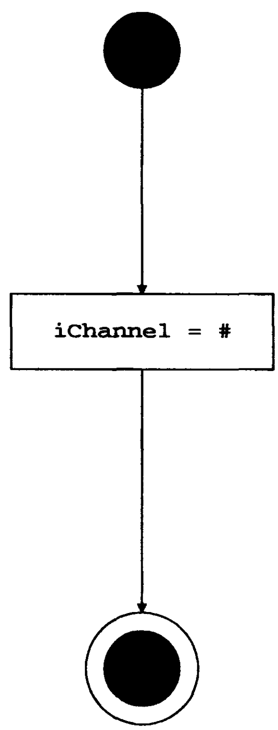

Rev	Who	Date	Notes
02	tnt	2001-06-25	upgraded form for easier usage
01	tnt	2001-06-20	additions of functions

National Radio Astronomy Observatory		
Temperature Monitor Data Collection Program		
Creator: tthacker	Edit Date: 2001/6/27 13:24	
File: TempMtr Diagrams 1.doc	Rev: 01	Page 4 of 9

Figure 4: Option#_Click

The Option# routine lets the user choose which channel on the temperatuer monitor they wish to look at.

```
Private Sub ArraySize_Click()
```

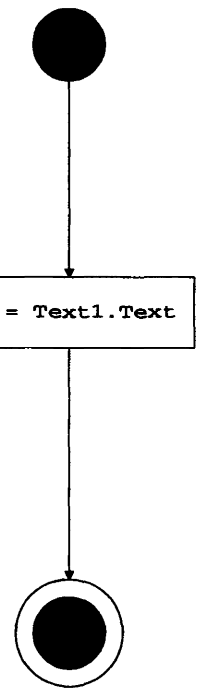

02	tnt	2001-06-25	upgraded form for easier usage
01	tnt	2001-06-20	additions of functions
Rev	Who	Date	Notes
National Radio Astronomy Observatory			
Temperature Monitor Data Collection Program			
Creator: tthacker		Edit Date: 2001/7/24 10:46	
File: TempMtr Diagrams 1.doc		Rev: 01	Page 5 of 9

Figure 5: ArraySize_Click

The user inputs the number of reading they desire into the text window, and when the button is pushed the number is recorded as the array size and loop counter's size.

Private Sub Quit_Click()

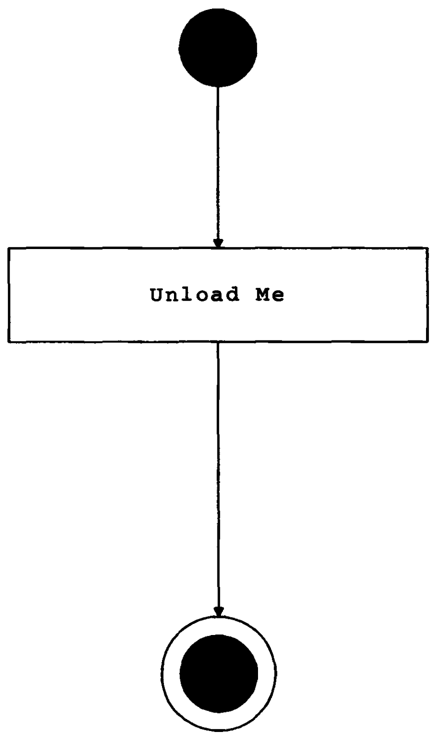

02	tnt	2001-06-25	upgraded form for easier usage
01	tnt	2001-06-20	additions of functions
Rev	Who	Date	Notes
National Radio Astronomy Observatory			
Temperature Monitor Data Collection Program			
Creator: tthacker		Edit Date: 2001/7/24 10:49	
File: TempMtr Diagrams 1.doc		Rev: 01	Page 6 of 9

Figure 6: Quit_Click

This function's purpose is to kill the program if the user so desires to exit and change or work on something else. It is a quick link to the UserForm_Terminate routine.

```
Public Sub UserForm_Terminate()
```

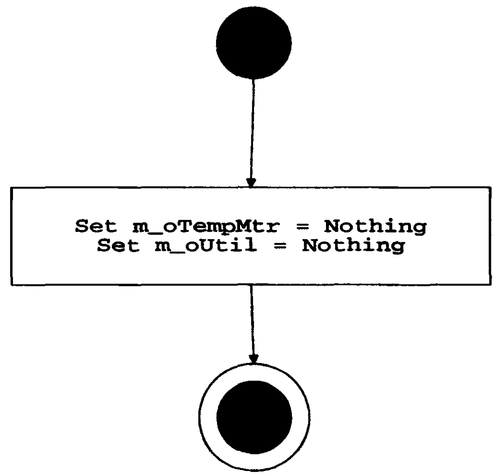

02	tnt	2001-06-25	upgraded form for easier usage
01	tnt	2001-06-20	additions of functions
Rev	Who	Date	Notes
National Radio Astronomy Observatory			
Temperature Monitor Data Collection Program			
Creator: tthacker		Edit Date: 2001/8/6 16:14	
File: TempMtr Diagrams 1.doc		Rev: 01	Page 3 of 9

Figure 7: UserForm_Terminate
This sub-routine unloads all the form objects and exits the program.

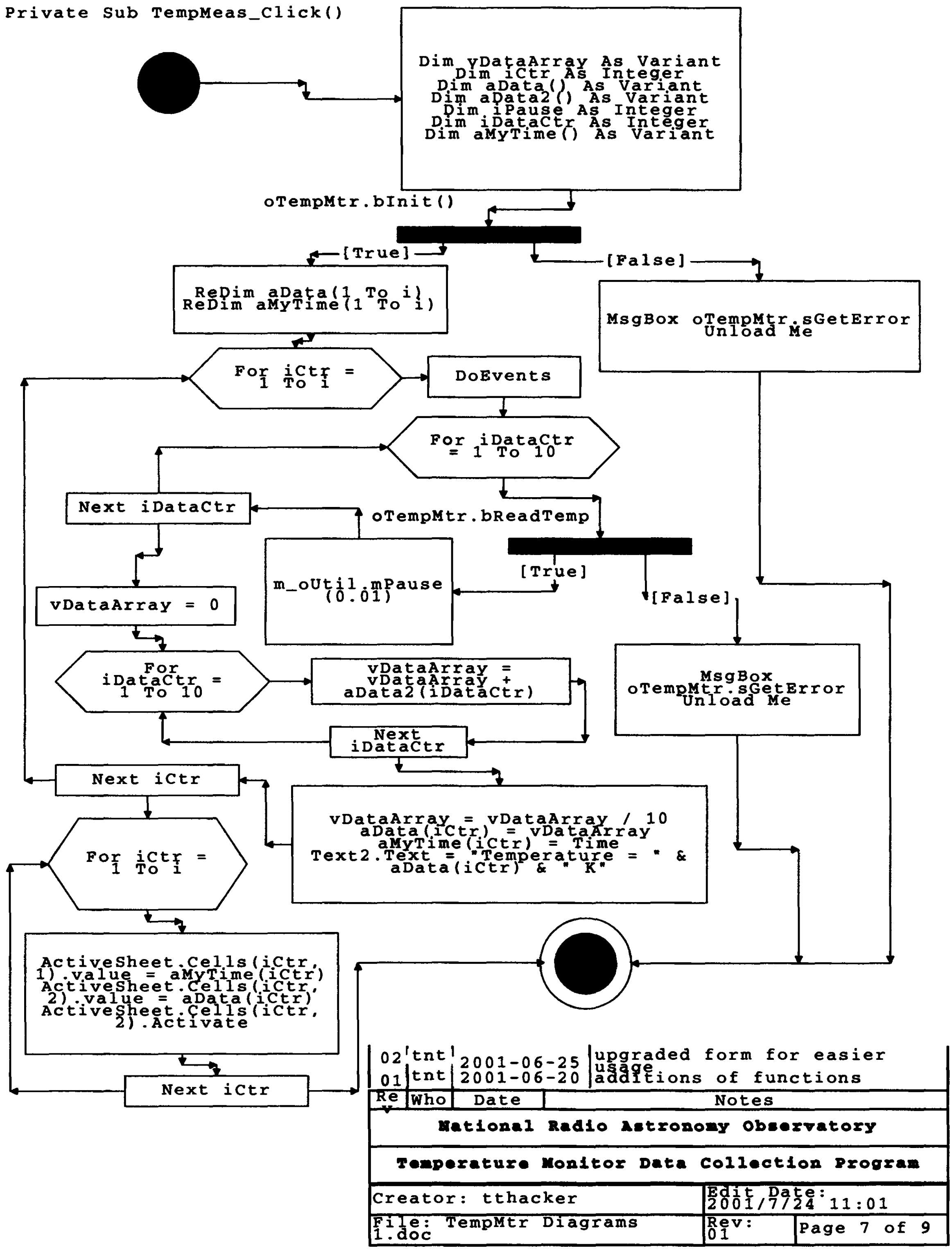

Figure 8: TempMeas_Click

When invoked, this routine calls funcitons to send out commands to the temperature monitor to receive temperature measurements back and store those readings into an array of user defined length in Figure 5.

CLS218.bReadTemp(iChannel, vDataArray)

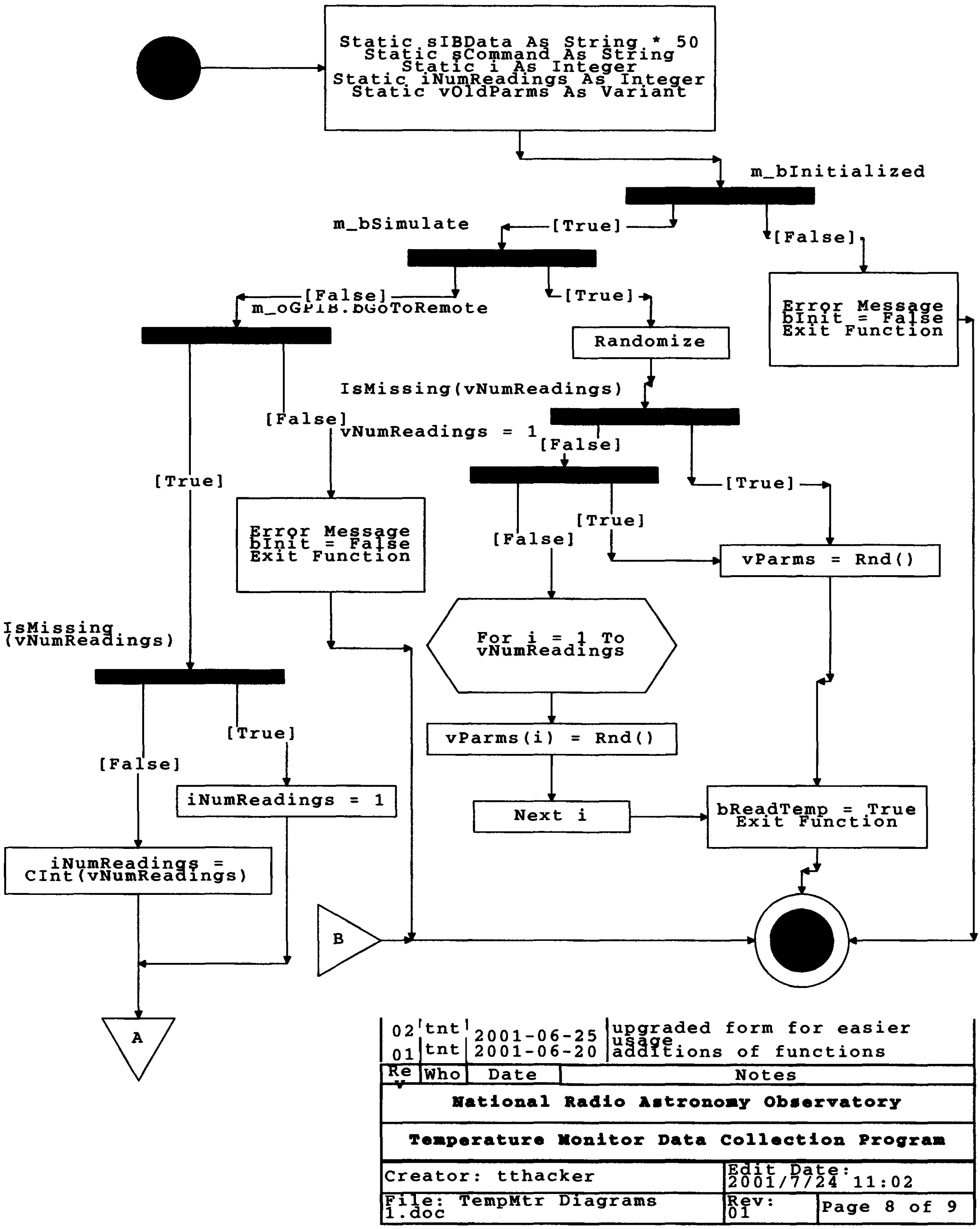

Figure 9: CLS218.bReadTemp
This is the function that receives temperature monitor measurements.

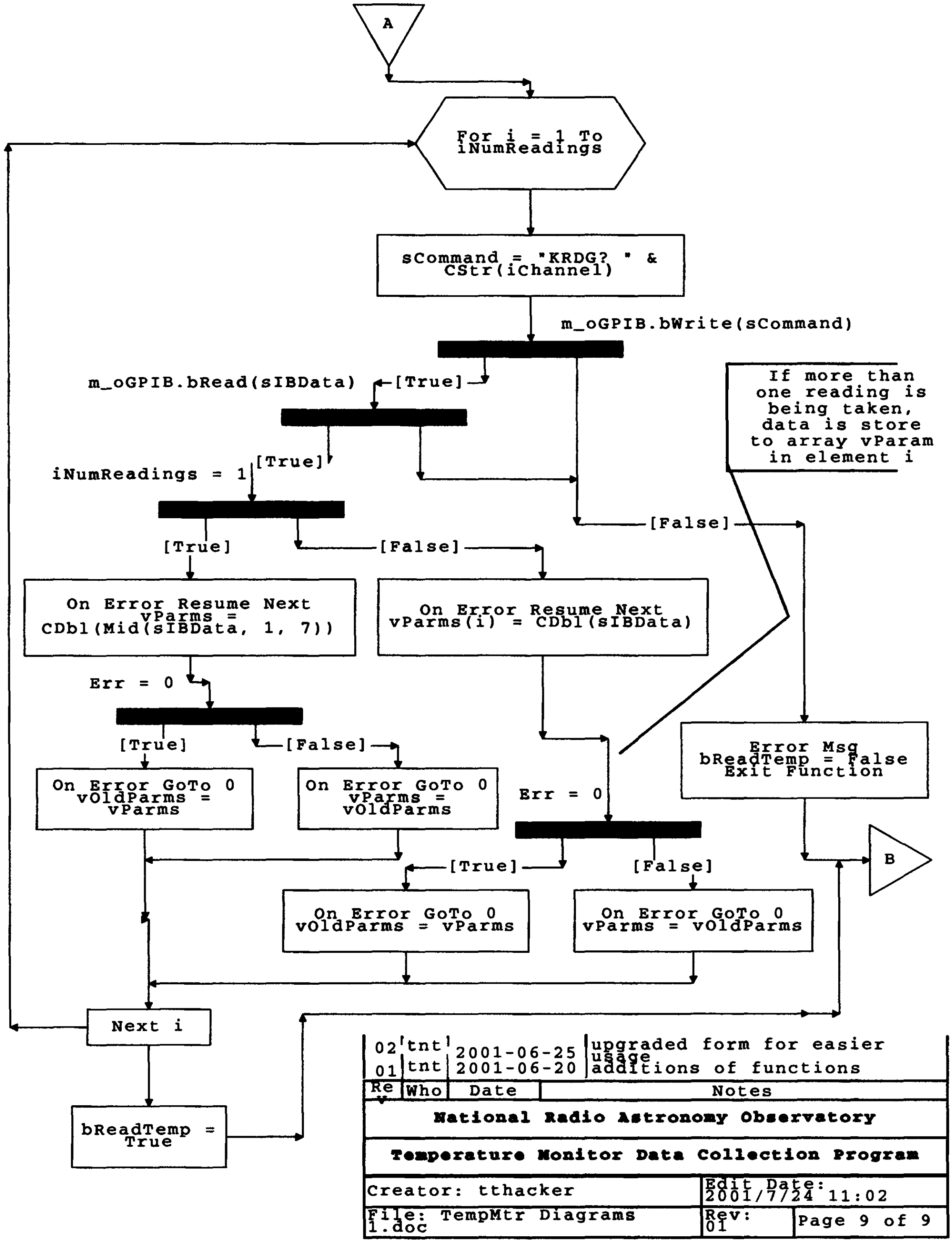

Figure 10: CLS218.bReadTemp (con't)

This figure continues the read function. The function loops the commands to tell the monitor to make data available and to read the data the number of times the user has defined, and exits upon completion.

```
)ption Explicit
'ublic m_lNumReadings As Long
'ublic iChannel As Integer
)im m_oTempMtr As CLS218
)im m_oUtil As CUtil

*********************************************************************
'ublic Sub UserForm_Initialize()
   'initializes keypress sub routine to kill program
   DoEvents

   iChannel = 1
   m_lNumReadings = 1

   'sets up m_oTempMtr as the meter address
   Set m_oTempMtr = New CLS218
   Set m_oUtil = New CUtil

   If m_oTempMtr.bInit() = False Then
       MsgBox m_oTempMtr.sGetError
       Unload Me
   End If
:nd Sub
*********************************************************************
'rivate Sub UserForm_Terminate()
   Set m_oTempMtr = Nothing
:nd Sub
*********************************************************************
'rivate Sub Option1_Click()
   iChannel = 1
:nd Sub
*********************************************************************
'rivate Sub Option2_Click()
   iChannel = 2
:nd Sub
*********************************************************************
'rivate Sub Option3_Click()
   iChannel = 3
:nd Sub
*********************************************************************
'rivate Sub Option4_Click()
   iChannel = 4
:nd Sub
*********************************************************************
'rivate Sub Option5_Click()
   iChannel = 5
:nd Sub
*********************************************************************
'rivate Sub Option6_Click()
   iChannel = 6
:nd Sub
*********************************************************************
'rivate Sub Option7_Click()
   iChannel = 7
:nd Sub
*********************************************************************
'rivate Sub Option8_Click()
   iChannel = 8
:nd Sub
*********************************************************************
'rivate Sub ArraySize_Click()
   m_lNumReadings = Text1.Text
:nd Sub
*********************************************************************
'rivate Sub Quit_Click()
   Unload Me
:nd Sub
*********************************************************************
'rivate Sub TempMeas_Click()
```

```
    '
    ' 2001-07-03 JEE added lNUm_Averages, Progressbar
    ' 2001-08-06 tnt added CUtil class, and used it's mPause function to replace ibwait

    Dim vDataArray As Variant
    Dim iCtr As Integer
    Dim aData() As Variant
    Dim aData2() As Variant
    Dim iPause As Integer
    Dim iDataCtr As Integer
    Dim aMyTime() As Variant
    Const lNUM_AVERAGES As Long = 30

    If m_oTempMtr.bInit() = False Then
        MsgBox m_oTempMtr.sGetError
        Unload Me
    End If

    ReDim aData(1 To m_lNumReadings)
    ReDim aMyTime(1 To m_lNumReadings)
    ReDim aData2(1 To lNUM_AVERAGES)

    Me.ProgressBar1.Max = m_lNumReadings
    Me.ProgressBar1.value = 0

    For iCtr = 1 To m_lNumReadings

        DoEvents

        For iDataCtr = 1 To lNUM_AVERAGES

            If m_oTempMtr.bReadTemp(iChannel, vDataArray) = False Then
                MsgBox m_oTempMtr.sGetError
                Unload Me
            End If

            m_oUtil.mPause (0.01)

            aData2(iDataCtr) = vDataArray
        Next iDataCtr

        vDataArray = 0

        For iDataCtr = 1 To lNUM_AVERAGES
            vDataArray = vDataArray + aData2(iDataCtr)
        Next iDataCtr

        vDataArray = vDataArray / lNUM_AVERAGES

        aData(iCtr) = vDataArray
        aMyTime(iCtr) = Time
        Text2.Text = "Temperature = " & aData(iCtr) & " K"

        Me.ProgressBar1.value = iCtr
    Next iCtr

    Me.ProgressBar1.value = 0

    For iCtr = 1 To m_lNumReadings
        ActiveSheet.Cells(iCtr, 1).value = aMyTime(iCtr)
        ActiveSheet.Cells(iCtr, 2).value = aData(iCtr)
        Me.ProgressBar1.value = iCtr
    Next iCtr

:nd Sub
```

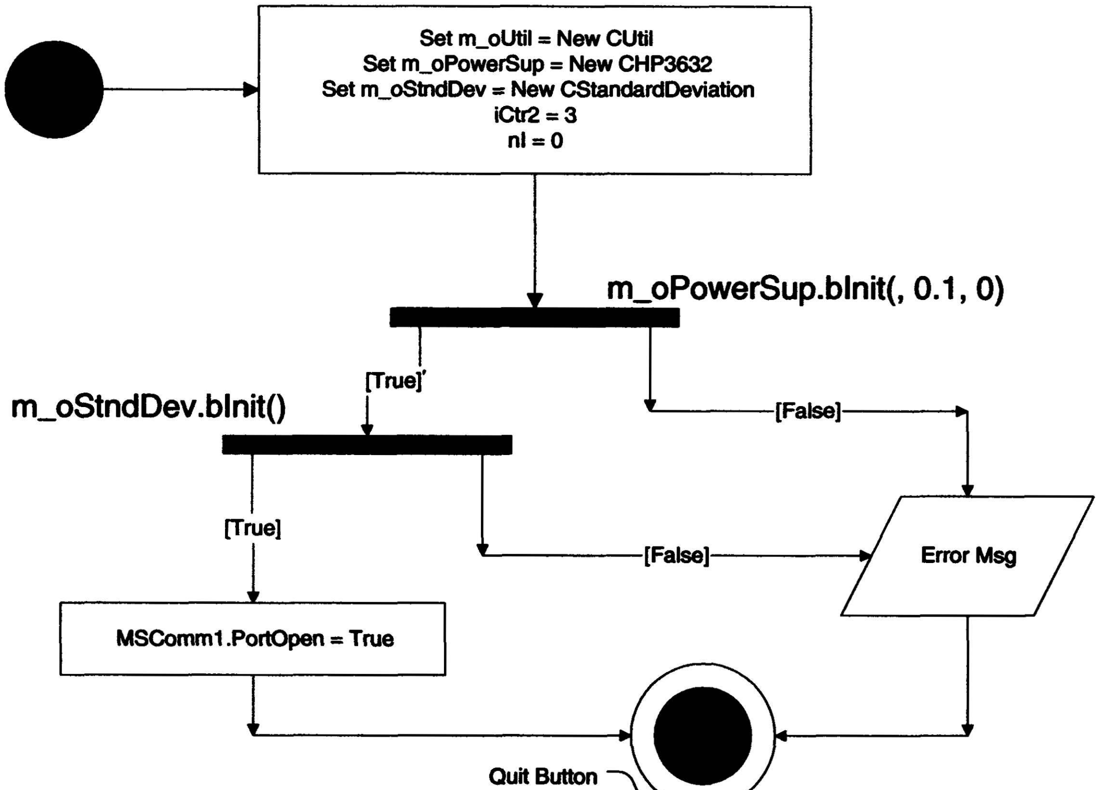

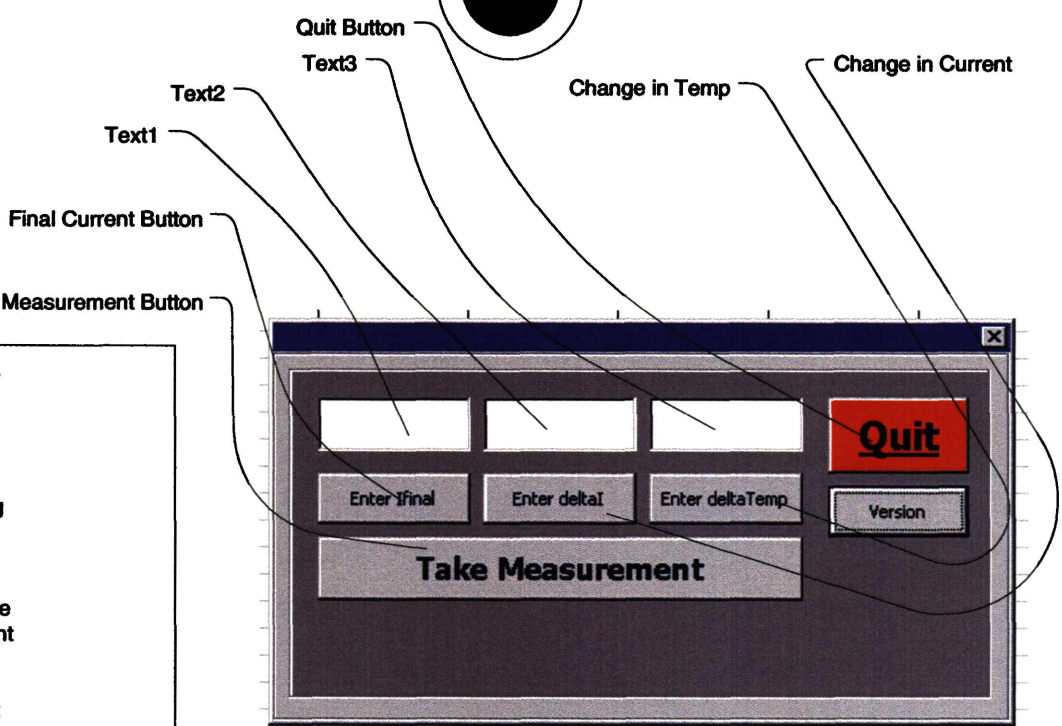

These variable are initialized when the program is started

```
Dim iChannel As Integer
Dim iCtr1 As Integer
Dim iCtr2 As Integer
Dim iCtr3 As Integer
Dim iCtr4 As Integer
Dim sTempUnit As String
Dim nI As Single
Dim nIfinal As Single
Dim ndeltaI As Single
Dim ndeltaTemp As Single
Dim vJ(1 To 25) As Variant
Dim MyTime As Variant
Dim vCurrent As Variant
Dim vVoltage As Variant
Dim vTo3 As Variant
Dim m_oUtil As CUtil
Dim m_oPowerSup As CHP3632
Dim m_oStndDev As CStandardDeviation
```

Figure 1: UserForm_Initialize()

This section of the program initializes all the variables and meters, opens comm port to temp meter, and initializes objects and variables to specific values.

01	tnt	2001-07-23	Creation of flowchart for Omega temp meter
Rev	Who	Date	Notes
National Radio Astronomy Observatory			
Dan's Omega Temperature Meter Data Acquisition Program			
Creator: tthacker		Edit Date: 2001/8/6 09:45	
File: \\Eagle\cv-cdl-sis\TThacker\Temperature Meter\Dan's TempMtr\omega temp.vsd		Rev: 01	Page 1 of 16

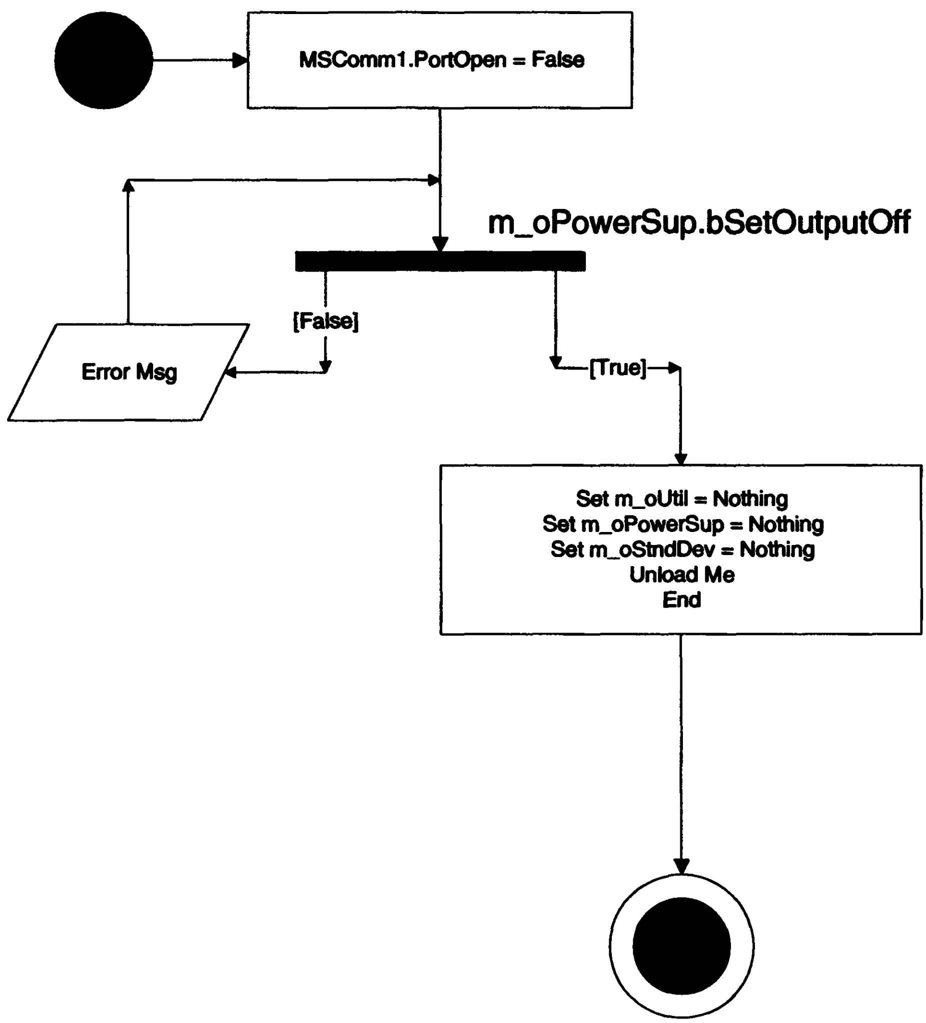

Figure 2: UserForm_Terminate()

This section of the program unloads all the objects, closes the comm port, turns off the outout of the power supply and closes the program.

01	tnt	2001-07-23	Creation of flowchart for omega temp meter	
Rev	Who	Date	Notes	
National Radio Astronomy Observatory				
Dan's Omega Temperature Meter Data Acquisition Program				
Creator: tthacker			Edit Date: 2001/8/6 09:45	
File: \\Eagle\cv-cdl-sis\TThacker\Temperature Meter\Dan's TempMtr\ omega temp.vsd			Rev: 01	Page 2 of 16

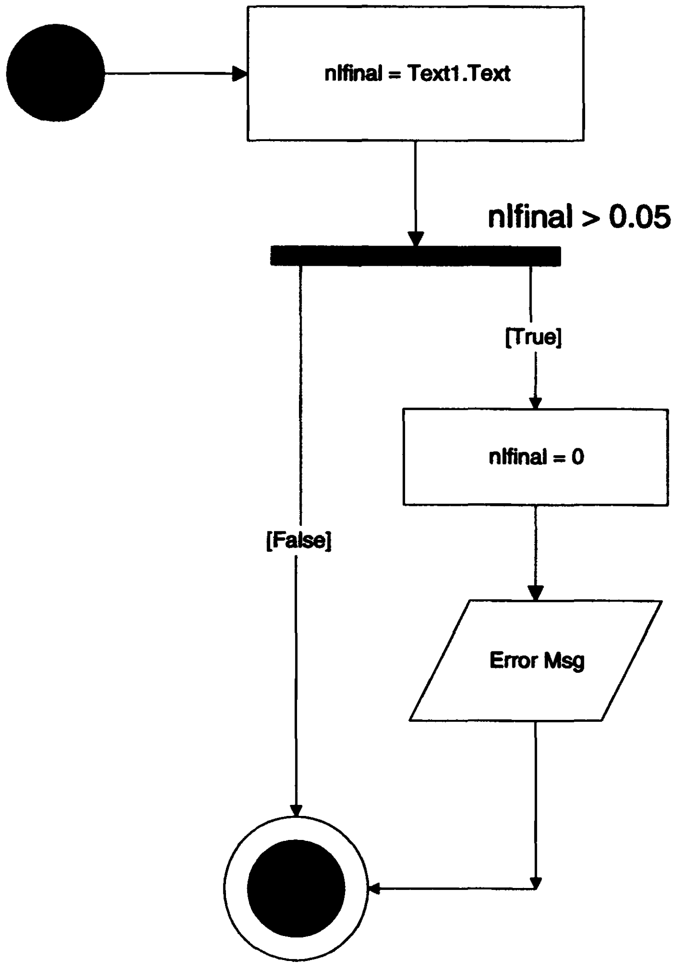

Figure 3: Ifinal_Click()

Ifinal_Click allows the user to set the final value of I. The program will later then take temp measurements at different currents until it is done. Tests to ensure that the final current cannot exceed 50 mA are also included.

Rev	Who	Date	Notes
01	tnt	2001-07-23	Creation of flowchart for omega temp meter

National Radio Astronomy Observatory		
Dan's Omega Temperature Meter Data Acquisition Program		
Creator: tthacker	Edit Date: 2001/8/6 09:45	
File: \\Eagle\cv-cdl-sis\TThacker\Temperature Meter\Dan's TempMtr\ omega temp.vsd	Rev: 01	Page 3 of 16

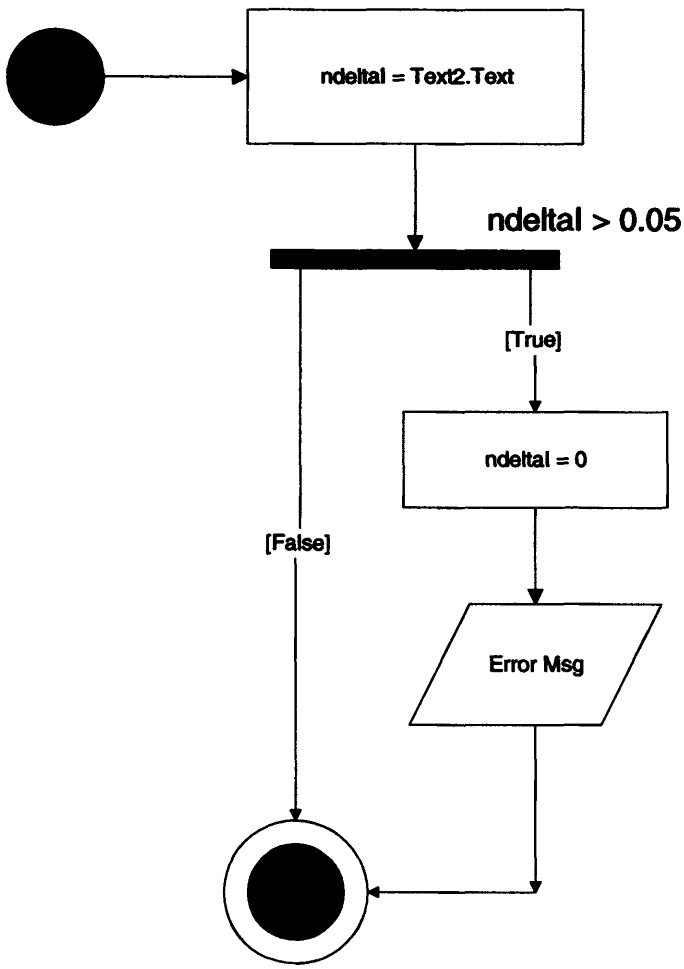

Figure 4: deltal_Click()

deltal_Click() allows the user to set the step value for the current. Tests to ensure that the change in current cannot exceed 50 mA are also included.

Rev	Who	Date	Notes
01	tnt	2001-07-23	Creation of flowchart for omega temp meter

National Radio Astronomy Observatory		
Dan's Omega Temperature Meter Data Acquisition Program		
Creator: tthacker	Edit Date: 2001/8/6 09:45	
File: \\Eagle\cv-cdl-sis\TThacker\Temperature Meter\Dan's TempMtr\ omega temp.vsd	Rev: 01	Page 4 of 16

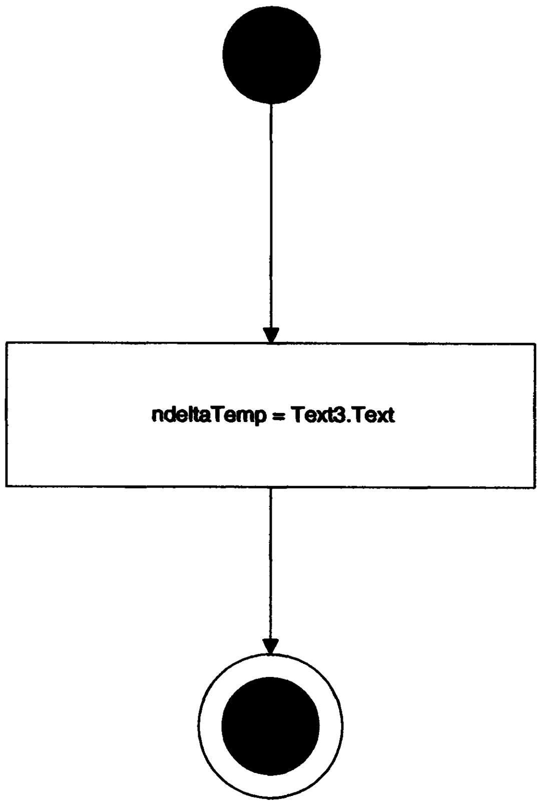

Figure 5: deltaTemp_Click()

deltaTemp_Click() allows the user to set the value to test to see if the meter has changed it's temperature significantly. The program uses this value in the TestTemp function when it compares the standard error on the readings.

Rev	Who	Date	Notes
01	tnt	2001-07-23	Creation of flowchart for omega temp meter

National Radio Astronomy Observatory		
Dan's Omega Temperature Meter Data Acquisition Program		
Creator: tthacker	Edit Date: 2001/8/6 09:45	
File: \\Eagle\cv-cdl-sis\TThacker\Temperature Meter\Dan's TempMtr\ omega temp.vsd	Rev: 01	Page 5 of 16

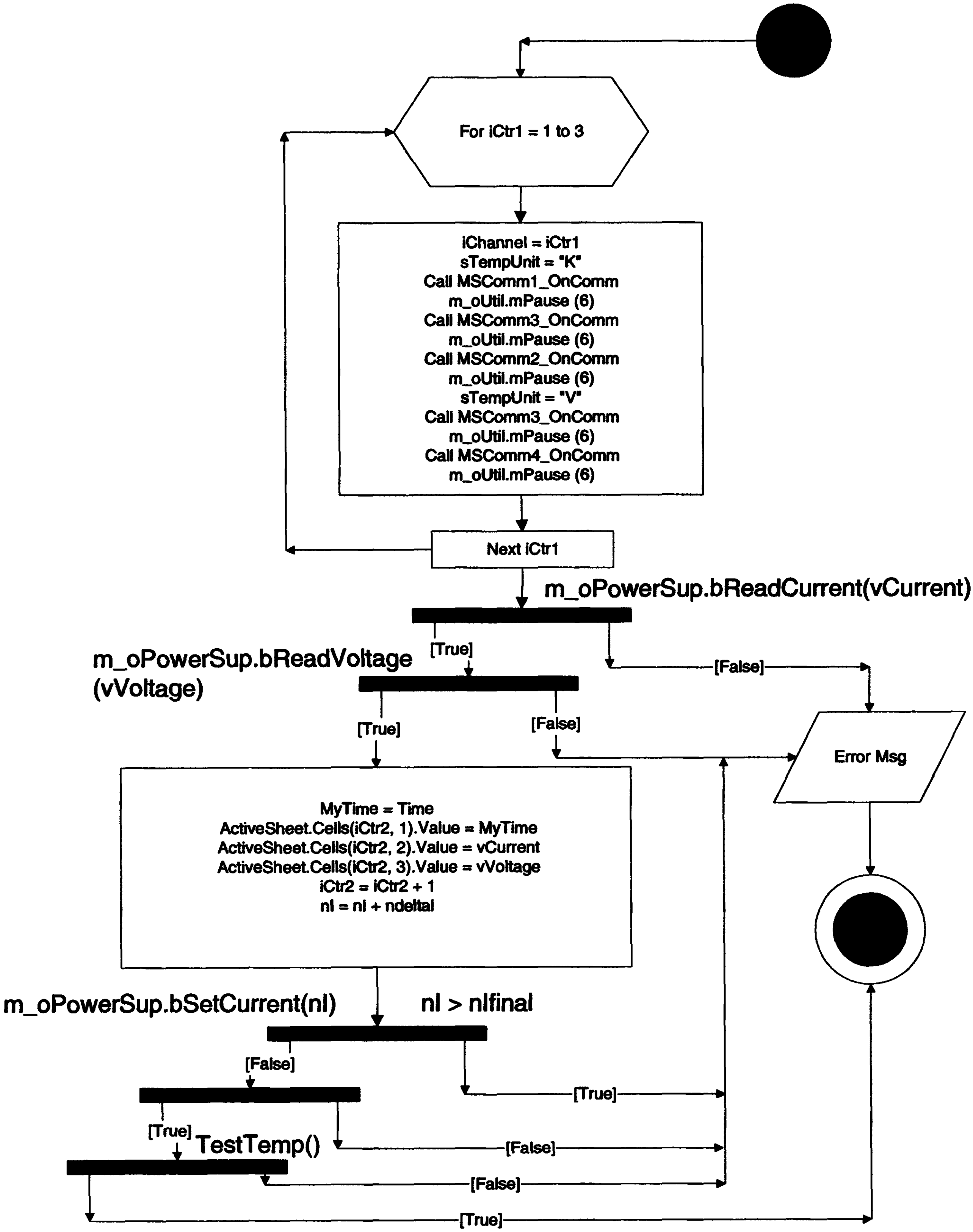

Figure 6: TempMeas_Click()

This sub-routine calls out to different functions to tell the meter to set the meter's channel, set it's units to kelvin, take a reading, set units to voltage, take a reading, for 3 channels. The routine then reads the power supply current and voltage, writes all of the readings to excel, increases the current by deltaI, and finally calls the function TestTemp to check that the temp meter isn't malfunctioning

Rev	Who	Date	Notes
01	tnt	2001-07-23	Creation of flowchart for omega temp meter

National Radio Astronomy Observatory		
Dan's Omega Temperature Meter Data Acquisition Program		
Creator: tthacker	Edit Date: 2001/8/6 09:45	
File: \\Eagle\cv-cdl-sis\TThacker\Temperature Meter\Dan's TempMtr\omega temp.vsd	Rev: 01	Page 6 of 16

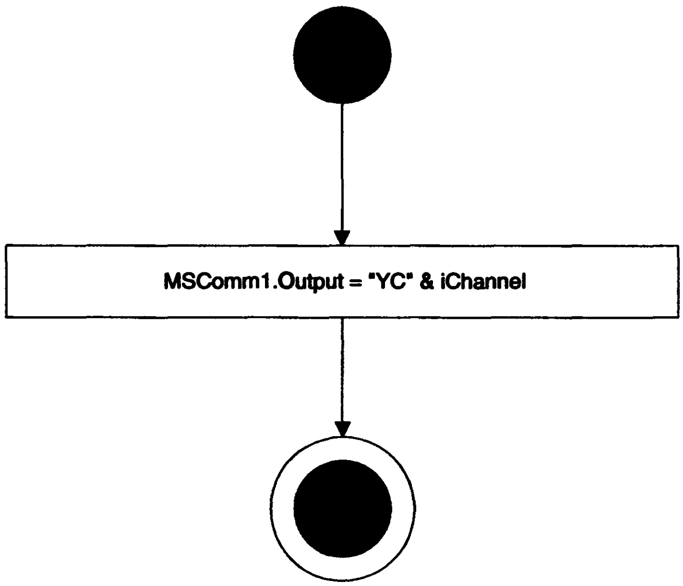

Figure 7: MSComm1_OnComm()

MSComm1_OnComm() writes to the Omega temp meter through the comm port the message to change the channel to iChannel.

01	tnt	2001-07-23	Creation of flowchart for omega temp meter
Rev	Who	Date	Notes

National Radio Astronomy Observatory		
Dan's Omega Temperature Meter Data Acquisition Program		
Creator: tthacker	Edit Date: 2001/8/6 09:45	
File: \\Eagle\cv-cdl-sis\TThacker\Temperature Meter\Dan's TempMtr\ omega temp.vsd	Rev: 01	Page 7 of 16

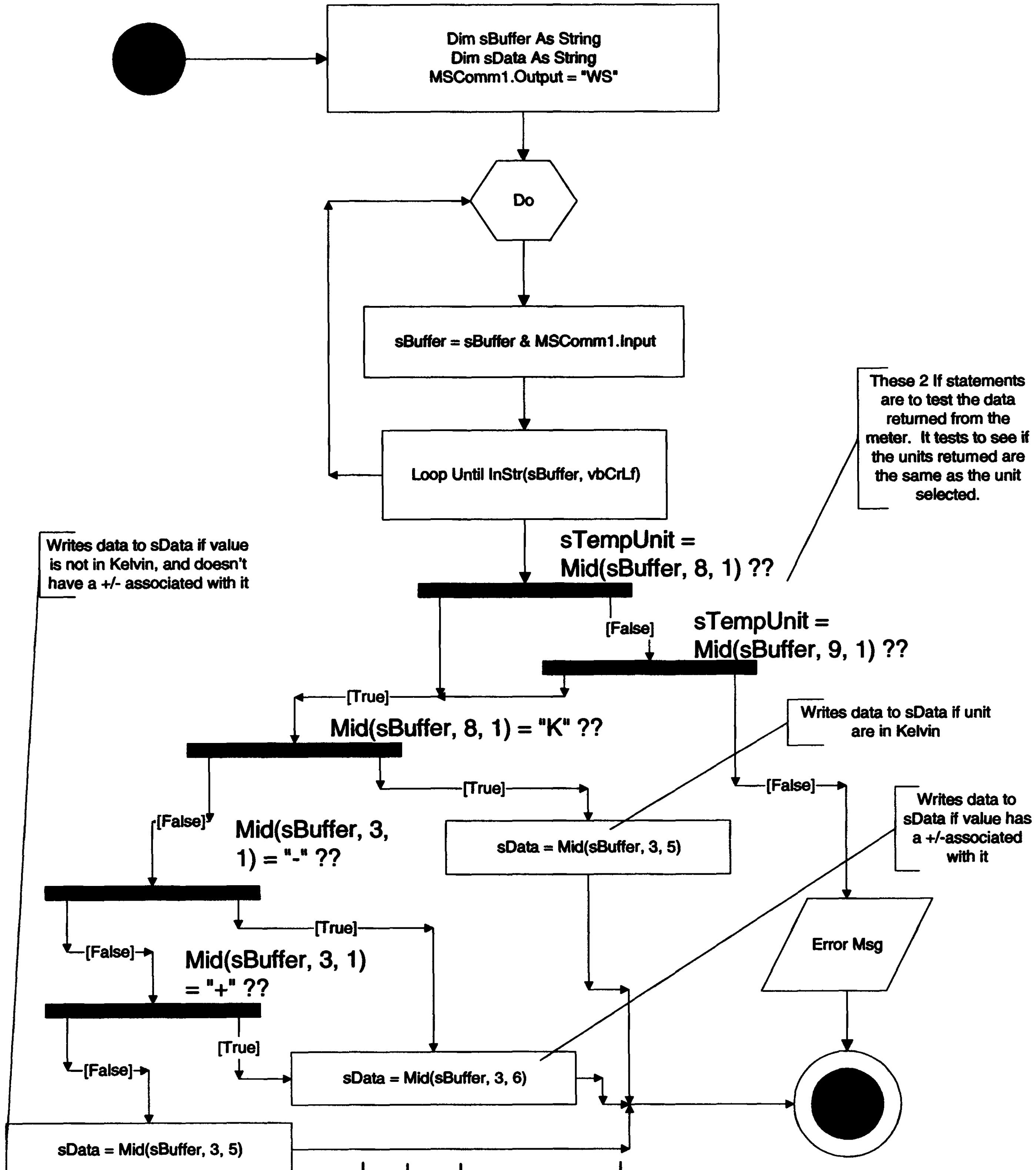

Figure 8: MSComm2_OnComm()

MSComm2_OnComm() writes to the Omega temp meter through the comm port and tells it to start sending back data. It then collects the data, determines if the units are correct, and then sorts out which part of it is raw numerical data, and stores it in sData.

Rev	Who	Date	Notes
01	tnt	2001-07-23	Creation of flowchart for omega temp meter

National Radio Astronomy Observatory		
Dan's Omega Temperature Meter Data Acquisition Program		
Creator: tthacker	Edit Date: 2001/8/6 09:45	
File: \\Eagle\cv-cdl-sis\TThacker\Temperature Meter\Dan's TempMtr\omega temp.vsd	Rev: 01	Page 8 of 16

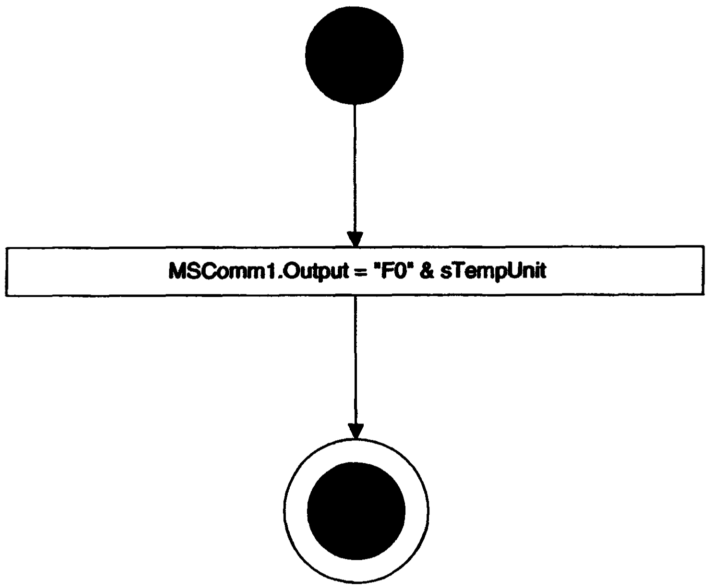

Figure 9: MSComm3_OnComm()

MSComm3_OnComm() writes to the Omega temp meter through the comm port to change the units it is reading to sTempUnit.

Rev	Who	Date	Notes
01	tnt	2001-07-23	Creation of flowchart for omega temp meter

National Radio Astronomy Observatory	
Dan's Omega Temperature Meter Data Acquisition Program	
Creator: tthacker	Edit Date: 2001/8/6 09:45
File: \\Eagle\cv-cdl-sis\TThacker\Temperature Meter\Dan's TempMtr\omega temp.vsd	Rev: 01
	Page 9 of 16

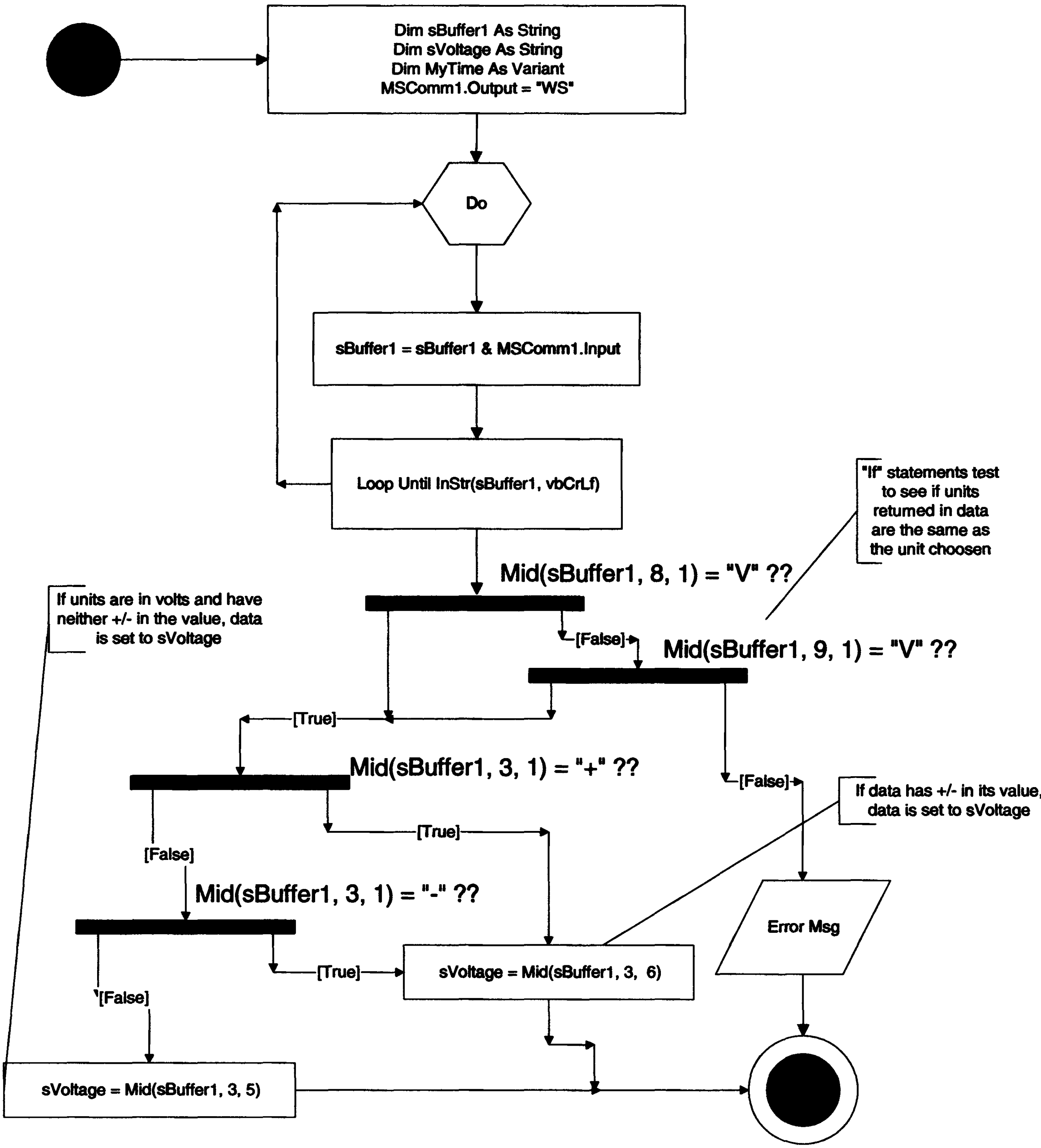

Figure 10: MSComm4_OnComm()

MSComm4_OnComm() writes to the Omega temp meter through the comm port and tells it to start sending back data. It then collects the data, determines if the units are correct, and then sorts out which part of it is raw numerical data, and stores it to sVoltage.

Rev	Who	Date	Notes
01	tnt	2001-07-23	Creation of flowchart for omega temp meter

National Radio Astronomy Observatory		
Dan's Omega Temperature Meter Data Acquisition Program		
Creator: tthacker	Edit Date: 2001/8/6 09:45	
File: \\Eagle\cv-cdl-sis\TThacker\Temperature Meter\Dan's TempMtr\omega temp.vsd	Rev: 01	Page 10 of 16

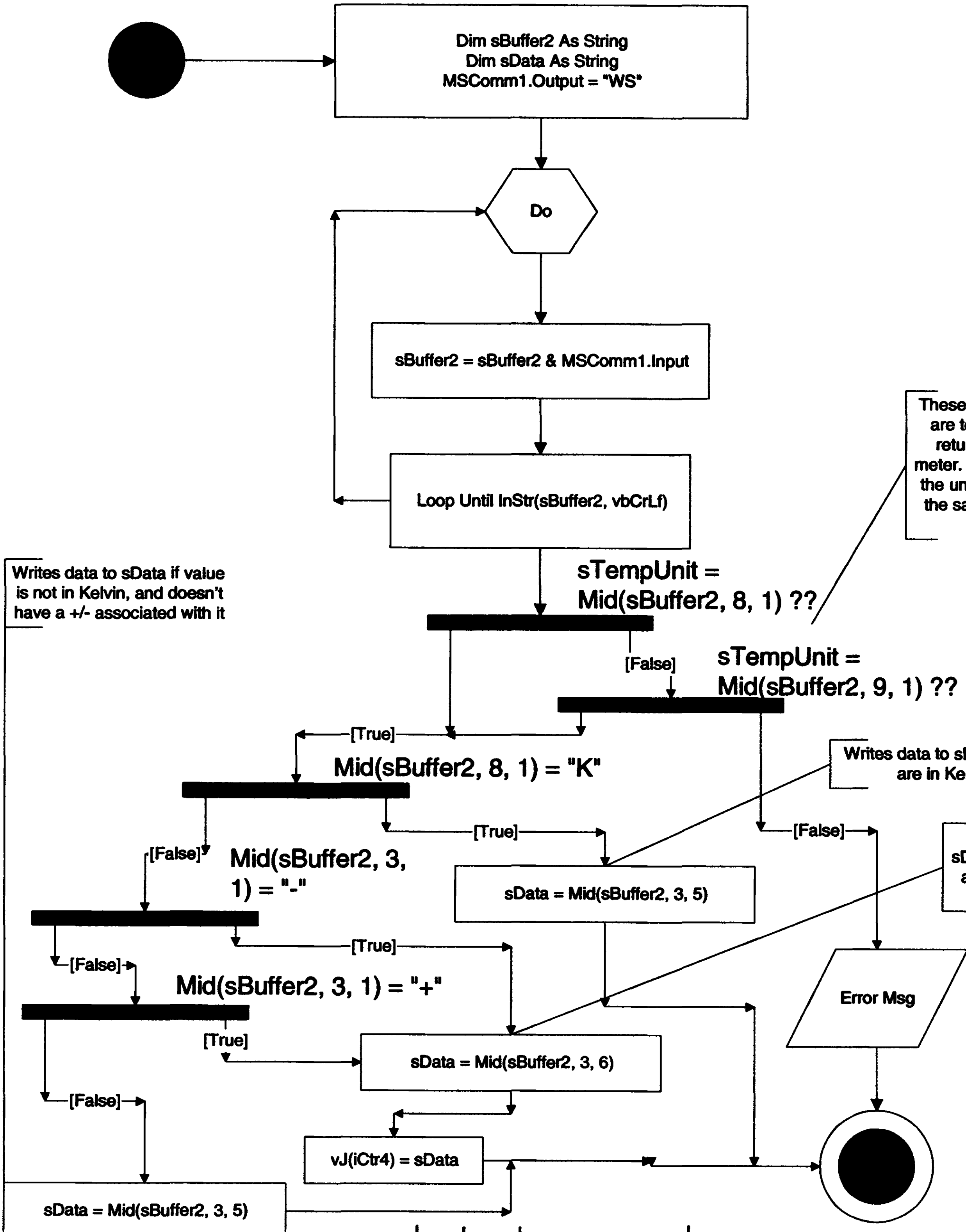

Figure 11: MSComm5_OnComm()

MSComm5_OnComm() writes to the Omega temp meter through the comm port and tells it to start sending back data. It then collects the data, determines if the units are correct, and then sorts out which part of it is raw numerical data, and stores it in sData. It then stores sData into the array vJ, with position iCtr4.

Rev	Who	Date	Notes
01	tnt	2001-07-23	Creation of flowchart for omega temp meter

National Radio Astronomy Observatory		
Dan's Omega Temperature Meter Data Acquisition Program		
Creator: tthacker	Edit Date: 2001/8/6 09:45	
File: \\Eagle\cv-cdl-sis\TThacker\Temperature Meter\Dan's TempMtr\omega temp.vsd	Rev: 01	Page 11 of 16

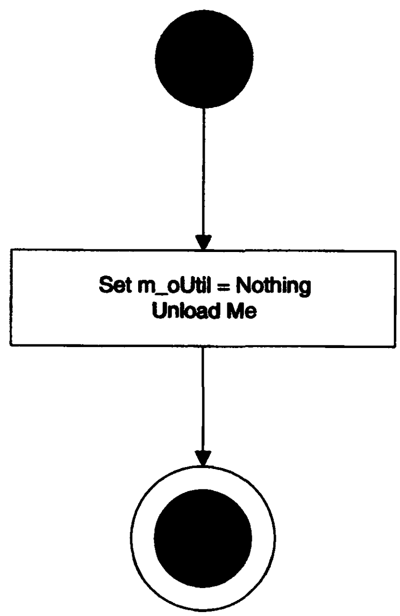

Figure 12: Quit_Click()

Quit_Click() is a button the user can press to activate the UserForm_Terminate sub-routine.

01	tnt	2001-07-23	Creation of flowchart for omega temp meter
Rev	Who	Date	Notes
National Radio Astronomy Observatory			
Dan's Omega Temperature Meter Data Acquisition Program			
Creator: tthacker		Edit Date: 2001/8/6 09:45	
File: \\Eagle\cv-cdl-sis\TThacker\Temperature Meter\Dan's TempMtr\ omega temp.vsd		Rev: 01	Page 12 of 16

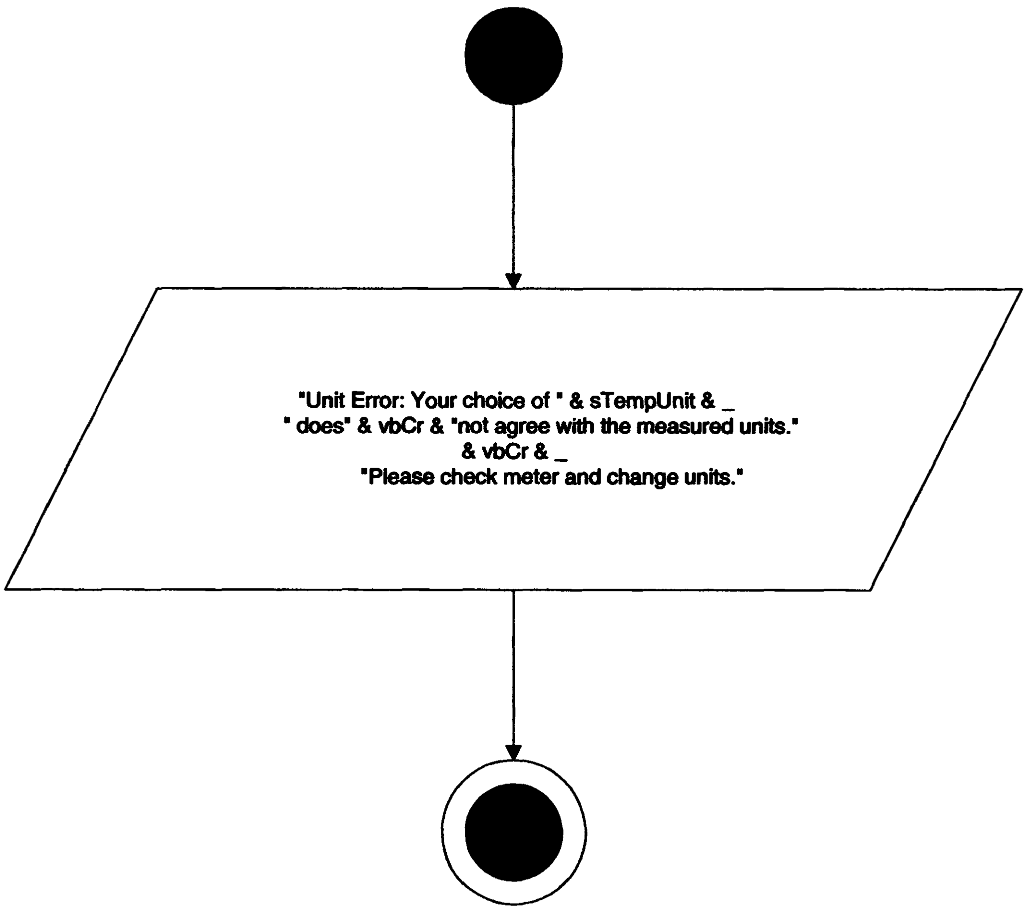

Figure 13: ErrorMsg()

ErrorMsg() is the function called to display the error message if the program determines the units read are not the same as the units choosen.

Rev	Who	Date	Notes
01	tnt	2001-07-23	Creation of flowchart for omega temp meter

National Radio Astronomy Observatory		
Dan's Omega Temperature Meter Data Acquisition Program		
Creator: tthacker	Edit Date: 2001/8/6 09:45	
File: \\Eagle\cv-cdl-sis\TThacker\Temperature Meter\Dan's TempMtr\omega temp.vsd	Rev: 01	Page 13 of 16

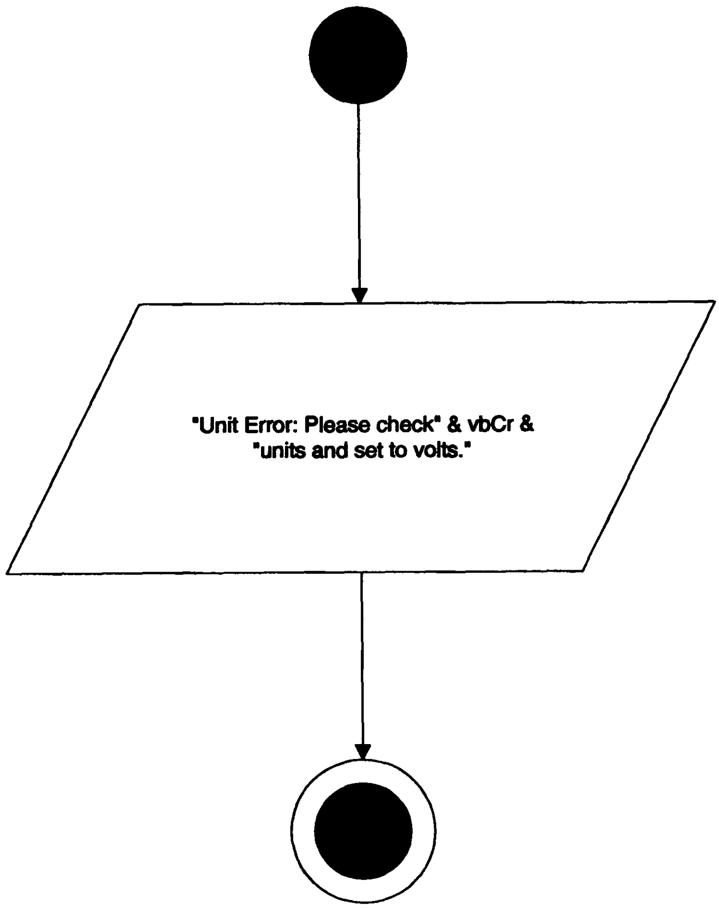

Figure 14: ErrorMsg1()

ErrorMsg() is the function called to display the error message if the program determines the units read are not in volts.

Rev	Who	Date	Notes
01	tnt	2001-07-23	Creation of flowchart for omega temp meter

National Radio Astronomy Observatory

Dan's Omega Temperature Meter Data Acquisition Program

Creator: tthacker	Edit Date: 2001/8/6 09:45	
File: \\Eagle\cv-cdl-sis\TThacker\Temperature Meter\Dan's TempMtr\ omega temp.vsd	Rev: 01	Page 14 of 16

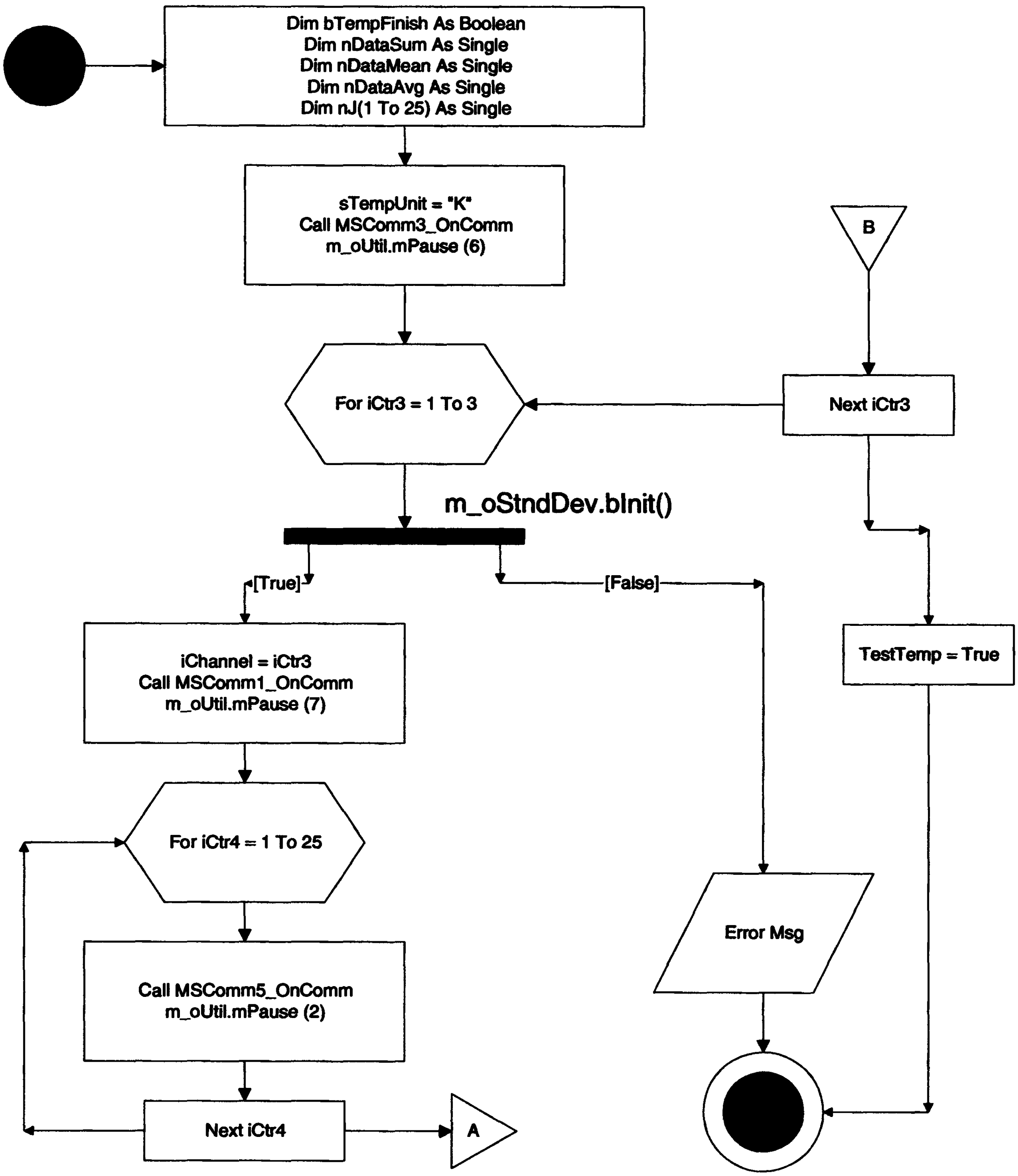

Figure 15: TestTemp()

This section of code, cycles through numerous readings to check to see if the temp meter is still settling. It takes 25 readings, computes the standard error and compares it to the deltaTemp the user input at the beginning.

Rev	Who	Date	Notes
01	tnt	2001-07-23	Creation of flowchart for omega temp meter

National Radio Astronomy Observatory

Dan's Omega Temperature Meter Data Acquisition Program

Creator: tthacker	Edit Date: 2001/8/6 09:45	
File: \\Eagle\cv-cdl-sis\TThacker\Temperature Meter\Dan's TempMtr\omega temp.vsd	Rev: 01	Page 15 of 16

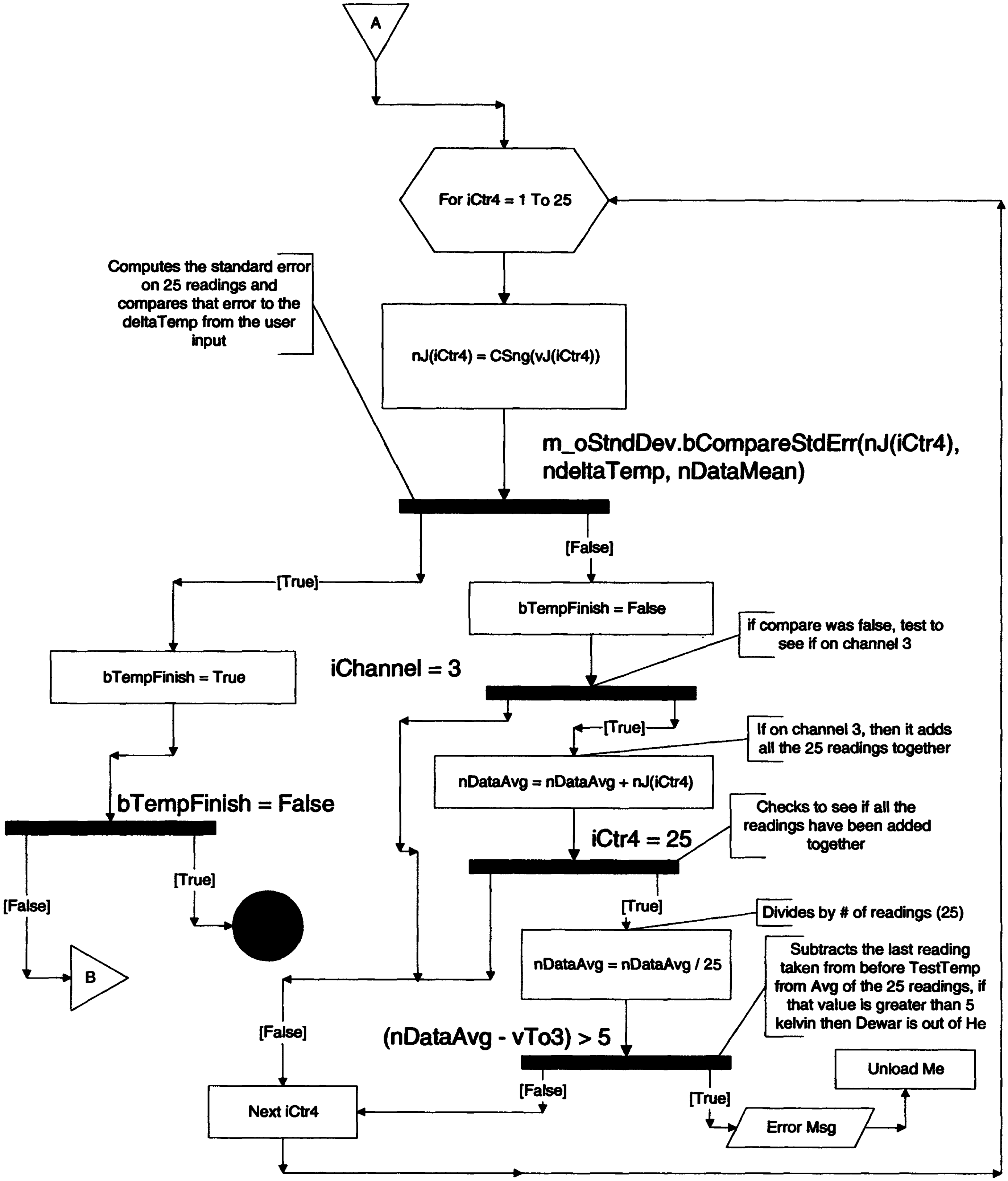

Figure 16: TestTemp() (con't)

Here one can see how the function cycles through the different readings and tests the standard error. One can also see that if the standard error is not met, and certain conditions hold true, the function tests to see if the Dewar is out of He, and exits the program if so.

Rev	Who	Date	Notes
01	tnt	2001-07-23	Creation of flowchart for omega temp meter

National Radio Astronomy Observatory

Dan's Omega Temperature Meter Data Acquisition Program

Creator: tthacker	Edit Date: 2001/8/6 09:45	
File: \\Eagle\cv-cdl-sis\TThacker\Temperature Meter\Dan's TempMtr\omega temp.vsd	Rev: 01	Page 16 of 16

REU Program
NRAO, Vol. Charlottesville, Va, 2001
Summer 2001

Stray Radiation Correction

Paul E. Robinson

Appalachian State University

1. Introduction

I was fortunate enough this year to be chosen as a summer intern at the National Radio Astronomy Observatory(NRAO)'s site in Green Bank, WV. I was informed of my appointment by phone by my NRAO advisor himself, Dr. F. Jay Lockman. I later received paperwork by mail concerning the nature of the employment.

As a radio astronomer, Dr. Lockman is concerned with neutral hydrogen(HI) in the plane of our Milky Way Galaxy. For about a period of five years, from 1994-1999, Dr. Lockman and some colleagues used NRAO-GB's 140' telescope to perform a galactic plane survey for HI, covering much of the sky, with a resolution of twenty-one arc minutes. An HI survey of such resolution has never been done before, so Dr. Lockman's survey is especially important for astronomy.

This past summer, it was my job to refine a computer program, written in the C language, that corrects the 140' data for stray radiation. The program in its original form would take too much computing time to correct the nearly 400,000 data scans. I worked to increase the performance of the program and streamline the code to make it easier to handle such a large data set. In the process of reworking the computer program, I had to learn a great deal about basic radio astronomy techniques, technical aspects of the telescope itself, and computer programming in general.

The bulk of my time was spent manipulating a large data "cube" of previous HI surveys that the stray radiation program uses to compare with the 140' data. Since much of the computing time was being spent reading from that data cube, I worked for nearly a month to shrink the size of the cube, while still maintaining the integrity of the data. I did this by writing a separate program in C that effectively converted the 77MB data cube into an array that is only about 6MB in size. I also changed the way in which the stray radiation program performs some of its calculations. For instance, at one point in the program, a cubic spline interpolation subroutine is called, an action that is taxing on the processing time. I replaced the cubic spline interpolation with a linear interpolation that does not require calling a subroutine. Precision was not lost in the changing of the interpolation procedures.

The end result of my work is a stray radiation program that processes data at least an order of magnitude greater that the original program. The survey data can now be stray corrected and then properly reduced for analysis. I plan to be involved in the later stages of the reduction and analysis of Dr. Lockman's HI survey in the upcoming year.

Dr. Lockman did not hold a monopoly on my advising. The original stray radiation program was written by Edward Murphy, a professor at the University of Virginia in Charlottesville, Virginia. I made several trips to the UVa campus to work with Dr. Murphy on the program. His advice and explanations of the program and in radio astronomy in general were valuable. When I had questions about programming in C, I was able to enlist the help of Jim Braatz here in Green Bank. Jim was very patient with my constant calls for assistance.

In addition to doing work for Dr. Lockman, I was able to take advantage of many educational opportunities in Green Bank. My first week in Green Bank was spent attending a conference of radio astronomers concerning HI Surveys(the very topic that my summer work would entail!). The conference was my first glimpse of the radio astronomy community. Indeed, previous to the conference, I had little to no knowledge of radio astronomy at all. I met astronomers from many different countries, including Canada, Germany, and the Netherlands.

The observatory also hosted several 'institutes in radio astronomy' for college and high school teachers. During these institutes, scientists and engineers would give talks on basic science and technical research at the NRAO. I attended as many talks as I could. Many of the NRAO scientists and engineers also gave presentations to the summer interns. I am leaving the NRAO this summer with much more knowledge than I entered with.

I enjoyed the community in Green Bank. I feel that my fellow interns and I have had an advantage over those students in other REU programs in the large amount of resources we have compared to the small community of scientists, engineers, and technicians that live here. In such an environment, we have made many friends with those in the NRAO community, and I am going to miss the people of Green Bank. Another advantage that NRAO-GB has is the number of visiting scientists that come here. I have met science faculty from literally across the country here in West Virginia. It is just these kinds of acquaintances that help me to learn about potential places to continue my education into graduate school.

My job here at the NRAO in Green Bank has been a fulfilling one. I truly cannot imagine a better job, and if I could intern here again, I would.

Hello! I'm Tucker Freismuth, NRAO Summer Student

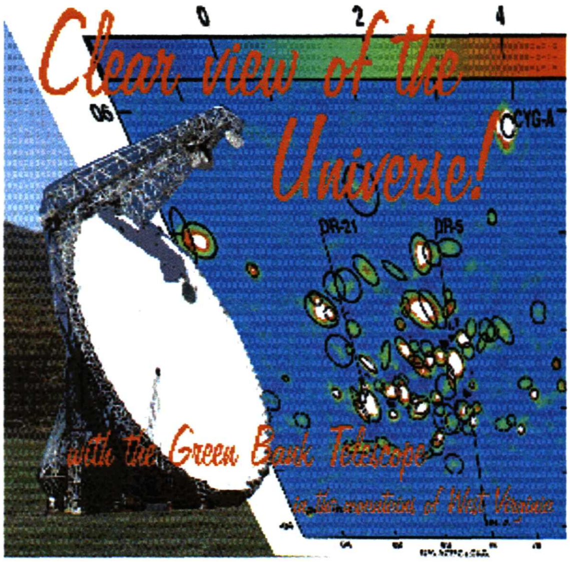

I'm in Green Bank to advance my understanding of Radio Astornomy.

I am currently a student at the College of Charleston, SC, but I call wild and wonderful Wheeling, WV my home. I will be entering my junior year as a physics major with a concentration in astronomy. My previous research experience has been with Bob Dukes at the Department of Physics and Astronomy at the College of Charleston and Shay Holmes (student collaborator) analyzing Galactic Double Mode Cepheid Variable Stars. This research won the South Carolina Academy of Sciences award for outstanding undergraduate research in astronomy in April, 2001.

I have also done work with Jon Hakkila (Dept. of Physics and Astronomy, College of Charleston) analyzing gamma-ray burst data from the Burst and Transient Source Experiment (BATSE) that was located on NASA's Compton Gamma-Ray Observatory. This work will help with the sky exposure for the BATSE 5B Catalog.

This summer I am working on the second Galactic Plane survey at 8.35 and 14.35 GHz with Glen Langston at the National Radio Astronomy Observatory in Green Bank, WV.

Below are links to notable radio sources in our galaxy:

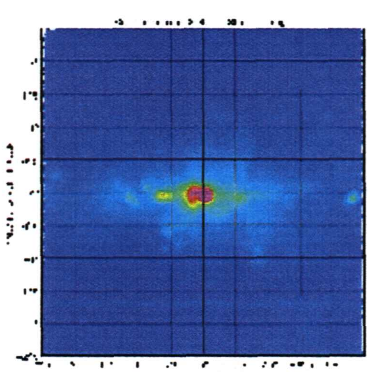

The Milky Way Galaxy (Our Home Galaxy) center is invisible at optical wavelengths but shows remarkable properties at radio wavelengths.

At left is a GBT commisioning observation of the Galactic center.

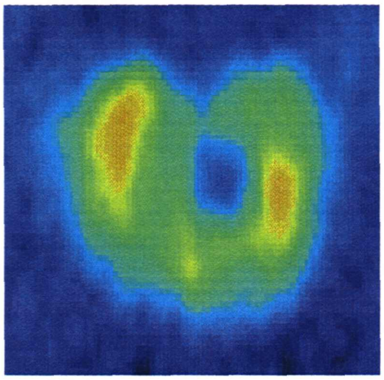

The Rosette nebula (NGC2237) in the constellation Monoceros, is a spherical shell of HI gas and dust surrounding an intense star forming region in the Milky Way Galaxy. The central region has been cleared by stellar " winds" from young OB stars. The Rosette nebula covers an area in the sky larger than six full moons. This image was created at the NRAO in Green Bank as part of the Galactic Plane "B" Survey.

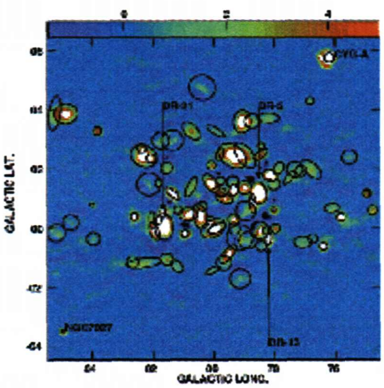

This image shows star forming region DR-21 in the constellation Cygnus

Radio observations have shown that there are many molecules present in the DR-21 region.

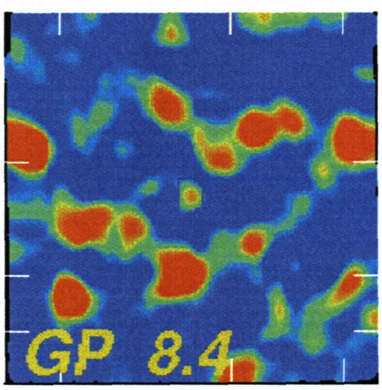

The Cygnus X-3 (A binary star system in our Milky Way) exhibited transient emission on 20 April, 2000.

The image shows Cygnus X-3 in the optical wavelengths, along with the comparison of the 20 April emission at 8.4 Ghz to the Galactic Plane A Survey at 8.4 Ghz. There is also a ROSAT image of the active Cyg X-3.

LINSLY
WHEELING, WV

Learn more about Radio Astronomy at the National Radio Astronomy Observatory in Green Bank.

tfreismu@gb.nrao.edu Last edited 2001 July 24

The Galactic Center: Sagitarius A

The center of our Milky Way Galaxy is difficult to study because of our Solar System is buried within a spiral arm of the galaxy. Astronomers are able to collect vast amounts of data from various galaxies primarily because they are inclined relative to the line of sight. This gives astronomers the ability to see within the galactic centers, unlike the Milky Way where astronomers are forced to look through the plane of the galaxy. Our location within a galactic spial arm lends itself to an extinction of close to 30 magnitudes in the V band of the Galactic Center. The Galactic Center, though, can be studied at longer wavelengths, ie. radio. The Galactic Center has been designated as Sagitarius A (Sgr A) and is part of what is commonly refered to as the "Sgr A Complex" (Zylka et al.,1990). Constituents of the Complex are: Sgr A East, a nonthermal shell source that is the remnant of an explosive event some 40 times the energy of a single supernova; and Sgr A West, a thermal source characteristic of an HII region. Within Sgr A West there is a compact synchrotron source known as Sgr A* (Metzger et al.,1995) about which Sgr A West orbits, and is the suspected galactic central point. Sgr A is about 8.5kpc distant.

Here we examine images of the center of the Milky Way Galaxy: X-Ray to Radio.

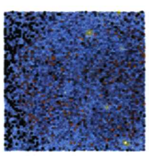

X-Ray

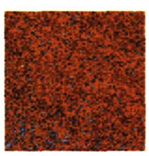

Optical

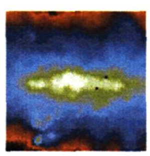

100 microns

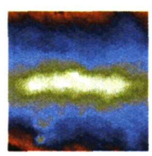

60 microns

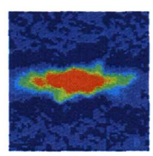

3.59 cm

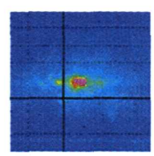

15 cm

- (click on the images below to retrieve FITS format images)

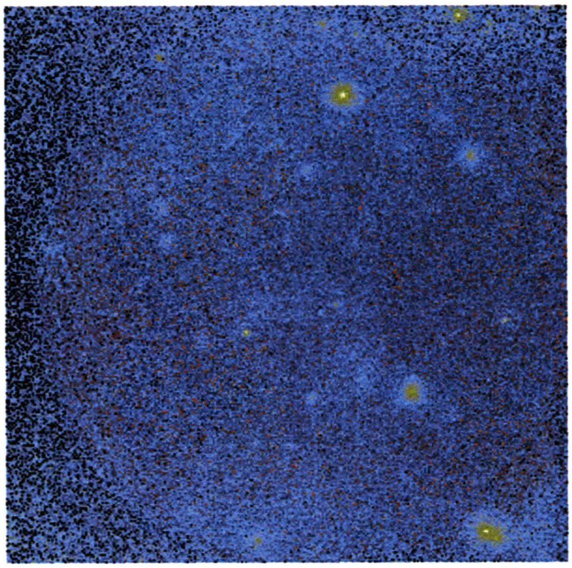

ROSAT X-Ray image of Sgr A (10^{16}-10^{19} Hz)

The Galactic Center at optical wavelengths (380-750 nm) from the Digitized Sky Survey. (400-790 THz)

- Notice that the galactic center is invisible at short wavelenghts.

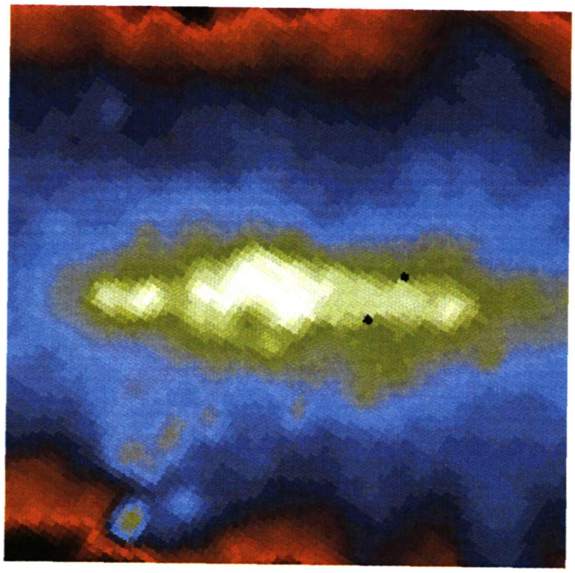

IRAS image at 60 microns (5 THz)

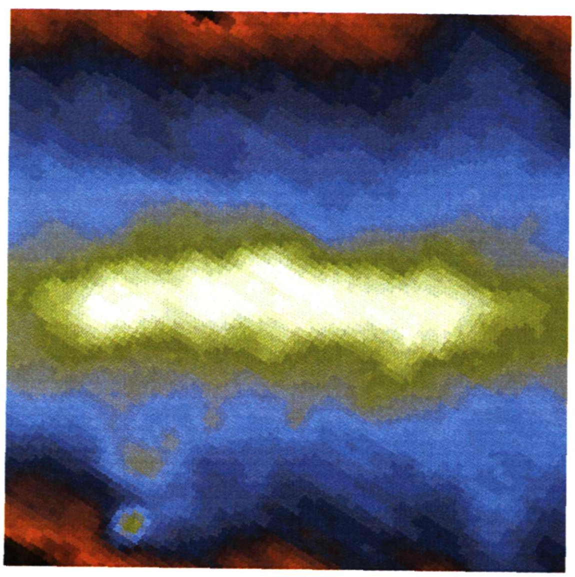

IRAS image at 100 microns (3 THz)

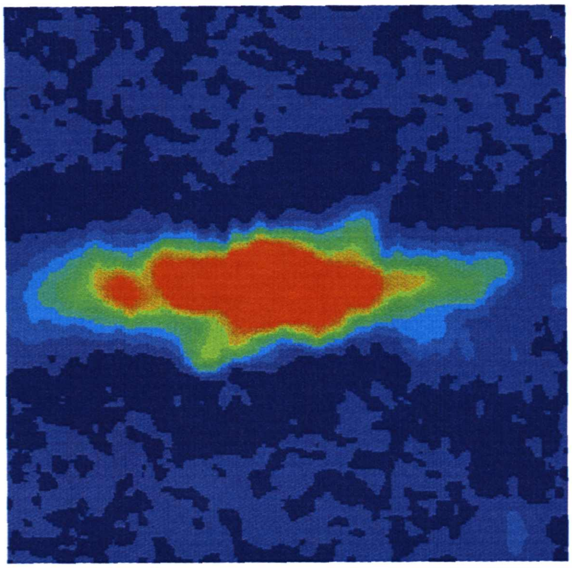

Sgr A at 8.35 GHz as taken from the Galactic Plane Survey A (GPA)

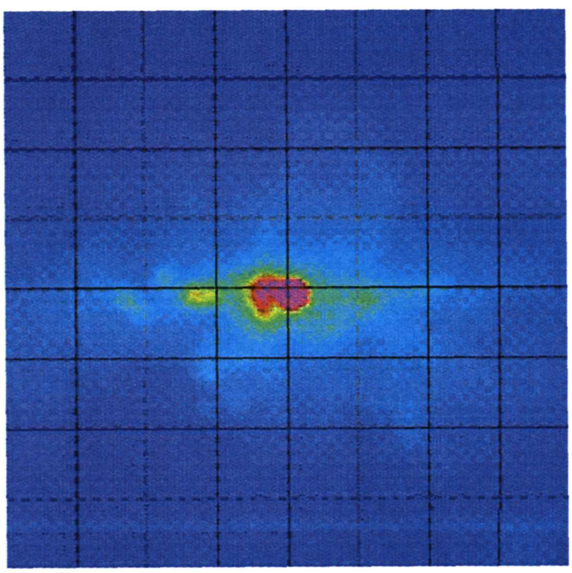

This is a Green Bank Telescope (GBT) commissioning image of Sgr A at 2 GHz

NRAO

SKYVIEW

Learn more about Radio Astronomy at the National Radio Astronomy Observatory in Green Bank.

tfreismu@gb.nrao.edu Last edited 2001 July 24

The Rosette Nebula: (NGC2237)

The Rosette nebula is an emission nebula about 1600pc distant. It is almost 100ly in diameter. The central region of the Rosette nebula is a star cluster designated as NGC2244. It is the hot, young OB type stars in this cluster that provide the strong stellar "winds" (radiative pressure) that blow the HI from the central region, leaving what appears to be a hole within the nebula. The HI shell is still expanding at a rate of 4.5km/s. If the rate of expansion is constant, then the Rosette nebula is about 4 million years old (Kuchar & Bania 1993). This age estimate is consistent with the suspected age of NGC2244. The nebula has an estimated mass 11,000 times that of the sun. Fast-moving molecular knots in NGC2237 are currently being investigated. This beautiful object can be found in the constellation Monoceros (RA 6:30, Dec +5:03).

The Rosette nebula from radio to visible wavelengths:

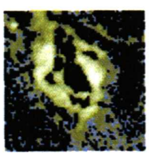
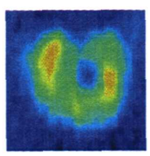
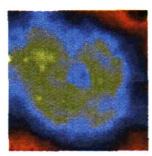
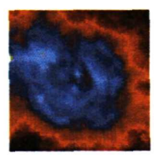
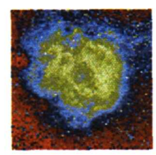

6.19 cm 3.59 cm 60 microns 25 microns Optical

- (click on the images below to retrieve FITS format images)

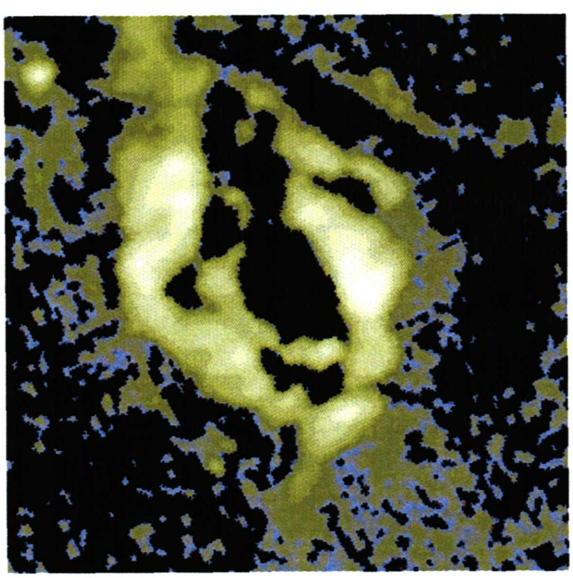

A radio image of the Rosette nebula from GB6 at 4850 MHz.

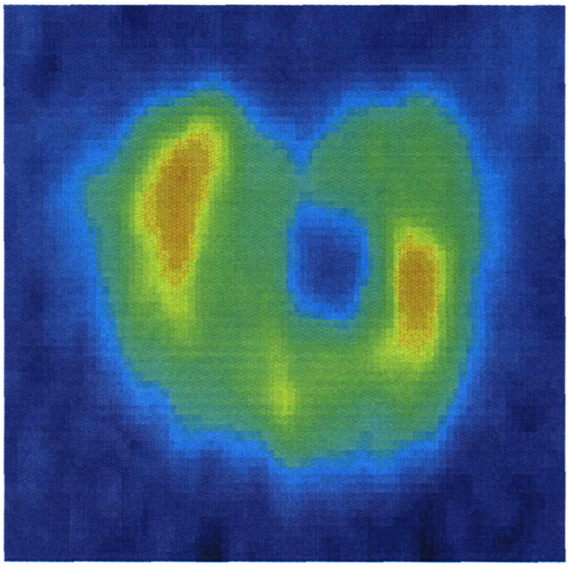

A radio image of the Rosette nebula from the Galactic Plane "B" Survey at 8.35 GHz.

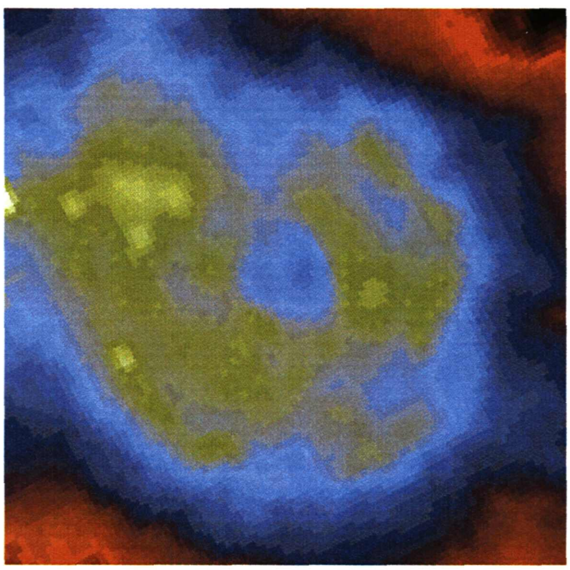

The Rosette nebula at 60 microns (5 THz) from IRAS.

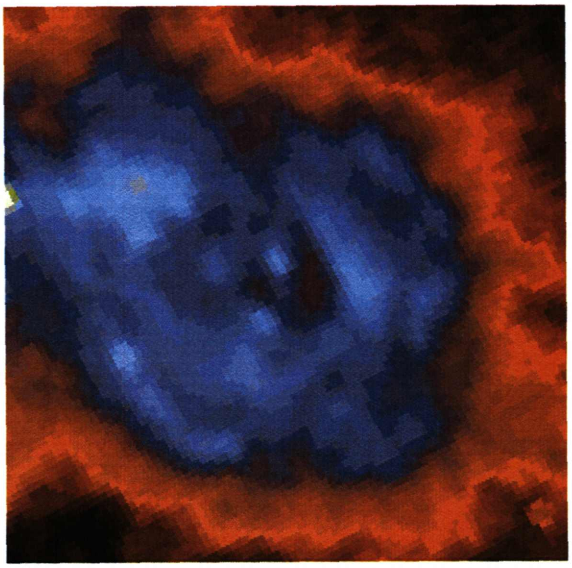

An IRAS image at 25 microns (120 THz).

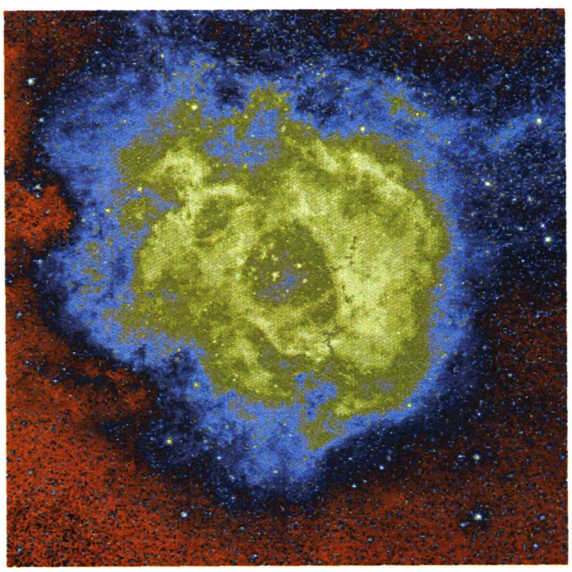

The Rosette nebula at optical wavelengths (380-750 nm) from the Digitized Sky Survey. (400-790 THz)

NRAO

SkyView

Learn more about Radio Astronomy at the National Radio Astronomy Observatory in Green Bank.

tfreismu@gb.nrao.edu Last edited 2001 July 24

How I spent my summer in Green Bank

By Michael Wallace
August 10, 2001

The laser metrology group runs a tight outfit. They can discern the movement of a large structure to an accuracy as small as the thickness of two sheets of paper. The ironworkers at the GBT site were a little scared of them because of the half thousandths accuracy measuring the movement of the GBT azimuth track and Elevation Gear. This was the place to work for a summer student who wanted to see how real and accurate measurements were made. The measurements I did participate in were the azimuth track and elevation gear motion measurements and accurate alignment and pointing of the Laser Range-finding System.

GBT Track and Elevation Gear Measurements

The GBT Azimuth Track previous to my employment had a number of revisions performed to it to minimize movement between the wear strip and the base plate and the base plate and the concrete foundation. The most recent revision was drilling out old holes to put larger bolts through the wear strip to hold down the track. On June 27, 2001 the track needed to be tested to see if the wheels would hit the bolts. John Shelton, Bill Radcliff, Dave Parker, Tim Weadon, and I set up digital indicators to log the movement of the wear strip and the base plate, and we also measured track strain to check wheel alignment.

Results from these measurements were as follows:

1) The wheels seemed to be well aligned when looking at the track strain data.
2) The wheels were not cocked to one side in any way, but their weight caused tension in the top of the base plate where the gauges were placed.
3) Movement of the wear strip was minimal and had a maximum value of around 5 thousandths of an inch.
4) Movement of the base plate was also minimal with the greatest movement around 3 thousandths of an inch.
5) Both of the indicator measurements turned out better than the 140 thousandths movement seen fall of last year.

The revisions appear to be working and that is good news. The improvements to the track were the last big project that needed to be finished on the GBT before COMSAT could leave.

Tim Weadon in July wanted the group to measure the horizontal and vertical run-out of the elevation gear. There are two stands setup under the gear teeth at the front and back of the telescope. A U-shaped bracket was made to be clamped to the stand and fitted around the gear. One-inch indicators rested on a flat place to the side and above the gear teeth. Data was taken one Thursday on the vertical run-out and the next Thursday on the horizontal run-out.

Results from these measurements were as follows.

1. Repeatability holds true for all the measurements. The gear deflects the same way for each change in elevation.
2. The max vertical deflection was about .3 to .4 inches, which is within the .5 inch absolute design specs.
3. The twist of the gear was under .020 in. except for a few spikes at segment joints.
4. The horizontal movement is within the .5 inch design spec but at low elevations the gear moves about .6 inches in the +X direction.
5. The differential horizontal movement shows the change in width of the gear. The large spikes are do to COMSAT grinding the rough edges off of the segment joints.

The Elevation Gear for the most part meets the design specs established, but segments are moving at their joints. If this continues, it could cause problems later on when high frequency observing becomes a priority.

Laser Alignment and Pointing

The Laser Range Finder is a precision instrument any misalignment degrades the overall performance. The laser range finder's primary mirror must reflect a nearly collimated laser beam. If this does not happen then the laser beam will not travel to the target uniformly. Parts of the beam will diverge more than other parts depending on the mirror misalignment. Ultimately a mirror that is not adjusted for correct alignment will affect the signal being received in the detector and the data will suffer as a result.

To collimate the mirror in the field we setup a flat mirror in front of the primary and angled the light toward an autocollimator set to one side of the ranger. An umbrella and piece of cardboard were used to keep to much light from entering the auto-collimator. A program called camera.exe can steer the mirror; we set the mirror servomotor controls so that the mirror could move to four perpendicular positions in elevation while azimuth stayed constant. I would change the primary mirror's orientation while John Shelton tweaked the clips on the back of the mirror and looked into the auto-collimator to see how far out of alignment the mirror was. The autocollimator had rings denoted by minutes or seconds and a set of cross hairs to tell how far off center the mirror is. For the mirror to be auto-collimated all four-elevation orientations had to be within the fifteen seconds circle.

Most of the rangers collimated were off by 1-3 minutes and after auto-collimation became better than fifteen seconds. There was one ranger that must have had a twisted axle because in two of the four quadrants the ranger was slightly outside of fifteen seconds circle while in the other two quadrants it was inside of fifteen seconds.

Now that the mirrors are aligned we checked and tweaked the pointing of all the laser rangers. To check the pointing of the laser rangers we took the covers of all 12 and sequentially went around the loop pointing a rangers beam at it's two adjacent neighbors. If the beam missed or the power received was low then the optics on the ranger were adjusted until the beam hit the target with an amplitude of seven volts. Then we would switch to the other adjacent ranger and tweak the beam until the amplitude was about seven volts. This switching back and forth continued until both sides showed amplitude greater than six volts. Each ZY except 108 points well now.

One other problem arose when we tried to check the pointing. ZY-104 and 105's rangers would not point right at all out at the GBT site and inside on the test range. This problem led us to check the monuments with an inclinometer to see if their tilt angles had changed. ZY-104's had changed slightly but the test range monument was off by over two minutes in the flat angle. This two minutes change made the beam point high on one side and low on the other.

Conclusions

Precision and accuracy makes for a job well done. In my labs at college it has not been stressed as much, but I see now where it becomes a premium. I hope that in the future I can use this knowledge I acquired to provide useful measurements like the measurements I participated in this summer. This summer student position was a great experience for learning about the engineering required for a large mobile structure such as the GBT

HP-5528A Laser Measurement System Data Logging Procedure

By Michael Wallace
August 10, 2001

This is a description of the apparatus setup and computer commands necessary to log distance measurements with HP-5528A Laser Measurement System accurately to 10^-5 millimeters.

Parts List

HP 5528A Laser Measurement System consists of the HP 5518A Laser Head and the HP-Material temperature sensor, the HP-10751B air sensor and the HP-5508A Measurement Display. The laser head is connected to the Laser Source connector on the back of the Measurement Display. The temperature sensor is connected to connector on the back of the measurement display labeled T1, and the sensor is referred to in the program as T1. The air sensor is connected to the connector labeled air sensor, which is also on the back of the measurement display.

The HP-5528A has an IEEE-488 port on the back of the measurement, which is connected to the OMB-SERIAL488A BUS CONVERTER. This bus converter allows for rapid conversion of bus instructions between RS-232 and IEEE-488.

The OMB-SERIAL488A bus converter connects to the computer through a nine pin serial connector cable. The computer is a windows based machine with two serial connectors, keyboard, mouse, and SVGA monitor. The serial connector from the bus converter must be connected to the top serial connector because the program is setup to run on COM1 only. The mouse can use COM2 or the bottom connector.

Power to the HP-5528A Interferometer plugs into the back of the measurement display and is distributed to the other components through their connector cables. The OMB-SERIAL488A BUS CONVERTER needs a power supply rated at less than 9 volts dc. A pin connector is plugged into the back of the converter. The computer and monitor both need 120V AC and the plugs are in the back. The power switches for both the monitor and the computer are in the front.

Software Description and Operation

The software is an executable compiled from Forth code written with LMI URFORTH 16 bit. The executable is HPINT.exe, which resides in the c:\forth directory on the computer called Rocky. HPINT.OVL and MODE.COM must be in this directory for the software to run. To run the program either type **hpint** from the DOS prompt in this directory or click on the executable from the directory window in Win95.

When the program has loaded, a list of command options appear and the note, to toggle a command press a number key. Numbers 1-9 toggle the command listed beside them.

After typing a number, either one of two things will happen another menu will appear asking for input or a command will be transmitted to the Interferometer. For the menu options, read all the text that appears on the screen because there are limits to the input that can be given or a person may have to hit the **ENTER** key after typing there input. If you hit the **ESC** key, then the program will stop.

The program stores logged data in **INTT.dat**. The time is the first column and the measurement is the second column. This data can be plotted in Excel by opening the .dat file with spaces being the delimiters between columns.

Example of Setup and Operation

To measure something that is suspect to move a slight amount, mount the set of two retro reflectors onto the suspect piece and then mount the beam splitter on a stable surface in line with the laser and the mounted retro reflector. There should be two reflections hitting the laser head's bottom aperture. The two reflections need to be aligned so that they both are aimed into the bottom aperture of the laser head. Correct Alignment can be checked by seeing if the laser head's signal LED is on or hit **RESET** on the measurement display making sure that there is no PA ERROR on the screen.

If all the optics have been aligned properly, then attach the temperature sensor to the back of the retro-reflector mount. The air sensor can be attached near to the experiment site on the side of a table or other piece of metal. Both sensors must be plugged in to the back of the measurement display.

To connect the computer to the Measurement Display, an IEEE cable needs to be connected to the back of the measurement display and then to the OMB-SERIAL488A converter. The converter then connects to the computer through a 39 pin to 9 pin serial cable. The nine pine serial connector connects to COM1 or the first serial port since the program is designed for COM1.

All right now to turn on the devices, the measurement displays power switch is on the front. When the system is turned on it checks itself out, I would make sure that the address parameter is set to twenty-six so you can talk back and forth to the converter. After the computer turns on and boots up, initialize HPINT.EXE by going to the forth directory in c-drive. **The first command sent will always cause an error, so hit button 9 on the keyboard and then hit RESET on the panel to clear the error.** Otherwise the program should run without errors.

To correctly set the preset and the resolution you must set the measurement mode first. This is due to the use of a common variable set at the time of the measurement mode. Refer to the attached appendices for activating and viewing temperature sensors and compensation numbers. To initialize compensation go into direct command transmit mode and type in the corresponding command. The direct command transmit mode allows for transmitting any command string to the Measurement System.

Data taking consists of typing button eight at the command menu and waiting for the time and measurement data to appear on the screen. To stop data logging, **Press any Key but ESC key because ESC quits the program** and of course to quit the program press **ESC**.

Appendices

Copy of HP-5528A Commands and Error Descriptions
Dip Switch settings for HP-5528A and OMB-SERIAL488A

For Help with this software the author's email address is either wallis_98@yahoo.com or WallaceM@hsc.edu.

I do not know my phone number for the time being but you can call the HSC switchboard at (804) 223-6000 and ask for Michael Wallace.

REU Program
NRAO, Green Bank, W. Va., Vol. 1, 2001
Summer 2001

Reduction of 21cm HI Galactic Plane Survey

Melissa K. Williams
Valdosta State University, Department of Astronomy, Valdosta, GA, 31698; mkwillia@valdosta.edu

Abstract.
I am a third year student at Valdosta State University in Valdosta, Georgia seeking my Bachelor of Science degree in astronomy. I will receive my undergraduate degree in December 2003. This internship during the summer of 2001 with the National Radio Astronomy Observatory of Green Bank, West Virginia was my first internship. I chose to pursue this opportunity in the hopes of narrowing my desired field of research for graduate school, which I should enter in January or August of 2003. I was assigned to work with Dr. Felix J. Lockman in the reduction of data from his HI galactic plane survey designed to study the hydrogen envelope of the Milky Way galaxy far from the galactic disk where it begins to be affected by the interstellar environment. The survey was a project undertaken by Dr. Lockman in conjunction with Dr. Edward M. Murphy of the University of Virginia. A second student, Paul Robinson, of Appalachian State University, was also assigned to work with Dr. Lockman on the reduction effort. His portion of the research was dedicated to correcting the survey data for stray radiation.

1. Introduction

The data set taken by Lockman and Murphy consists of approximately 400,000 individual spectral scans, which is a considerably large data set. Reduction of such a large data set requires several major steps. The first step is to calibrate data taken for several standard regions, S6 and S8, which will eventually be used to calibrate the survey data to find the beam-averaged brightness temperature. The second step is to correct the calibration data for stray radiation. The data must then also be corrected for atmospheric attenuation. Once the calibration data is fully reduced, it can be applied to the survey data in one calibration factor. The survey data must be corrected for stray radiation and atmospheric attenuation before the calibration factor can be applied. The final outcome after all data has been reduced is a three dimensional map of the galactic plane. I was responsible for reducing the calibration data of standard regions S6 and S8. This reduction is a miniature version of the entire survey reduction. Once the two major portions of the reduction process are completed, that is, the calibration reduction and the stray radiation correction, it is a simple process to complete the averaging and differencing of the survey data using AIPS++.

2. Equipment

The 21cm data was taken with the140 Foot Telescope of the NRAO in Green Bank, WV. The project spanned a period of four years between June of 1996 and May of 1999. The telescope has an angular resolution of 21' at the wavelength of the 21cm HI line. Plans were made to complete several follow-up observations using the newly commissioned Green Bank Telescope, the world's largest fully steerable telescope. Unfortunately, the GBT was not completely operational until after the internship period was complete.

3. Reduction Programs

Initially, I was instructed to reduce the data using AIPS++, but after careful consideration, Dr. Lockman decided to use UniPOPS for the first portion of the reduction process. AIPS++ is designed so that it can handle large data set reductions at one time. However, the process of calibration reduction is easiest using the same program that was used to collect the data, in this case UniPOPS. Dr. Lockman decided to use AIPS++ only for the full reduction after the calibration factors were determined and for the final map production. The first four weeks of my internship, I learned the basic operation of the AIPS++ reduction process under the direction of Dr. Jim Braatz, who was extremely helpful in my learning the operation of the program. The next two weeks were devoted to learning the same reduction processes using UniPOPS under the direction of its author, Dr. Ronald Maddalena.

4. Corrections

Edward Murphy had previously written a program to correct the data for stray radiation. The program was not capable of handling the entire data set at once and so was being modified by Paul Robinson in order to do so. It was, however, sufficient for correcting only the calibration data in a timely manner. Therefore, this was the program that I used to begin reducing the calibration data. Each scan had to be individually differenced with its stray correction. Of the two resulting corrected polarizations of each scan, one was then baselined to correct for noise interference from the telescope and then corrected for atmospheric attenuation. The two final polarizations were left in a state where they could be averaged together to determine the final calibration correction. I was, due to the lack of time, unable to perform this averaging. Once the average is taken, the calibration constant can be determined. Normally, both polarizations of each scan would be corrected simultaneously. This was not done here to preserve continuity throughout the entire survey reduction. Of the survey data, one polarization was corrected for stray radiation using Paul Robinson's modified program. The program was only capable of correcting one polarization at a time. The other polarization was left to be baselined and corrected for atmospheric attenuation. Once both polarizations are corrected individually, they can be averaged and the calibration factor applied. The calibration constant is multiplied by the antenna temperature and differenced for the near and far sidelobe correction of the survey data that is determined by the stray radiation correction program. The result is the brightness temperature for each scan. These results can be used to create a three dimensional map of the galactic plane area surveyed.

5. Comments

This being my first internship experience and my first experience working in the area of radio astronomy, I felt that I needed more guidance than I received. Perhaps this is the best way to learn, having to figure out things on your own. I do feel that I learned a great deal from my experiences at the observatory. I learned a great deal of computer skills that I did not posses previously and I now have a more detailed impression of work in radio astronomy. As much as I would like to find my niche in astronomy, I did not yet come to a decision about my research choices for graduate work. I feel that I will need to complete other internships in other areas of astronomy to accurately determine my area of choice. I am therefore very grateful for the opportunity to have begun my search for a career through the generosity of the National Radio Astronomy Observatory and the National Science Foundation. This opportunity was a great way for me to make friends and acquaintances that will affect my life's work. I have been introduced to other students, to teachers, and to professional astronomers and computer scientists who will have the opportunity to evaluate my work and help determine what some of my career paths will be. Overall, my experience at Green Bank, WV was a good one. Although I do not feel that I completed my work this summer, I do feel that it prepared me to develop good working habits. This internship has helped to prepare me for the kind of work I will be expected to do as a scientist. I had a great deal of fun taking new risks and learning new things that will help me in the remainder of my undergraduate courses. I am very appreciative of this opportunity and I hope that it will present itself again in my future. I would like to acknowledge the help I received from Jay Lockman, Ed Murphy, Jim Braatz, Ron Maddalena, and Al Wooten. I would also like to thank the National Radio Astronomy Observatory, Associated Universities, Inc. and the National Science Foundation.

The CLASS Project

Jason Adelstein, Columbia University

Dr. Steve T. Myers, NRAO

CLASS Project

The Cosmic Lens All-Sky Survey (CLASS) is a large international project aimed at observing more than 10,000 radio sources in the Northern Sky. The primary purpose of this survey is to identify cases where these objects have been multiply imaged by flat spectrum radio sources (e.g. an intervening galaxy). [The classification of "flat spectrum" sources for the purposes of the survey is those sources whose spectral index $\alpha \geq -0.5$ between 1.4 GHz and 4.85 GHz.] An important use of gravitational lenses is to aid in the determination of cosmological parameters, such as the Hubble constant, H_0. This requires a well-selected sample of lenses.

The VLA observations for CLASS were completed two years ago. Combining earlier JVAS survey results with CLASS, a database of over 15,000 sources has been compiled. From this large database, fourteen new gravitational lens systems have been discovered (with nineteen total systems in the database). Thanks to the CLASS, this more than doubled the number of radio-loud lens systems known before the survey. Now that the VLA's observations are complete, multi-wavelength follow-up observations on gravitational lens system candidates identified in the survey are being conducted.

The primary goals of my summer research were to work with Dr. Steve Myers in building a world wide web accessible CLASS archive, do morphological studies, classify the CLASS radio sources, and to make sure that no gravitational lensing cases had been overlooked. (Recently, a "missed" lens was found on recalibration of the survey.)

1. ***Build the CLASS Archive at the NRAO:*** The CLASS archive has been built at the NRAO. Within the archive are the calibrated UV FITS files. In addition, output from the automap scripts such as modelfit data (number of components automap found for source),

source images (plots of the sources), and logfiles (the record of the automap's run on the source) are located in the archive.

2. ***Categorizing the Morphologies:*** The CLASS data's main use has been to identify any new gravitational lenses. However, there are many more uses for the survey if an easily accessible archive is constructed. There are only nineteen known gravitational lensing systems in an archive of over fifteen thousand sources. Approximately eight percent of the CLASS archive is composed of multiple component sources. Being able to identify sources as multiple compact components (lens candidates and compact double/symmetric sources), core-jet or core-lobe sources (one compact object, others extended), extended sources (radio lobes and blended compact sources), or artifacts (sidelobes, etc.) is an important part to the developing archive and its accuracy.

   Currently, I am in the process of categorizing the distinct morphologies of multiple component sources. In addition to the multiple sources, I am attempting to identify interesting individual sources from the morphological study. Due to the vast number in the archive, I have concentrated on mapping a subset of the CLASS-4 (1999) observations.

3. ***Quantify the completeness and robustness of the automap products in the archive:*** Automap scripts process sources very quickly in the Difmap mapping program automatically. This saves the user much time going through the sources individually. Once the automap has run on all the sources, the user can study the results. However, first the results must be accurate to proceed.

   Another phase of my summer research entailed making sure the data gathered from the automapping products was valid. This entailed testing the latest round of CLASS data (CLASS 4). If fake multiple sources were found, they had to be remapped and put back in the archive. This called for modifying multiple automapping scripts. Each modification corrected previous problems, but others arose in their place. While there was advancement in some areas of the scripts, further work needs to be done with the automapping materials.

During the course of this analysis, it became clear that there were differences between the 1998 and 2001 versions of the difmap program. These differences, although not major, caused dissimilar results when using the same automap script. The problem with this finding is that the previous CLASS archives had used the 1998 edition and we had used the 2001 version. Previous archives must now be tested using the 2001 version of difmap to correct for the deficiencies in the older edition and to provide consistency in the whole archive.

4. Tools: The final element of the summer project was to use and develop tools to index (via HTML), catalogue (via text files), and visualize (via images) the archive contents. Even though there has been little in new tool development for the archive, the basic indices have been completed. Employing multiple scripts of different languages, all of the necessary basic items are there to start the database. In the table below are a listing of the scripts used and their function for aiding in the development of the web archive. The index to the archive can be found at *http://www.aoc.nrao.edu/~smyers/class/archive.html*.

Language	Script Name	Use	Author
C	pos.c	■ take difmap modelfit output .gmod files and create a catalog	C. Fassnacht

Perl	classgen.pl ghead.pl	■ for the main index ■ aids in creating VLA header information	S. Myers S. Myers
C Shell	ghead.csh	■ aids in creating VLA header information	S. Myers
C++	classhtml.C	■ for individual source HTML indexes	D. Rusin
Fortran	catalogue.f	■ cross-index versus GB6/NVSS surveys; selects sub samples from .gmod catalog	S. Myers

Summary

The groundwork for the web database is in place. However, there are issues that must be resolved before going further with the online archive. Completing the categorization of the distinct morphologies of multiple component sources is vital. In addition, remapping false multiple component sources and reinserting them into the archive is key to the database's accuracy. Finally, further modification of the automapping materials is needed to allow the archive to be set up in less time.

References

"CLASS: A Gravitational Lens Survey of Flat-Spectrum Radio Sources –I. Source selection and observations." By Steve T. Myers et al.

Figure 1 – B1608+656 → A quadruple lens from the CLASS archive now at the NRAO.

Figure 2 – B2108+213 → The newest confirmed lens to date. A double lensing system from the newest CLASS data that I was working with this summer.

Figure 3 – An extended source categorized from the morphological study this summer.

Figure 4 – A double extended source categorized from the morphological study this summer.

Figure 5 – A flow chart of how an automap script works.

Clean I map. Array: VLA
16156554 at 8.440 GHz 1994 Mar 01

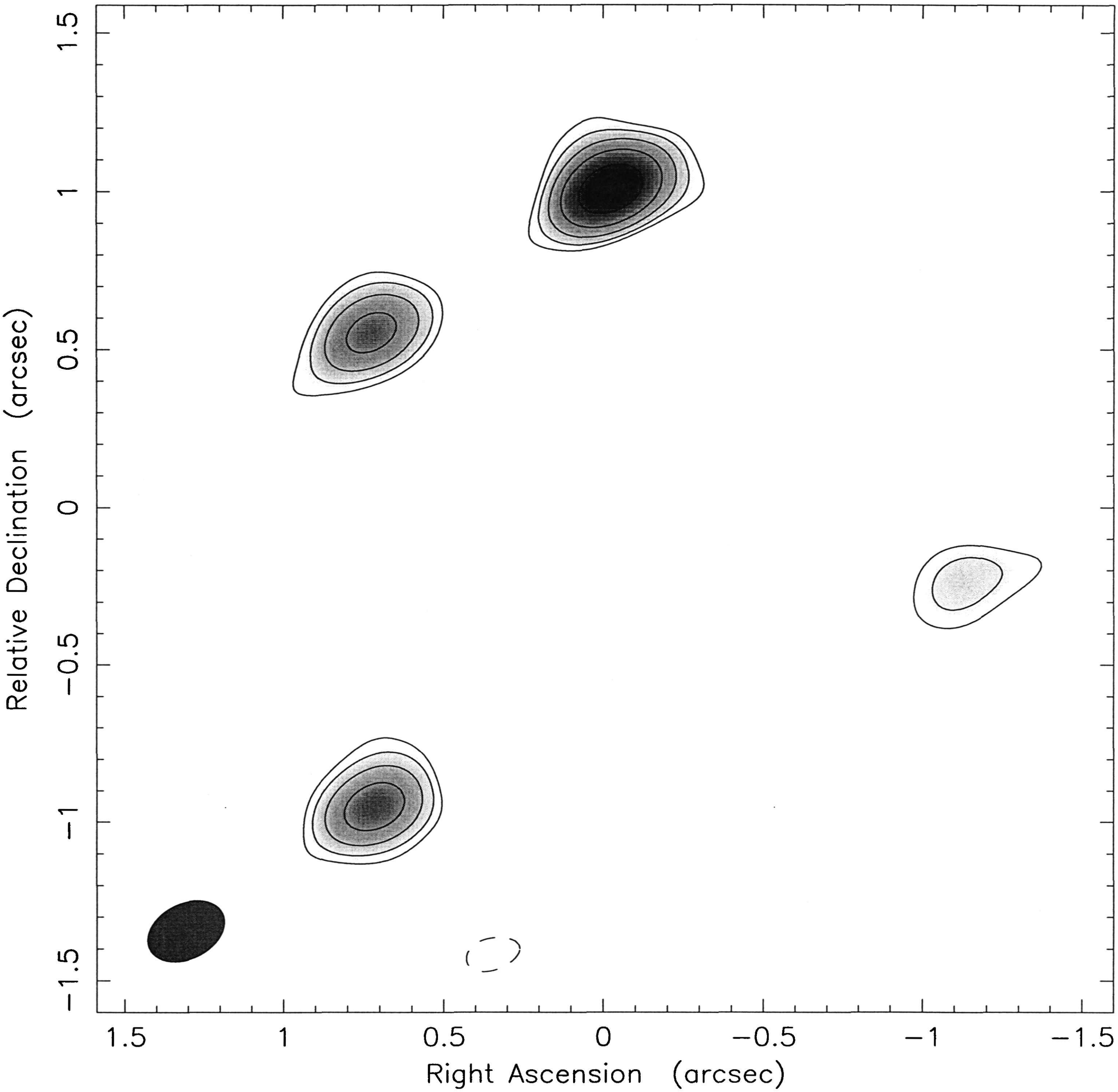

Map center: RA: 16 09 13.960, Dec: +65 32 27.966 (2000.0)
Map peak: 0.0359 Jy/beam
Contours %: −4 4 8 16 32 64
Beam FWHM: 0.256 x 0.174 (arcsec) at −63.6°

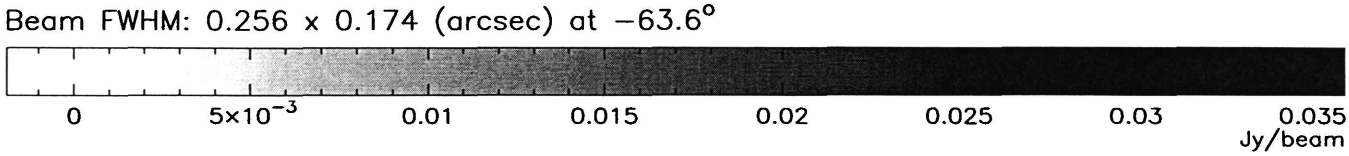

Clean I map. Array: VLA

21182151 at 8.460 GHz 1999 Aug 17

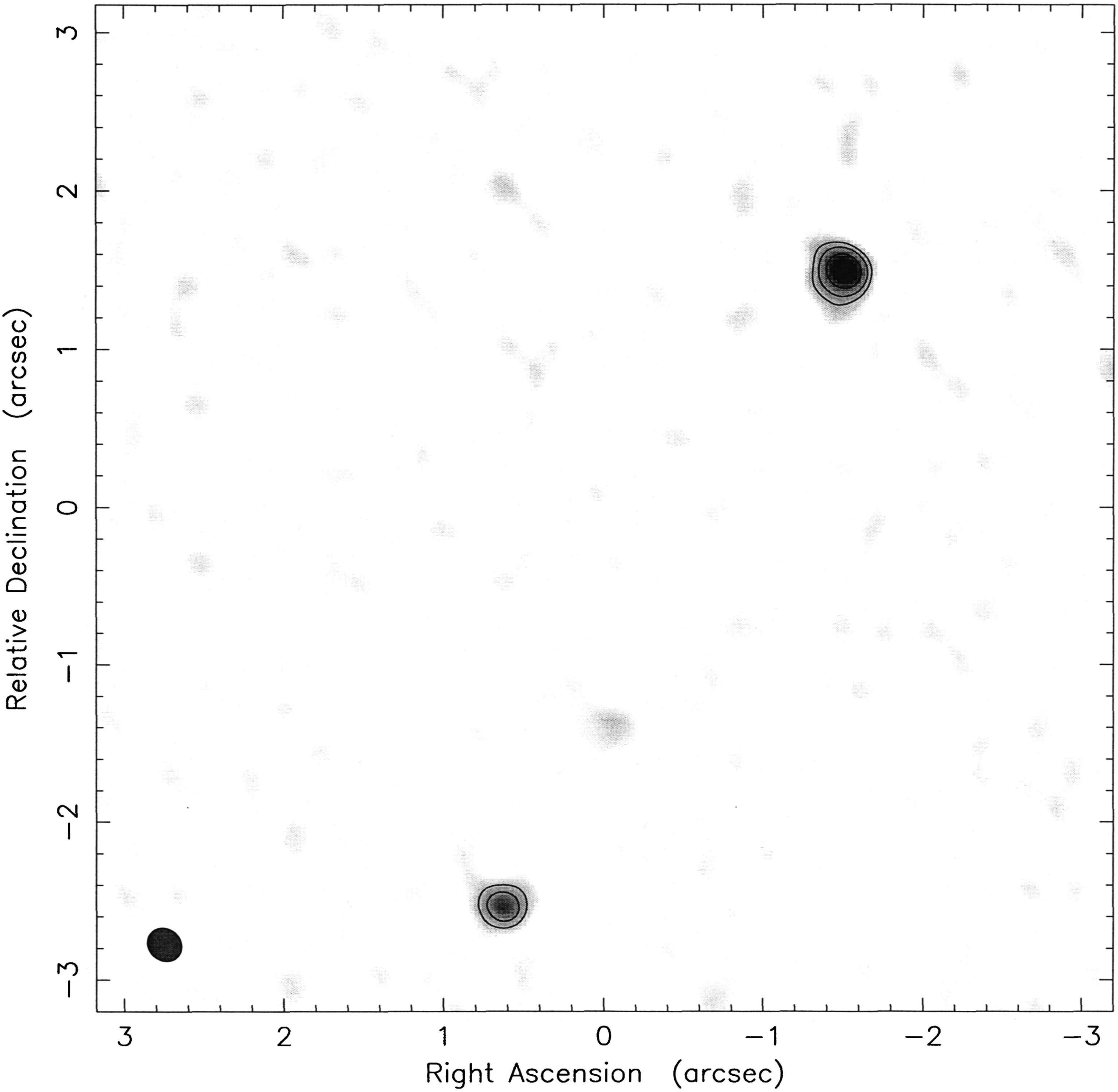

Map center: RA: 21 10 54.133, Dec: +21 30 59.100 (2000.0)

Map peak: 0.0112 Jy/beam

Contours %: 12.5 25 50

Beam FWHM: 0.226 x 0.2 (arcsec) at 48°

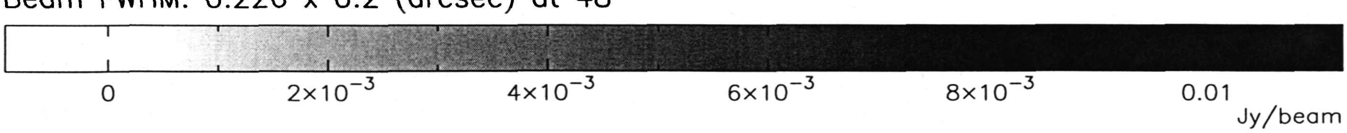

Clean I map. Array: VLA
05610882 at 8.460 GHz 1999 Aug 17

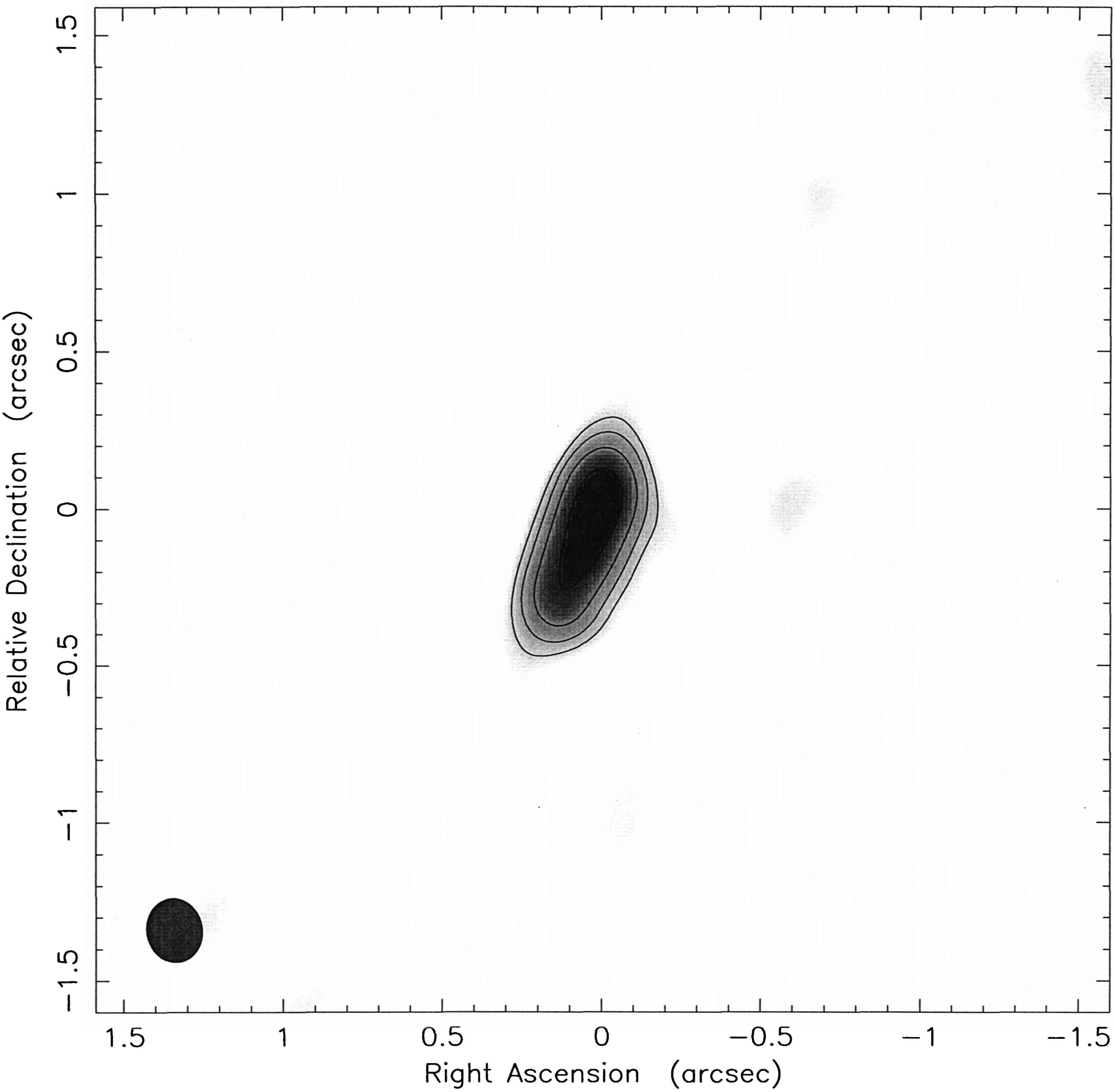

Map center: RA: 05 36 40.419, Dec: +08 51 05.499 (2000.0)
Map peak: 0.0541 Jy/beam
Contours %: 8 16 32 64
Beam FWHM: 0.203 x 0.173 (arcsec) at 11.2°

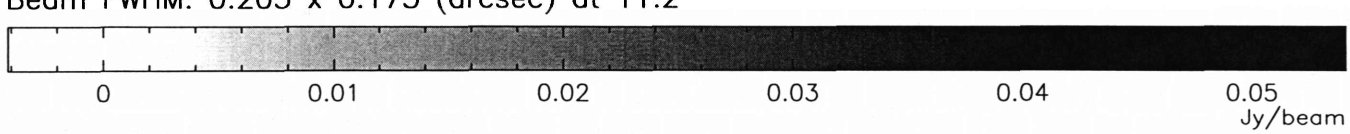

Clean I map. Array: VLA
23392913 at 8.460 GHz 1999 Aug 17

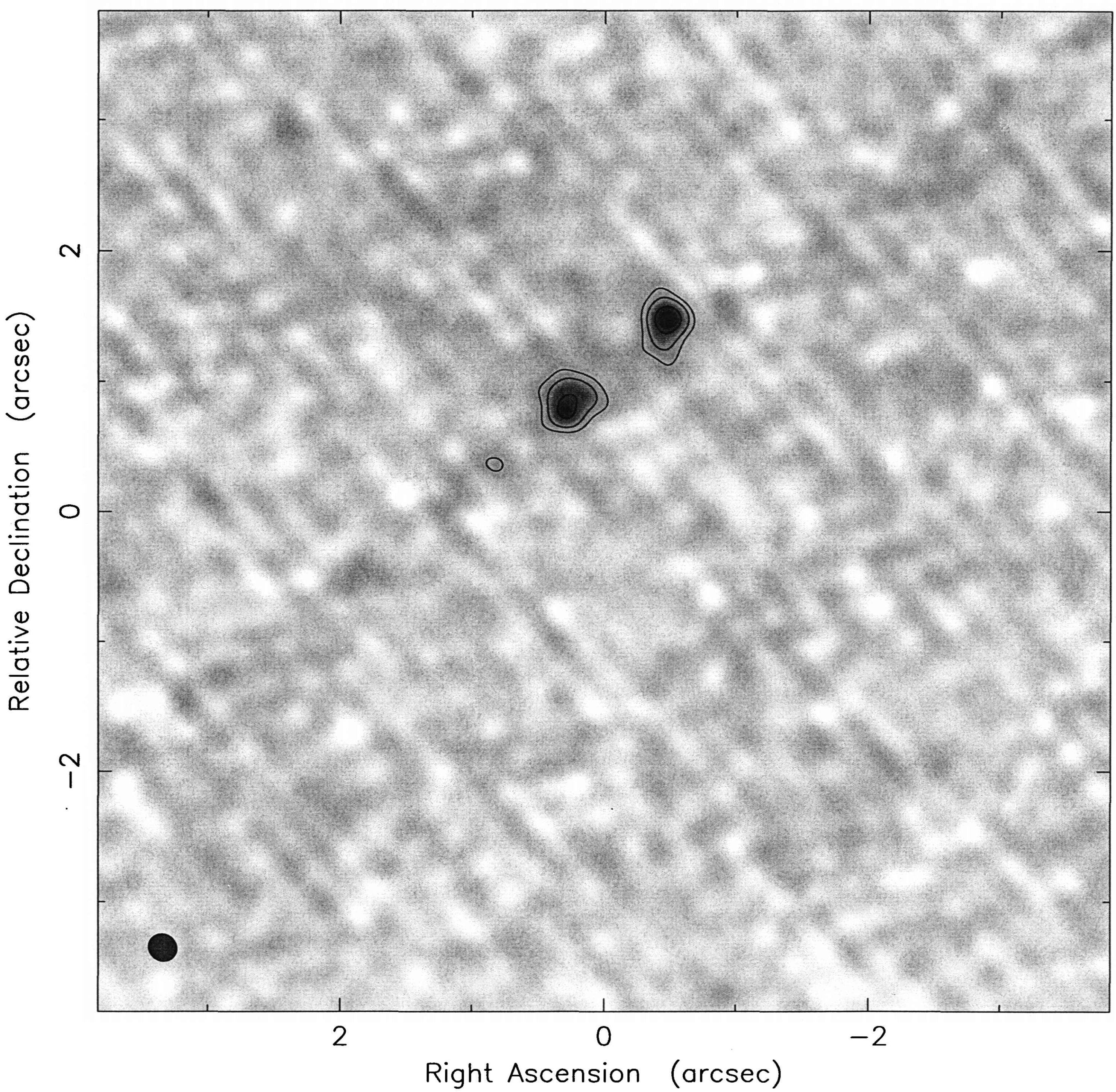

Map center: RA: 23 23 50.220, Dec: +29 08 23.200 (2000.0)
Map peak: 0.00868 Jy/beam
Contours %: 16 32 64
Beam FWHM: 0.222 x 0.204 (arcsec) at 58.9°

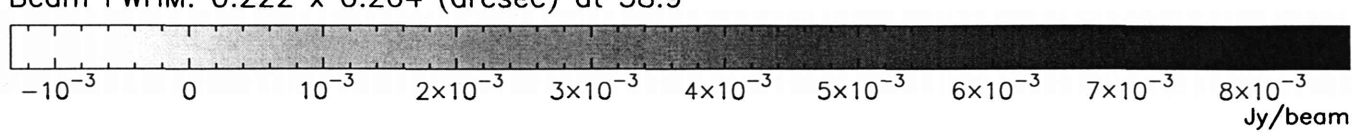

What the Automap Does

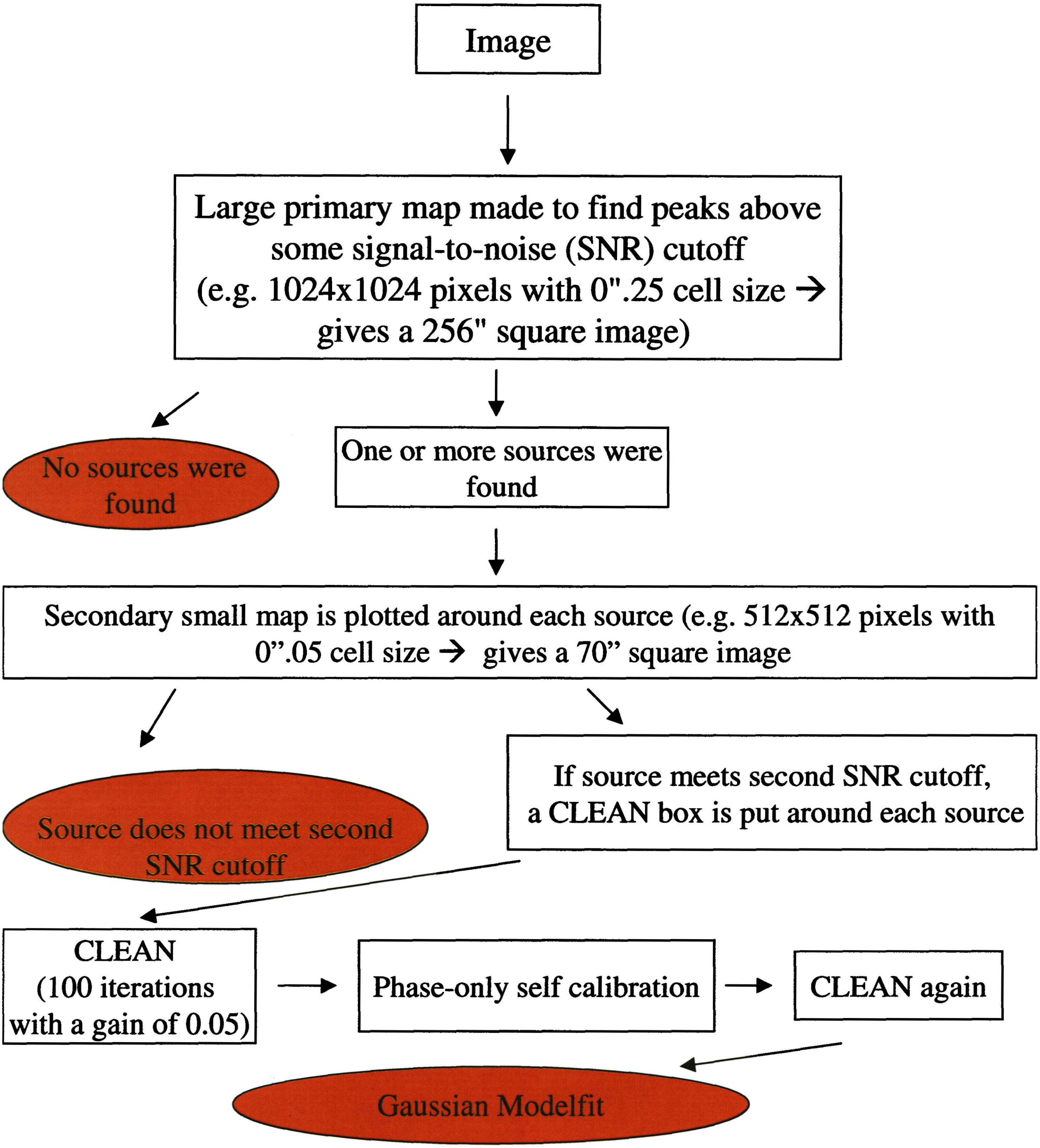

Radio Limits on the Proposed Supernova in NGC 7582

James M. Anderson[1] and James S. Ulvestad

National Radio Astronomy Observatory, P.O. Box 0, Socorro NM 87801

janderso@aoc.nrao.edu

Received ______________; accepted ______________

Draft for AJ Paper?

[1]Department of Physics, New Mexico Institute of Mining and Technology, 801 Leroy Place, Socorro NM 87801

ABSTRACT

Subject headings: galaxies: Seyfert — galaxies: individual (NGC 7582) — supernovae: general — radio continuum: galaxies — X-rays: general

1. Introduction

In the standard unification model for active galactic nuclei (AGN), Seyfert 1 and Seyfert 2 objects are believed to represent members of the same intrinsic class of objects which are viewed from different angles. Gas and dust fall toward a supermassive black hole located at the center of the AGN. Conservation of angular momentum of the infalling material leads to the formation of an a disk (torus) surrounding the black hole. The gravitational potential energy released as the gas falls onto the black hole powers the AGN, heating the gas to very high temperature. In this region close to the black hole the hot gas produces strong continuum emission and broad emission lines. The width of these broad lines is presumably determined by the high temperature and rotational velocity of the gas near the black hole. Farther from the black hole, outside of the torus region, narrow emission lines are produced by particles having a smaller spread in relative velocity differences. An observer looking at the AGN from the direction of the rotational pole of the torus would see the central broad line region, leading to a Seyfert 1 classification. On the other hand, the high optical depth of the gas and dust in the torus prevents light from the broad emission line region to pass, so that an observer in the plane of the torus would only see the narrow line emission, leading to a Seyfert 2 classification. Observations at intermediate viewing angles will produce similar results, with classification changing from 2 to 1 around the opening angle of the torus. Under certain conditions, some objects may be giving intermediate classifications (Seyfert 1.5, 1.8, etc.) as the broad line region becomes less and less extincted.

An alternative to this model has been developed by Terlevich and collaborators. In this model, the broad line components of AGN are explained by supernovae at the cores of galaxies. The broad lines result from the initial rapid expansion of the supernova material after the explosion of a star. After a period of several years, the supernova ejecta is sufficiently slowed by the interstellar medium that only narrow emission lines are observed. For galaxies with low supernova rates, the galaxy will spend most of its time with only narrow emission lines being produced in the core. However, at random intervals a supernova will go off, creating broad emission lines for a short period of time.

Such an even was proposed to have happened to the galaxy NGC 7582. Broad emission lines developed some time between spectroscopic observations on 1998 Jun 0 and 1998 Jul 11. An increase in the continuum level of the optical emission was also observed at this time. These broad emission lines were again observed in 1998 Oct. The characterization of the emission lines classified the galaxy as a Seyfert 1 galaxy, whereas the galaxy has previously been classified as a Seyfert 2.

Supernovae in dense interstellar environments are expected to produce radio emission from the acceleration of particles in the shock front of the supernova. To test whether or not this broad line appearance in NGC 7582 was due a supernova, radio observations of the galaxy were undertaken.

2. Radio Observations

2.1. Observations

A search for the radio counterpart to the proposed supernova was conducted with the VLA[2] (Thompson et al. 1980). New A array observations were made at 3.5 and 6 cm on 1999 Sep 04 and 2000 Dec 12 (approximately 420 and 519 days after the initial detection of broad lines in NGC 7582). All VLA archive observations of NGC 7582 made in the A configuration were accessed to provide comparison measurements prior to the broad line event. Table 1 shows the date, wavelength (λ), sky frequency (ν), bandwidth ($\Delta\nu$), and integration time (τ) for individual observations.

Observations of NGC 7582 were usually interspersed with observations of nearby calibrator sources to provide phase calibration for the VLA. Various calibrators were used for the archive data. Source 2314-449 was used for the new observations except for the end of the 2000 Dec 12 run when this source had set and 2324-372 was used. The standard source 3C 48 was used for amplitude calibration for all observations except 1980 Aug 08 for which no amplitude calibrations were made by the original observer. These observations are therefore uncalibrated in amplitude and only useful in a relative sense within the final image. For the remainder of the observations, visibility amplitudes were calibrated by first assuming flux densities of 3C 48 on the scale of Baars et al. (1977), as confirmed or adjusted by VLA personnel. Flux densities of the other calibrators were found relative to 3C 48. The antenna gains (amplitudes and phases) for NGC 7582 observations were set using the values of the nearby calibrators.

---

[2]The VLA is a facility of the National Radio Astronomy Observatory, which is operated by Associated Universities, Inc., under a cooperative agreement with the National Science Foundation.

Following the initial calibration sequence, phases were adjusted on an antenna-by-antenna basis using a standard self-calibration process provided by the task SCMAP in the Astronomical Image Processing System (AIPS). A solution interval of 20 s was generally used for the self-calibration procedure and amplitudes were not adjusted. Observations on 2000 Dec 12 were made during a snowstorm at the VLA site, and the short solution interval produced unsatisfactory results. SCMAP was run with an initial solution interval of 2 minutes; this interval was incrementally decreased to 1 minute during as the task worked on the data. After self-calibration, all data were reimaged using the AIPS task IMAGR with a ROBUST parameter of zero to provide a balance between high resolution and sensitivity (Briggs 1995).

2.2. Results

Figure 1 shows a contour image of NGC 7582 from the 2000 Dec 12 3.5 cm data. The source has an extended emission region approximately $5''$ across, as originally seen by Ulvestad & Wilson (1984). At a distance of 17.6 Mpc Tully (1988), this corresponds to $\sim$ 400 pc. A N-S bar of strong emission lies at the center of the source. A separate, bright compact source lies to the NW of this bar. A 1.6 μm *HST* greyscale image of the region (Regan & Mulchaey 1999) has been overlaid on the radio contours. The core of the near-infrared emission corresponds to the center of the radio emission bar. The radio morphology is suggestive of a core of radio emission with a double-sided jet extending to the North and South. The four brightest separable peaks in the emission have been labelled 1–4 in the figure. Component 2 corresponds to the core of the AGN, where the broad line detection was identified optically. The other three components are separated from component 2 by at least $1''$ on the sky, or at least 85 pc at the distance of NGC 7582. Therefore, a change in the environment of the core during 1998 has not yet had time to influence the emission from any of the other three radio components. Figure 2 shows the corresponding 6 cm image from the 2000 Dec 12 data. The lower resolution of the 6 cm data compared to the 3.5 cm data has smoothed out the individual emission peaks of the radio bar, leaving only components 2 and 4 as distinguishable features.

The AIPS task JMFIT was used to measure the peak and integrated flux densities of the distinguishable radio peaks for each observation of NGC 7582. Figure 3 shows the radio light curves for the peak flux densities — a plot of the integrated flux densities is virtually identical. Recall that the 6 cm observations from 1981 are uncalibrated in amplitude. The relative amplitudes of the components for 1981 should, however, be a good measurement within the noise uncertainty of the image. The figure suggests a rise in emission through approximately 1997.0, followed by a decline thereafter. A decline in emission from 1997.0 onward is inconsistent with the appearance of a radio supernova. However, all four components show essentially the same behavior. Because of their linear separations, the four components cannot be causally related, and therefore the similar behavior by all of them suggests an amplitude calibration problem. The 2000 Dec 12 measurements are known to be affected by the snowstorm during observations. The remaining amplitude changes may reflect the uncertainty in amplitude calibrations of the VLA itself for low Declinations objects. NGC 7582 always remains below an elevation of 13°, so the emission changes in this object may be due to insufficient gain corrections for elevation or a problem in the atmospheric absorption correction used by AIPS.

If these variations are due to amplitude offsets for the entire image, then the ratios of emission values remains a valid measurement. Figure 4 shows the ratios of the emission in component 2 (the core) to the other three components. All of the ratios have been normalized to unity for the 1999 Sep observations to improve readability of the figure. Errorbars for the flux density ratios represent uncertainty estimates obtained from varying the starting conditions used by JMFIT to calculate the peak flux values for individual components. The data are suggestive of a small decline in the relative flux of the core component through 1999,but any change is less than the 1σ uncertainty in any individual measurement. For the 2000 Dec observations, the data are significantly more scattered, but are consistent with no change from 1999 Sep within the measurement uncertainty.

Based on these measurements, the radio observations are consistent with no detection of a radio supernova in NGC 7582. From the measurement uncertainties, upper limits of 0.2 mJy at 3.5 cm and 0.4 mJy at 6 cm can be placed on the variation of the radio core component. At 6 cm, this corresponds to a possible spectral luminosity of approximately 1.5×10^{19} W Hz^{-1}. From figure 1 of van Dyk et al. (1996), this spectral luminosity is consistent with many other non-detections of other Type IIn supernovae. Therefore, the non-detection of radio emission from the broad-line event in NGC 7582 cannot rule out a Type IIn supernova.

3. X-ray Data

3.1. Background

In their *BeppoSAX* observations of NGC 7582 shortly after the broad line event started, Turner et al. (2000) found an increase in X-ray emission compared to *ASCA* observations prior to the broad line event (Xue et al. 1998). Their measurements indicated nearly a factor of two increase in emission for soft (0.5–2 keV) X-rays and nearly 30% for hard (2–10 keV) X-rays compared to the 1994 *ASCA* observations. The data are most consistent with an *increase* in the total neutral hydrogen column depth with the appearance of holes in the absorption screen, providing clear lines of site to the nuclear broad-line region and allowing $\lesssim 1\%$ of the nuclear emission to be seen directly. However, Turner et al. (2000)

cannot rule out an increase in X-ray emission from a supernova near the core of NGC 7582.

X-ray data for NGC 7582 have been collected from various publications extending back more than 25 years. *Ariel 5* (Ward et al. 1978), *HEAO 1* (Mushotzky 1982), *Einstein* (Maccacaro & Perola 1981), *EXOSAT* (Turner & Pounds 1989), *Ginga* (Warwick et al. 1993), *ASCA* (Xue et al. 1998), *BeppoSAX*, and *RXTE* (Turner et al. 2000) measurements are collectively shown in Figure 5. These data show the long-term variability of the X-ray emission from this Seyfert galaxy. Variations of factors of 2 in a single day have also been observed (e.g. Mushotzky 1982). Measurements of the absorption column of neutral hydrogen also show large variability over the past 25 years. A variation of nearly a factor of two can be seen since 1994. Although these data are consistent with the standard unification model for AGN, they do not rule out a supernova event in 1998.

3.2. Supernova Radio to X-ray Relation

Although the X-ray measurements alone may not be able to rule out a supernova in 1998, the radio upper limits from section 2.2 combined with the X-ray measurements suggest that the increase in X-ray emission is not likely to be associated with a supernova. Table 2 provides soft and hard X-ray measurements for *all* known supernovae detected in X-rays (through 2001 Aug). The X-ray fluxes shown are taken from measurements as close as possible to 90 days after the outburst of the supernova to correspond to the time of *BeppoSAX* measurements of NGC 7582 (Turner et al. 2000). Also shown are radio measurements of these same supernovae, taken approximately 900 days after the outburst to correspond to the new VLA measurements of NGC 7582 presented in this paper. The surprising result seen in this table is that all but 2 of the X-ray supernovae also have detections in the radio. One of the radio non-detections is for supernova 1999gi, which possibly has not yet had time to sufficiently brighten in the radio to become visible. The other non-detection is 1994W, which may have had observing difficulties in detecting the radio supernova (R. Sramek, private communication).

Another interesting feature of X-ray supernovae is shown in Figures 6 and 7. The ratio of radio flux density to X-ray flux is confined to a narrow range despite the enormous range in X-ray luminosity. The *BeppoSAX* increase in soft X-rays is a factor of 40 below the lowest point in Figure 6, and a factor of 80 below the lowest point in Figure 7 using the upper limits from the VLA 3.5 cm data. In contrast, the standard deviation of the measured supernovae data about their mean is only 0.58 in the log, or a factor of 3.8. Thus, the NGC 7582 radio to X-ray ratio represents at least a 10σ outlier if the event is indeed a supernova.

4. Hot Spot Modeling

5. Conclusions

Radio observations of NGC 7582 do not detect an emission increase in the galaxy core at a moderate detection level. This level is insufficient by itself to rule out a supernova in the core of NGC 7582. A comparison of radio to X-ray fluxes for known supernovae suggests that the increase in X-ray emission around the time of the broad line event in NGC 7582 was not due to a supernova. Finally, modeling of the variation in redshift of the optical broad line emission is consistent with a clump of hot gas orbiting about a supermassive object at the center of the galaxy.

REFERENCES

Baars, J. W. M., Genzel, R., Pauliny-Toth, I. I. K., & Witzel, A. 1977, A&A, 61, 99

Beuermann, K., Brandt, S., & Pietsch, W. 1994, A&A, 281, L45

Briggs, D. S. 1995, PhD thesis, New Mexico Institute of Mining and Technology, Socorro, NM

Canizares, C. R., Kriss, G. A., & Feigelson, E. D. 1982, ApJ, 253, L17

de Vaucouleurs, G. 1963, ApJ, 137, 720+

Fabian, A. C. & Terlevich, R. 1996, MNRAS, 280, L5

Feldmeier, J. J., Ciardullo, R., & Jacoby, G. H. 1997, ApJ, 479, 231+

Fox, D. W., Lewin, W. H. G., Fabian, A., Iwasawa, K., Terlevich, R., Zimmermann, H. U., Aschenbach, B., Weiler, K., Van Dyk, S., Chevalier, R., Rutledge, R., Inoue, H., & Uno, S. 2000, MNRAS, 319, 1154

Freedman, W. L., Hughes, S. M., Madore, B. F., Mould, J. R., Lee, M. G., Stetson, P., Kennicutt, R. C., Turner, A., Ferrarese, L., Ford, H., Graham, J. A., Hill, R., Hoessel, J. G., Huchra, J., & Illingworth, G. D. 1994a, ApJ, 427, 628

Freedman, W. L., Madore, B. F., Stetson, P. B., Hughes, S. M. G., Holtzman, J. A., Mould, J. R., Trauger, J. T., Gallagher, J. S., Ballester, G. E., Burrows, C. J., Casertano, S., Clarke, J. T., Crisp, D., Ferrarese, L., Ford, H., Graham, J. A., Griffiths, R. E., Hester, J. J., Hill, R., Hoessel, J. G., Huchra, J., Kennicutt, R. C., Scowen, P. A., Sparks, B., Stapelfeldt, K. R., Watson, A. M., & Westphal, J. 1994b, ApJ, 435, L31

Groenewegen, M. A. T. 2000, A&A, 363, 901

Houck, J. C., Bregman, J. N., Chevalier, R. A., & Tomisaka, K. 1998, ApJ, 493, 431+

Immler, S., Pietsch, W., & Aschenbach, B. 1998a, A&A, 336, L1

—. 1998b, A&A, 331, 601

Lewin, W. H. G., Zimmermann, H.-U., & Aschenbach, B. 1996, IAU Circ., 6445, 1+

Maccacaro, T. & Perola, G. C. 1981, ApJ, 246, L11

Mushotzky, R. F. 1982, ApJ, 256, 92

Pian, E., Amati, L., Antonelli, L. A., Butler, R. C., Costa, E., Cusumano, G., Danziger, J., Feroci, M., Fiore, F., Frontera, F., Giommi, P., Masetti, N., Muller, J. M., Nicastro, L., Oosterbroek, T., Orlandini, M., Owens, A., Palazzi, E., Parmar, A., Piro, L., in't Zand, J. J. M., Castro-Tirado, A., Coletta, A., Dal Fiume, D., Del Sordo, S., Heise, J., Soffitta, P., & Torroni, V. 2000, ApJ, 536, 778

Pooley, D. et al. 2001, X-ray, Optical, and Radio Observations of SN 1999em and SN 1998S, astro-ph, 0103196

Regan, M. W. & Mulchaey, J. S. 1999, AJ, 117, 2676

Richmond, M., Schmidt, B., Challis, P., Kirshner, R., Berland, P., Phillips, M., Sramek, R. A., Rupen, M. P., van Dyk, S. D., Weiler, K. W., & Panagia, N. 1994, IAU Circ., 5966, 1+

Rupen, M. P., van Gorkom, J. H., Knapp, G. R., Gunn, J. E., & Schneider, D. P. 1987, AJ, 94, 61

Sakai, S., Ferrarese, L., Kennicutt, R. C., Graham, J. A., Silbermann, N. A., Mould, J. R., Freedman, W. L., Bresolin, F., Ford, H. C., Gibson, B. K., Han, M., Harding, P., Hoessel, J. G., Huchra, J. P., Hughes, S. M., Illingworth, G. D., Kelson, D., Macri, L., Madore, B. F., Phelps, R. L., Saha, A., Sebo, K. M., Stetson, P. B., & Turner, A. 1999, ApJ, 523, 540

Schlegel, E. M. 1999, ApJ, 527, L85

— 2001, ApJ, 556, L25

Schlegel, E. M., Ryder, S., Staveley-Smith, L., Petre, R., Colbert, E., Dopita, M., & Campbell-Wilson, D. 1999, AJ, 118, 2689

Sohn, Y. & Davidge, T. J. 1998, AJ, 115, 130+

Staveley-Smith, L., Briggs, D. S., Rowe, A. C. H., Manchester, R. N., Reynolds, J. E., Tzioumis, A. K., & Kesteven, M. J. 1993, Nature, 366, 136+

Theureau, G., Bottinelli, L., Coudreau-Durand, N., Gouguenheim, L., Hallet, N., Loulergue, M., Paturel, G., & Teerikorpi, P. 1998, A&AS, 130, 333

Thompson, A. R., Clark, B. G., Wade, C. M., & Napier, P. J. 1980, ApJS, 44, 151

Tinney, C., Stathakis, R., Cannon, R., Galama, T., Wieringa, M., Frail, D. A., Kulkarni, S. R., Higdon, J. L., Wark, R., & Bloom, J. S. 1998, IAU Circ., 6896, 1+

Tully, R. B. 1988, Nearby galaxies catalog (Cambridge and New York, Cambridge University Press, 1988, 221 p.)

Turatto, M., Cappellaro, E., Danziger, I. J., Benetti, S., Gouiffes, C., & della Valle, M. 1993, MNRAS, 262, 128

Turner, T. J., Perola, G. C., Fiore, F., Matt, G., George, I. M., Piro, L., & Bassani, L. 2000, ApJ, 531, 245

Turner, T. J. & Pounds, K. A. 1989, MNRAS, 240, 833

Ulvestad, J. S. & Wilson, A. S. 1984, ApJ, 285, 439

Uno, S., Mitsuda, K., Inoue, H., Takahashi, T., Makino, F., Hirayama, M., Takizawa, K., Makishima, K., Ishisaki, Y., Kohmura, Y., Itoh, M., & Lewin, W. 1997, in X-Ray Imaging and Spectroscopy of Cosmic Hot Plasmas, 399+

van Dyk, S. D., Weiler, K. W., Sramek, R. A., & Panagia, N. 1993, ApJ, 419, L69

van Dyk, S. D., Weiler, K. W., Sramek, R. A., Rupen, M. P., & Panagia, N. 1994, ApJ, 432, L115

van Dyk, S. D., Weiler, K. W., Sramek, R. A., Schlegel, E. M., Filippenko, A. V., Panagia, N., & Leibundgut, B. 1996, AJ, 111, 1271+

Ward, M. J., Wilson, A. S., Penston, M. V., Elvis, M., Maccacaro, T., & Tritton, K. P. 1978, ApJ, 223, 788

Warwick, R. S., Sembay, S., Yaqoob, T., Makishima, K., Ohashi, T., Tashiro, M., & Kohmura, Y. 1993, MNRAS, 265, 412+

Weiler, K. W., Sramek, R. A., Panagia, N., van der Hulst, J. M., & Salvati, M. 1986, ApJ, 301, 790

Wieringa, M. H., Kulkarni, S. R., & Frail, D. A. 1999, A&AS, 138, 467

Xue, S., Otani, C., Mihara, T., Cappi, M., & Matsuoka, M. 1998, PASJ, 50, 519

This manuscript was prepared with the AAS LaTeX macros v5.0.

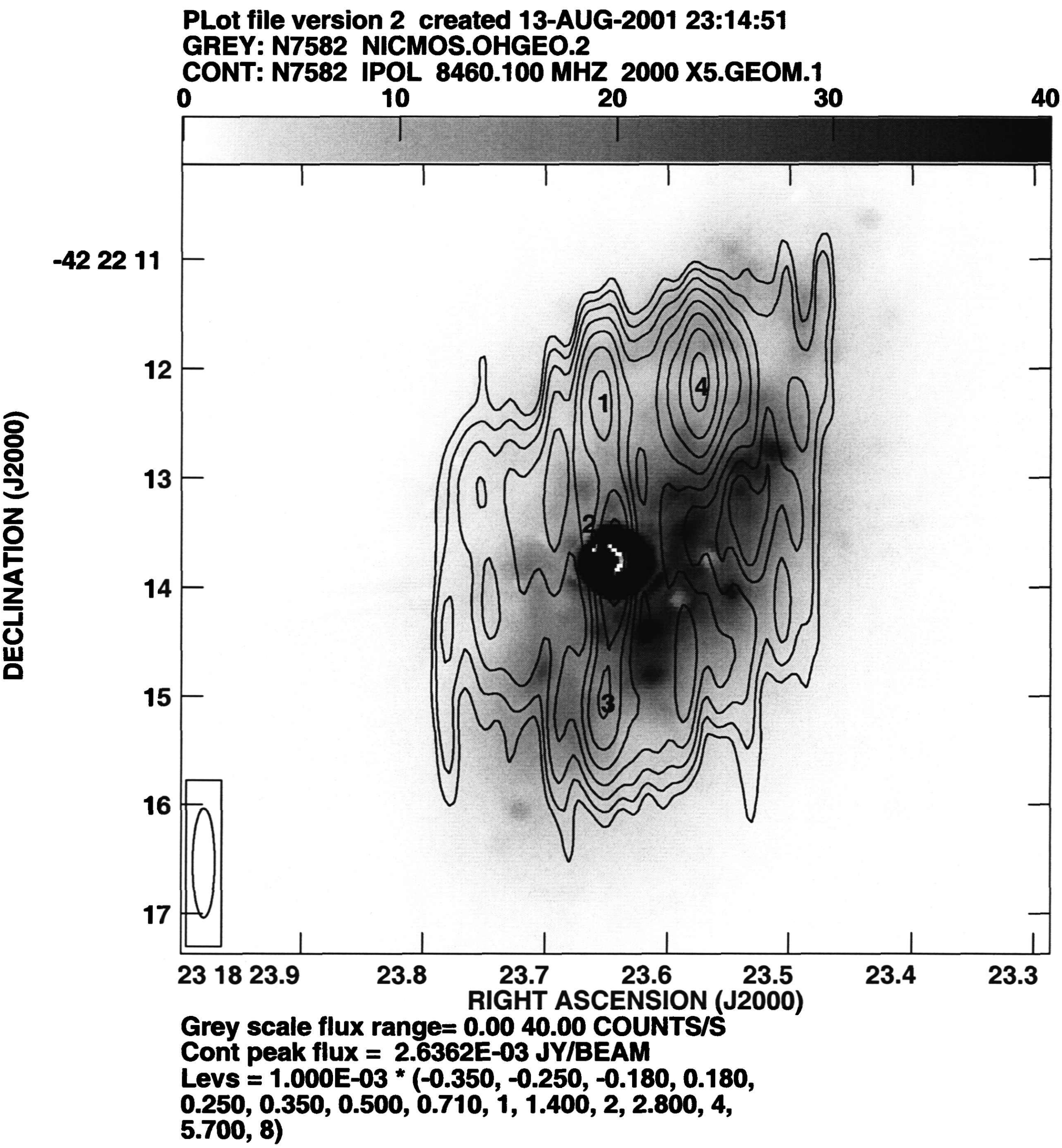

Fig. 1.— NGC 7582. The 2000 December 3.5 cm data (contours) are shown overlaid on a 1.6 μm *HST* NICMOS image (greyscale) (Regan & Mulchaey 1999) taken prior to the broad-line event. Radio contours are spaced at $\sqrt{2}$ intervals, starting at 0.18 mJy beam^{-1}. The four brightest radio components are labeled 1–4 in the image. The *HST* image has been shifted approximately 0$''$.5 on the sky to line up the bright core with radio component 2. Components 1 and 3 could possibly be jet features extending from the AGN core. The

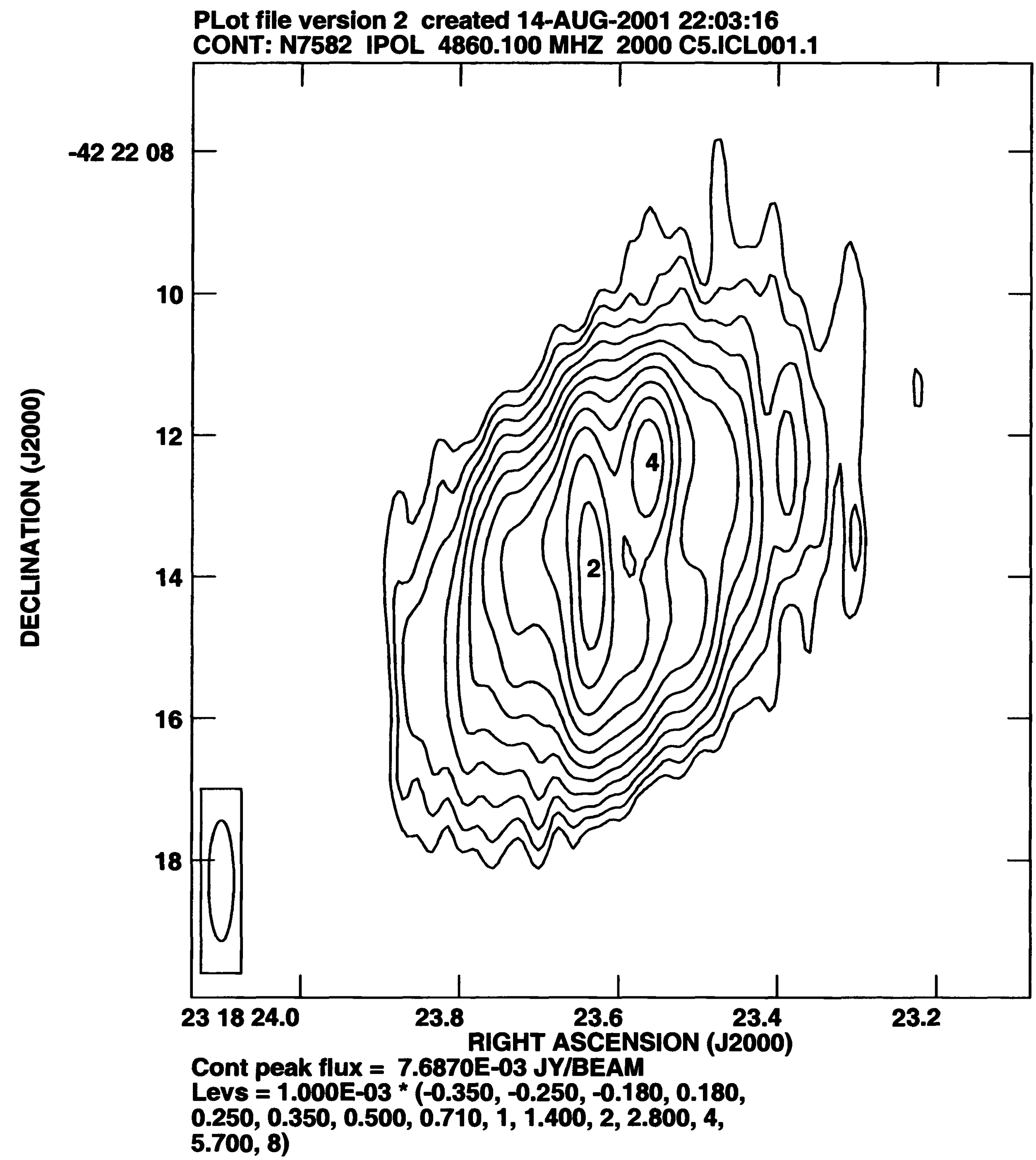

Fig. 2.— NGC 7582. The 2000 December 6 cm radio data are shown as a contour map. The contours are spaced at $\sqrt{2}$ intervals starting at 0.18 mJy beam^{-1}. Components 1 and 3 are not distinguishable at the somewhat lower resolution of the 6 cm data, so only components 2 and 4 are labeled. The size of the synthesized beam is shown at the lower left.

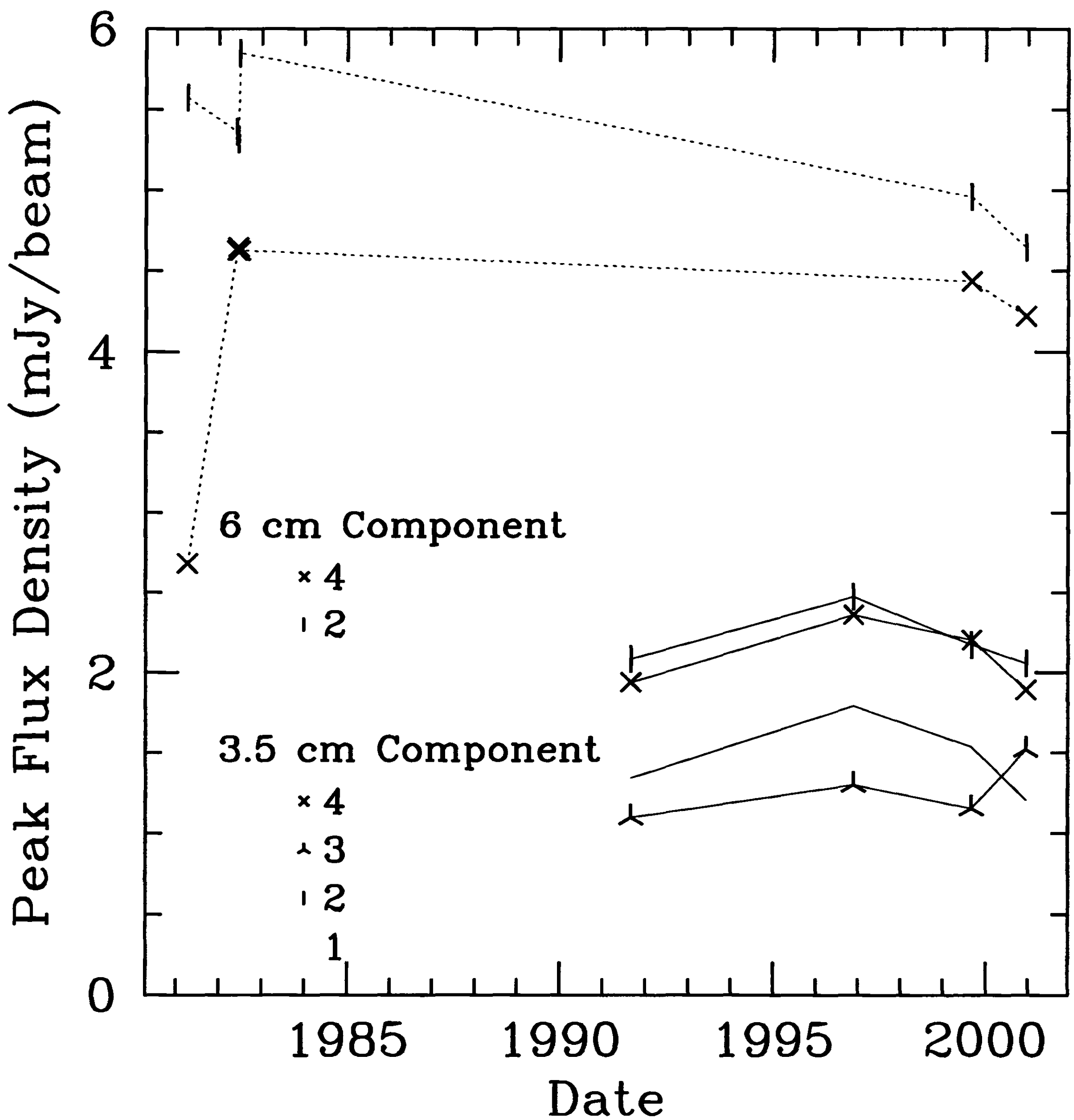

Fig. 3.— Radio Flux Density History. 6 cm (dotted lines) and 3.5 cm (solid lines) measurements of the central components of NGC 7582 are shown as a function of date. Variations in flux density are highly correlated between components and are probably due to calibration effects.

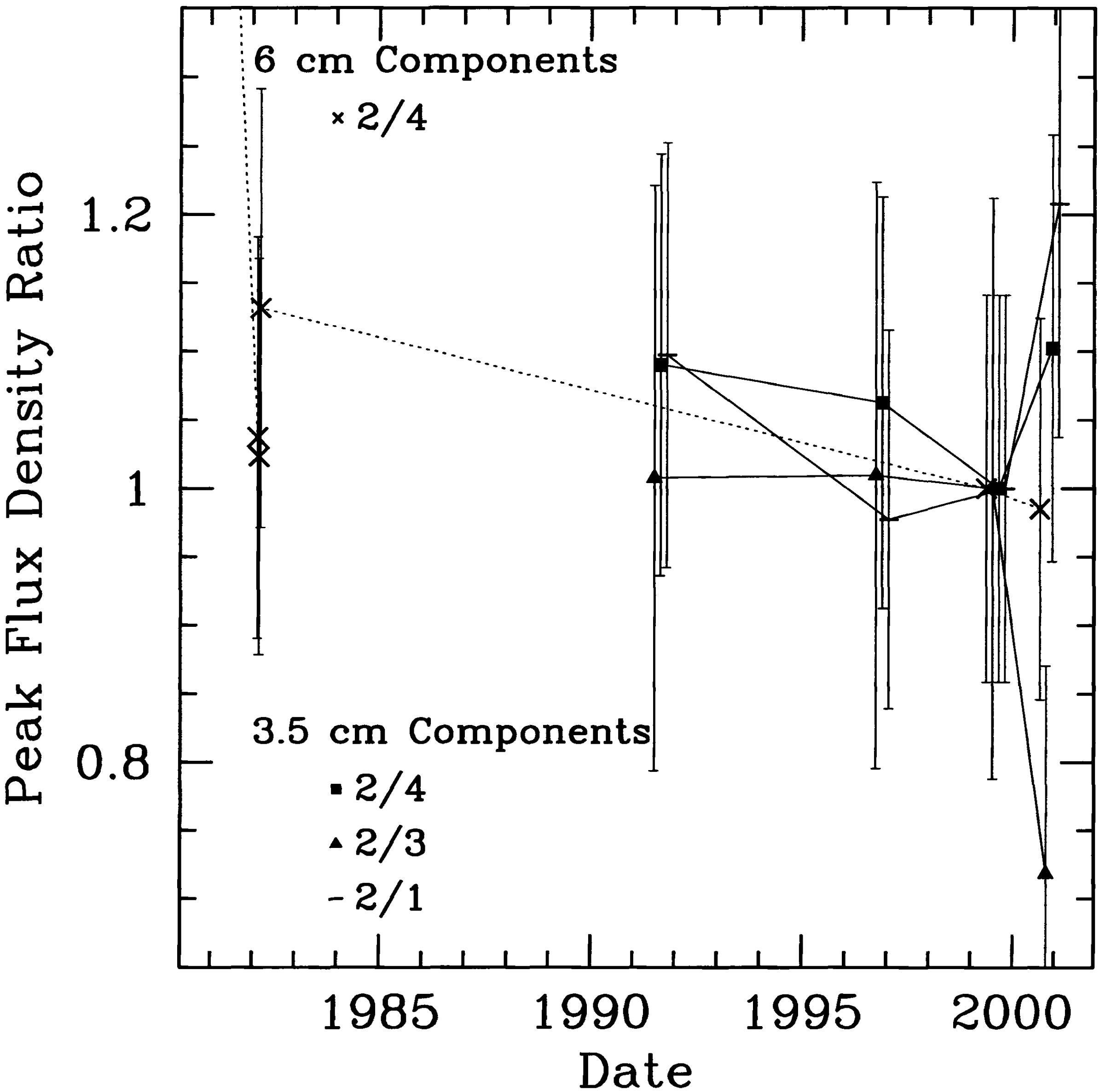

Fig. 4.— Radio Flux Density Ratio History. The peak flux density in the core (component 2) relative to the other central components is shown as a function of date. 6 cm data are connected by dotted lines, 3.5 cm data are connected by solid lines. The component ratios have all been multiplicatively normalized to unity for the 1999 observations. Errorbars represent the expected fit uncertainty in the individual peak flux densities. Ratios to different components have been slightly shifted in time to uniquely identify errorbars. The 1981 6 cm ratio is ~ 1.9 with a large errorbar.

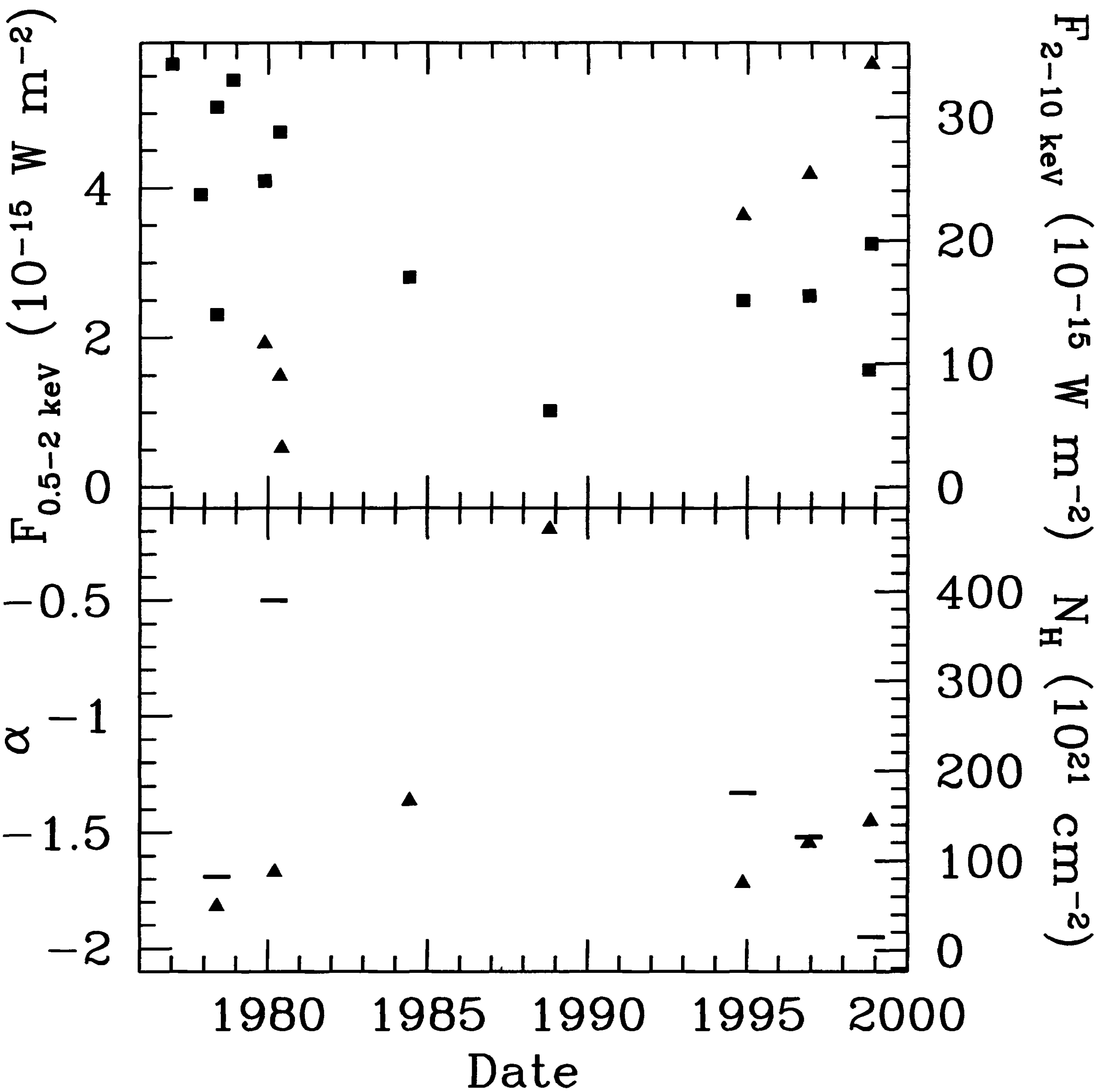

Fig. 5.— NGC 7582 X-ray Observations. X-ray measurements and derived parameters for NGC 7582 are shown as a function of observation date. The upper region contains soft (triangle) and hard (square) X-ray flux measurements. The lower region shows calculated values for the spectral shape (bar) and column density of neutral hydrogen (triangles). Measurements prior to 1990 are somewhat contaminated by other nearby X-ray sources and are probably less reliable. See the text for further information.

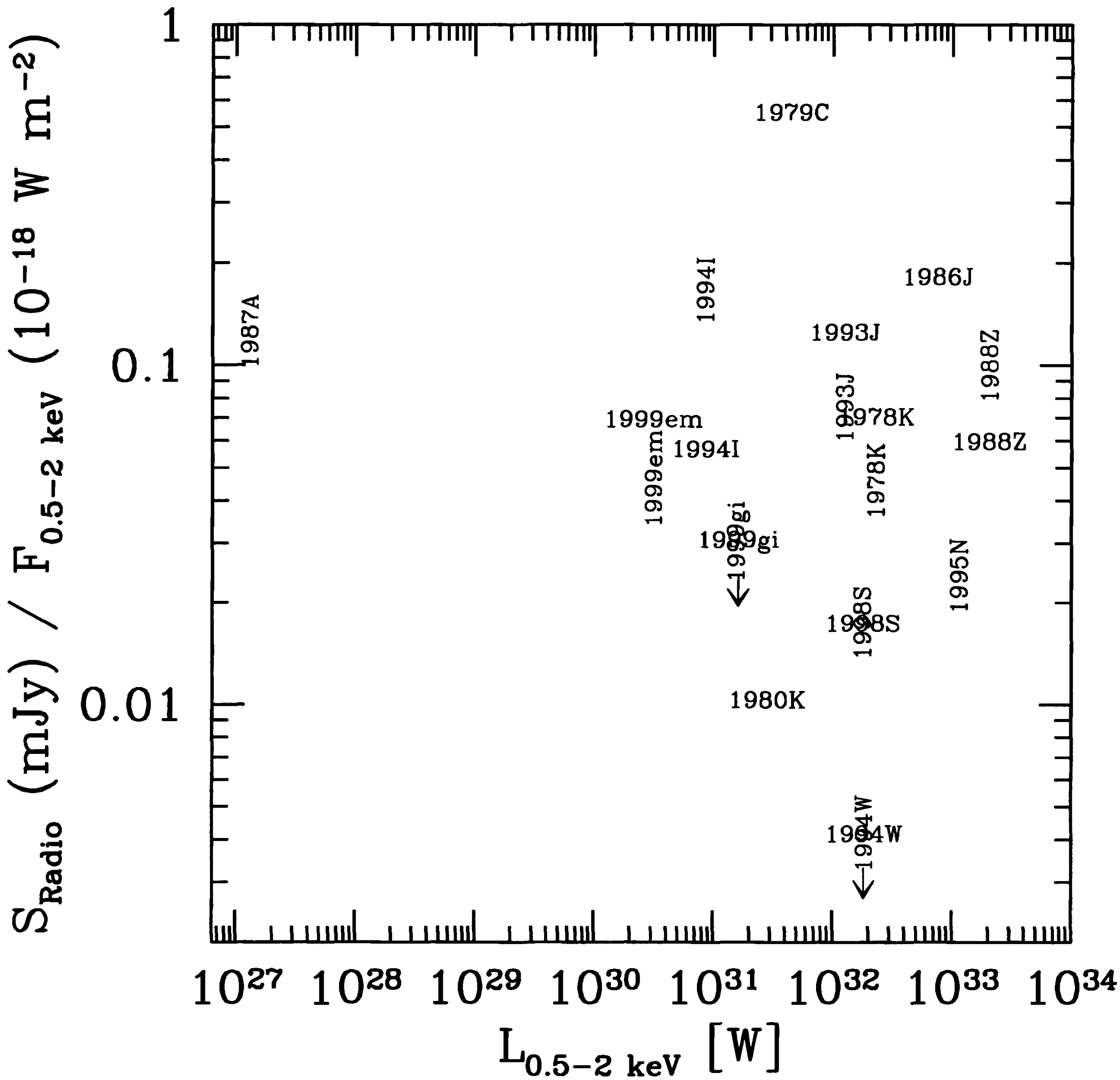

Fig. 6.— Supernova Radio to Soft X-ray Relation. The radio flux density to soft X-ray flux ratios for all supernovae with detected X-ray emission are plotted as a function of soft X-ray luminosity. 6 cm radio supernovae data are indicated by horizontal names; 3.5 cm data are represented by vertical lettering.

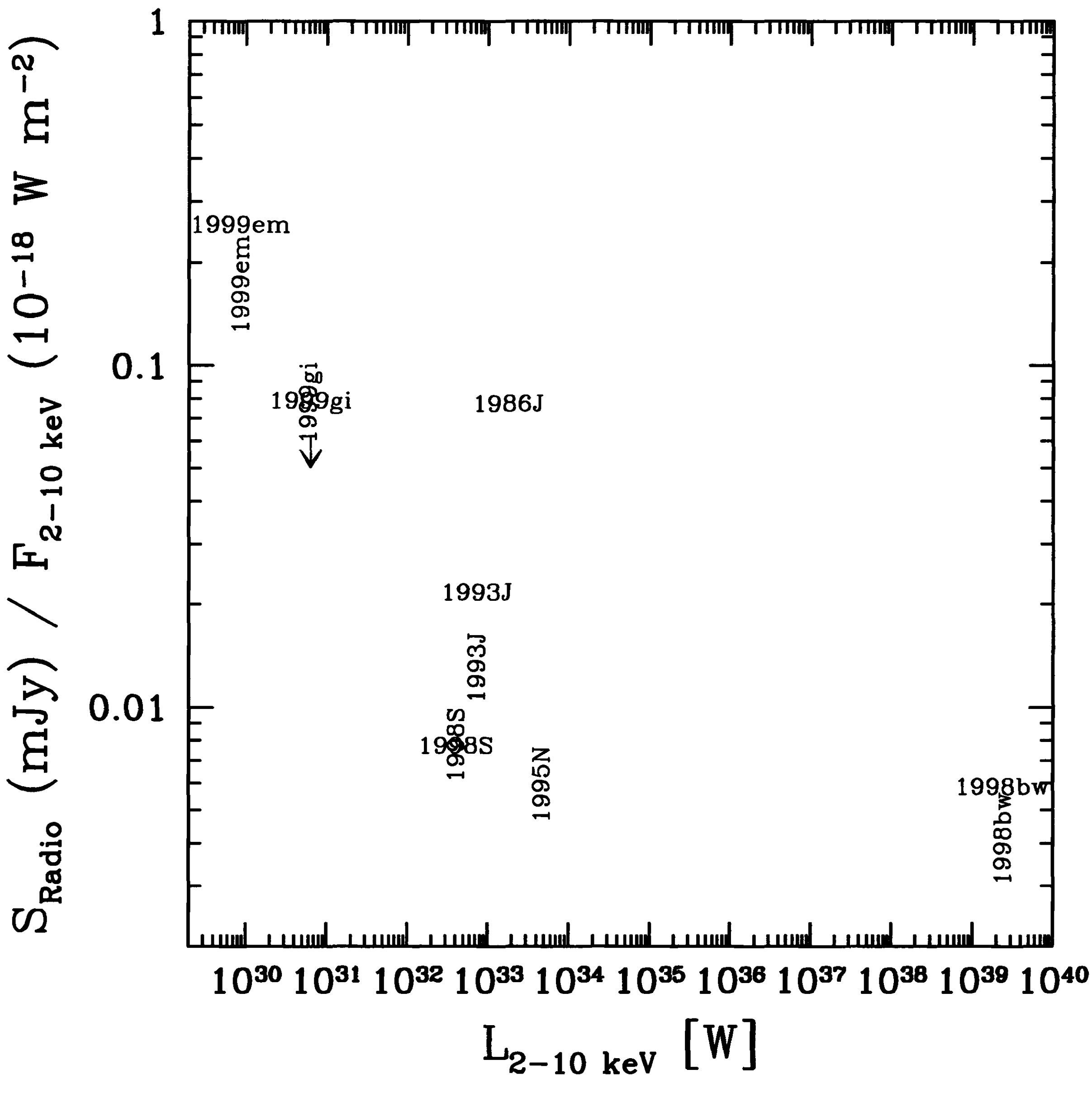

Fig. 7.— Supernova Radio to Hard X-ray Relation. The radio flux density to hard X-ray flux ratios for all supernovae with detected X-ray emission are plotted as a function of hard X-ray luminosity. 6 cm radio supernovae data are indicated by horizontal names; 3.5 cm data are represented by vertical lettering.

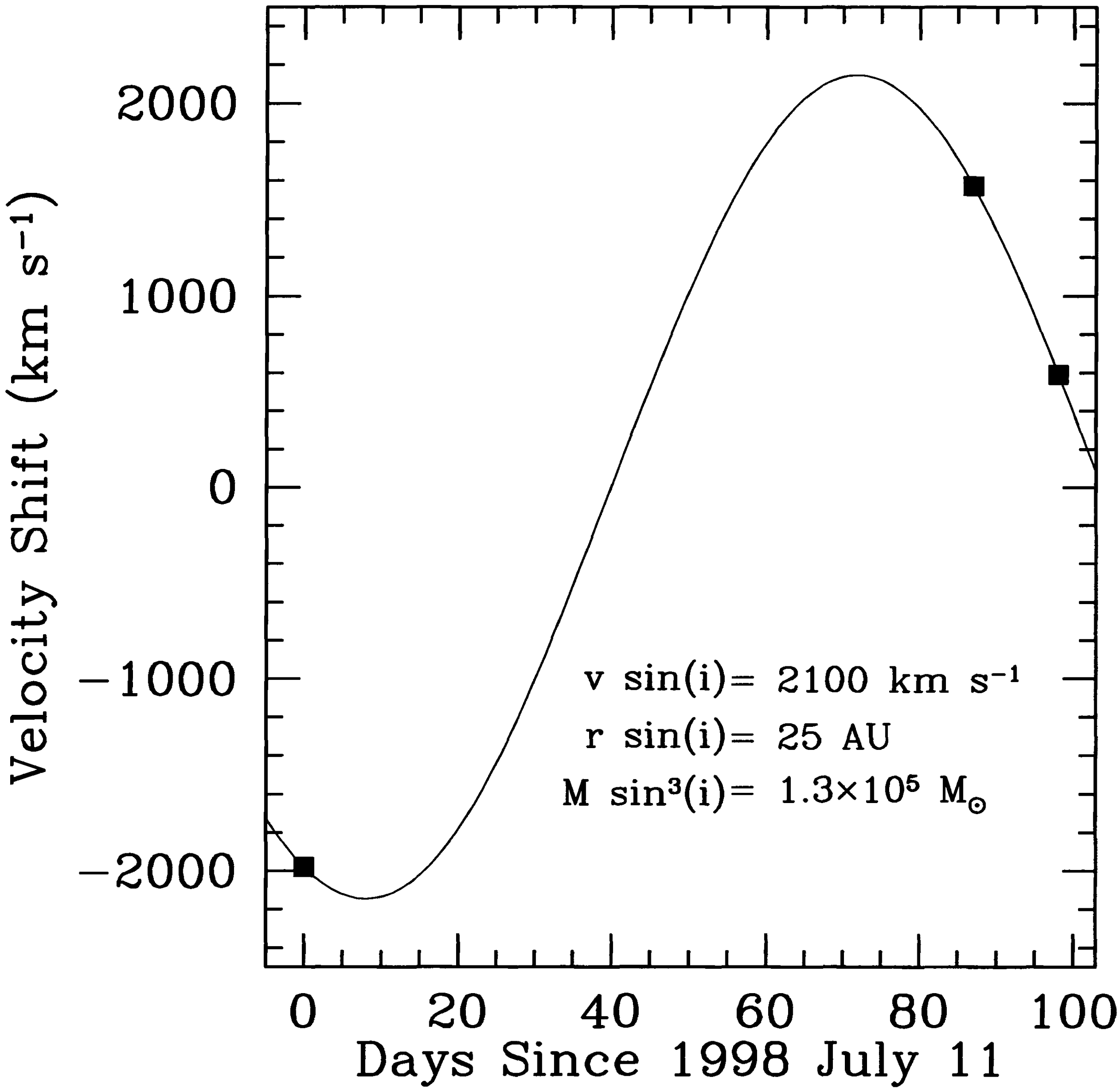

Fig. 8.— Circular Orbit Fitting. A best fit circular orbit is shown for the velocity shift of the broad optical component relative to the narrow optical lines. The fit is consistent with a central mass of at least 10^5 $M_\odot$ inside a radius of 25 AU.

Table 1. VLA Observations of NGC 7582

Date	λ (cm)	ν (GHz)	$\Delta\nu$ (MHz)	τ (min)
1980 Aug 08	6	4.885	50	9
1982 Jun 04	6	4.885	50	24
1982 Jun 28	6	4.885	50	29
1991 Sep 01	3.5	8.440	100	59
1996 Nov 25	3.5	8.460	100	14
1999 Sep 04	6	4.860	100	15
1999 Sep 04	3.5	8.460	100	15
2000 Dec 12	6	4.860	100	76
2000 Dec 12	3.5	8.460	100	72

Table 2. X-ray Supernovae

Supernova[a]		Host Galaxy			Radio Data[b]			X-ray Data[c]		
Name	Type	Name	Distance[d] Mpc	Ref	$S_{4.9\ \mathrm{GHz}}$ mJy	$S_{8.5\ \mathrm{GHz}}$ mJy	Ref	$F_{0.5-2\ \mathrm{keV}}$ 10^{-18} W m^{-2}	$F_{2-10\ \mathrm{keV}}$ 10^{-18} W m^{-2}	Ref
1978K	$\mathrm{II_{L/P}}$	NGC 1313	4.5	1	67.1	43.2	2	950	...	2
1979C	$\mathrm{II_L}$	NGC 4321	17.1	3	7.0	...	4	13	...	5
1980K	$\mathrm{II_L}$	NGC 6946	5.5	7	0.8	...	4	77	...	7
1986J	$\mathrm{II_{pec}}$	NGC 891	9.6	6	124	...	8	680	1600	9
1987A	$\mathrm{II_p}$	LMC	0.052	10	...	5.0	11	40	...	12
1988Z	$\mathrm{II_{pec}}$	MCG +03-28-022	89.9	13	1.26	2.10	14	21	...	15
1993J	$\mathrm{II_{pec}}$	NGC 3031	3.63	16	100	60	17	800	4600	18
1994I	Ic	NGC 5194	8.4	19	0.57	1.66	20	10	...	21
1994W	$\mathrm{II_p}$	NGC 4041	17.9	6	$\lesssim 0.2$	$\lesssim 0.2$	22	48	...	23
1995N	$\mathrm{II_{pec}}$	MCG -02-038-017	24.5	24	...	3.8	25	580	640	25,26
1998bw	Ic	ESO 184-G82	34 000	27	1.0	0.7	28	...	170	29
1998S	$\mathrm{II_n}$	NGC 3877	17.0	6	0.9	0.9	30	520	120	30
1999em	$\mathrm{II_p}$	NGC 1637	7.8	31	0.3	0.2	30	4.3	1.2	30
1999gi	$\mathrm{II_?}$	NGC 3184	14.3	32	$\lesssim 0.2$	$\lesssim 0.2$	22	6.6	2.6	33

[a]List of X-ray Supernovae taken from the University of Massachusetts High Energy Astrophysics Group.

[b]Radio data refer observations $\sim$ 800–1000 days after outburst wherever possible.

[c]X-ray data refer to detection closest to $\sim$ 90 days after outburst. Fluxes have been converted from published bands assuming $S_\nu \propto \nu^{-1}$.

[d]Distances are calculated assuming $H_0 = 75$ km s^{-1} Mpc^{-1} when only velocity information is available.

Note. — References are as follows: (1) de Vaucouleurs (1963); (2) Schlegel et al. (1999); (3) Freedman et al. (1994b); (4) Weiler et al. (1986); (5) Immler et al. (1998b); (6) Tully (1988); (7) Canizares et al. (1982); (8) Rupen et al. (1987); (9) Houck et al. (1998); (10) Groenewegen (2000); (11) Staveley-Smith et al. (1993); (12) Beuermann et al. (1994); (13) Turatto et al. (1993); (14) van Dyk et al. (1993); (15) Fabian & Terlevich (1996); (16) Freedman et al. (1994a); (17) van Dyk et al. (1994); (18) Uno et al. (1997); (19) Feldmeier et al. (1997); (20) Richmond et al. (1994); (21) Immler et al. (1998a); (22) R. Sramek (2001, private communication); (23) Schlegel (1999); (24) Theureau et al. (1998); (25) Fox et al. (2000); (26)